Suramin Resistance

in African Trypanosomes

INAUGURALDISSERTATION

zur

Erlangung der Würde eines Doktors der Philosophie

vorgelegt der

Philosophisch-Naturwissenschaftlichen Fakultät

der Universität Basel

von

Natalie Wiedemar

aus Bern (BE)

Basel, 2019

Genehmigt von der Philosophisch-Naturwissenschaftlichen Fakultät

auf Antrag von

Prof. Dr. Pascal Mäser

Prof. Dr. André Schneider

Basel, den 19.02.2019

Prof. Dr. Martin Spiess

Dekan

Abbreviations

BSA	Bovine serum albumin
BSD	Blasticidine resistance gene
cds	Coding sequence
ConA	Concanavalin A
ESAG	Expression-site associated gene
GPI	Glycosylphosphatidylinositol
HAT	Human African trypanosomiasis
HMI-9	Iscove's Modified Dulbecco's Media supplemented acc. to Hirumi
HpHb	Haptoglobin-haemoglobin
IC50	50% inhibitory concentration
IMDM	Iscove's Modified Dulbecco's Media
ISG75	invariant surface glycoprotein 75
LDL	Low density lipoprotein
MPXR	Melarsoprol-pentamidine cross-resistance
PCR	Polymerase chain reaction
qPCR	Quantitative polymerase chain reaction
Rab	Ras-related protein
STIB	Swiss Tropical Institute Basel
TLF1	Human trypanolytic factor 1
TLF2	Human trypanolytic factor 2
UBP1	Uridine-rich-binding protein 1
UTR	Untranslated region
VSG	Variant surface glycoprotein

Summary

Drug resistance is a wide-spread phenomenon and affects medical fields from infection biology to oncology. In the protozoan parasite *Trypanosoma brucei*, the causative agent of sleeping sickness, a number of resistance mechanisms have been described so far, most of them affecting drug uptake. In the presented PhD study I have investigated resistance of trypanosomes against the drug suramin. Suramin is a very old drug but its mode of action in trypanosomes is not well understood. By investigation of suramin-resistant parasites on their genomic and transcriptomic level I aimed to gain new insights into the pathway by which trypanosomes take up suramin and the mode of action of suramin.

I analyzed the transcriptome of a *T. brucei rhodesiense* line with a very quickly emerging *in vitro* suramin resistance. By combination of a mapping-based approach with a *de novo* transcriptome assembly, a new variant surface glycoprotein, VSG^{Sur}, was identified. Subsequent experiments showed that the expression of VSG^{Sur} is enough to cause ~100-fold suramin resistance in *T. brucei*. The phenotypic changes in these parasites were not limited to drug resistance; the uptake of a number of different substrates and nutrients was highly reduced. This suggests on the one hand that the VSG^{Sur}-mediated resistance phenotype is caused by lower levels of intracellular suramin due to a reduced suramin uptake, linked to a decreased uptake of transferrin and low density lipoprotein. On the other hand, these results demonstrate that VSGs have an impact on the cell biology of trypanosomes that is broader than previously believed and reaching beyond immune evasion.

I further selected these trypanosomes for even higher levels of suramin resistance. Analysis of sequence variations revealed a non-synonymous mutation in the RuvB-like helicase. This mutation was absent in the sensitive parent clone, heterozygous after suramin selection for three months, and turned homozygous during the course of further selection. Even though this finding needs further experimental validation, we have strong indications that RuvB-like helicase is a suramin target in trypanosomes, since (i) an unrelated suramin-resistant *T. evansi* isolate bears a mutation of the same residue, and (ii) suramin was shown to inhibit helicases in viruses.

Taken together, the transcriptome analysis of suramin-resistant trypanosomes led to the identification of two new resistance mechanisms: A VSG^{Sur}-mediated resistance that causes a reduced suramin uptake; and a mutation in the RuvB-like helicase that might protect this potential drug target from suramin action.

1. Trypanosomes, drugs and drug resistance – an introduction

1.1. The phenomenon of drug resistance

Drug resistance is a widespread problem in many fields of modern medicine. It hampers the combat of all infectious diseases in the field: viral [1], bacterial [2], fungal [3] and parasitic [4] pathogens are all able to develop resistance against the respective drugs and to impede successful treatment. But drug resistance is not restricted to infection biology. In the field of oncology, it poses a major problem as cancer cells very often become resistant against cytostatic drugs during the course of treatment [5], which is the reason for the poor prognosis of many late-stage neoplastic diseases. Even healthy human cells can develop resistance or tolerance to certain drugs: neurons, for instance, can become tolerant to opioids during analgesic treatments of acute and chronic pain conditions [6,7]. Under the flagship “antibiotics crisis”, the topic of drug resistance has gained a lot of attention in the last two decades as antibiotic resistance has reached the levels of an epidemic [2]. This is reflected in the number of publications about the topic: both, the absolute and the relative (compared to the whole biomedical scientific literature) numbers of publications on drug resistance constantly rose since the '60s with a jump at the turn of the millennium (Fig 1).

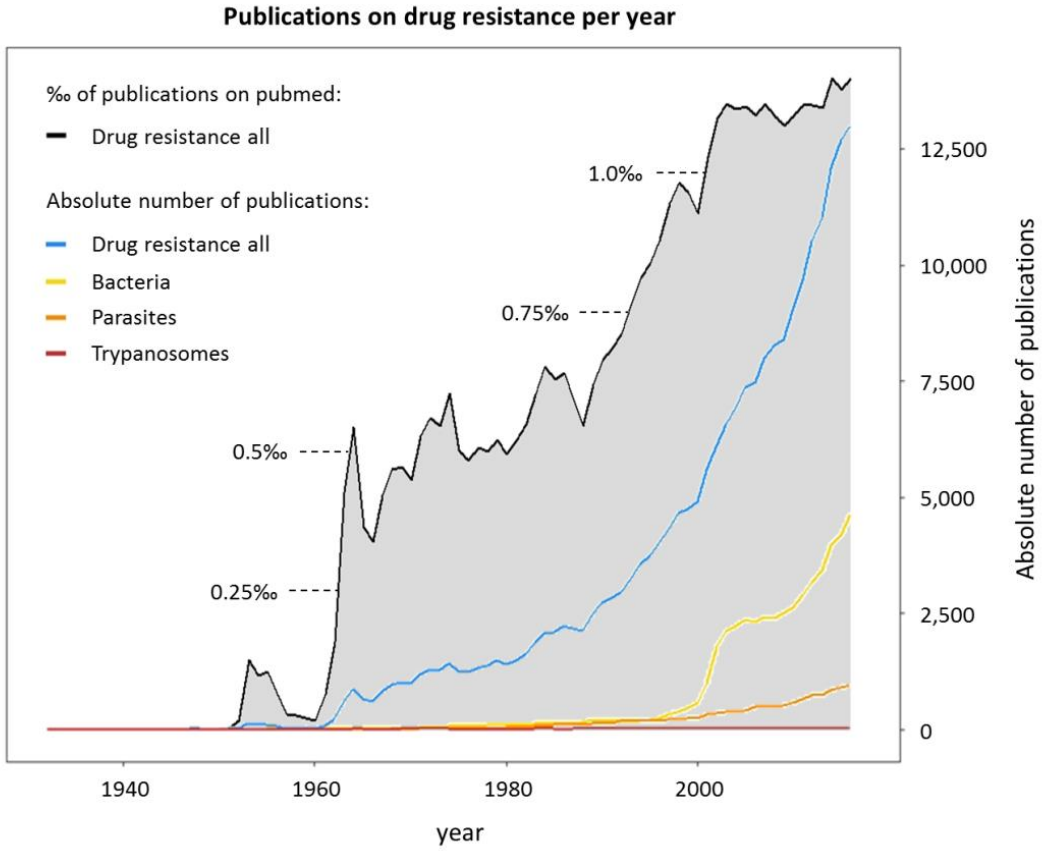

Figure 1: Number of publications about drug resistance on PubMed.

The black line with the grey filling corresponds to the per-mil publications containing the string 'drug resistance'of all publications on PubMed. The coloured lines show the absolute numbers of publications per year using the search strings 'drug resistance' (blue); '"bacterial drug resistance" OR "antibiotic resistance" OR "antimicrobial drug resistance"' (yellow); '"parasitic drug resistance" OR "parasite drug resistance"' (orange); and '"drug resistance" AND (trypanosoma OR trypanosomes OR "sleeping sickness" OR trypanosomiasis)' (red).

Amongst different types of drug resistance, the mechanisms of antibiotic resistance have been studied most extensively and many different bacterial resistance mechanisms have been described on the cellular and biochemical levels. They can be divided into five main categories: decrease of drug uptake, increase of drug efflux, inactivation of the drug, lack of drug activation and alterations of the drug target (Fig 2). A decreased drug uptake can be caused by a reduced expression and/or modifications of drug transporters [8]. Complementary to a decreased drug uptake, an increased drug efflux can be conferred through overexpression of efflux pumps or modifications of the pumps that change their substrate specificity [9]. Notably, efflux pumps often confer resistance not only to one drug

but act on various drugs [10]. Once the drug has entered the cell, additional mechanisms can confer resistance. Drug-inactivating or drug-degrading enzymes can be overexpressed [11] or more active forms can evolve through modifications of less active enzymes [12]. In case the drug enters the cell as a pre-drug that needs to be activated enzymatically, these enzymes can be mutated [13] or downregulated [14] leading to a lack of activation. Finally, the resistance mechanism can act on the drug target itself. The target can be modified in a way that decreases drug binding affinity while maintaining the function of the protein [9]. Proteins that bind to and protect the target [15] or target protein homologues that are less sensitive to the drug [9] can be upregulated. Finally, overexpression of the target protein itself can confer resistance [16].

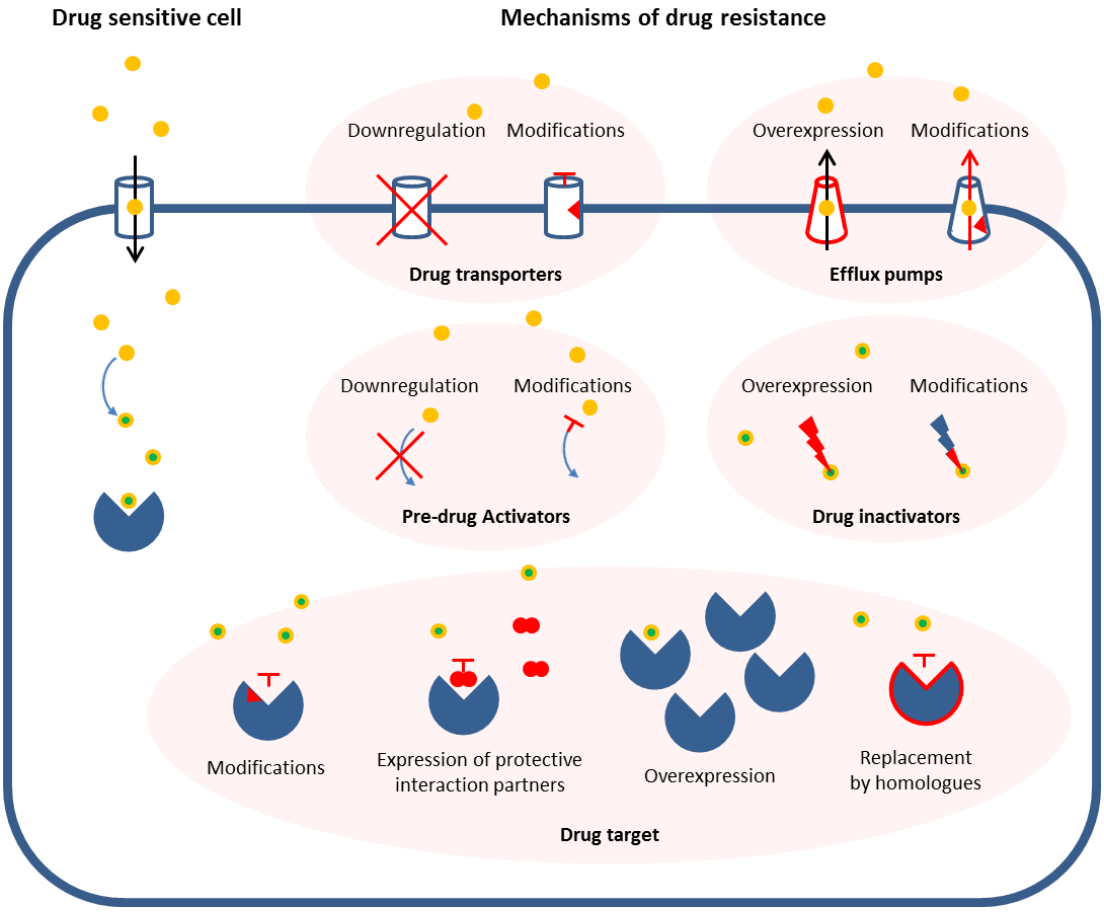

Figure 2: Mechanisms of drug resistance.

On the left hand side, the action of the drug in drug sensitive cells is shown: The pro-drug is taken up through its transporter, activated and binds to and inactivates its target. On the right hand side, different resistance mechanisms are shown.

In comparison to antibiotic resistance, parasitic drug resistance seems to be a rather small field of research. Nevertheless, the very first observations and investigations of drug resistance were carried out in protozoan parasites, predominantly in trypanosomes, the causing agents of Human African Trypanosomiasis (HAT). Even before the first drugs against HAT were introduced in the field, Ehrlich described at the beginning of the 19th century, that trypanosomes can become resistant against different drugs such as against arsenic compounds, azo-dyes (trypan red and trypan blue) and basic triphenylmethane dyes (e.g. fuchsin) if infected mice were repeatedly treated with these compounds [17,18]. He observed that resistant parasites were cross-resistant to other compounds of the same class of molecules and suspected changes in the affinity of chemo-receptors on the surface of the parasites and consequently a reduced drug uptake to be responsible for the resistance [18]. In the following years this theory was heavily disputed [19], but was later-on solidified by Yorke, who observed in first *in vitro* tests that drug sensitive trypanosomes accumulated the arsenic tryparsamide intracellularly, whereas resistant parasites did not [20]. Even though, retrospectively this observation could have also been attributed to an increased drug efflux, a decreased drug uptake is still the predominant resistance mechanism in trypanosomes known nowadays. In the following, the most important resistance mechanisms against the drugs used for the treatment of HAT will be described starting with a brief overview about the disease and the drugs currently used in the field.

1.1.1. Human African Trypanosomiasis and the drugs used for the treatment

Human African trypanaosomiasis, also called sleeping sickness, is transmitted by the bite of the tsetse fly (genus *Glossina*) and therefore its occurrence depends on the geographic distribution of the fly. The disease is caused by two subspecies of the kinetoplastid *Trypanosoma brucei*: The East African *T. b. rhodesiense* causes an acute, and the Central and West African *T. b. gambiense* causes a chronic form of the disease. In both cases, the parasites first multiply in the blood and lymph system and cause the first stage of the disease, also called the haemolymphatic stage. After weeks to years they invade the central nervous system and lead to the second or neurological stage of the disease. The choice of the drug used for HAT treatment depends on the causal trypanosome species and the staging of the disease. The first stage of rhodesiense HAT is treated with suramin, the oldest drug currently used, introduced 100 years ago [21]. The first stage of gambiense HAT is treated with pentamidine, which was introduced in the forties of the 20th century [22]. The

treatment of second stage HAT relies on drugs that are able to cross the blood-brain barrier. This is not the case for suramin and pentamidine, therefore, highly toxic arsenic compounds were the only option to treat second stage HAT for a very long time. In the forties the arsenic melarsoprol was introduced [23], replacing its arsenic precursors [24]. Melarsoprol is still used to treat the second stage of rhodesiense HAT, even though it is less toxic than its precursors, its toxicity is still unacceptable and causes an encephalopathic syndrome in up to 10% of treated patients with case fatality rates of up to 50% [25]. In the '80s, a second drug that is able to cross the blood-brain barrier was introduced: eflornithine [26]. Eflornithine is much less toxic than melarsoprol but it is not active against the rhodesiense subspecies and therefore only used for the treatment of second stage gambiense HAT [27]. Since the turn of the century it is used in combination with nifurtimox [28].

What all these drugs have in common is their parenteral administration requiring hospitalization, which complicates the treatment in the remote areas where HAT is prevalent. Even though African trypanosomes have been intensively used to study basic cell biology in the last few decades, the development of new drugs against HAT was neglected for long periods over the last century. Only in the last decades, fexinidazole [29,30], the first oral drug for the treatment of both stages of gambiense HAT, has been developed and tested in clinical trials. It recently received a positive opinion from the European Medicines Agency and will hopefully facilitate future treatment of the disease [31].

1.1.2. Melarsoprol and Pentamidine

The mode of action of melarsoprol and pentamidine has been studied but is not completely understood. The highly trypanocidal action of melarsoprol is probably carried out through the formation of stable adducts with the kinetoplastid specific antioxidans trypanothione [32]. The diamidine pentamidine interacts electrostatically with polyanions such as the circular mitochondrial (kinetoplast) DNA. It leads to a loss of kinetoplast DNA and of the mitochondrial membrane potential [33,34].

It had already been observed in the fifties that trypanosomes resistant to melarsen, a precursor of melarsoprol, are cross-resistant to pentamidine [35]. This melarsoprol-pentamidine cross-resistance (MPXR) later-on became the first resistance mechanism extensively studied in trypanosomes. The reason for MPXR was found in a decreased drug uptake [36] and was attributed to a defective adenosine transporter P2 [37,38]. The gene

encoding P2 was identified as *adenosine transporter 1* (*TbAT1*) by expression of a *T. b. brucei* cDNA library in yeast with deficient purine biosynthesis [39]. Mutations in *TbAT1* were found in *in vitro* selected *T. b. brucei* with a MPXR phenotype [39] and in resistant *T. b. rhodesiense* and *gambiense* patient isolates [40]. Homozygous disruption of *TbAT1* resulted in ~2-fold resistance to melarsoprol and pentamidine, even though resistance was much stronger to other diamidines [41]. A second gene involved in MPXR was identified by reverse genetics. In a genome-wide RNAi-library screen, knock-down of *aquaglyceroporin 2* (*TbAQP2*) and *aquaglyceroporin 3* (*TbAQP3*) expression caused MPXR [42]. Subsequent genetic knock-out of both genes increased the IC50 by two-fold for melarsoprol and 15-fold for pentamidine [42]. Subsequent experiments with inducible expression of *TbAQP2* and *TbAQP3* in a *TbAQP2/3* knockout, showed that loss of the gene *TbAQP2* was responsible for the resistance phenotype. In addition, mRNA and whole-genome sequencing of two *in vitro* selected *T. b. rhodesiense* lines with a pronounced MPXR phenotype, revealed a deletion of *TbAQP2* in addition to mutations and loss of *TbAT1* [43]. It was furthermore shown, that mutations in *TbAQP2* were also present in resistant field isolates and thus most probably confer drug resistance in the field [44]. It was somewhat surprising to find a channel that physiologically transports small, uncharged molecules to be involved in transport of positively charged molecules like pentamidine. Indeed, expression of a *TbAQP2/3* chimera with the TbAQP2 selectivity filter sensitized the *TbAQP2/3* null cells to melarsoprol but not to pentamidine [45]. Song et al. further showed that pentamidine binds to and inhibits TbAQP2 but does not permeate the channel, thus they hypothesized that AQP2 is a pentamidine receptor, and that the uptake is subsequently carried out through endocytosis [46]. The aforementioned *in vitro* selected *T. b. rhodesiense* lines [43] additionally had both acquired heterozygous mutations in the *TbUBP1* gene encoding for an RNA-binding protein. However, follow-up experiments were not fully conclusive and did not support a role of UBP1 in MPXR (Appendix 2).

1.1.3. Eflornithine and Nifurtimox

Eflornithine is the only drug against HAT whose mode of action is well understood: It inhibits polyamine synthesis or more specifically the decarboxylation of ornithine to putrescine by the enzyme ornithine decarboxylase [47]. In a forward genetics approach, a *T. b. brucei* line was selected *in vitro* and developed resistance within only two months [48]. Eflornithine is an amino acid analogue and since the resistant cells showed a decreased drug

accumulation, the amino acid transporters were screened for mutations. Indeed the *amino acid transporter 6* gene (*TbAAT6*) was found to be heterozygously deleted [48]. Subsequent reverse genetic experiments confirmed the involvement of *TbAAT6* in drug resistance and thus its key role in elfornithine uptake [48–50]. Treatment failures of eflornithine monotherapy were reported from the field, but these were not further investigated, therefore it is unknown whether drug resistance was involved and whether *TbAAT6* mutations play a role in the field [51]. The easy and fast selection for eflornithine resistance *in vitro* is alarming, but development of resistance in the field might be hindered through the combination of eflornithine with nifurtimox as used nowadays. In contrast to *T. b. gambiense*, the *T. b. rhodesiense* subspecies is innately less susceptible to eflornithine, which has been attributed to a faster turnover of ornithine decarboxylase in *T. b. rhodesiense* [52].

The nitroheterocyclic pro-drug nifurtimox probably enters *T. brucei* by passive diffusion through the plasma membrane as shown for the South American *Trypanosoma cruzi* [53]. Intracellularly, nifurtimox has to be activated in order to become cytotoxic. Cytotoxicity is probably mediated by free radicals and oxidative stress [54,55]. Studies on *in vitro* selected nifurtimox resistant *T. cruzi* showed a decrease of nifurtimox reducing activity and an abnormal karyotype with loss of a chromosome that contains a putative *type I nitroreductase* (*NTR*) [56]. Subsequent heterozygous and homozygous *NTR* deletion in *T. cruzi* and *T. brucei* [56] as well as RNAi library screens [49] confirmed the involvement of NTR in nifurtimox resistance. This is the only known resistance mechanism in trypanosomes that is conferred by a lack of intracellular drug activation.

1.1.4. Suramin and suramin resistance

Suramin is a highly anionic polysulphonated naphthylurea that inhibits different intracellular targets in trypanosomes [57] and whose mode of action is not well understood (Chapter 2). Given the large size of the molecule (compared to other drugs) and its 6-fold negative charge, suramin is likely taken up through receptor-mediated endocytosis [58,59]. The presence of different plasma proteins has a major impact on suramin uptake by trypanosomes as suramin shows very high levels of plasma-protein binding [59]. Suramin resistant trypanosomes have not been described in human patients, but suramin resistance is widely spread in animal pathogenic trypanosomes [60,61]. In a genome-wide RNAi screen, knock-down of the invariant surface glycoprotein 75 (*TbISG75*) and of a number of

lysosomal and endosomal genes was found to confer suramin resistance, substantiating the proposed uptake route through endocytosis [42]. Knock-down of *TbISG75* further led to a decreased suramin binding, therefore TbISG75 was proposed to act as the suramin receptor in *T. brucei* [42].

1.1.5. Resistance mechanisms in T. brucei - a matter of drug uptake?

It is striking that most identified drug resistance mechanisms in *T. brucei* affect drug uptake (Fig 3). In case of melarsoprol and eflornithine, the genes involved in resistance encode transporters that directly carry out drug uptake (TbAAT6, TbAT1 and TbAQP2). For pentamidine, the role of TbAQP2 is not completely understood and it was proposed to be a receptor rather than a channel, while the uptake might be mediated through endocytosis [46]. However, it is somewhat surprising that genome-wide RNAi screens for pentamidine resistance did not identify genes encoding for endosomal proteins as observed for suramin [42]. Suramin first binds to its receptor and is subsequently taken up through endocytosis, whereby it passes through the endosomal system until it reaches the lysosome. Thus, a large number of different proteins are involved in uptake and intracellular drug transport, which is reflected in the high number of hits detected in the genome-wide RNAi-library screen [42]. Nifurtimox is the only drug for which a resistance mechanism distinct from drug uptake has been identified. Do these results reflect a biological feature of *T. brucei*? Do trypanosomes acquire resistance mainly through reduction of drug uptake or are these findings one-sided due to the applied methodologies?

We cannot answer these questions at the moment. But the applied methodologies are indeed predisposed to identify resistance mechanisms involving drug uptake. The older studies on drug resistance were usually carried out by selective investigation of candidate genes in drug selected resistant parasites. As the mode of action of most of the trypanocidal drugs are not well understood, the investigators have focused on transporter genes. The more recent studies usually used RNAi knock-down to generate resistance. As shown in Figure 2, downregulation of genes, and thus loss-of-function, predominantely leads to resistance if the protein encoded by the downregulated gene is involved in drug uptake or drug activation. For genes that encode proteins involved in drug efflux, drug inactivation, or the drug target itself, downregulation will usually not lead to resistance but instead sensitize the parasites. These genes could be identified through overexpression libraries or by whole genome or mRNA sequencing of resistant parasites rather than with RNAi. Furthermore,

one should keep in mind that not only the genes encoding proteins directly in contact with the drug can be modified, but their whole regulatory network can cause resistance. Loss or downregulation of certain repressors of drug target synthesis could for example lead to higher expression of the drug target and hence drug resistance. These regulators could very well be identified also by RNAi, and indeed such a mechanism wa s already described for suramin: Knock-down of de-ubiquitinating enzymes led to suramin resistance through a decrease of ISG75 abundance; thus suramin resistance was a secondary effect of the altered turnover of ISG75 [42,62]. In Figure 3 the described resistance mechanisms of *T. brucei* are summarized graphically.

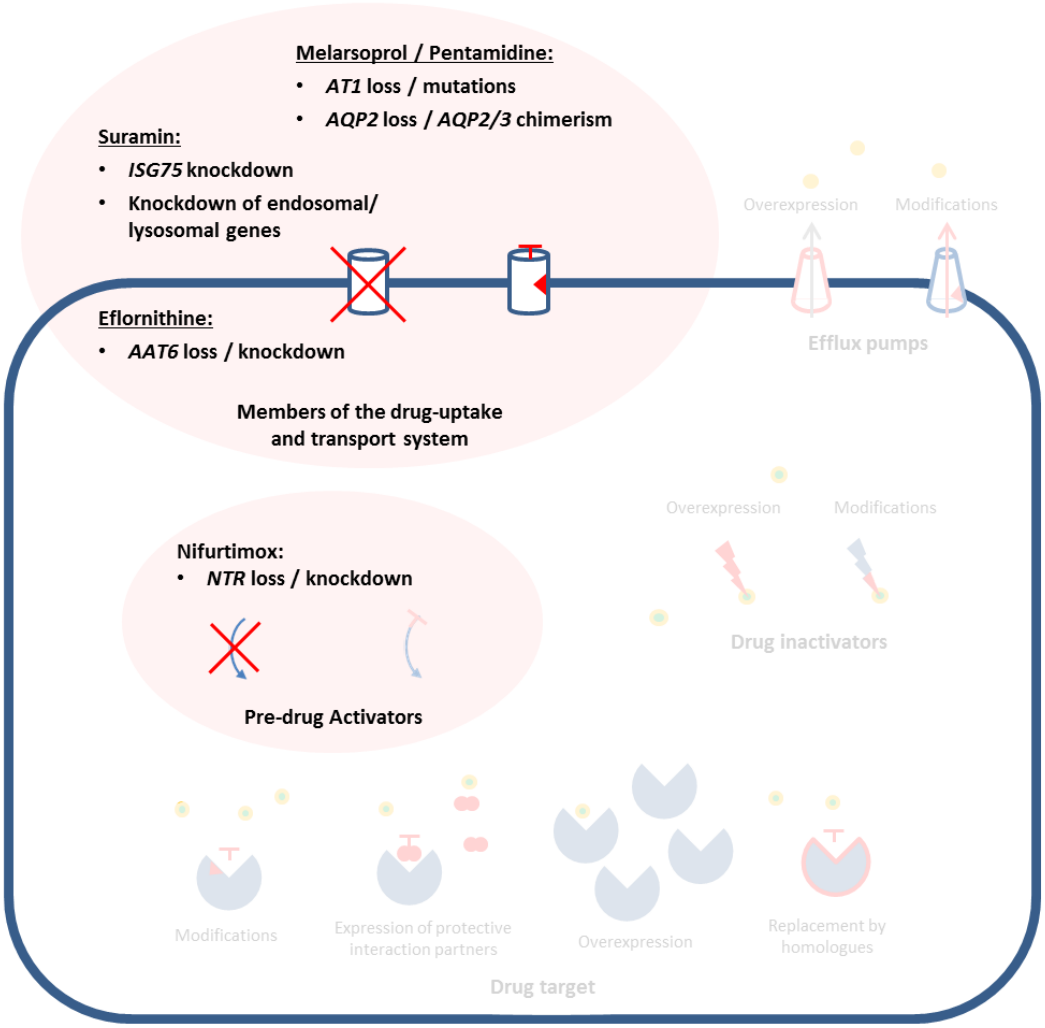

Figure 3: Mechanisms of drug resistance in *T. brucei*.

T. brucei can become resistant to melarsoprol, pentamidine, suramin or eflornithine through alterations of the uptake systems, notably through reduced expression, gene loss or mutations of the involved receptors and transporters. Nifurtimox resistance in *T. brucei* is acquired through loss or knock-down of the drug-activator nitroreductase. The other resistance mechanisms known from bacteria and other organisms, such as an increased drug efflux, enzymatic drug inactivation or alterations of the drug targets, have not been identified in *T. brucei*. The finding that drug resistance in *T. brucei* is predominantly caused by loss-of-function is all the more suprising since the trypanosomes, in contrast to bacteria or malaria parasites, are diploid.

1.2. Objectives

The presented PhD thesis investigated drug resistance with a focus on suramin, aiming to better understand this elusive molecule, its uptake and mode of action in *T. brucei*.

The work begins with a literature review about suramin, its broad clinical assessment for different diseases, and its potential biochemical targets (Chapter 2).

The thesis continues with the experimental investigation of suramin resistance in *T. brucei*. Starting with forward genetics of resistant parasites (Chapter 3), the results obtained by bioinformatics and molecular biology were corroborated by reverse genetic experiments, establishing a new link between suramin resistance and antigenic variation (Chapter 3 and 4).

Further, cell biological consequences of suramin resistance were examined with a special focus on ISG75 and receptor-mediated endocytosis, opening up new questions about the basic cell biology of trypanosomes (Chapter 4).

In the last chapter, high-level suramin-resistant parasites were generated and characterized by mRNA sequencing with the goal to find additional resistance mechanisms. This finally identified a potential drug target for suramin in African trypanosomes (Chapter 5).

2. One Hundred Years of Suramin

Natalie Wiedemar[1,2], Dennis A. Hauser[1,2] and Pascal Mäser[1,2]

[1] Swiss Tropical and Public Health Institute, Socinstrasse 57, 4051 Basel, Switzerland

[2] University of Basel, Petersplatz 1, 4001 Basel, Switzerland

Under Review

2.1. Abstract

Suramin is a hundred years old and still being used to treat the first stage of acute human sleeping sickness, caused by *Trypanosoma brucei rhodesiense*. Suramin is a multifunctional molecule with a wide array of potential applications, from parasitic and viral diseases to cancer, snakebite and autism. Suramin is also an enigmatic molecule: What are its targets? And how does it get into cells in the first place? Here we provide an overview on the many different candidate targets of suramin, discuss modes of action, and routes of cellular uptake. We reason that once the polypharmacology of suramin is understood at the molecular level, new, more specific, and less toxic molecules can be identified for the numerous potential applications of suramin.

2.2 A versatile molecule

2.2.1. Suramin, the fruit of the first medicinal chemistry program

When suramin was introduced for the treatment of African sleeping sickness in 1922, it was one of the first anti-infective agents that had been developed in a medicinal chemistry program. Starting from the antitrypanosomal activity of the dye trypan blue, synthesized in 1904 by Paul Ehrlich, Bayer made a series of colorless and more potent derivatives. Molecule 205 was suramin (Figure 1), synthesized by Oskar Dressel, Richard Kothe and Bernhard Heymann in 1916. Sleeping sickness (also known as human African trypanosomiasis, HAT) was at the forefront of research at that time, not a neglected disease as it is today, and the development of suramin was a breakthrough for the emerging field of chemotherapy. While the history of suramin has been reviewed elsewhere [21], we focus here on the many potential applications of suramin and its enigmatic mode of action.

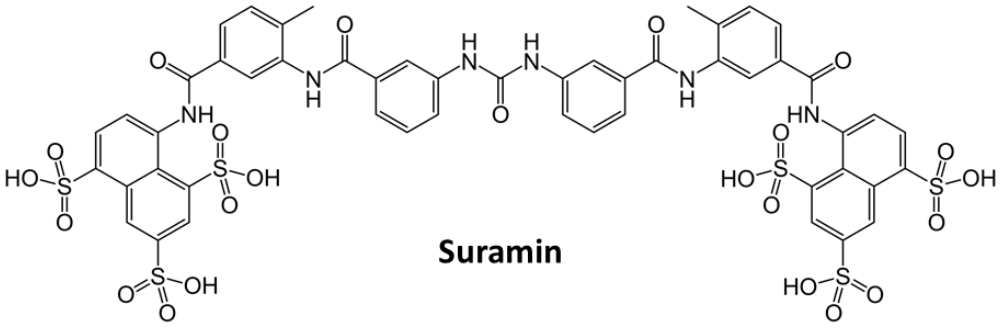

Suramin

Molecular weight	1297 Da
H-bond donors	12
H-bond acceptors	23
logP	0.00023
Protein binding	99.7%
Metabolites	none
Biological half-life	44-54 days
Metabolites	none
Elimination pathway	urinary

Figure 1. Suramin structure and medicinal chemistry parameters.

Except for its good solubility in water, suramin lacks lead-like properties as defined/stipulated by Lipinsky's rule of 5.

2.2.2. Suramin as an antiparasitic drug

Suramin is still being used for the treatment of *Trypanosoma brucei rhodesiense* infections [63]. However, it does not cross the blood-brain barrier and therefore is administered only for the first, hemolymphatic stage of sleeping sickness, when the trypanosomes have not yet invaded the patient's CNS. The standard treatment regimen for suramin is an initial test dose of 4-5 mg/kg followed by five weekly doses of 20 mg/kg (but not more than 1 g) injected i.v. [64]. Suramin is also used for Surra (mal de caderas), caused by *T. evansi*, in particular for the treatment of camels [65]. The treatment regimen is a single injection i.v. of 10 mg/kg suramin, i.e. about 6-10 g [65]. *In vitro*, suramin also has some activity against *T. cruzi* [66]. However, it is not used for Chagas' disease, and studies in mice even suggested that suramin would exacerbate the disease [67]. *In vitro* activity of suramin against *Leishmania major* and *L. donovani* has recently been described [68]. Furthermore, suramin blocks host cell invasion by the malaria parasite *Plasmodium falciparum*. This was observed for both the invasion of erythrocytes by *P. falciparum* merozoites [69] and the invasion of HepG2 hepatoma cells by *P. falciparum* sporozoites [70].

Suramin had been in use for river blindness, caused by the filarial parasite *Onchocerca volvulus* [71]. It acts on both microfilariae and, to a larger extent, on adult worms [72,73]. However, suramin was subsequently replaced by the less toxic, and orally bioavailable, ivermectin [74,75]. The adverse effects of suramin are indeed manifold, including nephrotoxicity, hypersensitivity reactions, dermatitis, anemia, peripheral neuropathy and bone marrow toxicity [64,76]. But despite its potential toxicity, the lack of bioavailability, and absence of lead-like properties (Figure 1), suramin has found a surprising variety of repurposing applications. Table 1 provides an overview on the biological activities of suramin and Table 2 lists clinical trials performed with suramin.

2.2.3. Suramin as an antiviral agent

The antiviral and antibacteriophage activities of suramin are known since the mid-20th century [77,78]. Soon after the discovery of retroviruses, suramin was found to inhibit retroviral reverse transcriptase [79], which served as a rationale to test suramin against human immunodeficiency virus (HIV). Suramin protected T-cells from HIV infection *in vitro* [80], and in AIDS patients it reduced the viral burden in some of the study subjects; however, no improvement of the immunological features and clinical symptoms was achieved [81–83]. Later-on suramin was found to inhibit host cell attachment through

binding to the HIV-1 envelope glycoprotein gp120, indicating that the *in vitro* protection against HIV infection is mediated through inhibition of viral entry [84].

Suramin also inhibits the binding of Dengue virus to host cells through a direct effect on the viral envelope protein [85]. Inhibition of host cell attachment was also found for Herpes simplex [86] and Hepatitis C viruses [87], which explained the previously reported protective effects of suramin against *in vitro* herpes simplex infections [88] and *in vivo* infections of ducks with Duck Hepatitis B Virus [89]. Similar to the experience with HIV, suramin had initially been tested against Hepatitis viruses due to its inhibitory effect on the viral DNA polymerase [90,91]. But in a small clinical trial suramin was found to be ineffective and toxic in chronic active Hepatitis B patients [92]. Suramin neutralized enterovirus 71 (EV71) in cell culture and in a mouse model by binding to capsid proteins [93–95].

Suramin also bears potential against emerging viruses. It was shown to inhibit both RNA synthesis and replication in Chikungunya virus [96]. *In vitro* suramin conferred protection if present at the time of infection, and this was attributed to a reduction of viral host cell binding and uptake [97]. In the murine model suramin led to a reduction of pathognomonic lesions if injected prior to Chikungunya infection [98]. Suramin also inhibited host cell invasion by Ebola virus [99] and Zika virus, even when added after viral exposure of the cell cultures [100].

2.2.4. Suramin against cancer

The first studies on the effects of suramin on neoplasms in animals were carried out in the 1940's; mice engrafted with lymphosarcoma developed significantly smaller tumors when simultaneously treated with suramin [101]. In the 1970's it was shown that suramin can enhance the action of cyclophosphamide and adriamycin in mice engrafted with Ehrlich carcinoma [102]. A first clinical trial with suramin was carried out in the 1980's in advanced-stage adrenal and renal cancer patients [103]. Around half of the patients showed either partial or minimal responses, none showed complete remission. Nevertheless, a number of subsequent clinical trials with suramin were carried out (Table 2). In particular, suramin was tested against prostate cancer [104–112], non-small cell lung cancer [113], breast cancer [113], bladder cancer [114,115] and brain tumors [116,117]. Most of these studies were based on the potential of suramin to act as an antagonist of growth factors

[118–120], which are often overexpressed by tumors. In addition, suramin directly exhibits cytostatic activity on cultured tumor cells [121–123]. However, the initial clinical tests did not warrant the further development of suramin as an anticancer monotherapy.

Subsequent tests focused on suramin as a chemosensitizer, based on the findings that at sub-cytotoxic levels (<50 µM), it enhanced the efficacy of anticancer drugs such as mitomycin C, taxol or doxorubicin in *ex vivo* cultures and in animal models [124–126]. Suramin combined with taxol inhibited invasiveness and prevented metastasis in a xenograft mouse model [127]. Different explanations are conceivable for the chemosensitizing effects of suramin on tumor cells, including inhibition of telomerase [128] or inhibition of fibroblast growth factors and angiogenesis [129]. A phase II clinical study was performed in patients with advanced, drug-resistant, non-small cell lung cancer treated with taxol or carboplatin; supplementation with nontoxic doses of suramin did not overcome drug resistance [130]. Randomized controlled studies to validate the use of suramin as a chemosensitizer in chemotherapy-naive lung cancer patients remain to be performed. A combination of estramustine, docetaxel and suramin gave promising results in hormone-refractory prostate cancer patients [112].

2.2.5. Suramin as an antidote

Three of the many biological activities of suramin support a potential use as a protective agent: the inhibition of thrombin, the inhibition of phospholipase A2, and the inhibition of purinergic signaling. Several vipers possess toxins that mimic thrombin [131], perfidiously triggering the coagulation cascade in the mammalian blood. Suramin not only inhibits thrombin itself [132] but also the thrombin-like proteases of snake venom [133], and was therefore proposed as an antidote for snakebite. Other common constituents of metazoan venoms are phospholipases A2 that convert phospholipids into lysophospholipids. Again, suramin inhibits mammalian phospholipase A2 [134] as well as the orthologs from snake venom [135–137] and bee venom [138], suggesting that it can act as an antidote. A certain degree of protection from venoms by suramin was confirmed in mouse models [138–140]. The potential use of suramin as an antidote is attractive given the high global burden of snakebites [141] and the current shortage of antivenom [142].

Suramin's ability to block P2 purinergic, G protein-coupled receptors [143] may counteract the action of neurotoxins that trigger arachidonic acid signaling, e.g. via

phospholipase A2 activity [144]. A possible explanation is that suramin prevents the activation of ATP receptors at the motor nerve ending, which otherwise would depress Ca^{2+} currents and reduce acetylcholine release at the presynaptic membrane [145]. Suramin was also proposed to serve as a neuroprotective agent [146,147], as an antidote for kidney toxicity during cancer chemotherapy [148] and, based on its antiapoptotic effect, to protect from liver failure [149]. Suramin also inhibits connexin channels of the tight junction, thereby suppressing ATP release and protecting cells from pore-forming bacterial toxins such as hemolysin [150]. The suramin analogs NF340 and NF546 were cardioprotective in a mouse model for heart graft rejection, presumably via inhibition of the purinergic G protein-coupled receptor P2Y11 [151].

2.2.6. Further potential uses of suramin

Suramin was found to have beneficial effects in a rat arthritis model [152] and to suppress fear responses in the rat [153]. It also promoted the expansion of T cells during immunization of mice and was therefore considered as a small molecule adjuvant for vaccination [154]. Based on the cell danger hypothesis, suramin has recently been tested for the treatment of autism spectrum disorders (ASD). The cell danger hypothesis suggests that a systemic stress response, which involves mitochondria and purinergic signaling, contributes to the development of psychopathologies like autism. Suramin had been shown to act as an inhibitor of purinergic signaling [155] and mitochondrial function [156], and was therefore proposed as a potential therapy for ASD [157]. First tests in mouse models showed correction of symptoms in juveniles [157] as well as in adults [158]. A first small human trial was carried out and, even though difficult to quantify, showed improvement of ASD symptoms [159].

Table 1. Diseases and pathogens susceptible to suramin.

Disease, pathogen	Activity in cell culture	Activity in animal model	Activity in patient
Parasitic infections			
T. b. rhodesiense HAT	x	x	x
T. b. gambiense HAT	x	x	x
Surra, *T. evansi*	x	x	n.a.
River blindness, *O. volvulus*	x	x	x
Trypanosoma cruzi	x		
Leishmania spp.	x		
Plasmodium falciparum	x		
Viral infections			
Hepatitis	x	x	x
AIDS, HIV	x		x
Herpes simplex	x	x	
Chikungunya	x	x	
Enterovirus 71	x	x	
Dengue	x		
Zika	x		
Ebola	x		
Neoplastic diseases			
Non-small cell lung cancer	x	x	
Breast cancer	x	x	
Bladder cancer	x	x	
Brain tumors	x	x	
Prostate cancer	x	x	x
Other uses			
Snake bite	x	x	
Arthritis	x	x	
Autism	n.a.	x	x

Table 2. Clinical trials with suramin. Trials with a registered NCT number are from ClinicalTrials.gov; others are from the literature.

Registry ID	Disease	Phase	Year
NCT02508259	Autism spectrum disorders	I, II	2015
NCT01671332	Non-small cell lung cancer	II	2012
NCT01038752	Non-small cell lung cancer	II	2010
NCT00083109	Recurrent renal cell carcinoma	I, II	2004
NCT00066768	Recurrent non-small cell lung cancer	I	2003
NCT00054028	Recurrent breast cancer	I, II	2002
NCT00006929	Recurrent non-small cell lung cancer	II	2000
NCT00006476	Bladder cancer	I	2000
NCT00004073	Brain and central nervous system tumors	II	1999
NCT00002921	Adrenocortical carcinoma	II	1997
NCT00003038	Advanced solid tumors	I	1997
NCT00002723	Prostate cancer	III	1996
NCT00002881	Prostate cancer	III	1996
NCT00002652	Multiple myeloma and plasma cell neoplasm	II	1995
NCT00002639	Brain and central nervous system tumors	II	1995
NCT00001381	Bladder neoplasms, transitional cell carcinoma	I	1994
NCT00001266	Prostatic neoplasm	II	1990
NCT00001230	Filariasis	observ.	1988
[103]	Solid tumors	observ.	1987
[82]	AIDS	observ.	1987
[92]	Hepatitis B	observ.	1987

2.2.7. (Too) many targets

Suramin is a large molecule that carries six negative charges at physiological pH (Figure 1). It is likely to bind to, and thereby inhibit, various proteins [160]. Thus the many and diverse potential applications of suramin reflect the polypharmacology of suramin. Indeed, a large number of enzymes have been shown to be inhibited by suramin (Table 3). Suramin inhibits many glycolytic enzymes [161,162], enzymes involved in galactose catabolism (PubChem

BioAssay: 493189) and enzymes of the Krebs cycle [163]. Suramin further decreases the activity of a large number of enzymes involved in DNA and RNA synthesis and modification: DNA polymerases [164,165], RNA polymerases [164,166,167], reverse transcriptase [79,164], telomerase [128], and enzymes involved in winding/unwinding of DNA [168,169] are inhibited by suramin, as well as histone- and chromatin modifying enzymes like chromobox proteins [170], methyltransferases [171] and sirtuin histone deacetylases [172]. Suramin is also an inhibitor of other sirtuins [173] and protein kinases [174,175], glutaminase (PubChem BioAssay: 624170), phospholipase A2 [176,177], protein tyrosine phosphatases [178], lysozyme [179] and different serine- and cysteine-proteases [180–182]. For caspases, cysteine proteases involved in apoptosis, suramin was described to act as either inhibitor or activator [183,184]. Suramin further inhibits the Na^+,K^+-ATPase and other ATPases [185–187], certain classes of GABA receptors [188,189], and several G protein-coupled receptors [190] including P2 purinoceptors and follicle-stimulating hormone receptor [191,192]. Suramin also showed inhibitory effects against components of the coagulation cascade [132,193] and the complement system [194–196], and against deubiquitinating enzymes (PubChem BioAssay: 504865; 463106). It also interacts with prion protein, inhibiting the conversion into the pathogenic form PrP^{Sc} [197]. Beside the many inhibitory activities, suramin also activates certain nuclear receptors that act as transcription factors [198], and intracellular calcium channels [199].

Table 3. Putative target proteins of suramin, biological processes and mechanisms. Suramin acts as an inhibitor or antagonist in all cases except for the pregnane X receptor and the ryanodine receptor. The mode of action against caspase is controversial.

Putative target	Reference
Metabolism	
6-Phosphofructokinase	[161]
Fructose-l,6-bisphosphate aldolase	[161]
Glucose-6-phosphate isomerase	[161]
Glyceraldehyde-3-phosphate dehydrogenase	[161]
Glycerol-3-phosphate dehydrogenase	[161,200]
Glycerol kinase	[161]
Hexokinase	[161]
Phosphoglycerate kinase	[161]
Pyruvate kinase	[162]
Triose-phosphate isomerase	[161]
Succinic dehydrogenase	[163]
Galactokinase	493189*
Glutaminase	624170*
Glycerophosphate oxidase	[200]
Nucleoside triphosphate diphosphohydrolase 1 & 2	[186,187,201–204]
Nucleotide pyrophosphatase/phosphodiesterase 1 & 3	[205]
Nucleic acids	
DNA polymerase alpha	[164,165]
DNA polymerase beta	[164,165]
DNA polymerase gamma	[164]
DNA polymerase delta	[165]
DNA polymerase I	[164,165]
Terminal deoxynucleotidyltransferase	[164]
DNA primase	[164]
DNA dependent RNA polymerase	[164,167]
RNA dependent RNA polymerase	[166]
Reverse transcriptase	[79,164]
Telomerase	[128]
RNAse H	[206]
Flavivirus RNA helicase	[100,168,207]
DNA Topoisomerase II	[169]
Tyrosyl-DNA phosphodiesterase 1	[208]
Human antigen R	[209]
DNA-binding protein MCM10	[210]
Epigenetics	
Chromobox protein homologue 1 beta	488953*
Chromobox protein homologue 7	[170]
Histone methyltransferases	[171,211]
Precorrin-4 C(11)-methyltransferase	[212]

Sirtuin 1, 2, 5	[172,173,213]
Protease	
Kallikrein	[182]
Alpha Thrombin	[132]
Human neutrohphil cathepsing G	[181]
Human neutrophil elastase	[181]
Human neutrophil proteinase 3	[181]
Rhodesain	[180]
Caspases 1, 2, 8, 9, 10	[183,184,214,215]
Falcipain-2	[216]
Extracellular matrix	
Hyaluronidase	[217,218]
Iduronate sulfatase	[218]
β-glucuronidase	[218]
Membrane channels and signaling	
Non-junctional connexin 43 hemichannels	[150]
Na^+,K^+-ATPase	[185]
Cystic fibrosis transmembrane regulator	[219]
Ryanodine receptor 1	[199]
$GABA_A$ receptors	[188,189]
P2X Purinergic receptors	[155]
P2Y Purinergic receptors	[155]
N-methyl-D-aspartate receptor	[220]
DNA-dependent protein kinase	[174]
Protein kinase C	[175]
Protein tyrosine phosphatases	[178]
VIP receptor	[190]
Follicle-stimulating hormone receptor	[192]
Pregnane X receptor	[198]
Diadenosine tetraphosphate hydrolase	[221]
Other	
Prion (Prp^C)	[197]
Complement factors	[182,194–196]
Phospholipase A_2	[177,222]
Lysozyme	[179]
Antimicrobial Peptide CM15	[223]
Ubiquitin carboxyl-terminal hydrolases 1 & 2	504865; 463106*
HSP 60 chaperonin system	[224,225]
GroEL chaperonin system	[224,225]

*PubChem BioAssay, last retrieved 29.04.2019

2.2.8. Enigmatic mechanisms of action against African trypanosomes

Somewhat ironically, much less appears to be known about the targets of suramin in African trypanosomes, where it has been in use for a century, than in tumor cells or viruses. Suramin was shown to inhibit glycolytic enzymes of *T. brucei* with selectivity over their mammalian orthologues, in particular hexokinase, aldolase, phosphoglycerate kinase and glycerol-3-phosphate dehydrogenase [161]. Intriguingly, the trypanosomal enzymes have higher isoelectric points (>9), which is due to extra arginines and lysines that are absent in the mammalian orthologues [226]. These residues form positively charged, surface exposed 'hot spots' that were proposed to be bound by the negatively charged suramin [161]. Inhibition of trypanosomal glycolysis by suramin is in agreement with the dose-dependent inhibition of oxygen consumption and ATP production observed in trypanosomes isolated from suramin-treated rats [58]. However, the glycolytic enzymes of *T. brucei* are localized inside glycosomes [227], and it is unclear how suramin could penetrate the glycosomal membrane, or if suramin could bind to glycolytic enzymes in the cytosol, before they are imported into the glycosomes [57]. Alternative targets proposed for the trypanocidal effect of suramin are glycerophosphate oxidase [200,228], a serine oligopeptidase termed OP-Tb [229], and REL1 [230], the RNA-editing ligase of the trypanosome's kinetoplast. It is unclear how suramin would pass the inner mitochondrial membrane, but suramin inhibited oxidative phosphorylation in mitochondrial preparations of the trypanosomatid *Crithidia fasciculate* [231]. Suramin also appeared to inhibit cytokinesis in *T. brucei*, as indicated by the finding that suramin treatment resulted in an increased number of trypanosomes with two nuclei [232].

2.2.9. Uptake routes of suramin into cells

The negative charges of suramin (Figure 1) not only promote binding to various proteins, they also prevent diffusion across biological membranes. However, the majority of targets (Table 3) are intracellular, and radiolabeled suramin was shown to be taken up by human endothelial and carcinoma cells [233,234] and by *T. brucei* bloodstream forms [58,59]. Suramin is not a of P-glycoprotein substrate [235], nor of any other known transporter. Thus suramin must be imported by endocytosis. Mammalian cells can take up suramin in complex with serum albumin by receptor-mediated endocytosis [236]. This had originally also been thought to happen in *T. brucei* [58]. However, the trypanosomes do not take up albumin by receptor-mediated endocytosis [237], and LDL (low density lipoprotein) was

proposed to act as the vehicle instead [59]. Suramin bound to LDL and inhibited the binding and uptake of LDL, while LDL enhanced the uptake of suramin in bloodstream-form *T. brucei* [59]. In contrast, overexpression in procyclic *T. b. brucei* of Rab4, a small GTPase involved in the recycling of endosomes, decreased suramin binding and uptake without affecting LDL binding or uptake [238]. In the same study, overexpression of a mutant Rab5, which was locked in the active, GTP-bound form, increased LDL uptake without affecting suramin uptake [238]. These findings indicated that, at least in the procyclic trypanosomes of the tsetse fly midgut, LDL and suramin are imported independently of each other.

The development of genome-wide RNAi screens in bloodstream-form *T. brucei* combined with next-generation sequencing offered new opportunities to address the genetics of drug resistance. This approach identified genes, silencing of which reduced the sensitivity to suramin [42]. These included a number of genes encoding for endosomal and lysosomal proteins, in agreement with uptake of suramin through endocytosis. The invariant surface glycoprotein ISG75 was identified as a likely receptor of suramin since knock-down of ISG75 in bloodstream-form *T. brucei* decreased suramin binding and suramin susceptibility [42]. ISG75 is a surface protein of unknown function whose abundance is controlled by ubiquitination [62]. Thus, there appear to be (at least) two pathways for receptor-mediated endocytosis of suramin in *T. brucei* bloodstream forms: either directly with ISG75 as the receptor or, after binding of suramin to LDL, together with the LDL receptor.

Table 4. Solved structures of suramin complexed to target proteins.

PDB id	Protein	Reference
6CE2	Myotoxin I from *Bothrops moojeni*	[136]
4YV5	Myotoxin II from *Bothrops moojeni*	[135]
1Y4L	Myotoxin II from *Bothrops asper*	[177]
3BJW	Ecarpholin S from *Echis carinatus*	[137]
1RML	Acid fibroblast growth factor	[239]
n.a.	Human epidermal growth factor (hEGF)	[240]
4X3U	CBX7 chromodomain	[170]
3BF6, 2H9T	Human thrombin	[241]
2NYR	Human sirtuin homolog 5	[173]
3PP7	*Leishmania mexicana* pyruvate kinase	[162]
3GAN	*Arabidopsis thaliana* At3g22680	n.a.
3UR0	Murine norovirus RNA-dependent RNA polymerase	[166]
4J4V	Pentameric bunyavirus nucleocapsid protein	[242]
4J4R	Hexameric bunyavirus nucleocapsid protein	[242]

2.3. Conclusion

Suramin remains controversial. Is its polypharmacology a liability or an asset? Is it toxic or protective? Dated or timeless? Whatever the verdict on suramin, there is hardly a molecule with as many biological activities. The list of potential targets is indeed impressive, and the publication stream on suramin is not stagnating. The large majority of papers is not about trypanosomes or trypanosomiasis (Figure 2). The list of potential targets has to be taken with a grain of salt, though, since the negative charges of suramin, and its promiscuity in protein binding, can cause all kinds of artefacts. Suramin can dissolve matrigel [243], resulting in a false positive signal in cell-based screening campaigns that use matrigel for support, e.g. for inhibitors of angiogenesis [243]. On the other hand, suramin's high affinity to albumin [244] may give false negative results in cell-based tests that contain mammalian serum. But in spite of the various confounders, a number of different drug-target interactions for suramin have been experimentally validated, and are directly supported by crystal structures (Table 4).

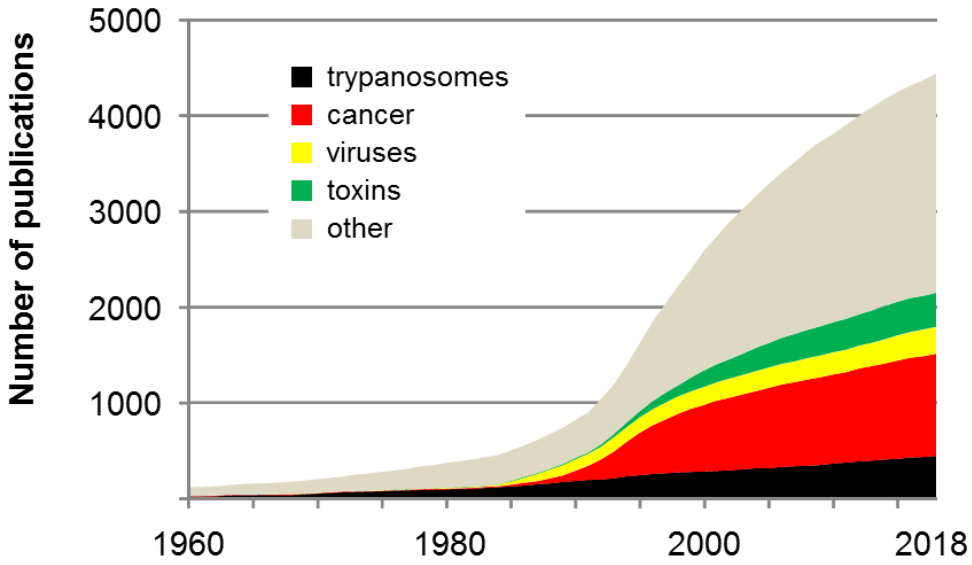

Figure 2. Publications on suramin in PubMed. Cumulative numbers are shown for papers on suramin and trypanosomes or trypanosomiasis (black, search term "trypanosom*"), cancer (red, "cancer OR tumor"), viruses (yellow, "virus OR viral OR hiv OR aids"), and toxins (green, "toxin OR venom"). Other papers on suramin are shown in beige. There is no saturation yet. And it is surprising that only a minority of the publications on suramin actually deal with trypanosomes.

Several routes of investigation on the bioactivities of suramin have culminated in clinical trials with healthy volunteers (i.e. phase I) or patients (i.e. phases II and III; Table 2). Yet, to our knowledge, none of these trials was a striking success, and it is unclear whether suramin will ever find medical applications outside the field of parasitology. However, molecules that act in a similar way than suramin may be identified via target-based screening once the mode of action is understood – new molecules that are more specific, less toxic, and possess better pharmacological properties than suramin. Thus it will be important to dissect the polypharmacology of suramin at the molecular level. We hope that the compiled list of targets (Table 3) will serve this purpose.

Acknowledgments

We are grateful to the Swiss National Science Foundation for financial support and to Prof. Alan Fairlamb for sharing insights into the possible molecular interactions of suramin.

3. Beyond immune escape: A variant surface glycoprotein causes suramin resistance in *Trypanosoma brucei*

Natalie Wiedemar[1,2], Fabrice E. Graf[1,2,+], Michaela Zwyer[1,2], Emiliana Ndomba[1,2,*], Christina Kunz Renggli[1,2], Monica Cal[1,2], Remo S. Schmidt[1,2], Tanja Wenzler[1,2,∘], Pascal Mäser[1,2]

[1] Swiss Tropical and Public Health Institute, CH-4002 Basel, Switzerland

[2] University of Basel, CH-4001 Basel, Switzerland

2018

Mol Microbiol. 107:57-67

I have performed all experiments and analysis, except for the microcalorimetry (Figure 1), which was carried out by Tanja Wenzler; the trypan blue assays (Figure 7) and the growth curves (Figure S2), which were performed by Michaela Zwyer under Remo Schmidts and my supervision.

3.1. Abstract

Suramin is one of the first drugs developed in a medicinal chemistry program (Bayer, 1916), and it is still the treatment of choice for the hemolymphatic stage of African sleeping sickness caused by *Trypanosoma brucei rhodesiense*. Cellular uptake of suramin occurs by endocytosis, and reverse genetic studies with *T. b. brucei* have linked downregulation of the endocytic pathway to suramin resistance. Here we show that forward selection for suramin resistance in *T. brucei* spp. cultures is fast, highly reproducible, and linked to antigenic variation. Bloodstream-form trypanosomes are covered by a dense coat of variant surface glycoprotein (VSG), which protects them from their mammalian hosts' immune defenses. Each *T. brucei* genome contains over 2000 different *VSG* genes, but only one is expressed at a time. An expression switch to one particular VSG, termed VSG^{Sur}, correlated with suramin resistance. Reintroduction of the originally expressed *VSG* gene in resistant *T. brucei* restored suramin susceptibility. This is the first report of a link between antigenic variation and drug resistance in African trypanosomes.

3.1.1. Abbreviated summary

Suramin is still in use to treat sleeping sickness caused by *Trypanosoma brucei rhodesiense*. Here we show that in culture, trypanosomes can quickly become suramin-resistant by expressing one particular variant surface glycoprotein (VSG) gene, and they revert to sensitive upon replacement of that VSG gene with the originally expressed VSG gene. This is the first reported link between antigenic variation and drug resistance in African trypanosomes.

3.2. Introduction

Sleeping sickness, also called human African trypanosomiasis (HAT), is still a prevalent disease in sub-saharan Africa. It is transmitted by the blood-feeding tsetse flies and caused by two subspecies of *Trypanosoma brucei*: *T. b. gambiense* causes the chronic form, *T. b. rhodesiense* the acute form of HAT. Untreated, both typically end with coma and death. Among the four currently available drug therapies, suramin is the oldest one and is used for the treatment of the first, hemolymphatic stage of *T. b. rhodesiense* HAT. Suramin is a big and highly charged molecule (Fig. S1) and therefore not able to passively diffuse through biological membranes. It is supposedly taken up by receptor-mediated endocytosis [58] with an involvement of low-densitiy lipoprotein [59]. More recent high-throughput RNAi-screens [42] have shown a variety of endosomal and lysosomal genes to render trypanosomes less susceptible to suramin when knocked-down, which is in agreement with an uptake via endocytosis. Furthermore, knock-down of the invariant surface glycoprotein ISG75 led to a 50% reduction of suramin susceptibility. ISG75 was therefore proposed to be the binding partner of suramin on the cell surface [42,245]. The mode of action of suramin has been elusive since it was shown to have diverse intracellular targets [57].

Despite its use for about a hundred years now, there have been no reports of suramin resistance in human pathogenic trypanosomes. The cure-rates of first stage *T. b. rhodesiense* HAT are typically high. Suramin treatment failures were mainly observed in context of a miss-staging of the disease [246], since suramin has a low brain permeability and is ineffective once the trypanosomes have crossed the blood-brain barrier. However, suramin resistance is prevalent among animal pathogenic trypanosomes, for example in *T. evansi* isolates from Sudanese camels [60] and Chinese buffaloes and mules [61]. Selection for suramin resistance is feasible under laboratory conditions. After 550 days of *in vitro* selection *T. evansi* were 1800-fold less susceptible to suramin [247], and *T. brucei* showed a resistance factor of 20-140 after *in vivo* selection with subcurative doses [248]. The suramin resistance phenotype was lost after transformation of the trypanosomes to insect-stage, procyclic forms.

We have observed the appearance of strong drug resistance in *T. brucei* bloodstream forms after exposure to high suramin concentrations for only a few days. Here we use

transcriptomics and reverse genetics to elucidate the genetic mechanism behind this phenomenon.

3.3. Results

3.3.1. *In vitro* selection for suramin resistance monitored in real-time

Isothermal microcalorimetry allows to monitor the growth of axenic *T. brucei* cultures in real-time based on the heat emitted by the cells' metabolism [249]. Here we use the technology to track the emergence of drug resistance. Incubated at presumably lethal concentrations of suramin, i.e. the 5-fold and 25-fold of the IC_{50}, *T. b. rhodesiense* bloodstream-form cultures appeared to be dead after two days, started to regrow after three, and had fully recovered by day five (Fig. 1). This phenomenon was consistently observed: we have performed the same experiment with *T. b. brucei*, which also recovered from suramin pressure within one week. In all cases, the recovered trypanosomes were suramin-resistant by factors between 30 and 100 as compared to the starting population. No such phenomenon was observed with other drugs: melarsoprol or pentamidine completely killed the *T. brucei* cultures at concentrations of 5- and 25-fold their IC_{50} [249] (Fig. 1).

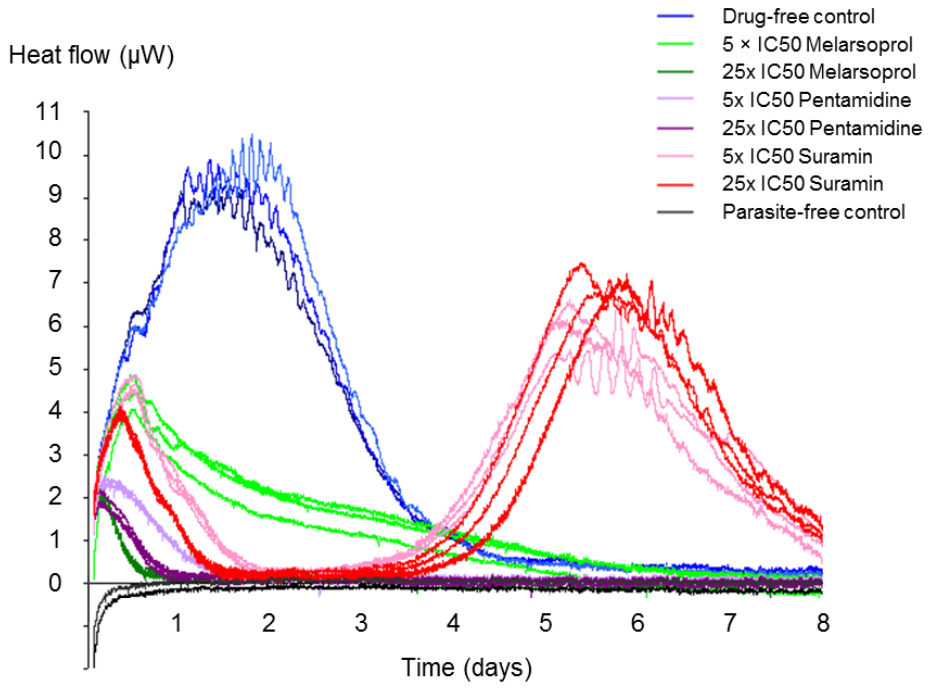

Figure 1. Bloodstream-form *T. brucei* incubated with presumably lethal concentrations of suramin rapidly became resistant and regrew. No such phenomenon was observed with the drugs melarsoprol or pentamidine.

3.3.2. Rapid emergence of resistance also in clonal populations

The microcalorimetric experiment was performed with an inoculum of 10^5 cells. To rule out that a subpopulation of suramin-resistant trypanosomes had been present all along and was simply selected for under drug pressure, we repeated the experiment with fresh *T. b. rhodesiense* STIB900 clones. Incubated at concentrations between 500 and 1700 nM suramin (i.e. 5-80 fold their respective IC_{50}), drug-resistant progeny was again obtained within one week for all tested clones [n=11]. Table 1 summarizes the results for one clone (named *T. b. rhodesiense* STIB900_c1) and four independent suramin-resistant derivatives thereof (named *T. b. rhodesiense* STIB900_c1_sur1 to _sur4), selected at 1050 nM suramin (80-fold the IC_{50}). All four derivatives were at least 90-fold resistant to suramin as compared to the parent clone STIB900_c1 ($p < 0.0001$ by One Way Anova with Tukey's multiple comparisons test). While their sensitivity to melarsoprol and pentamidine was unchanged (Table 1), the suramin-resistant lines were cross-resistant to the structurally related trypanocidal dye trypan blue ($p<0.001$, Ehrlich, 1904; Fig. S1).

Table 1. Drug sensitivities of the parental clone *T. b. rhodesiense* STIB900_c1 and four independently selected derivatives (sur1-4). Values are 50% inhibitory concentrations in nM ± standard deviation (n≥5).

	Suramin	**Trypan Blue**	**Melarsoprol**	**Pentamidine**
STIB900_c1	13 ±4	2,700 ±900	22 ±1.2	1.1 ±0.4
STIB900_c1_sur1	1,250 ±40	16,200 ±5,600	23 ±2.3	1.0 ±0.3
STIB900_c1_sur2	1,240 ±10	16,300 ±5,300	24 ±1.9	1.5 ±1.1
STIB900_c1_sur3	1,240 ±90	16,300 ±5,200	24 ±2.2	1.2 ±0.5
STIB900_c1_sur4	1,270 ±100	16,600 ±5,700	26 ±3.3	1.5 ±1.2

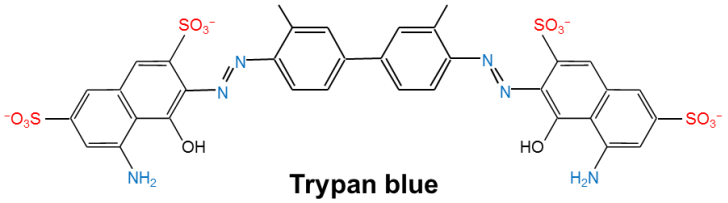

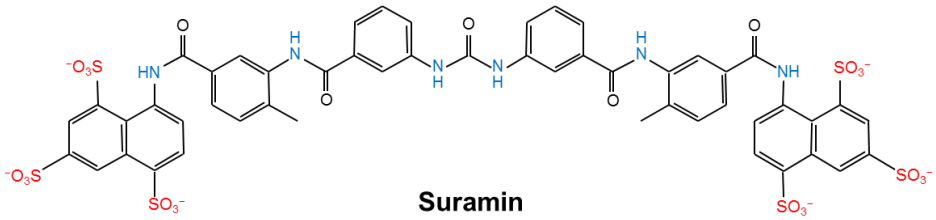

Figure S1. Suramin (Bayer & Co, 1916) is a colorless derivative of the azo-dye trypan blue (Ehrlich, 1904).

The cross-resistance phenotype was stable in the absence of drug pressure for several weeks. After 80 days of cultivation, however, the resistance factor had decreased to 10- to 50-fold in the four lines (Fig. 2). Cumulative growth curves (Fig. S2) demonstrate slightly longer population doubling times of the resistant derivatives (8.2 h for STIB900_c1_sur1 and 8.3 h for STIB900_c1_sur4) as compared to the suramin sensitive parent clone (7.7 h).

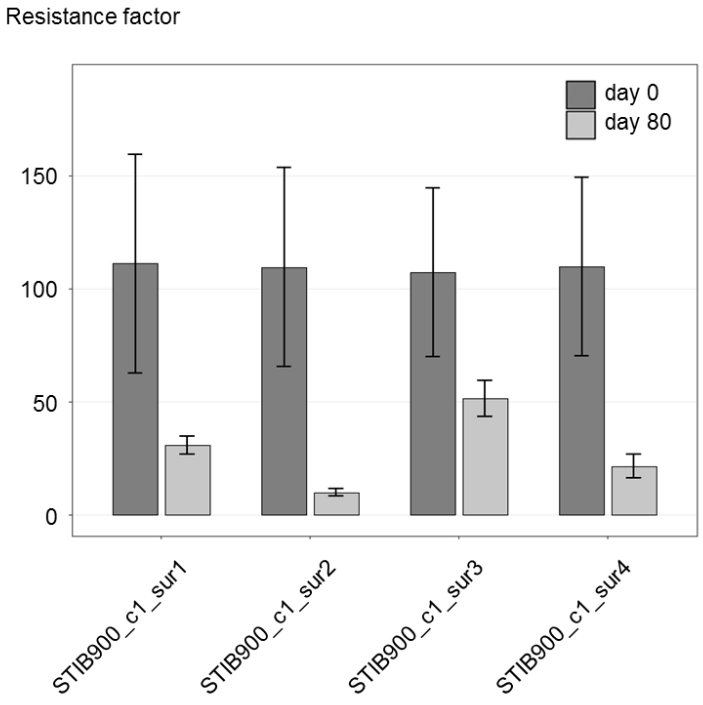

Figure 2. Stability of suramin resistance in the absence of selection. The resistance factor was defined as the IC_{50} of the derivatives of *T. b. rhodesiense* STIB900_c1 divided by the IC_{50} of *T. b. rhodesiense* STIB900_c1 itself, grown in parallel.

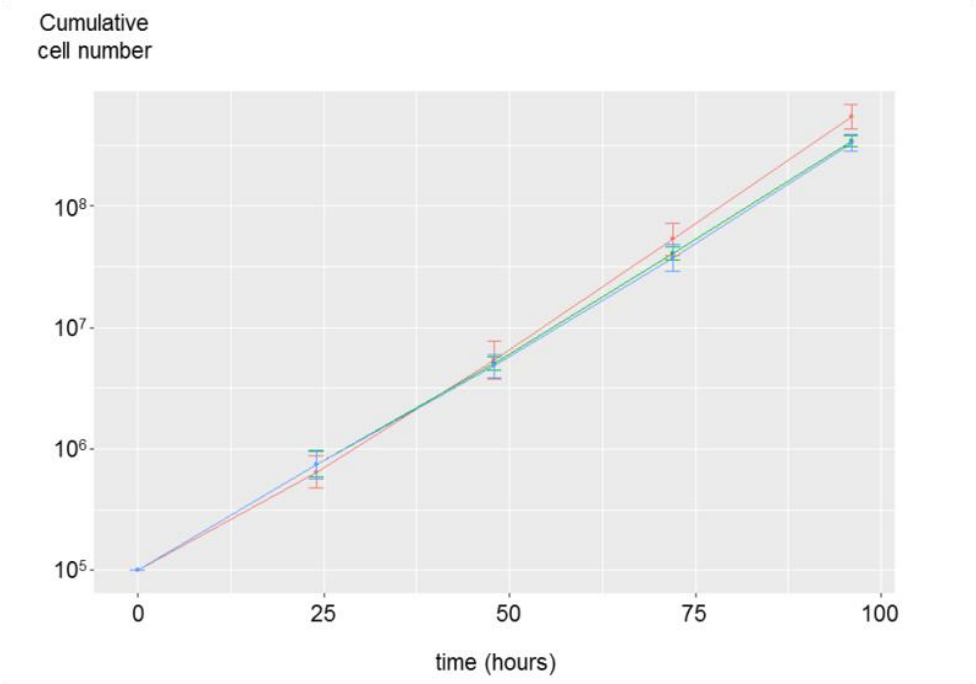

Figure S2. Cumulative growth curves of suramin sensitive and resistant parasites.
Growth rates are displayed as cumulative cell number of STIB900_c1 (red), STIB900_c1_sur1 (green) and STIB900_c1_sur4 (blue), error bars represent the standard deviation. Cumulative cell counts were significantly different between resistant and sensitive parasites after four days (p-value = 0.00042 for STIB900_c1 versus STIB900_c1_sur1 and p-value = 0.00042 for STIB900_c1 versus STIB900_c1_sur4, n=6).

3.3.3. *VSG*s are differentially expressed in resistant and sensitive parasites

The finding that suramin resistance reproducibly developed even in cultures from freshly cloned trypanosomes, indicated that the underlying mutation – whatever its nature – had occurred during the selection period. However, the reproducible acquisition of a particular point mutation is unlikely to happen within days. We therefore reckoned the mechanism of suramin resistance more likely to be reflected at the level of gene expression than gene sequence. Total RNA from *T. b. rhodesiense* STIB900_c1 and the four selected lines, grown in the absence of suramin, was subjected to quantitative transcriptomics by mRNA-Seq. Over 50 million high-quality reads were obtained for each line (European Nucleotide Archive accession PRJEB20650). As expected given the short interval between suramin-sensitive parent and suramin-resistant derivatives, there were hardly any differences in transcript abundance (Fig. S3). Genes encoding proteins that had been shown to be involved in suramin resistance in *T. brucei* [42], i.e. the invariant surface glycoprotein ISG75, the

putative major facilitator superfamily transporter MFST or the lysosomal proteins CatL, CBP1 and GLP-1, were not differentially expressed in the suramin-resistant lines. The only hits that were differentially expressed mapped to *VSG* genes (Fig. S3). Thus all four selected lines had undergone an expression switch to a new *VSG*.

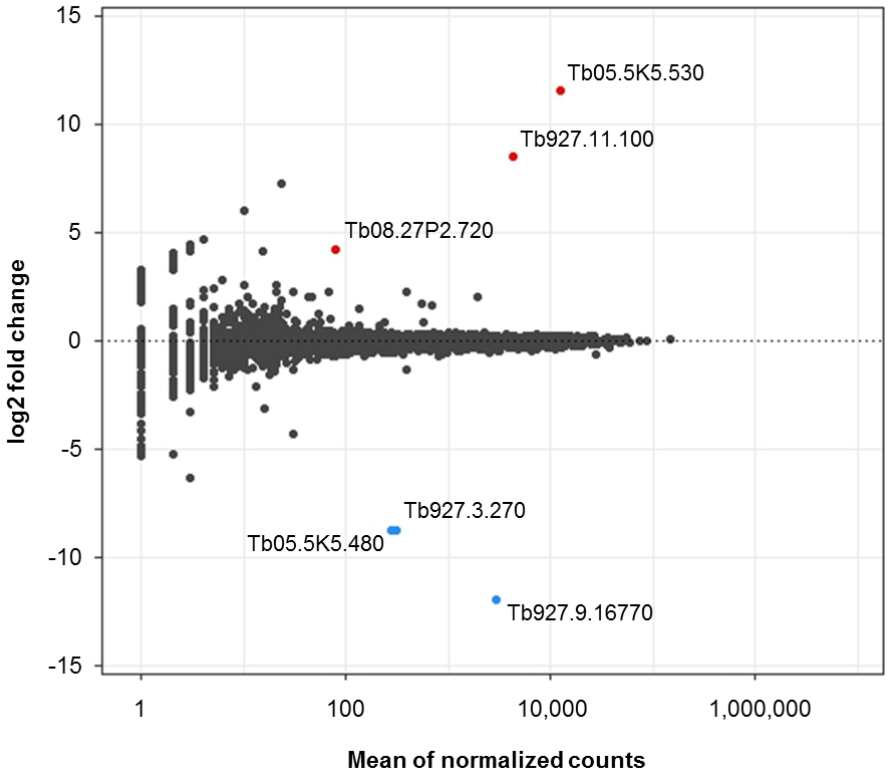

Figure S3. Transcriptomics of suramin sensitive and resistant *T. brucei*.
Analysis as described in figure legend 3, the data shows the original mapping to the TREU927 reference genome complemented with the Lister 427 bloodstream expression sites prior to the identification of VSG^{Sur} and VSG^{900}. A number of genes seem to be over- (red) or under-expressed (blue); all of the significant hits are *VSG* genes.

3.3.4. The suramin-resistant lines have all switched to the same *VSG*

The sequence of this newly expressed *VSG* was reconstructed by *de novo* assembly from the Illumina reads. The reconstructed sequence was verified by reverse transcriptase PCR followed by direct sequencing, making use of the fact that all *T. brucei* mRNAs possess the same spliced leader sequence at the 5' end [250]. Three of the four resistant lines had switched to the identical *VSG* gene, which was termed VSG^{Sur} (GenBank accession MF093647). *T. b. rhodesiense* STIB900_c1_Sur2 expressed a gene that was almost

identical to *VSG*^{Sur} (GenBank accession MF093648), differing only in four SNPs (two of which were non-synonymous); and a different 3' UTR. The sequence of the *VSG* expressed in the parental clone STIB900_c1 was reconstructed in the same way and termed *VSG*^{900} (GenBank accession MF093646). Re-mapping of the Illumina reads upon inclusion of these two *VSG* sequences resulted in more than 10% of reads mapping to *VSG*^{900} in the sensitive parent clone, and more than 10% of reads mapping to *VSG*^{Sur} in all the resistant derivatives (Fig. 3).

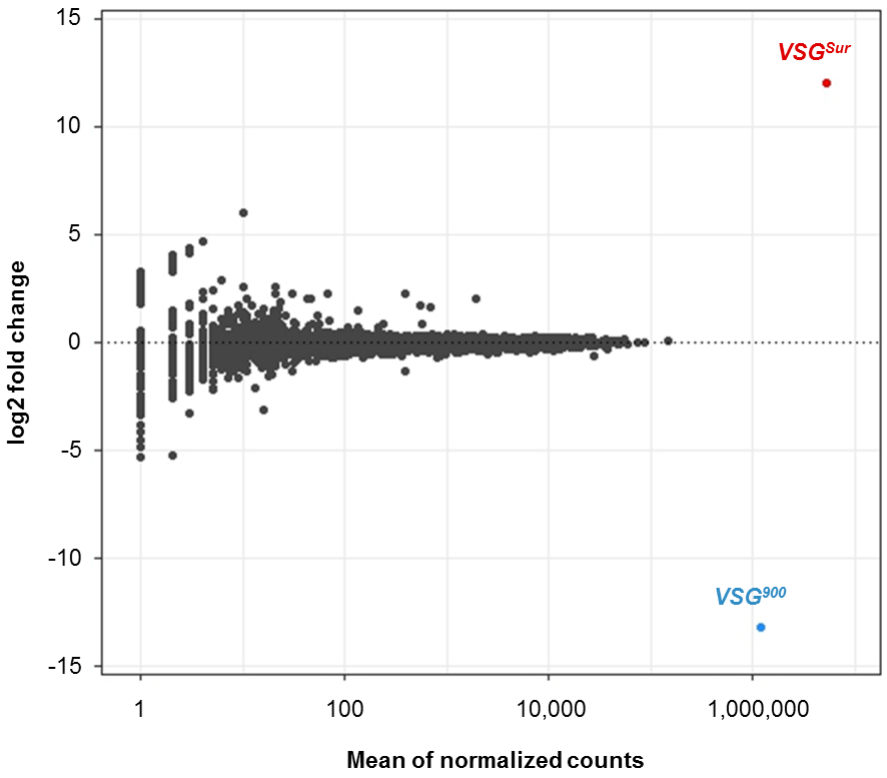

Figure 3. Differential gene expression of resistant derivatives vs. suramin-sensitive parental *T. b. rhodesiense* STIB900 clone as analyzed with DESeq2. Illumina reads were mapped to the TREU927 reference genome supplemented with Lister 427 bloodstream expression sites and with the sequences of *VSG*^{Sur} and *VSG*^{900}. The x-axis displays transcript abundance (mean read count over all samples normalized for library size) and the y-axis displays the logarithmic fold-change of transcript abundance (all four resistant derivatives vs. the sensitive parent clone). Genes with a significant ($p<0.01$) fold-change are colored in red if overexpressed, and in blue if underexpressed in the resistant derivatives.

Reverse-transcriptase qPCR confirmed the switch from VSG^{900} to VSG^{Sur} in the resistant lines as they all showed a more than 10,000-fold upregulation of VSG^{Sur} (Fig. 4). We also analyzed the suramin-selected derivatives of another clone of *T. b. rhodesiense* STIB900 (STIB900_c2), and they had switched to VSG^{Sur} as well (Fig. 4). Moreover, the suramin-resistant population derived from *T. b. brucei* strain BS221 had undergone a switch to a *VSG* with 97% nucleotide sequence identity (Needleman-Wunsch global alignment) to VSG^{Sur} (Fig. 4; GenBank accession MF093649).

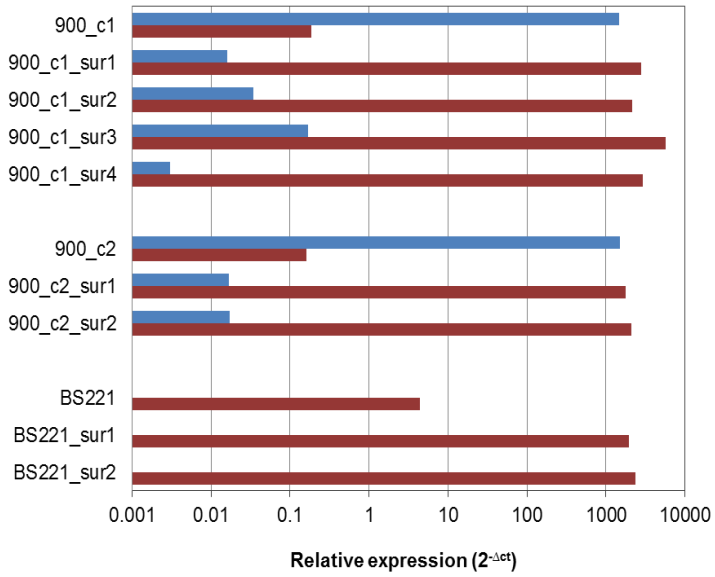

Figure 4. Expression of VSG^{Sur} and VSG^{900} as determined by qRT-PCR in resistant *T. b. rhodesiense* and *T. b. brucei*, normalized to telomerase reverse transcriptase (*TERT*).

3.3.5. Suramin resistance correlates with expression of VSG^{Sur} but not *ESAG7*

VSG^{Sur} encodes a bona fide variant surface glycoprotein of 491 amino acids with an N-terminal export signal and a C-terminal GPI-anchoring signal as predicted by SignalP [251] and GPI-SOM [252], respectively. Profile scans against the Procite and Pfam databases of sequence motifs did not return significant hits beside the entry for the *T. brucei* VSG conserved C-terminal domain (PF10659; E-value of 0.0002). A Blastp search with VSG^{Sur} as the query against the non-redundant protein sequence database at NCBI returned significant hits on variant surface glycoproteins, the best one on VSG 522 (GenBank: AGH61081.1) with a sequence identity of 72%. The same search against all organisms other than *Trypanosoma* spp. did not return a single hit. In the absence of any particular feature that would distinguish it from other VSGs, we initially presumed that it is not VSG^{Sur} itself that caused drug resistance but one of the expression site associated genes (*ESAG*s), which are polycistronically co-transcribed with each *VSG* and which could have

failed to correctly map due to sequence divergence between STIB900 and the reference sequence used. If an antigenic switch results from activation of a new *VSG* expression site, new alleles of *ESAG*s will be expressed as well. If the switch is due to replacement of the active *VSG* by gene conversion, the expressed *ESAG*s will remain the same.

ESAG7 encodes the non-anchored part of the heterodimeric transferrin receptor and differs in sequence among the *T. brucei* VSG expression sites [253,254]. For each of the five sequenced *T. b. rhodesiense* lines, the whole transcriptome was assembled *de novo* from the Illumina reads and the expressed *ESAG7* was extracted using a blast search (Tb927.7.3260, 2175 nt). Three of the suramin-resistant lines expressed exactly the same *ESAG7* gene as the parental *T. b. rhodesiense* STIB900_c1 (GenBank accession MF093650); the fourth expressed an *ESAG7* that differed in five nucleotides, two of which were non-synonymous (GenBank accession MF093651). Thus in one of the suramin-selected lines, the switch to VSG^{Sur} appears to have occurred by activation of a new expression site, while in the remaining three it happened by gene conversion, replacing the originally expressed VSG^{900} gene while maintaining the *ESAG*s. This strongly suggests that it is the expression of VSG^{Sur} itself, and not of the *ESAG*s, that causes suramin resistance. This hypothesis was corroborated by reverse genetic manipulation of *VSG* expression.

3.3.6. Reversal of the VSG^{900}-VSG^{Sur} switch restores suramin sensitivity

We made a genetic construct (Fig. 5A) to target the active *VSG* expression site of the suramin-resistant *T. b. rhodesiense* STIB900_c1_sur1. In order to exchange the expressed VSG^{Sur} with VSG^{900}, the construct was framed with the 5' and 3' UTR of VSG^{Sur} and contained the coding sequence of VSG^{900} together with a blasticidin resistance gene. Positive transfectants were selected with blasticidin and cloned by limiting dilution. The construct had integrated in the genomes of all the analyzed clones [n=6] as determined by PCR using primers binding to the 5' and 3' UTR of VSG^{Sur} as the adjacent genomic context was unknown. Reverse-transcriptase qPCR confirmed a high expression of the re-introduced VSG^{900} (Fig. 5B). Subsequent drug sensitivity assays with three of the transfectants showed a complete loss of resistance in all of them, with IC_{50} values between 10 and 12 nM (Fig. 5c).

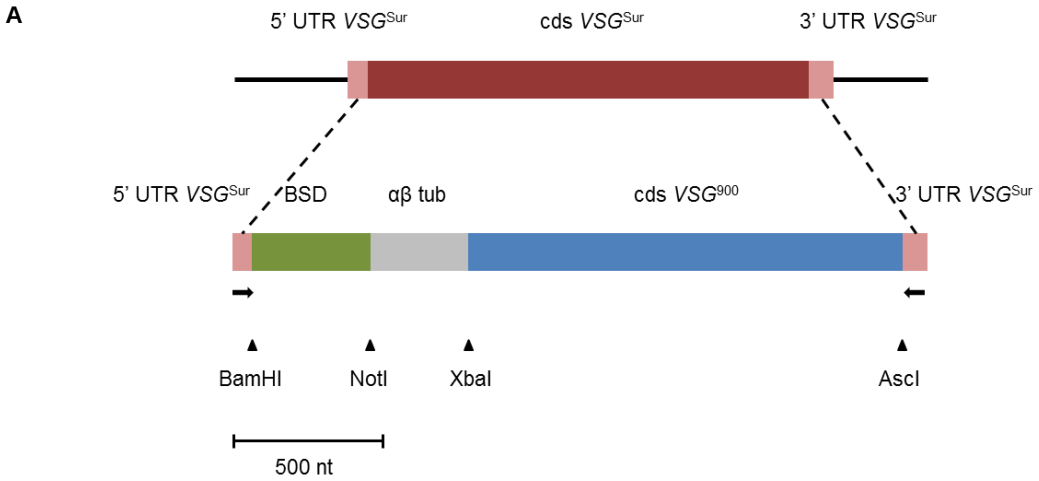
A
5' UTR VSG^Sur
cds VSG^Sur
3' UTR VSG^Sur
5' UTR VSG^Sur
BSD
αβ tub
cds VSG^900
3' UTR VSG^Sur
BamHI
NotI
XbaI
AscI
500 nt

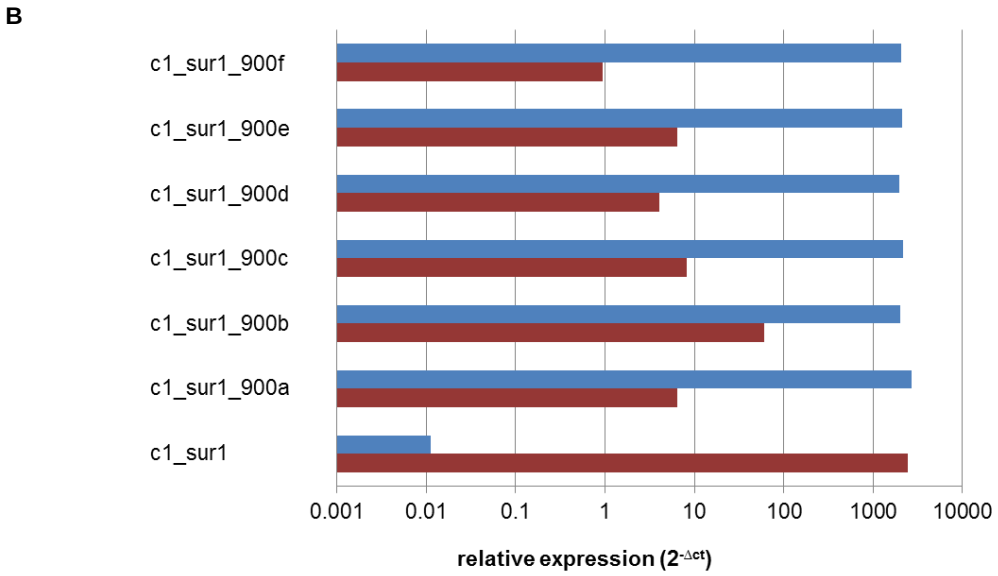
B
c1_sur1_900f
c1_sur1_900e
c1_sur1_900d
c1_sur1_900c
c1_sur1_900b
c1_sur1_900a
c1_sur1
0.001
0.01
0.1
1
10
100
1000
10000
relative expression (2^-Δct)

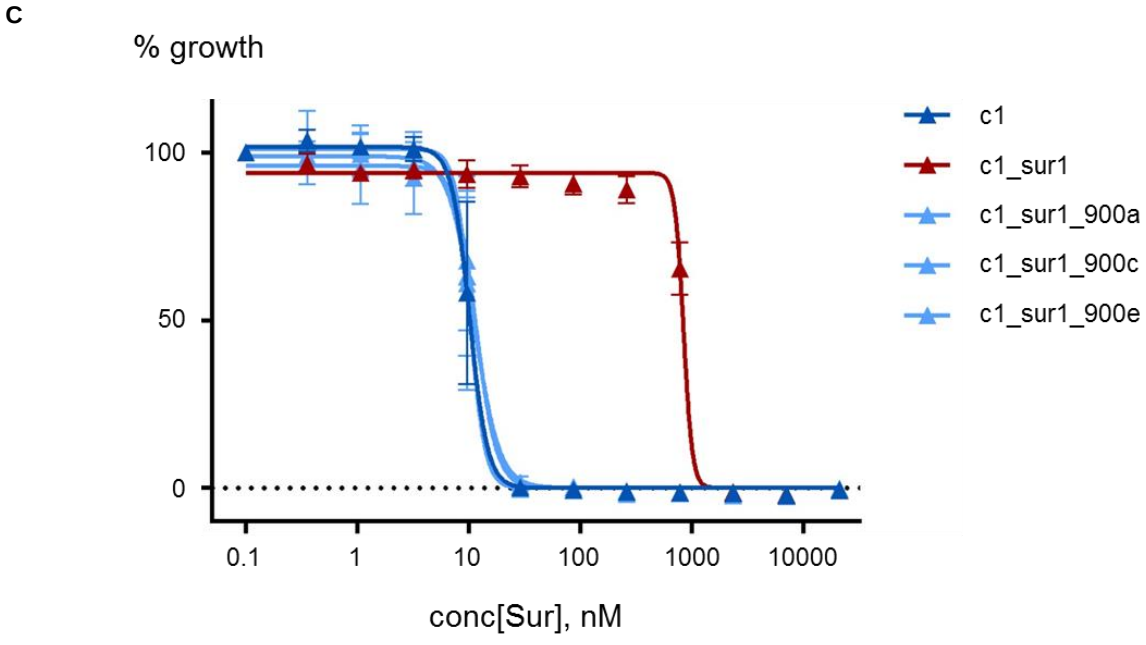
C
% growth
100
50
0
0.1
1
10
100
1000
10000
conc[Sur], nM
c1
c1_sur1
c1_sur1_900a
c1_sur1_900c
c1_sur1_900e

Figure 5. Reverse genetic re-introduction of *VSG^{900}*. A) Schematic illustration of *VSG^{Sur}* (top) and the construct (bottom) used for re-introduction of *VSG^{900}* into the active bloodstream expression site of the resistant derivative STIB900_c1_sur1. The construct is framed with the 5' and 3' untranslated region (UTR) of *VSG^{Sur}*, it contains a blasticidin resistance gene (BSD), an αβ tubulin splice site (αβ tub) and the coding sequence (cds) of *VSG^{900}*. Binding sites of primers used for the verification of the genomic integration of the construct are indicated with black arrows. B) qRT-PCR, normalized with *TERT*. Expression of *VSG^{Sur}* (red) and *VSG^{900}* (blue) are shown for STIB900_c1_sur1 and six transfected clones thereof, with *VSG^{900}* introduced into the active bloodstream expression site. C) Suramin dose-response curves for STIB900_c1_sur1 and three transfected clones expressing *VSG^{900}*.

One of the transfectants was once more subjected to suramin pressure. It quickly reestablished suramin resistance with a resistance level similar to STIB900_c1_sur1 (Fig 6). Since these re-selected parasites could have undergone either expression site switch or gene conversion in order to re-express *VSG^{Sur}*, we investigated three lines selected from one transfectant by PCR using primers binding to the 5' and 3' UTR of *VSG^{Sur}*. Two of them (c1_sur1_900a_sur1 and c1_sur1_900a_sur2) had lost the construct, thus had undergone a gene conversion in order to switch back to *VSG^{Sur}*. In the third line (c1_sur1_900a_sur3) the construct was still present, therefore it had undergone an expression site switch in order to express *VSG^{Sur}*. We subsequently exposed the three lines to blasticidin; as expected the two lines that had undergone gene conversion were killed. The line that had undergone an expression site switch recovered under blasticidine pressure and the obtained parasites (c1_sur1_900a_sur3_bl1, _bl2 and _bl3) had completely lost the suramin resistance (Fig 6).

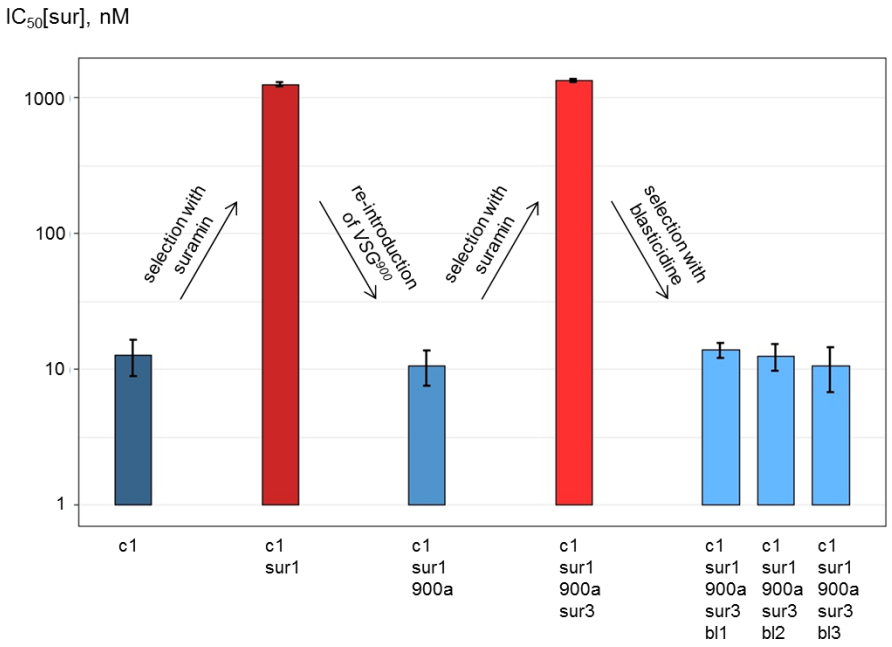

Figure 6. Ups and downs of suramin sensitivity in the course of the experiment. IC_{50} values are shown for the sensitive parent clone c1 before selection (dark blue), one of the resistant derivatives after suramin selection (dark red), a transfected clone thereof with *VSG*^{900} re-introduced into the active bloodstream expression site (blue), one suramin selected derivative of that clone (light red), and three blasticidine selected lines thereof (light blue).

3.3.7. Binding and uptake of trypan blue

We exploited the facts that the suramin-selected lines were cross-resistant to trypan blue, and that trypan blue becomes fluorescent when bound to protein [255], to further examine the observed phenomenon of drug resistance. The fluorescence of trypanosomes was quantified by flow cytometry after incubation for two hours with different concentrations of trypan blue (Fig 7). Since dead cells are strongly perfused by trypan blue, we first compared dead and living cells. The dead cells showed a much higher fluorescence and could be clearly separated from the living cells by setting the gate accordingly in a cell-size versus fluorescence plot (Fig. S4). Fluorescence of living cells incubated at physiological temperature is derived from both, surface bound and endocytosed trypan blue. At 37°C the two tested resistant derivatives (STIB900_c1_sur1 and STIB900_c1_sur4) showed significantly lower fluorescence levels when compared to the sensitive parent clone (STIB900_c1) over all concentrations (Fig. 7A). As endocytosis in trypanosomes is inactivated at low temperatures [256], we performed the same experiment at 4°C to quantify the fluorescence of surface-bound trypan blue (Fig 7B). The resistant parasites showed

similar levels of fluorescence as the sensitive clone at concentrations of 5 to 200 µg ml^{-1} but significantly differed at 390 µg ml^{-1}, where the sensitive clone showed a strong increase in fluorescence. If the fluorescence at 37°C represents binding plus uptake, and the fluorescence at 4°C represents binding, then the curve obtained by subtraction (Fig. 7C) represents the trypan blue which had been endocytosed during the two hours of incubation. These values were lower for the resistant parasites than for the sensitive clone at concentrations up to 200 µg ml^{-1}. There was no difference at 390 µg ml^{-1} trypan blue, possibly due to toxicity and inhibition of endocytosis in the sensitive clone.

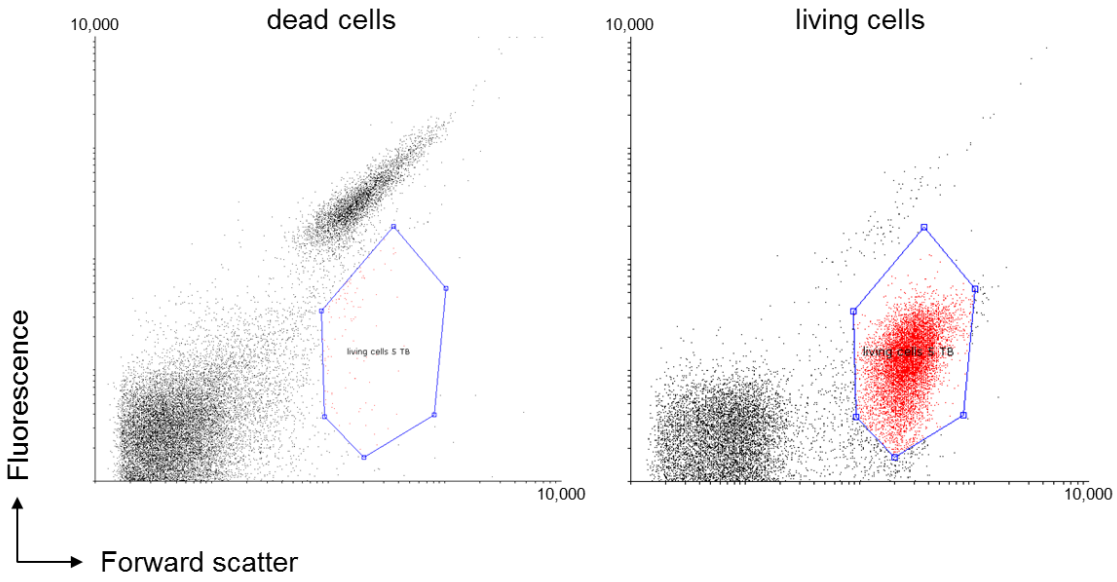

Figure S4. Size (forward scatter, x-axis) versus fluorescence intensity (y-axis) of dead (left) and alive (right) cells after incubation with 5 µg ml^{-1} trypan blue for two hours. The dead cells had been incubated for 5 min at 56 °C beforehand. Cells in the gate defined for the living cells are labeled in red

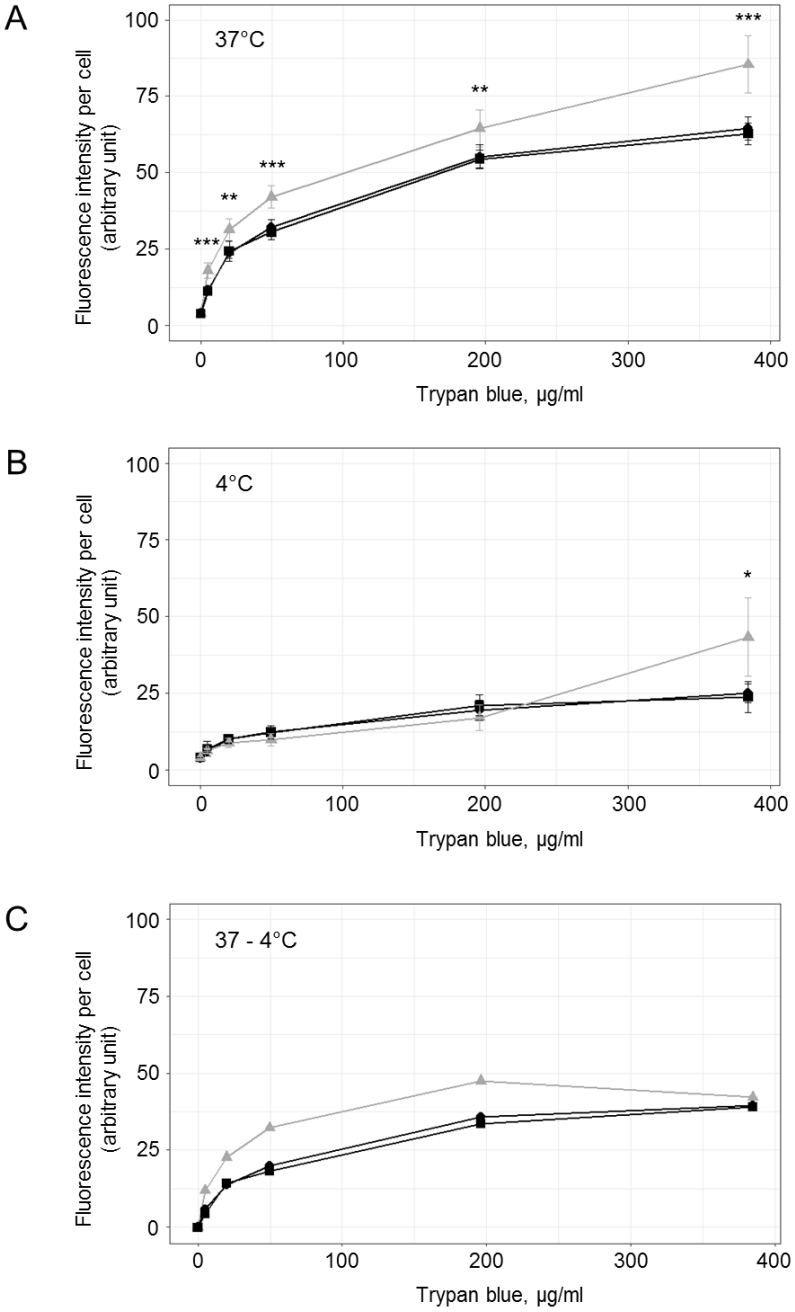

Figure 7. Fluorescence of suramin sensitive and resistant cells incubated at different concentrations of trypan blue for two hours. Significantly different fluorescence levels between the sensitive and the resistant lines are indicated (*, $p<0.05$; **, $p<0.01$; **, $p<0.001$; $n\geq5$, pairwise t-test); there were no significant differences between the two resistant lines. (A) Cells incubated at 37°C: the fluorescence levels represent surface bound plus endocytosed trypan blue. (B) Cells incubated at 4°C: the fluorescence levels represent surface-bound trypan blue. (C) The difference between the fluorescence at 37°C and 4°C therefore represents an estimate of the endocytosed trypan blue.

3.4. Discussion

The famous parasitologist Frank Hawking (father of the even more famous physicist Stephen Hawking) stated that "Strains of trypanosomes may be made suramin-resistant in the laboratory, but this resistance takes much longer to develop than with arsenicals" [257]. Here we show that >90-fold suramin resistance emerges in *T. brucei* spp. bloodstream forms after only few days of *in vitro* selection at high drug pressure. In contrast, it had taken us almost two years to select for melarsoprol-resistant derivatives of *T. b. rhodesiense* STIB900 with resistance factors of the same magnitude [258]. Comparative analysis of gene expression showed an association of a particular VSG with suramin resistance. Our first suspicion, that VSG^{Sur} was only a marker and the actual cause of resistance was one of the ESAGs, was rebuted by the finding that three of the four resistant lines had switched their *VSG* gene while maintaining the VSG expression site, as indicated by perfect conservation of expressed *ESAG7*. The finding that one of the resistant lines expressed a slightly different *ESAG7* indicated that VSG^{Sur} in parental *T. b. rhodesiense* STIB900 localized to a (silent) telomeric *VSG* expression site rather than to the chromosome-internal or minichromosomal *VSG* repository [259]. The suramin resistance phenotype was slowly reversible over time, which might be explained by the slightly longer population doubling times of the resistant derivatives.

The causality between VSG^{Sur} expression and suramin resistance was confirmed by reverse genetic re-introduction of the originally expressed *VSG* into the resistant parasites, which completely restored susceptibility. The finding that the expression of VSG^{Sur} causes suramin resistance, explains the fast emergence of the resistance and the high reproducibility of the *in vitro* selection. It also explains the discrepancy with Hawking's observation cited above, because he was using subcurative treatment of infected mice to select for resistance (*in vitro* cultivation of *T. brucei* was not possible at the time).

In vivo, parasites that are bound to express a particular VSG under suramin pressure will be eliminated by host antibodies. This might be the reason why suramin, after one century of use, is still effective in the treatment of early-stage east-African sleeping sickness. The commonly used regimen is five injections of 20 mg/kg, leading to suramin plasma levels over 100 µg ml^{-1} for several weeks [25], which is clearly above the *in vitro* IC_{50} of trypanosomes expressing VSG^{Sur}. The situation would be different if lower doses of suramin were administered. One could speculate that such a mechanism could have

facilitated the emergence of suramin resistance in animal-pathogenic trypanosomes, as the usual treatment regimen in horses and camels is a single dose of 10 mg/kg suramin, and the disease typically leads to immunosuppression [65]. Thus if the trypanosomes escaped the effects of suramin in the short term by switching to a certain VSG, this would give them more time to develop other resistance mechanisms. It has been reported that a functional immune system is important for effective suramin treatment of animal trypanosomiasis [260].

VSGs could be either directly or indirectly involved in binding and uptake of suramin, and VSG^{Sur} might be non-functional in this respect. Previous studies which proposed an uptake of suramin via endocytosis [58,59] are in accordance with this, as VSG in *T. brucei* bloodstream forms is endocytosed at a very high rate [261]. An involvement of VSG in suramin binding or uptake could also explain the insensitivity of procyclic trypanosomes to suramin [248] as they don't express *VSG* genes.

Binding of trypan blue at 4°C to suramin-sensitive trypanosomes suggests a saturable high-affinity component plus a low affinity component that becomes apparent at 390 µg ml^{-1} trypan blue (testing of higher concentrations was not possible because of toxicity and solubility problems). This implies the presence of more than one binding partner on the cell surface of the sensitive clone. The low affinity component appeared to be missing in the suramin-resistant clones (Fig. 7B). However, the uptake of trypan blue at 37°C by the suramin-resistant lines was impaired at concentrations between 5 and 200 µg ml^{-1} (Fig. 7C), indicating that the low-affinity binding component may not be responsible for drug resistance. Thus while the genetic basis for fast suramin resistance in *T. brucei* is an expression switch to VSG^{Sur}, the biochemical basis remains to be elucidated.

3.5. Experimental Procedures

T. brucei isolates and cultivation

The *T. b. rhodesiense* strain STIB900 is a derivative of STIB704, which was originally isolated from a male patient at St. Francis Hospital in Ifakara, Tanzania in 1982. It was passaged several times in rodents and once in a tsetse fly (*Glossina morsitans morsitans*) before a cloned population was adapted to axenic *in vitro* culture. The *T. b. brucei* strain BS221 is a derivative of 427 (not to be confounded with Lister427), which was originally isolated in Uganda in 1960. Parasites were cultivated in Iscove's Modified Dulbecco's Medium supplemented according to Hirumi [262] with 15% of heat-inactivated horse-serum. The parasites were grown at 37°C, 5% CO_2 and diluted three times a week.

Microcalorimetry with T. b. rhodesiense

T. b. rhodesiense strain STIB900 were cultivated in Minimum Essential Medium with Earle's salts, supplemented according to Baltz et al. [263] with minor modifications: 0.2 mM 2-mercaptoethanol, 1 mM sodium pyruvate, 0.5 mM hypoxanthine and 15% heat-inactivated horse serum. Trypanosome cultures in the late exponential growth phase were diluted with fresh culture medium to a density of 10^5 cells ml^{-1}. Ampoules were filled, in triplicate, with 3 ml cell suspension and supplemented with suramin, pentamidine or melarsoprol at concentrations corresponding to $5\times IC_{50}$ or $25\times IC_{50}$ in the identical medium [249]. Culture medium without trypanosomes served as baseline control. The heat flow was measured continuously over a period of 8 days at 37 °C in a TAM III isothermal microcalorimeter (thermal activity monitor, model 249; TA instruments, New Castle DE, USA).

Cloning of T. b. rhodesiense

A microdrop of a suspension with 10^4 cells ml^{-1} was made using a gilded paperclip and inspected by two persons under an inverted microscope. After confirmation of the presence of a single cell, the microdrop was supplemented with 50 µl of cloning medium. This consisted of 59% Iscove's modified Dulbecco's Medium, which had been supplemented according to Hirumi [262] for a total volume of 100%, 1% Mäser-mix [264], 20% inactivated horse-serum and 20% of pre-conditioned medium. The pre-conditioned medium was prepared by centrifugation of a dense trypanosome culture (10 min at 1840 g) and subsequent sterile filtering of the supernatant. After four days of incubation at 37°C, 5%

CO_2, the plate was inspected under an inverted microscope and 50 µl of cloning medium was added to the wells with a growing clonal colony. After another 3 days the clones were passaged to new plates and cultivated as described above.

In vitro selection for drug resistance and determination of growth rates

A fresh clone of *T. b. rhodesiense* STIB900 in the exponential growth phase was selected with 1050 nM suramin in four wells each containing 1 ml medium with 5×10^4 cells. After 6 days the parasites were removed from drug pressure by washing three times with fresh culture medium and cultured in drug-free medium as described above. For the BS221 strain 10^5 cells were selected with 1070 nM (BS221_sur1) and 4270 nM (BS221_sur2) suramin and removed from drug pressure after 5 days. Cell growth was measured between day 15 and day 26 after selection. Cumulative growth curves were determined by dilution of the cells to 10^5 ml^{-1}, incubation for 24 h, and measurement of cell density with a CASY Cell Counter (OMNI Life Science, Bremen). This procedure was repeated for four days. Cumulative cell numbers and the population doubling times were calculated and statistically evaluated with t-tests applying Benjamini-Hochberg correction using R Studio (R version 3.3.3).

Alamar blue assay

Suramin sodium salt and pentamidine isethionate were obtained from Sigma (S2671 and P0547 respectively), Trypan Blue from Fluka (93590) and melarsoprol from Sanofi-Aventis/WHO**.** Alamar blue assays [265] for determination of *in vitro* drug sensitivities were carried out at least three times independently. Serial drug dilutions were prepared on a 96 well plate in technical duplicates and cells were added to a concentration of 2×10^4. Parasite-free, drug-free wells were used for determination of background fluorescence. After an incubation time of 69 hours, plates were inspected microscopically and resazurin was added to a final concentration of 36 µM. Fluorescence intensity was measured after 3-4 hours incubation using a SpectraMax (Molecular Devices) and SoftMax Pro 5.4.5 software. The 50% inhibitory concentrations (IC_{50}) were calculated with GraphPad Prism 6.00 using a non-linear regression model to fit the dose-response curve (variable slope; four parameters, bottom value set to zero). Statistical analysis was performed with GraphPad Prism 6.00 using an ordinary one-way Anova with Tukey's multiple comparisons test.

Extraction of RNA, mRNA-Seq and comparative transcriptomics

Cultures in the exponential growth phase were centrifuged and washed once with PBS before total RNA was isolated using the RNeasy Mini Kit (Qiagen) including an on-column DNase treatment. RNA was shock-frozen in liquid nitrogen and stored at -80°C. Five microgram of RNA from two independent isolations were pooled for each sample. Library preparation and sequencing was performed at the Quantitative Genomics Facility (QGF) of the ETH Zurich in Basel. Sequencing libraries were prepared using the TruSeq Stranded mRNA Library preparation kit (Illumina). Single-end sequencing of 125 nucleotides was carried out on an illumina HiSeq 2500. The bioinformatic analysis was carried out on the sciCORE cluster of the University of Basel. Quality of the sequencing reads was controlled with fastqc software (Babraham Bioinformatics - FastQC A Quality Control tool for High Throughput Sequence Data. Available at: http://www.bioinformatics.babraham.ac.uk/projects/fastqc/. Accessed: 6th April 2017). Illumina adaptors, low quality ends and reads with a length of fewer than 36 nucleotides were removed with trimmomatic [266]. Sequencing reads were mapped to the TREU927 reference genome (version TriTrypDB-28) complemented with bloodstream expression sites from Lister427 [254]. Mapping was performed with bwa [267] using the default parameters (seedlength of 19 nucleotides, matching score of 1, mismatch penalty of 4, gap open penalty of 6 and a gap extension penalty of 1). The alignment files in the SAM format were converted to binary files using samtools [268] and sorted and indexed using picard tools (Broad Institute. Available at: http://broadinstitute.github.io/picard/. Accessed: 6th April 2017). Read counts per transcript were determined with the Python package HTSeq [269] using a combined gff file from TREU927 (version TriTrypDB-28) and bloodstream expression sites from Lister427 [254], default parameters with a minimal mapping quality of 10 were used. Raw counts were analyzed with the R package DESeq2 [270] (version 1.14.1), independent filtering was disabled.

The de novo assembly of transcripts was carried out using trinity [271] with the default parameters. The *de novo* assembled transcripts were screened with blastn for ESAG7-like genes using the sequence of gene Tb927.7.3260 as query.

Reverse transcription, PCR and quantitative PCR

Complementary DNA (cDNA) was synthesized with SuperScript III Reverse Transcriptase (Invitrogen via Thermo Fisher Scientific, Waltham MA, USA) according to the

manufacturer's protocol using oligo(dT) primer and 1-5 µg of total RNA. One microliter of the 1:100 diluted cDNA was used for PCR. Amplification of the VSGs was performed with one primer binding to the spliced leader sequence [250] at the 5' UTR and the other primer binding to the 3' end of the gene (Table S1). The sequences of the 3'ends were derived from the *de novo* assembly. For amplification of the VSG expressed in the BS221 strain, a primer binding unspecifically to the 3'ends of all VSGs [272] was used (Table S1). The PCR was carried out with Taq polymerase (Solis BioDyne, Estonia) or with KAPA HiFi HotStart DNA Polymerase (Kapa Biosystems, Cape Town, South Africa). PCR products were run on a 1% agarose gel, which was subsequently stained with GelRed Nucleic Acid Gel Stain (Biotium, Fremont CA, USA). The PCR products were purified with the Wizard® SV Gel and PCR Clean-Up System (Promega, Madison WI, USA) or the NucleoSpin® Gel and PCR Clean-up (Macherey-Nagel, Düren, Germany) and sent to Microsynth (Balgach, Switzerland) for sequencing. Primers for sequencing were the same as used for PCR, additional internal primers were designed for completion of the sequences. Quantitative PCR was carried out with Power SYBR® Green (Applied Biosystems via Thermo Fisher Scientific) on a StepOnePlus™ real-time PCR System (Applied Biosystems) in technical duplicates. StepOne Software v2.3 was used for analysis of the amplification plots and calculation of the C_T values, which were normalized to the housekeeping gene telomerase reverse transcriptase [273] (TERT; ΔC_T). All primers (Table S1) were designed using the Primer3Plus software (Available at: http://primer3plus.com/cgi-bin/dev/primer3plus.cgi. Accessed: 6th April 2017)

Table S1. Primers used for amplification of *VSG* and sequencing.

Name	**Sequence**	**Binding site**	**Use**
SLT_F	cgctattattagaacagtttctgtac	5' UTR of all mRNA	amplification of *VSG*
vsg01	agcaaaagaggggccttttttaataa	3' end of VSG^{Sur}	amplification of VSG^{Sur}
vsg02	tcattcgtttggccatacgc	internal VSG^{Sur}	sequencing of VSG^{Sur} and qPCR of VSG^{Sur}
vsg03	tctgggttcatatgcgctgc	internal VSG^{Sur}	sequencing of VSG^{Sur}
vsg04	gcaagcaaaagaggagaagtt	3' end of VSG^{900}	amplification of VSG^{900}
vsg05	caaggcaaaatccggctgtg	internal VSG^{900}	sequencing of VSG^{900} and qPCR of VSG^{900}
vsg06	ttactgacagacgaaccggc	internal VSG^{Sur}	qPCR of VSG^{Sur}
vsg07	gccgtagcagaatcagagct	internal VSG^{900}	qPCR of VSG^{900}

vsg08	gtgttaaaatatatc	3' UTR of *VSG* (unspecific)	Amplification of *VSG* in BS221
vsg16	gaaccgaaaatagtcacgaaggc	5' end of construct	amplification of construct VSG^{Sur} to VSG^{900} for transfection
vsg17	tttttcggtgaatttaaaggtgttaaa	3' end of construct	

Reverse genetics with T. brucei rhodesiense

For the gene exchange of VSG^{Sur} to VSG^{900} a construct was designed (Fig. 5A) containing the 3' and 5' UTRs of VSG^{Sur}, the coding sequence of VSG^{900}, an αβ tubulin splice site and a blasticidin-resistance gene (BSD). The DNA was synthesized by GenScript (Piscataway Township NJ, USA) and integrated between the HindIII and the EcoRI-site of a pUC57 vector. For amplification of the insert a PCR was performed using two flanking primers. Three µg of the purified PCR product were used for the transfection of 4×10^7 STIB900_c1_sur1 cells in 100 µl Tb-BSF buffer [50] with an Amaxa Nucleofector using program Z-001. Positive transfected clones were obtained by limiting dilution in standard culture medium. After 24 hours of incubation, blasticidin was added to a total concentration of 5 µg ml^{-1}. The construct integration was verified by PCR on genomic DNA: As the flanking genomic sequences upstream and downstream of VSG^{Sur} are unknown, primers binding to the 5' and 3' UTR of VSG^{Sur} were used for the PCR (Fig. 5), which resulted in a band of 1,624 nucleotides derived from the wildtype sequence of VSG^{Sur} and a second band of 2,356 nucleotides in the presence of the construct. Genomic DNA was isolated from 10 ml dense culture in the following manner: The culture was centrifuged at 1800 g for 5 minutes and washed with TE buffer (10 mM TrisHCl pH 8, 1 mM EDTA) once. Cells were eluted in 100 µl TE buffer and lysed by addition of 1 µl of 10% SDS and incubation for 10 min at 55°C. Subsequently 30 µl of 5 M potassium acetate were added to the lysate and incubated on ice for 5 min to precipitate SDS and proteins. The lysate was spun down for 5 min at full speed in a microcentrifuge and the supernatant transferred to a new tube. The DNA was precipitated with absolute ethanol, washed with 70% ethanol and eluted in 20 µl H_2O. PCR was carried out as described above. The expression of VSG^{Sur} and VSG^{900} was measured by quantitative PCR as described above.

Trypan blue binding and uptake

A total of 2×10^5 parasites per sample was exposed to trypan blue (5, 20, 50, 200 or 390 µg ml^{-1}) in 1 ml standard growth medium and incubated for two hours at 37°C or 4°C. After incubation, the parasites were centrifuged (5 min, 3000 g) and washed twice with 1 ml PBS

(Phosphate-buffered saline; 137 mM NaCl, 2.7 mM KCl, 10 mM Na_2HPO_4, 1.8 mM KH_2PO_4, pH 7.4) at room temperature or 4°C, respectively. The cells were resuspended in 250 µl PBS followed by the addition of 250 µl 10% formalin for fixation. The fluorescence intensity of the fixed cells was measured with a BD FACSCaliburTM flow cytometer (BD Biosciences, San Jose, CA, USA) using the FL3 channel (670 nm long pass) upon excitation at 488 nm. Ten thousand events were acquired within the parasite gate based on size versus granularity (FSC x SSC). Dot plots and their fluorescence were evaluated in FL3 histograms as trypan blue has its emission peak at 660 nm [255]. The measured fluorescence intensity was analyzed with Flowing Software (Version 2.5.1) by using a living parasite gate based on size versus fluorescence intensity (FSC x FL3) and statistically evaluated with R Studio, applying pairwise t-tests (Version 1.0.143, R version 3.3.3).

Acknowledgements

We are most grateful to Sebastian Hutchinson for helpful advice, to the Genomics Facility of the ETHZ in Basel for sequencing, to sciCORE of the University of Basel for data analysis runtime, and to Françoise Brand and Henning Stahlberg for the scanning electron microscopy picture. This study was funded by the Swiss National Science Foundation (grants 31003A_135746 and 310030_156264).

.

4. Expression of a specific variant surface glycoprotein has a major impact on suramin sensitivity and endocytosis in *Trypanosoma brucei*

Short title: A VSG, suramin and endocytosis in *T. brucei*

Natalie Wiedemar[1,2], Michaela Zwyer[1,2], Martin Zoltner[3], Monica Cal[1,2],

Mark C. Field[3], Pascal Mäser[1,2*]

[1] Swiss Tropical and Public Health Institute, Socinstrasse 57, 4051 Basel, Switzerland

[2] University of Basel, 4001 Basel, Switzerland

[3] School of Life Sciences, University of Dundee, Dundee, United Kingdom, DD1 5EH

2019

FASEB BioAdvances

Volume 1, Issue 10: 591-670

I performed all experiments and analysis, except for the reverse genetics (Figure 1A-C), which was carried out by Michaela Zwyer under my supervision. Further I am grateful to Martin Zoltner for help with the ISG75 turnover experiment (Figure 3A) and to Monica Cal for help with the wash-out assays (Figure 4)

4.1. Abstract

Suramin was introduced into the clinic a century ago and is still used to treat the first stage of acute human sleeping sickness. Due to its size and six-fold negative charge, uptake is mediated through endocytosis and the suramin receptor in trypanosomes is thought to be the invariant surface glycoprotein 75 (ISG75). Nevertheless, we recently identified a variant surface glycoprotein (VSG^{Sur}) that confers strong *in vitro* resistance to suramin in a *Trypanosoma brucei rhodesiense* line. In the present study we introduced *VSG^{Sur}* into the active bloodstream expression site of a *T. b. brucei* line. This caused suramin resistance and cross-resistance to trypan blue. We quantified the endocytosis of different substrates by flow cytometry and showed that expression of VSG^{Sur} strongly impairs the uptake of low density lipoprotein (LDL) and transferrin, both imported by receptor-mediated endocytosis. However, bulk endocytosis and endocytosis of the trypanolytic factor were not affected, and the *VSG^{Sur}*-expressors did not exhibit a growth phenotype in the absence of suramin. Knockdown of ISG75 was synergistic with *VSG^{Sur}* expression, indicating that these two proteins are mediating distinct suramin resistance pathways. In conclusion, VSG^{Sur} causes suramin resistance in *T. brucei* bloodstream forms by decreasing specific, receptor-mediated endocytosis pathways.

4.2. Introduction

Sleeping sickness, transmitted by the tsetse fly, is caused by two subspecies of the protozoan parasite *Trypanosoma brucei*: *T. b. gambiense* typically establishes a chronic infection, whereas *T. b. rhodesiense* causes a rather acute form of the disease. A third subspecies, *T. b. brucei*, is not infective to humans but, together with other trypanosome species, causes livestock trypanosomiasis. Trypanosomes are protected from the mammalian immune system by multiple mechanisms that confound both innate and acquired defenses. The surface coat consists of a dense layer of a single variant surface glycoprotein (VSG); with a reservoir of more than 2000 *VSG* genes and pseudogenes [274], trypanosomes evade their mammalian host's adaptive immune responses by antigenic variation. Thus there is no vaccine for sleeping sickness and chemotherapy relies on few available drugs, although more are entering the treatment pipeline [275]. Suramin is the oldest drug but remains used for the treatment of the first stage of *T. b. rhodesiense* infection.

Despite the use of suramin for a hundred years, its mode of action against African trypanosomes is not completely understood. Suramin inhibits a number of different enzymes including many in the glycolytic pathway [57]. As a negatively charged molecule, suramin cannot cross membranes by diffusion and was proposed to be taken up through receptor-mediated endocytosis [58,59]. More recent RNAi target sequencing studies showed that knock-down of a number of endosomal and lysosomal genes leads to up to about 11-fold suramin resistance [42], substantiating an uptake route through endocytosis. Invariant surface glycoprotein 75 (ISG75) was proposed to act as the suramin receptor, since its knock-down led to a decrease in suramin sensitivity [42]. Suramin shows a high plasma protein binding with approximately 70% bound to albumin, 15% to low density lipoprotein (LDL) and 15% free [59]. Based on findings that trypanosomes took up >20-fold more suramin in the presence of LDL than in the presence of plasma, while the binding and uptake of LDL were up to 70% reduced in the presence of high micromolar concentrations of suramin [59], suramin was proposed to be taken up in complex with LDL. However, procyclic trypanosomes overexpressing the trypanosome ortholog of Rab4 showed a 50% decrease of suramin binding and almost no suramin uptake when compared to parental cells, while the uptake of LDL was unchanged [276]. The expression of a

constitutively activated version of Rab5 lead to increased LDL uptake without affecting suramin uptake, indicating that uptake of LDL and suramin are likely independent [276].

While resistance to suramin is widespread in the animal pathogen *Trypanosoma evansi* with 50% inhibitory concentrations (IC_{50}) of up to 40 µg/ml [60,61], there have not been any reports of suramin resistance in *T. brucei* spp. from the field. Nevertheless, resistance can be selected for under *in vitro* and *in vivo* conditions in the laboratory [248]. We recently described a variant surface glycoprotein, VSG^{Sur}, which is linked to suramin resistance [277]. VSG^{Sur} was identified by forward genetics. We had exposed *T. b. rhodesiense* STIB900 clones to high suramin concentrations (80-fold the IC_{50}), and within only one week they became resistant. Transcriptome sequencing showed that all the resistant lines had switched to express VSG^{Sur}. This phenomenon was reproducible in multiple independent experiments. The VSG^{Sur} expressing parasites showed an increase in IC_{50} of almost 100-fold for suramin, and cross-resistance to trypan blue, a trypanocidal dye related to suramin. We quantified the amount of intracellular trypan blue and observed a reduced uptake by VSG^{Sur} expressing parasites [277]. In the present study we investigate the effects of enforced VSG^{Sur} expression in a suramin-sensitive *T. b. brucei* line, aiming to uncover the molecular mechanisms underlying the link between VSG^{Sur} expression and suramin resistance.

4.3. Material and Methods

Chemicals were purchased from Merck KGaA, Darmstadt, Germany, if not otherwise stated.

T. brucei strains and cell culture

The Lister 427 derived *T. b. brucei* 2T1 strain [278] was cultivated in Iscove's Modified Dulbecco's culture Medium complemented according to Hirumi [262] and supplemented with 10% heat-inactivated fetal calf serum. Cells were cultured at 37°C, 5% CO_2.

Introduction of VSG^{Sur} into 2T1 cells

The plasmid previously described [277] was modified for the genomic replacement of the VSG^{221} by VSG^{Sur} in 2T1 cells. First the coding sequence of VSG^{900} within the plasmid was replaced by the coding sequence of VSG^{Sur} (GenBank accession MF093647), which was derived by PCR from cDNA of STIB900_c1_sur1 with primers containing XbaI and AscI

restriction sites (VSGsur_XbaI_F: taatctagaatgcaagccgtaacacgc, VSGsur_AscI_R: aatggcgcgccttaaaaaagcaaaaatgcaagc). The construct's framing UTRs used for homologous recombination were replaced with the UTR-regions of *VSG^{221}*. For the 5' genomic UTR of *VSG^{221}* a PCR product amplified from 2T1 gDNA was cloned into the plasmid. Primer used for the amplification of the 5' genomic UTR of *VSG^{221}* contained HindIII and NcoI sites (VSG221_5'UTR_HindIII_f: tagaagcttcaagcacaatttcatcctcct and VSG221_5'UTR_NcoI_r: catccatgggccgcgttcgtgtcg). Correct cloning was validated by sequencing. The 3' UTR was replaced during the final PCR on plasmid DNA using a forward primer, which binds to the 221 5'UTR sequence (VSG221_5'UTR_HindIII_f), and a reverse primer, which binds to the stop-codon of *VSG^{Sur}* and contains an overhang of 71 nucleotides from the *VSG^{221}* 3'UTR sequence. The resulting PCR product was framed by the 3' and 5' UTRs of *VSG^{221}* and contained a blasticidine-resistance gene, an αβ tubulin trans-splice site and the coding sequence of *VSG^{Sur}*. Five micrograms of the purified PCR product were used for the transfection of 4×10^7 2T1 cells in 100 µl Tb-BSF buffer [50] with an Amaxa Nucleofector using program Z-001. Positive transfected clones were obtained by limiting dilution in standard culture medium and after 24 h of incubation, blasticidine was added to a total concentration of 10 and 20 µg/ml. Four positive transfected clones and the untransfected parent strain were analyzed by qPCR regarding the expression of *VSG^{Sur}* and *VSG^{221}*.

RNA isolation and quantitative PCR

Parasites in the exponential growth phase were washed once with PBS and total RNA was isolated using the RNeasy Mini Kit (Qiagen, Hombrechtikon, Switzerland) including an on-column DNase treatment. SuperScript III Reverse Transcriptase (Invitrogen via Thermo Fisher Scientific, Illkirch Cedex France) and an oligo(dT) primer was used to synthesize complementary DNA (cDNA) out of 1-5 µg total RNA according to the manufacturer's protocol. Quantitative PCR was carried out in a Power SYBR Green Mix (Applied Biosystems via Thermo Fisher Scientific, Illkirch Cedex France) on a StepOnePlus real-time PCR machine (Applied Biosystems) in technical duplicates. The primers used for qPCR were tcattcgtttggccatacgc and ttactgacagacgaaccggc for *VSG^{Sur}* and aaggccaagaaagcg and ttggtaacgcctgttttg for *VSG^{221}*. The amplification plots were analyzed with StepOne Software v2.3. and the Ct values were normalized to the housekeeping gene telomerase reverse transcriptase using the ΔΔCt method.

Drug and human serum sensitivity assays

Suramin (sodium salt) (S2671) and pentamidine isethionate (P0547) were obtained from Sigma (now Merck), trypan blue (93590) from Fluka (now Merck) and melarsoprol from Sanofi-Aventis/WHO. *In vitro* drug sensitivities were determined with Alamar blue assays [265] using standard growth medium. Serial drug dilutions were prepared on a 96-well plate and parasites were added to a final concentration of 1×10^4 cells/ml. After incubation for 69 hours, resazurin was added to a final concentration of 11.4 µg/ml. Cells were incubated for 2-4 more hours and fluorescence of viable cells was quantified using a SpectraMax reader (Molecular Devices, Wokingham, Berkshire, United Kingdom) and SoftMax Pro 5.4.5 Software. Dose-response curves were fitted with a non-linear regression model (variable slope; four parameters, lowest value set to zero) and IC50 values were calculated with GraphPad Prism 6.00. Human serum sensitivity was determined using Alamar blue assays as above. But, instead of drug addition, limited dilutions were prepared with human serum and the medium used was HMI-9 supplemented with 15% heat-inactivated horse serum (i-horse). Human serum was obtained through centrifugation of whole blood of volunteers, heat inactivated at 56°C and stored at -20°C. Specific killing due to trypanolytic factor was checked by incubation of *T. b. gambiense* in 5% human serum of the same batch. *T. b. gambiense* cells were not lysed.

Trypan Blue uptake

Cells were harvested in the logarithmic growth phase and resuspended in standard growth medium at a concentration of 4×10^5 cells/ml. Trypan blue was added to the respective concentrations and cells incubated for 2 hours at 37°C. Subsequently, cells were centrifuged for 5 min at 3000 g at room temperature and washed twice with PBS. Cells were resuspended in 250 µl PBS and fixed in 5% formalin. Fluorescence intensities of the cells were measured with a BD FACSCaliburTM flow cytometer (BD Biosciences, San Jose, CA, USA). A total of 10 000 events were acquired within a gate of intact cells based on size versus granularity (FSC/SSC) and fluorescence of the gated cells was measured in the FL3 filter. The measured fluorescence intensities were analyzed with Flowing Software (version 2.5.1) using a refined FSCxSSC gate to exclude cell debris and an additional size versus fluorescence gate to exclude parasites that had already been dead during incubation with trypan blue and thus gave a much stronger signal. Fluorescence values were defined as the geometrical mean fluorescence of gated particles (>6000 per replicate).

ISG75 turnover

For each cell line and each timepoint, 40 ml cell cultures were prepared the day before the experiment. The cell density was adjusted for each sample to reach 1.2 $\times 10^6$ cells/ml. The next day, at the respective time points, cycloheximide (C7698 Sigma, now Merck) was added to the cultures to a concentration of 100 µg/ml. At timepoint zero, the cell densities were measured and the same number of cells was taken from each replicate. Cells were centrifuged for 10 min, 1000 g at room temperature. The supernatant was removed and the cell pellet resuspended in 1 ml PBS supplemented with protease inhibitor (cOmplete™, Mini, EDTA-free Protease Inhibitor Cocktail, Roche: 1 tab in 20ml) and centrifuged for 10 min, 1000g at room temperature. The cells were washed one more time with PBS containing protease inhibitor, supernatant was removed and 10 µl of 3 × Laemmli buffer added. Cells were further diluted with Laemmli buffer to reach a density of 5×10^6 cells/ 10 µl. Cells were sonicated and incubated at 70°C for 10 min. Samples were centrifuged at full speed in a microcentrifuge for 2 minutes and subsequently 10 µl of sample was loaded on a NuPAGE 4-12% Bis-Tris Protein Gel (Fisher Scientific - UK Ltd, Loughborough, United Kingdom) and run for 1 hour at 200 V in NuPAGE™ MOPS SDS Running Buffer (Fisher Scientific - UK Ltd, Loughborough, United Kingdom). Separated proteins were transferred to a polyvinylidene difluoride (PVDF) membrane (Immobilon-P; Millipore) in a TE22 wet transfer tank (GE healthcare) in SDS-Page running buffer supplemented with 20% methanol. The membrane was blocked with blocking buffer consisting of Tris-buffered saline with 0.01% Tween-20 (TBST) and 5% milk powder. Subsequently the membrane was incubated for 1 hour in blocking buffer containing the primary antibody. For ISG75 a 1:2,500 diluted polyclonal rabbit antibody was used and for EF1α a monoclonal mouse antibody (clone CBP-KK1; Millipore) was used in a 1:20,000 dilution. Membranes were washed with TBST three times for 5 minutes and incubated for one hour with a secondary goat anti-rabbit peroxidase-conjugated IgG (A0545, Sigma, now Merck) at a 1:20,000 dilution. Membranes were washed once with TBS and twice with PBS before addition of 1 ml Amersham ECL Western Blotting Detection Reagent (GE Healthcare Life Sciences, Buckinghamshire, UK). After two minutes of incubation, chemiluminescence was detected with a G:box imager (Syngene). Signals were quantified using ImageJ (Fiji) software [279].

ISG75 knock-down

A previously described pRPa plasmid for RNAi-mediated knockdown of ISG75 [42] was amplified in DH5α cells and digested with XhoI. A total of 6 µg purified digested plasmid was used to transfect 4×10^7 *VSG^{221}* respectively *VSG^{Sur}* expressing 2T1 cells. Transfection was carried out as described above and positive transfectants were selected with 10 µg/ml Hygromycin (Invivogen, Toulouse, France). Pseudoclones were picked after five days and RNAi-knockdown was induced by the addition of 1 µg/ml Tetracycline. To quantify the level of ISG75 knock-down, 72 hours after induction, RNA of induced and non-induced clones was isolated and qPCR was performed as described above [277] (chapter 3). Primers used for qPCR were ISG75qPCR_F (gcttgggttgcttgtgttct) and ISG75qPCR_R (tcgtatttttgcttttagcattagc).

Suramin wash-out assay

Serial drug dilutions were prepared on a 96-well v-shaped plate with the following media: HMI-9 with 15% inactivated horse serum, HMI-9 without serum, HMI-9 without serum but complemented with 10 µg/ml LDL and HMI-9 without serum but complemented with 0.5% bovine serum albumin (BSA, A7030). Parasites were washed twice with pre-warmed IMDM, eluted in the respective media and added to the assay plates to a final volume of 100 µl/well and a concentration of 1×10^5 cells/ml for the HMI-9 medium with 15% inactivated horse serum. Since the cells in the media without serum were not dividing during the incubation time, higher inocula were used and parasites were added to a concentration of 2×10^5 cells/ml. Plates were incubated for 4 hours at 37°C, 5% CO_2 and subsequently centrifuged at 1000 g for 3 minutes. 50 µl of the supernatant were removed and 150 µl pre-warmed IMDM was added to all the wells. Cells were washed 3 more times, each time 150 µl supernatant were removed and 150 µl IMDM or, in case of the last wash, 150 µl HMI-9 with 15% i-horse were added. After the last centrifugation 150 µl supernatant were removed and 50 µl HMI-9 with 15% i-horse were added to elute the parasites. A new flat-bottom plate was prepared with 50 µl HMI-9 with 15% i-horse and 50 µl of the eluted parasites were transferred to the new plate. The flat-bottom plate was incubated for another 64 hours before resazurin was added to a final concentration of 11.4 µg/ml. After another 4-5 hours of incubation at 37°C, 5% CO_2, fluorescence of viable cells was measured with a SpectraMax (Molecular Devices, Wokingham, Berkshire, United Kingdom) and SoftMax Pro 5.4.5 Software. Dose-response curves were fitted with a non-linear regression model

(variable slope; four parameters, lowest value set to zero) and IC50 values were calculated with GraphPad Prism 6.00.

Uptake and binding of transferrin and low density lipoprotein

To quantify the uptake of transferrin and LDL, cells in the logarithmic growth phase were washed once with serum-free medium supplemented with 1% BSA and resuspended in serum-free medium supplemented with 1% BSA at a concentration of 2×10^6 cells/ml. 392 µl (for the transferrin uptake experiment) and 95 µl (for the LDL uptake experiment) of resuspended parasites were transferred to Eppendorf tubes. Cells were pre-incubated for 15 minutes at 37°C to internalize surface bound transferrin and LDL. At the respective timepoints fluorescently labeled transferrin (Alexa Fluor™ 488 Conjugate, T13342, Fisher Scientific, Illkirch Cedex, France) was added to a concentration of 50 µg/ml or fluorescently labeled LDL (Bodipy FL, I34359, Fisher Scientific, Illkirch Cedex, France) to a concentration of 10 µg/ml. At time point zero, cells were quenched by putting them on ice and by addition of 1 ml ice-cold PBS. Cells were centrifuged for 5 minutes at 1000 g at 4°C and washed once with ice cold PBS. Cells were fixed and fluorescence quantified as described above.

To quantify the impact of suramin on the uptake of transferrin and LDL, cells were washed once with IMDM and eluted in IMDM without BSA to a concentration of 2×10^6 cells/ml. The experiment was performed without BSA, since otherwise the majority of suramin would bind to BSA. Cells were pre-incubated for 15 minutes (transferrin) or for one hour (LDL) at 37°C. Suramin was added to concentrations between 0 and 1000 µM and subsequently transferrin or LDL were added to concentrations of 5 or 10 µg/ml respectively. Cells were incubated for 10 minutes (transferrin) or for 20 minutes (LDL) at 37°C, quenched, washed and fixed as described above.

For the quantification of transferrin and LDL binding to the cell surface, cells were washed with IMDM and eluted in IMDM to a concentration of 1×10^7 cells/ml. Cells were pre-incubated for 15 minutes (transferrin) or for one hour (LDL) at 37°C and subsequently chilled on ice for 15 minutes. Either suramin or cold PBS was added and subsequently transferrin or LDL were added to a concentration of 800 or 100 µg/ml respectively. Cells were incubated for 10 minutes on ice, subsequently washed twice with ice-cold PBS and fixed as described above.

Concanavalin A uptake and binding

Trypanosomes in the logarithmic growth phase were centrifuged at 1000 g for 5 minutes, the cell pellet was eluted in IMDM with 1% bovine serum albumin (BSA) to a concentration of 2×10^6 cells/ml. 498 µl of the eluted parasites were put in 1.5 ml Eppendorf tubes and pre-incubated at 37°C for 15 minutes. At the respective time points FITC conjugated Concanavalin A (C7642 Sigma, now Merck) was added to a concentration of 5 µg/ml. After incubation at 37°C cells were quenched on ice by addition of ice-cold PBS. Subsequently cells were centrifuged for 5 minutes at 1000 g at 4°C and washed once with PBS. Cells were eluted in 250 µl PBS and fixed by addition of 250 µl 10% formalin.

For the quantification of surface bound ConA, cells were centrifuged and eluted in IMDM with 1% BSA to a concentration of 2×10^6 cells/ml. These were pre-incubated on ice for 15 minutes and subsequently the ConA was added to concentrations of 0, 5, 20 and 50 µg/ml. After incubation on ice for 10 minutes, ice-cold PBS was added, the cells centrifuged at 4°C (5 minutes, 1000 g) and subsequently washed one more time with ice-cold PBS, eluted in 250 µl PBS and fixed by addition of 250 µl 10% formalin.

Fluorescent intensities of the cells were measured as described above but using the FL1 filter. Fluorescence values were defined as the geometrical mean fluorescence of >9000 events.

4.4. Results

4.4.1. Expression of *VSG^{Sur}* renders *T. b. brucei* resistant to suramin

To test the hypothesis that expression of *VSG^{Sur}* is sufficient to cause suramin resistance in *T. brucei*, we introduced the *VSG^{Sur}* gene into the active *VSG* expression site of *T. b. brucei* 2T1, a well-established *T. b. brucei* bloodstream-form laboratory line [278]. 2T1 cells naturally express *VSG^{221}* [280], also called MITat1.2 (GenBank: X56762.1). To replace *VSG^{221}* with *VSG^{Sur}* we made a construct (Fig 1A) which contained the coding sequence of *VSG^{Sur}* together with a blasticidine resistance gene, framed by the sequence of the 5'and 3' regions of *VSG^{221}*. Four transfected clones were recovered, all of which showed no expression of *VSG^{221}* and expressed *VSG^{Sur}* at the same level as the parental line expressed *VSG^{221}* (determined by qPCR using telomerase reverse transcriptase (TERT) as a reference; Fig 1B). Two of the *VSG^{Sur}* expressing transfectants (2T1_sur1 and 2T1_sur4) were chosen for further analysis. Proliferation was essentially indistinguishable from the parent cell line when cultivated in standard medium without blasticidine (Fig 1C). The 50% inhibitory concentration (IC_{50}) for suramin increased from 12 nM in the *VSG^{221}* expressing parent to 700 nM in the two *VSG^{Sur}* expressing transfectants ($p = 0.0036$, One-Way ANOVA; Fig 1D). No alterations of drug sensitivities were observed for melarsoprol or pentamidine, excluding a non-specific drug resistance mechanism. However, the *VSG^{Sur}* expressing cells showed weak cross-resistance to trypan blue, with an elevation of the IC_{50} from 13 µM in the *VSG^{221}* expressing parent to 19 and 21 µM in the *VSG^{Sur}* expressing transfectants, but this was statistically non-significant.

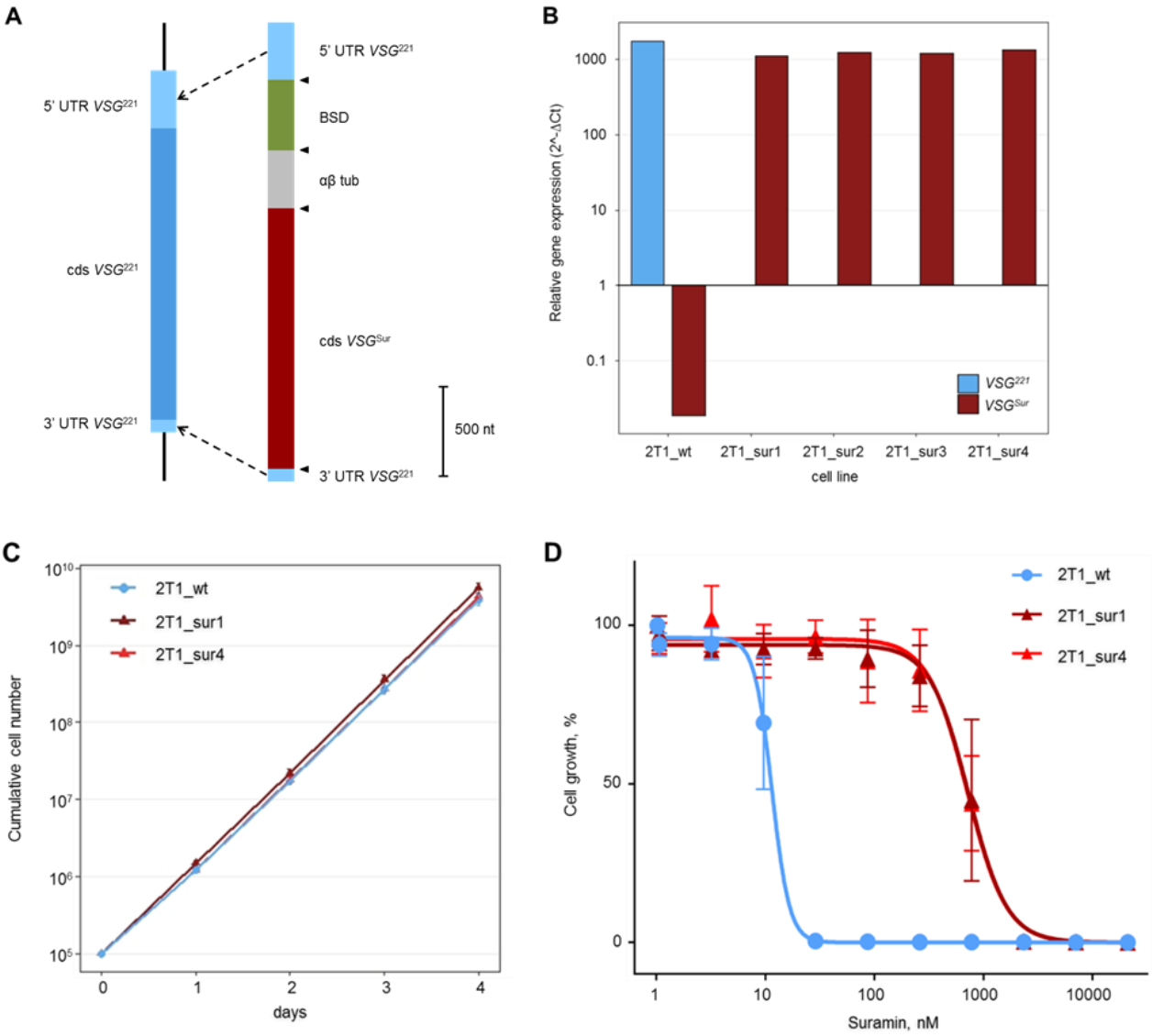

Figure 1: Introduction of VSG^{Sur} into the active bloodstream expression site renders 2T1 cells suramin-resistant. (A) Schematic illustration of VSG^{221} within the active bloodstream expression site of 2T1 cells before transfection and of the construct used for the *in situ* replacement of VSG^{221} with VSG^{Sur}. The construct is framed with the 5' region of VSG^{221} with adjacent sequence on one side and the 3' region of VSG^{221}on the other side; it contains a blasticidine resistance gene (BSD), an αβ tubulin splice site (αβ tub) and the coding sequence (cds) of VSG^{Sur}. Triangles indicate restriction-sites. (B) Expression of VSG^{Sur} and VSG^{221} as determined by qPCR in the parent 2T1 strain (2T1_wt) and in 4 transfected clones (2T1_sur1-4). Values shown are derived from technical duplicates; they represent expression levels normalized to the housekeeping gene *TERT*. The transfected clones show a high expression level VSG^{Sur}, comparable to the expression level of VSG^{221} in the 2T1 parent cells. (C) Cumulative cell number as measured over four days, error bars represent standard deviations (n=3). (D) Dose-growth curves for suramin show an 58-fold decrease in suramin sensitivity after introduction of VSG^{Sur} (n = 3).

4.4.2. *VSG^{Sur}* expressing cells show a reduced uptake of trypan blue

We exploited the fact that trypan blue becomes fluorescent when bound to proteins [255,281] to investigate drug uptake by *T. b. brucei* 2T1. Cells were incubated with different concentrations of trypan blue at 37°C and subsequently the fluorescence of cell-associated trypan blue quantified by flow cytometry. In the cell size versus fluorescence scatters, gates were set to exclude dead cells, which give a much stronger signal than live cells [255]. *VSG^{Sur}*-expressors showed a 30-50% reduction of fluorescence when compared to their *VSG^{221}* expressing parent (Fig 2). This is consistent with the small increase in the IC_{50} towards this compound.

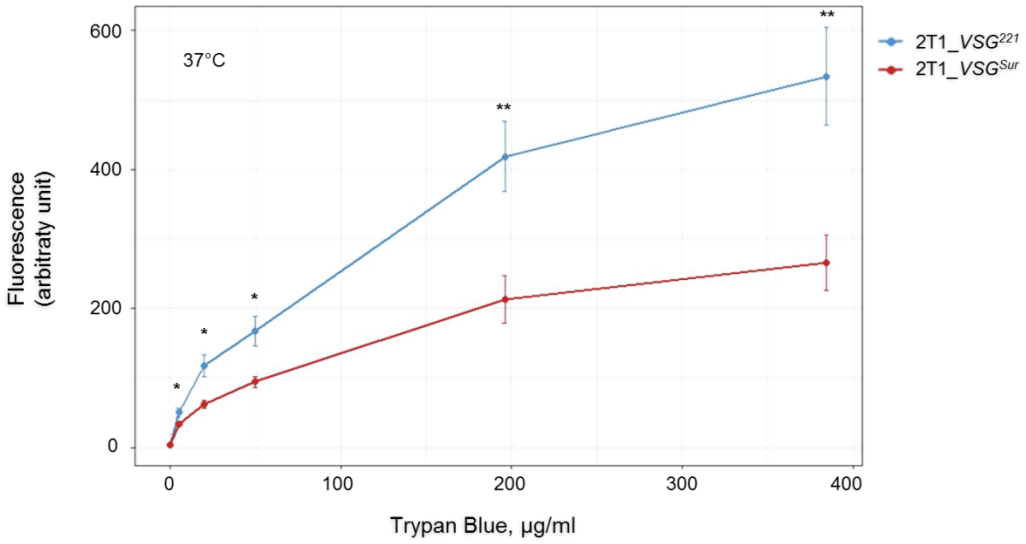

Figure 2: Trypan blue uptake

The trypan blue uptake of *VSG^{Sur}*and *VSG^{221}* expressing cells as determined by FACS after incubation for 2 hours at 37°C. Error bars represent standard deviations of three independent experiments (*= p<0.05; **= p<0.01, paired t-test).

4.4.3. VSG^{Sur}-mediated suramin resistance is not linked to ISG75

Since some suramin resistance can be caused by ISG75 depletion [42], we investigated a possible effect of VSG^{Sur} on ISG75 turnover. Therefore, cells were incubated with cycloheximide to block protein synthesis, and the steady-state ISG75 levels were determined after 0, 2, 4 and 6 hours by Western blotting. The ISG75 half-life was around 3 hours in both the *VSG^{221}* expressing and the *VSG^{Sur}* expressing trypanosomes (Fig 3A). We further investigated the effect of ISG75 depletion in *VSG^{Sur}*-expressors (2T1_sur1) and parental cells (2T1_wt) by introduction of a pRPA-based, tetracycline-inducible RNAi

knock-down construct. Induction of RNAi for 72 hours led to a 75-85% reduction of *ISG75* mRNA levels in 5 (2T1_wt_c1 and c3; 2T1_sur1_c1 to c3) out of 6 clones as determined by qPCR (Fig 3B). Growth was slightly faster under knock-down of *ISG75* with an average population doubling time of 6.9 h in the presence of tetracycline compared to 7.2 h without tetracycline (p-value = 0.003, paired t-test including all clones, Fig 3C). Suramin sensitivity decreased in all the tested clones upon down-regulation of ISG75 (Fig 3D). The presence of ISG75-dependent suramin uptake also in the VSGSur-expressors indicates that this is not the pathway affected by VSGSur. Moreover, the effect of ISG75 silencing on suramin sensitivity was clearly stronger (p = 0.009, Welch Two Sample t-test) in the VSGSur-expressors: the IC50 of suramin upon ISG75 knock-down increased 2.2 and 3.8 fold in parental 2T1 cells, and 7.9, 8.1 and 6.7 fold in *VSG*^{Sur}-expressors (Fig 3D). This is in agreement with the above hypothesis, that a pathway distinct from ISG75 is affected and hence, ISG75 confers a larger proportion of suramin uptake in the *VSG*^{Sur} expressing trypanosomes.

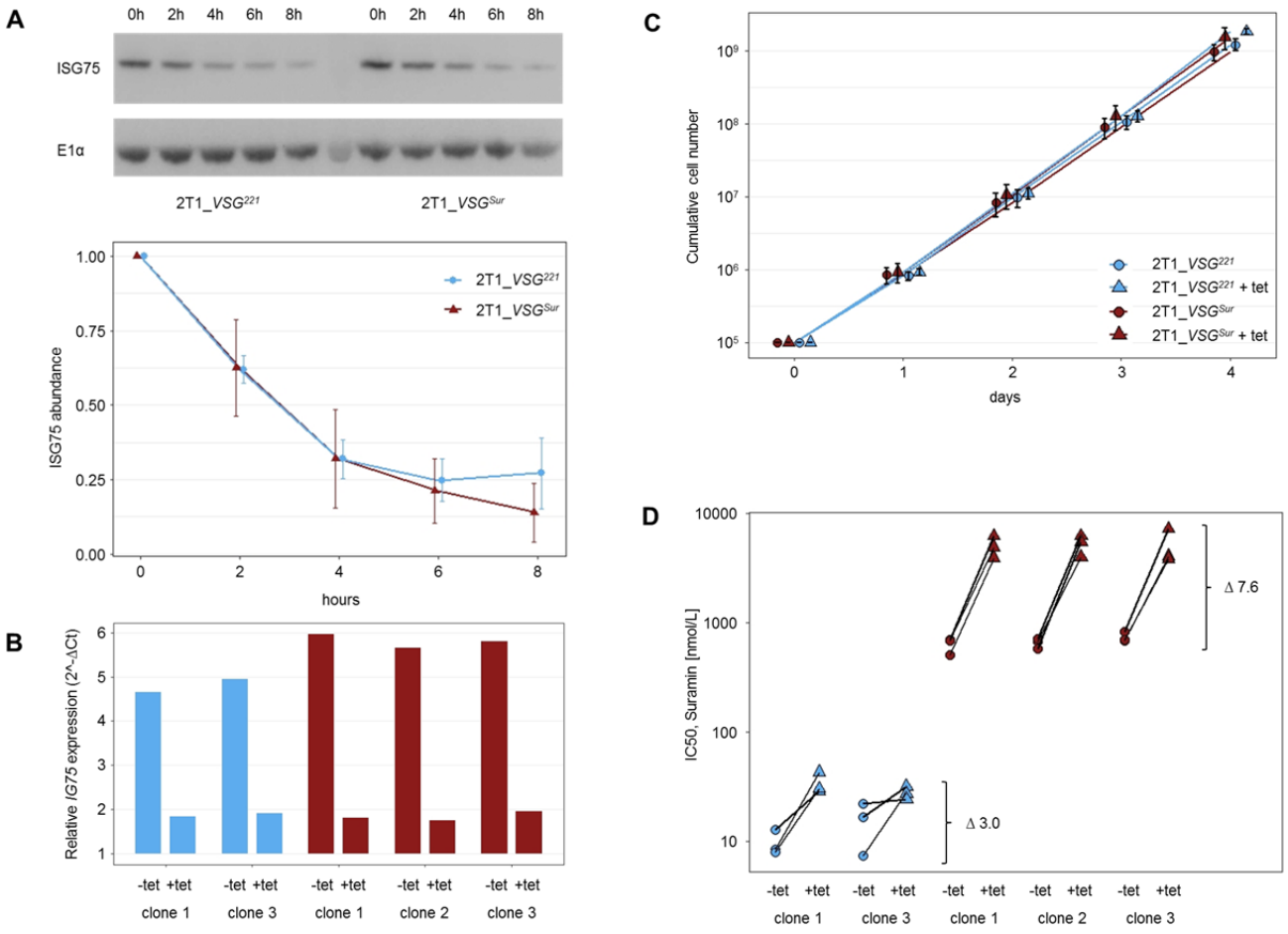

Figure 3: ISG75 expression and effect on suramin sensitivity (blue: parental, *VSG^{221}* expressing cells; red: *VSG^{Sur}* expressing cells).
(A) ISG75 turnover as determined by western blot after inhibition of translation for different time spans. Plotted data points represent mean amounts of protein from two independent experiments, for each experiment two technical replicates (western blots) were made. (B) Reduction of *ISG75* expression levels upon RNAi knockdown. Gene expression levels are normalized to the housekeeping gene *TERT*, values shown are derived from technical duplicates. (C) Cumulative growth curves of *VSG^{Sur}* and *VSG^{221}* expressing cells +/- ISG75 knockdown. Values shown are the averaged growth curves for each group, including two biological replicates from each clone (2T1_wt_c1 and c3 for the *VSG^{221}*-expressor and 2T1_sur_c1, c2 and c3 for the VSG^{Sur}-expressor). The data points represent mean cell numbers plotted with the position_dodge function in R to allow visual distinction between the groups. Error bars represent standard deviation. (D) 50% inhibitory concentrations for suramin of *VSG^{Sur}* and *VSG^{221}* expressing cells +/- ISG75 knockdown. Δ represents the factor of increase upon ISG75 knockdown.

4.4.4. Effects of serum proteins on suramin susceptibility

Having excluded defects towards ISG75 turnover as a reason for the decreased suramin sensitivity of *VSG^{Sur}* expressing cells, we tested for the involvement of serum proteins in VSG^{Sur}-mediated suramin resistance. This had to be performed with wash-out assays since the trypanosomes cannot be cultivated without serum proteins over long periods. Parental, *VSG^{221}* expressing 2T1 cells and *VSG^{Sur}*-expressors were incubated for 4 hours with suramin in HMI-9 medium without serum proteins, in HMI-9 supplemented with albumin, with LDL or with serum respectively, washed, and incubated in standard growth medium (without suramin) for 3 days. As expected, the IC_{50} in these assays (Fig 4) were higher than in the standard 72 h assay, since suramin was only present for the first 4 hours. Nevertheless, cells incubated in medium without any serum proteins were highly sensitive to suramin: they showed a decrease in IC_{50} of 98% for *VSG^{221}* and of 95% for *VSG^{Sur}*-expressing cells when compared to the IC_{50} of cells incubated in medium with serum. This demonstrates that free suramin is taken up by trypanosomes. Addition of bovine serum albumin (BSA) counteracted suramin toxicity, indicating that suramin is sequestered by binding to albumin, which is in agreement with previous findings [59]. The same effect can also explain why the trypanosomes were less suramin sensitive in the presence of serum than without serum. Addition of LDL further increased suramin susceptibility of serum-free cultures (50% decrease of IC_{50}; Fig. 4). However, this effect was only observed in parental, *VSG^{221}* expressing cells but not in the *VSG^{Sur}* expressing cells (p-value = 0.008, paired t-

test). These data suggest that *VSG*^{Sur} expression abolished LDL-mediated uptake of suramin.

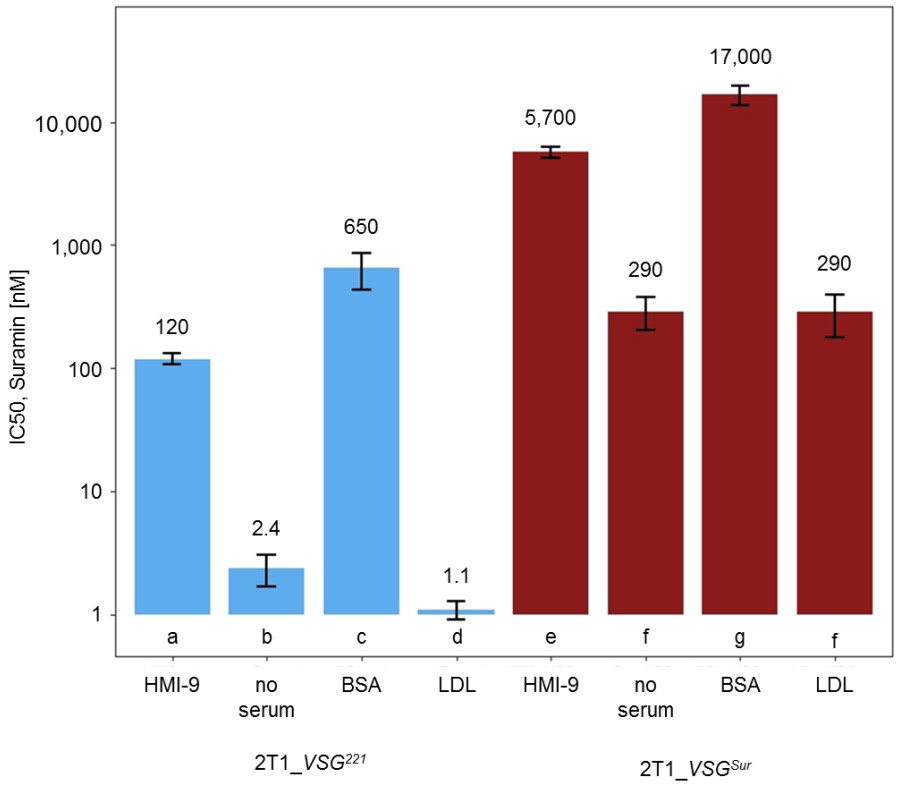

Figure 4: 50% inhibitory concentrations in presence of different serum proteins.
Parasites were incubated either in standard growth medium with 15% inactivated horse serum (HMI-9), in HMI-medium without any serum (no serum), in HMI-medium without serum supplemented with albumin (BSA), or in HMI-medium without serum supplemented with LDL (LDL). Values that differed significantly ($p<0.05$, Tukey's multiple comparison test on logarithmic data) are labeled with different letters (a-g) (independent biological replicates: n = 3 for "HMI-9" and "BSA"; n = 4 for "no serum" and "LDL"; each biological replicate consisted of two technical replicates).

4.4.5. The effect of VSG^{Sur} and suramin on LDL uptake

To measure uptake of LDL, *T. b. brucei* 2T1 cells were incubated for different times with fluorescently labeled LDL at 37°C to allow endocytosis, and the internalized LDL was quantified using FACS. No plateau was reached within 120 minutes incubation time, neither for *VSG*^{221} nor for *VSG*^{Sur} expressing cells (Fig 5A). LDL uptake was highly reduced in *VSG*^{Sur} expressing cells with an 80-90% lower fluorescence than *VSG*^{221}-expressors

throughout the 5 to 120 minute period (Fig 5A). The presence of suramin led to reduction of LDL uptake in wild type cells but not in *VSG^{Sur}*-expressors (Fig 5B). To differentiate whether the reduced LDL uptake is mediated through a reduced binding or endocytosis, we looked at the binding of LDL to the cell surface. LDL binding at 4°C was around 30 % reduced in *VSG^{Sur}* compared to *VSG^{221}* expressing cells (overall p-value = 0.0003, paired t-test). Thus, the highly reduced LDL uptake cannot be explained by a reduction of the binding alone and a reduced endocytosis seems to play a major role. No effect on binding was observed in the presence of suramin (Fig 5C).

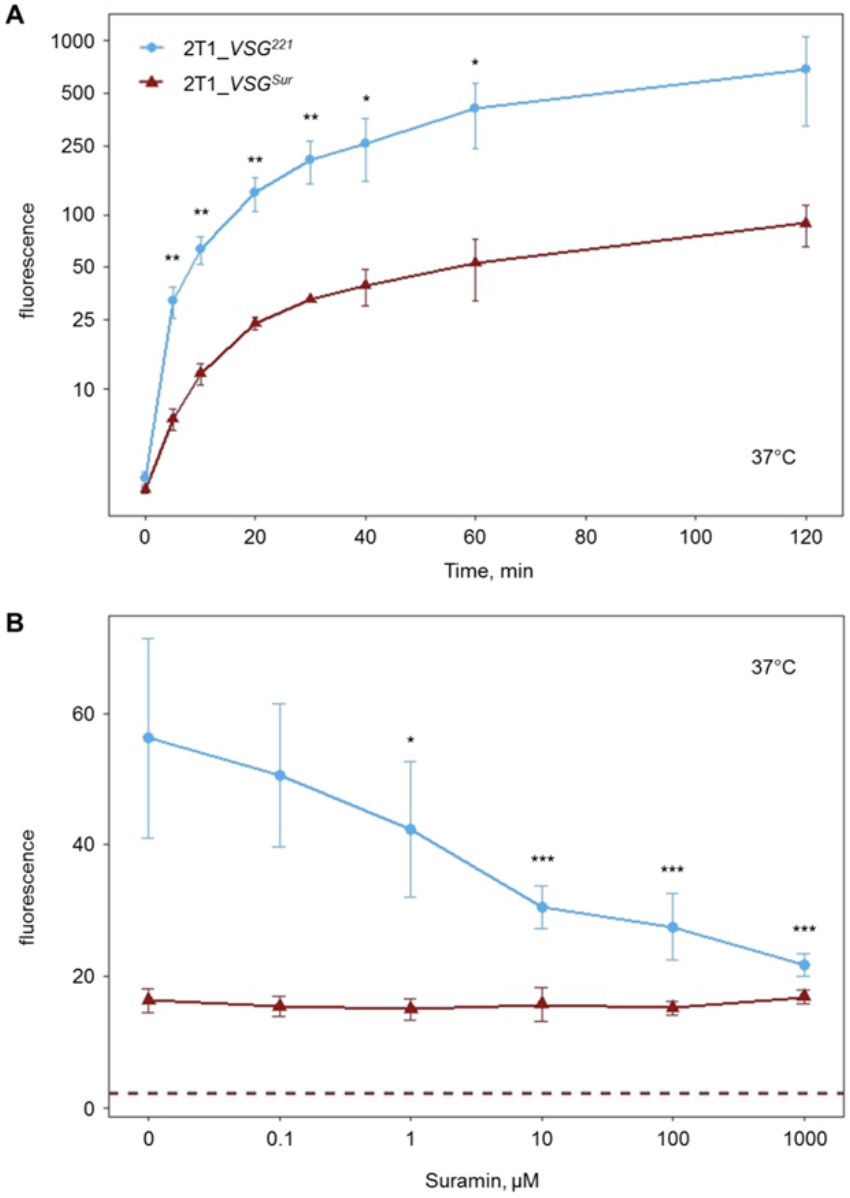

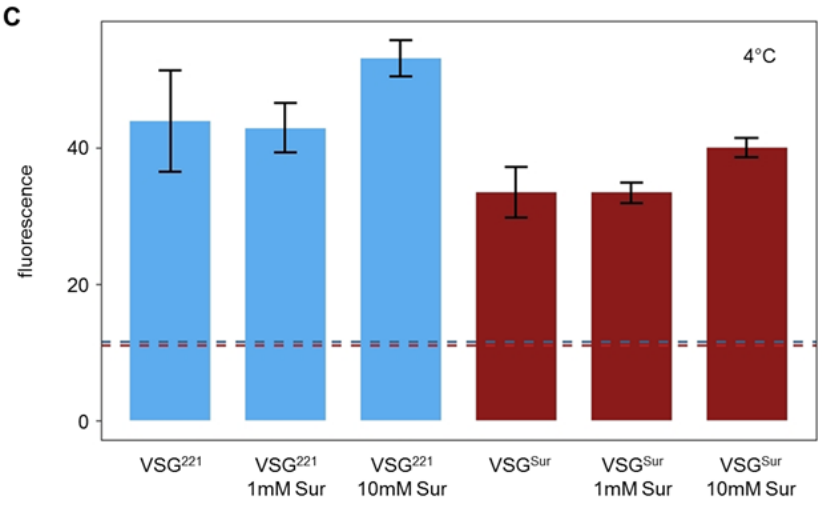

Figure 5: Uptake and binding of fluorescently labeled low density lipoprotein and the effect of suramin

(A) Uptake of low density lipoprotein over a period of 2 hours, error bars represent standard deviations (*= p<0.05; **= p<0.01; n=3 for timepoint 120 min; n=4 for timepoints 0-60 min; paired t-test). (B) Impact of suramin on the uptake of LDL during 20 minutes of incubation, asterisk represent significant p-values if fluorescence of *VSG^{221}* expressing cells under incubation with suramin is compared to the fluorescence of *VSG^{221}* expressing cells under incubation without suramin (*=p<0.05; **= p<0.01; ***=p<0.001; n=3, pairwise t-test with Bonferroni correction), error bars represent standard deviations. Dotted lines represent baseline, which was defined as fluorescence of cells which were incubated with the same amount of LDL but on ice to inhibit endocytosis. (C) Binding of LDL to the cell surface. Dotted lines represent background fluorescence of *VSG^{221}* expressing (blue) and *VSG^{Sur}* expressing (red) cells incubated without fluorescently labeled LDL. Error bars represent standard deviations of three measurements (two for 10 mM suramin).

4.4.6. The effect of VSG^{Sur} and suramin on transferrin uptake

We investigated uptake of transferrin as an additional substrate that is imported by receptor-mediated endocytosis [282,283]. Again, trypanosomes were incubated for different periods with fluorescently labeled transferrin at 37°C and analyzed by FACS. In *VSG^{221}* expressing 2T1 cells transferrin was quickly internalized, reaching a plateau of more than 4 times background fluorescence after ten minutes (Fig 6A). In contrast, *VSG^{Sur}* expressing 2T1 cells incubated with labeled transferrin only showed a slight increase of fluorescence to 1.5

times background level (Fig 6A), which corresponds to an 80% lower fluorescence than observed in parental cells. Since transferrin uptake had been described to be reduced in the presence of suramin in HeLa cells [284], we investigated the effect of suramin on transferrin uptake in *T. brucei*. Cells were incubated with fluorescently labeled transferrin in different concentrations of suramin for 10 minutes (the incubation time was kept short to limit the toxic effects of suramin). At concentrations below 300 µM, suramin had no effect on transferrin uptake; only at very high suramin concentrations, reduced amounts of intracellular transferrin were measured in *VSG^{221}* expressing cells (Fig 6B, p-values of 0.04 and 0.006 for concentrations of 300 and 1000 µM respectively, pairwise t-test with Benjamini Hochberg correction). To differentiate whether the reduced internalization of transferrin in *VSG^{Sur}* expressing cells was caused by reduced binding or reduced endocytosis, we quantified surface binding of transferrin to trypanosomes by incubating the cells on ice. The fluorescence of *VSG^{Sur}* expressing cells incubated without suramin was around 40% lower than the fluorescence of the *VSG^{221}* expressing cells (Fig 6). Thus again, the highly reduced transferrin uptake cannot be attributed to reduced binding. Upon addition of suramin at 1 mM and 10 mM, the difference between *VSG^{221}* and *VSG^{Sur}*-expressors became smaller (Fig 6C). However, at such high suramin concentrations we cannot exclude an ionic effect. The overall p-value of the difference between *VSG^{221}* and *VSG^{Sur}*-expressors was 0.03.

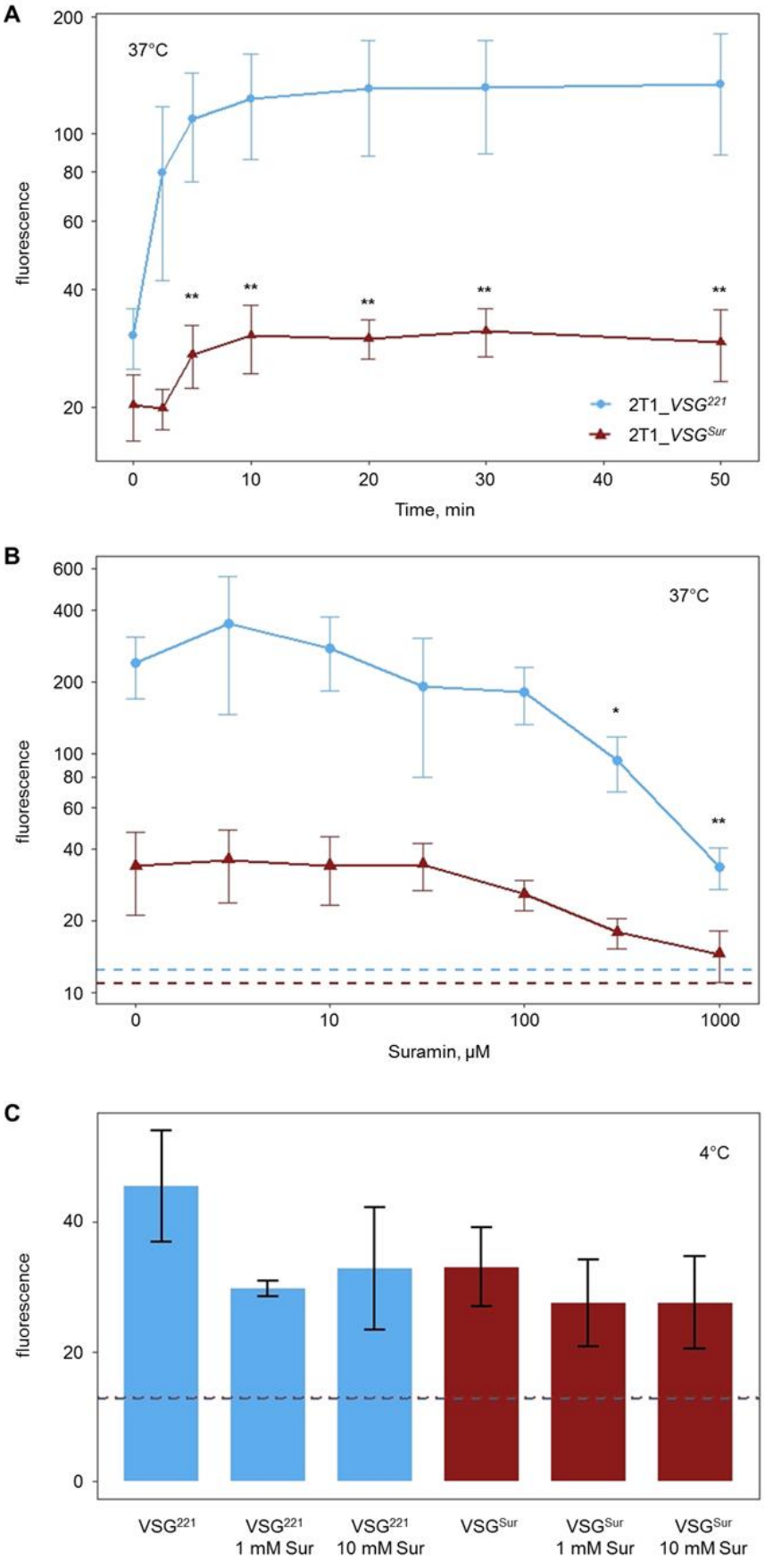
A
37°C
fluorescence
200
100
80
60
40
20
**
**
**
**
**
2T1_VSG221
2T1_VSGSur
0
10
20
30
40
50
Time, min
B
37°C
fluorescence
600
400
200
100
80
60
40
20
10
*
**
0
10
100
1000
Suramin, µM
C
4°C
fluorescence
40
20
0
VSG221
VSG221 1 mM Sur
VSG221 10 mM Sur
VSGSur
VSGSur 1 mM Sur
VSGSur 10 mM Sur

Figure 6: Uptake and binding of fluorescently labeled transferrin and the effect of suramin
(A) Transferrin uptake of *VSG^{Sur}* and *VSG^{221}* expressing cells at 37°C over time. Error bars represent standard deviation of four independent experiments (*= p<0.05; **= p<0.01, paired t-test). (B) Influence of suramin on transferrin uptake. Data of three independent experiments are shown, error bars represent standard deviations. Dotted lines represent baseline, which was defined as fluorescence of cells which were incubated with the same amount of transferrin but on ice to inhibit endocytosis. (C) Transferrin binding to the cell surface with and without suramin as determined after incubation of cells on ice. Dotted lines represent background fluorescence of *VSG^{221}* expressing (blue) and *VSG^{Sur}* expressing (red) cells incubated without fluorescently labeled transferrin. Error bars represent standard deviations of three measurements (two for 10 mM suramin).

4.4.7. The effect of VSG^{Sur} on VSG endocytosis

Variant surface glycoproteins are endocytosed at a very high rate with a turnover equivalent to the whole surface coat within 12 minutes [261]. To test whether *VSG^{Sur}* expression has a general impact on endocytosis, we investigated endocytosis of *VSG^{Sur}* and *VSG^{221}*. Concanavalin A (ConA) is a lectin that binds to glycosylated surface proteins, in case of trypanosomes mainly to VSG [285]. It is endocytosed together with the VSG and can therefore be used to measure VSG endocytosis rates. Cells were incubated for time periods of 0 to 60 minutes at 37°C with 5 µg/ml fluorescently labeled ConA. Subsequently cells were fixed, and the fluorescence of cell-associated ConA was measured by flow cytometry. Up to an incubation period of 20 minutes fluorescence levels were in the same range or even higher for *VSG^{Sur}* than for *VSG^{221}*-expressors. Thereafter *VSG^{Sur}*-expressors showed a slightly lower fluorescence than VSG221-expressors (Fig 7A). Since ConA does not bind equally well to all VSGs [285] we examined the ConA binding capacity of the two cell lines. The cells were incubated with different concentrations of ConA on ice to prevent endocytosis, and surface bound ConA was quantified by flow cytometry. VSGSur expressing cells showed a 22-34% higher fluorescence than VSG221-expressors (p-value = 0.0097, paired t-test, Fig 7B). Taken together, the facts that VSGSur-expressors showed similar levels of internalized ConA as VSG221-expressors at 37°C but more surface bound ConA at 4 °C, indicate that endocytosis of VSG may be slightly reduced in *VSG^{Sur}* expressing cells. However, we observed no enlargement of the flagellar pocket, which is a hallmark for blocked endocytosis.

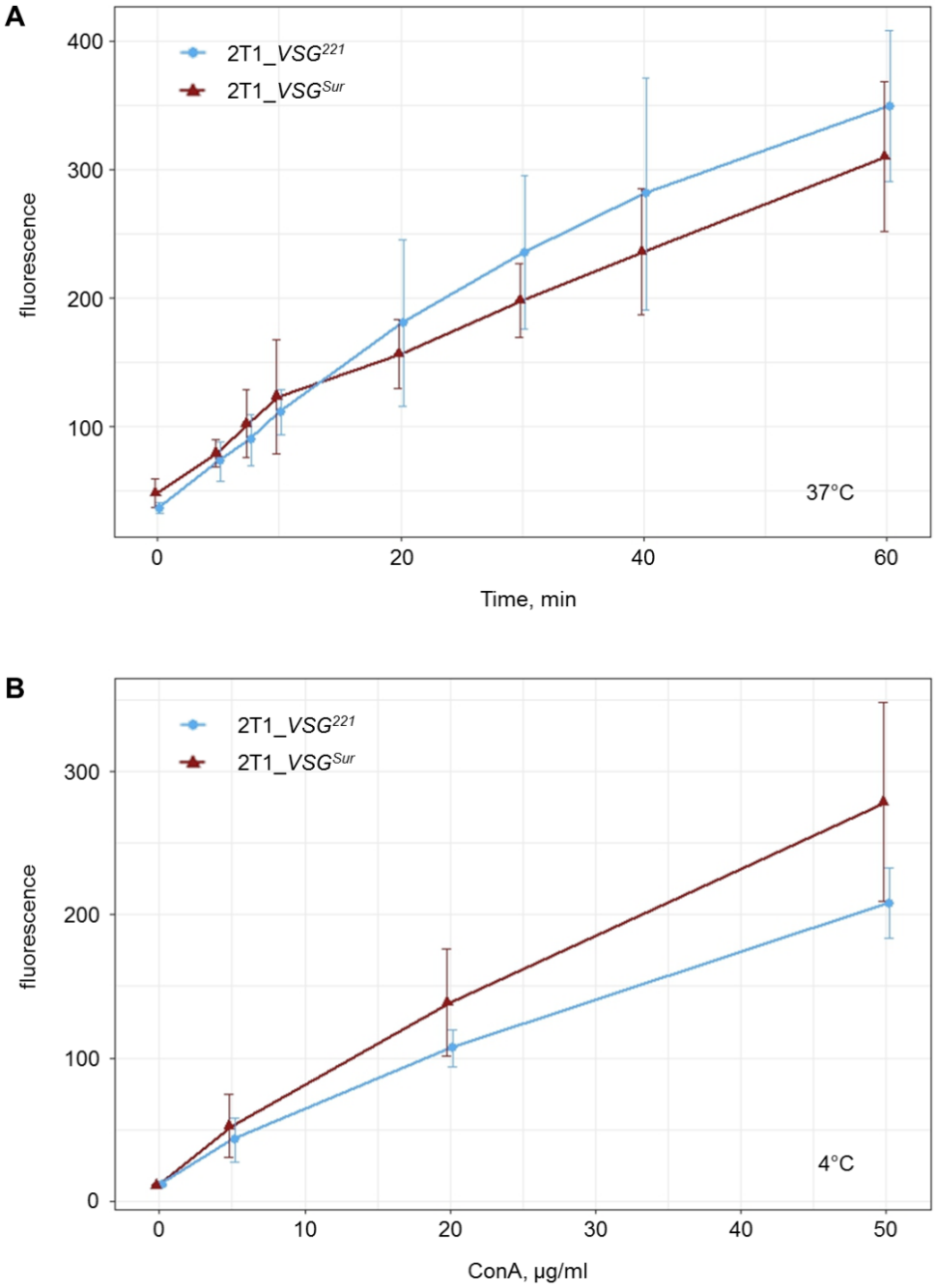

Figure 7: Concanavalin A uptake and binding in *VSG*^{Sur} and *VSG*^{221} expressing cells.

(A) Fluorescence of cells incubated with 5 µg/ml labeled ConA at 37°C, time point zero represents cells that were kept on ice before addition of ConA in order to allow binding but not uptake. Error bars represent standard deviations of five (for timepoint 60 only four) independent experiments.

(B) Fluorescence of surface bound ConA of cells incubated with different ConA concentrations at 4°C to prevent endocytosis. Error bars represent standard deviation of four independent experiments.

4.4.8. The effect of VSG^{Sur} on sensitivity to human serum

Most trypanosome species other than *T. b. rhodesiense* and *T. b. gambiense* are lysed by the two trypanolytic factors (TLF1 and TLF2) present in human serum. TLF1, a high density lipoprotein complex, and TLF2, a protein complex, both contain apolipoprotein L1 [286], which mediates trypanolysis [287]. TLF1 is much more active than TLF2 and kills *T. b. brucei* at very low concentrations in the absence of competing haptoprotein [288]. TLF1 binds to the haptoglobin-haemoglobin receptor (TbHpHbR) in the flagellar pocket and is subsequently endocytosed [289]. To test whether the endocytosis of the TbHpHbR is affected by *VSG^{Sur}* expression, sensitivity to human serum was tested. However, bloodstream-form *T. b. brucei* 2T1 expressing *VSG^{Sur}* or *VSG^{221}* were equally sensitive (Fig 8). This demonstrates that endocytosis of the trypanolytic factor of human serum, and the downstream mechanisms of cell lysis, are not affected by VSG^{Sur}.

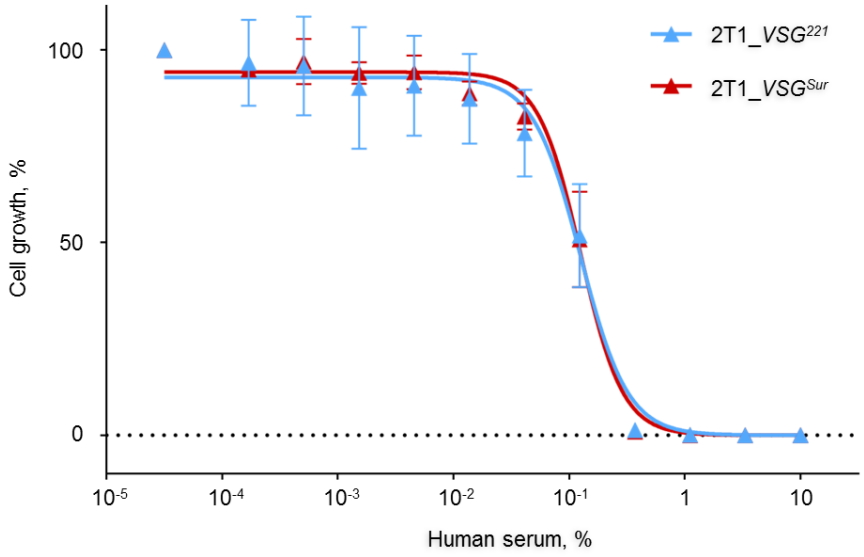

Figure 8: Sensitivity to normal human serum.

4.5. Discussion

We have originally identified VSG^{Sur} as the VSG expressed in bloodstream-form *T. brucei* spp. that had been selected *in vitro* for resistance to suramin [277]. The resistant cells had IC_{50} values to suramin of around 1.2 µM, which was almost 100-fold above the IC_{50} of the parental cells but still below the suramin plasma levels of 70 µM in the treated patients [25]. Thus expression of VSG^{Sur} is unlikely to cause suramin treatment failure in patients. Nevertheless, it is intriguing how a particular VSG can be linked to drug susceptibility.

Here we show that transgenic expression of *VSG^{Sur}* is sufficient to cause suramin resistance in *T. b. brucei*, which is otherwise highly sensitive to the drug. Based on the reduced uptake of trypan blue by the cells that express *VSG^{Sur}*, our working hypothesis is that suramin resistance is mediated by a reduced drug uptake. Trypanosomes take up suramin through receptor-mediated endocytosis [58,59]. Endocytosis in trypanosomes takes place at the flagellar pocket and the most abundantly endocytosed protein is VSG itself. VSGs are endocytosed into Rab5a endosomes [290] at a very high rate [261]. Subsequently the VSG is recycled back to the trypanosome surface by exocytosis via Rab11 exocytic carriers [291].

Concanavalin A, a lectin which binds to VSG, can be used as a marker to track VSG internalization [292]. We did not observe distinct alterations of ConA endocytosis in *VSG^{Sur}* expressing trypanosomes, neither by flow cytometry nor by fluorescence microscopy (not shown) and conclude that if there is an effect on VSG internalization at all, it is only marginal. Transferrin and low density lipoprotein (LDL) are important nutrients for African trypanosomes [293,294]. Transferrin binds to the transferrin receptor, which is a heterodimer of ESAG6 and ESAG7, and is subsequently endocytosed in Rab5a endosomes similar to the VSGs [290]. Once the ligand is removed, transferrin receptors are recycled to the cell membrane. Similar to VSG, this happens at a very high rate with a turnover of only 11 minutes [295]. LDL is imported via receptor-mediated endocytosis as well. The LDL receptor is supposedly located at the flagellar pocket and on the flagellar membrane [296], but it has not been identified. As determined by flow cytometry, the *VSG^{Sur}*-expressors showed highly reduced intracellular levels of fluorescently labeled transferrin and fluorescently labeled LDL after incubation at 37°C. This suggests that *VSG^{Sur}* expression impairs endocytosis of the LDL receptor and the transferrin receptor. However, expression of *VSG^{Sur}* did not alter sensitivity to human serum, indicating that endocytosis of the

TbHpHb receptor is not affected. The HpHb receptor is a glycosylphosphatidylinositol (GPI) anchored, glycosylated surface protein located at the flagellar pocket [289]. Taken together, *VSG^{Sur}*-expressors showed a normal growth and no enlarged flagellar pockets, thus we assume that VSG^{Sur} has no effect on bulk endocytosis. Receptor-mediated endocytosis is affected by VSG^{Sur}, but only specific pathways. While endocytosis of transferrin is highly reduced, endocytosis of the VSG may be moderately reduced, and endocytosis of the HpHb receptor unaffected by *VSG^{Sur}* expression. Additionally, and most importantly for suramin susceptibility, endocytosis of the elusive LDL receptor is highly reduced.

Suramin inhibited uptake of LDL by *VSG^{221}* expressing cells, in agreement with published results [59], but not in *VSG^{Sur}* expressing cells. Short-term suramin wash-out experiments in serum-free medium indicated that suramin uptake is lowest in the presence of albumin and intermediate in the presence of serum, which confirms the literature [59]. We further show for the first time that suramin is also taken up in the absence of serum. The addition of LDL appeared to increase suramin uptake in *VSG^{221}* expressing cells, which is in accordance with the literature [59], but not in *VSG^{Sur}*-expressors. On the other hand, knockdown of ISG75 had a stronger effect on suramin sensitivity in *VSG^{Sur}*-expressors than in *VSG^{221}* expressing cells.

Suramin remains an enigmatic molecule with polypharmacology and multiple potential uses. The effects of suramin on vesicular trafficking are likely to be complex, since suramin can interfere with vesicular transport and is imported via receptor-mediated endocytosis itself [58,59,276]. Our findings support a model of two independent pathways for endocytosis of suramin by trypanosomes: *via* the invariant surface glycoprotein ISG75 that directly binds suramin, and *via* the LDL receptor, a protein of unknown nature that binds suramin complexed to LDL. While the former is still active in cells expressing *VSG^{Sur}*, the latter is strongly impaired, causing suramin resistance in *T. brucei*.

Acknowledgement

We are grateful to Remo Schmidt and Christina Kunz Renggli for helpful advice.

5. Selection for high-level suramin resistance in *Trypanosoma brucei* highlights the importance of VSG^{Sur} and identifies a helicase as a candidate target

Natalie Wiedemar, Silvan Hälg, Pascal Mäser

Swiss Tropical and Public Health Institute, CH-4051 Basel, Switzerland
University of Basel, CH-4000 Basel, Switzerland

Working manuscript, 2019

The experiments were carried out as follows:
The suramin selection (Figure 1) was done by me;
the phenotypic characterization (Figure 2; Table 1), the reverse genetics experiment (Figure 4) and the mapping of sequencing reads and differential expression analysis (Figure 5) were done by Silvan Hälg under my supervision;
the analysis of sequence variants was carried out by me.

5.1. Abstract

Suramin is a fascinating molecule. In spite of the fact that it has successfully been used for the treatment of first-stage sleeping sickness for 100 years, very little is known about its mode of action against *Trypanosoma brucei*. The identification of the variant surface glycoprotein VSG^{Sur} as a determinant of suramin resistance in *T. brucei* has revealed a novel, surprising link between antigenic variation and drug resistance (Chapter 2). The subsequent characterization of VSG^{Sur}-mediated suramin resistance has identified LDL salvage as an uptake route for suramin that is affected in the resistant trypanosomes (Chapter 3). However, these studies have not revealed candidate targets of suramin. For this purpose, we have been further selecting a suramin-resistant, VSG^{Sur}-expressing *T. b. rhodesiense* line to obtain stable phenotypes of upto 1,100-fold resistance. Transcriptomics of these lines delivered three new pieces to the puzzle of suramin action: (i) the high-level suramin-resistant lines had acquired a set of point mutations in VSG^{Sur} that further increased suramin resistance; (ii) they over- and underexpress a larger number of genes including expression-site associated genes (ESAGs) and some of the previously known candidate genes for suramin resistance; (iii) amongst other mutations they have acquired a non-synonymous point mutation in the ATPase domain of a RuvB -like DNA helicase. Interestingly, exactly the same residue in RuvB -like helicase was found to be mutated in a suramin-resistant *T. evansi* field isolate. Thus we are confident that we have finally identified a primary candidate target for suramin in African trypanosomes.

5.2. Introduction

The drug suramin is a hundred years old and still being used to treat the first stage of acute human sleeping sickness, caused by *Trypanosoma brucei rhodesiense*. Suramin is a fascinating molecule with a wide array of potential applications, from parasitic and viral diseases to cancer and autism (Chapter 1). Despite its long term use against sleeping sickness, suramin remains an enigmatic molecule. *In vitro* it inhibits a number of *T. brucei* enzymes, among them many of the glycolytic pathway [57]. The 50% inhibitory concentrations for these enzymes are in the micromolar range, while *T. brucei* is killed by nanomolar concentrations and does not actively accumulate suramin [58]. This indicates the presence of additional or multiple targets in African trypanosomes. However, these targets together with the mode of action have remained elusive. Due to its large size and negative charge, suramin is likely imported via receptor-mediated endocytosis [58,59], and the receptor in *T. brucei* bloodstream forms is thought to be the invariant surface glycoprotein ISG75 [42].

By selecting *T. brucei* bloodstream forms *in vitro* for suramin resistance, we have identified a variant surface glycoprotein, termed VSG^{Sur}, expression of which is sufficient to increase the IC_{50} to suramin by a factor of 100 [277]; (Chapter 3 & 4). While VSG^{Sur}-mediated resistance is independent of ISG75, it is linked to the endocytosis of low density lipoprotein (Chapter 4). Expression of VSG^{Sur} in *T. brucei* affects selected membrane receptors, impairing the endocytosis of LDL and of transferrin, but not of the trypanolytic factor or of VSG itself (Chapter 4). These findings support the model of two independent pathways for suramin endocytosis, via ISG75 or via the LDL receptor, whereby the latter is impaired, via unknown interactions, by VSG^{Sur}.

While the investigation on VSG^{Sur} revealed a surprising link between antigenic variation and suramin resistance, it did not provide us with any new information about possible targets of suramin in trypanosomes. Therefore, we continued to expose the VSG^{Sur} expressing trypanosomes to increasing, sublethal concentrations of suramin, selecting for even higher resistance. Selection for high-level suramin resistance substantiated the role of VSG^{Sur} in suramin resistance and, finally, provided a candidate for the intracellular target of suramin.

5.3. Results

5.3.1. Further selection yields high-level suramin resistance

While the initial selection that yielded 100-fold resistance to suramin had been extremely fast, it took a year to further select for enhanced resistance. By continuously increasing the selective pressure, we finally obtained a *T. b. rhodesiense* line of 1,100-fold suramin resistance. The course of selection is summarized in Figure 1.

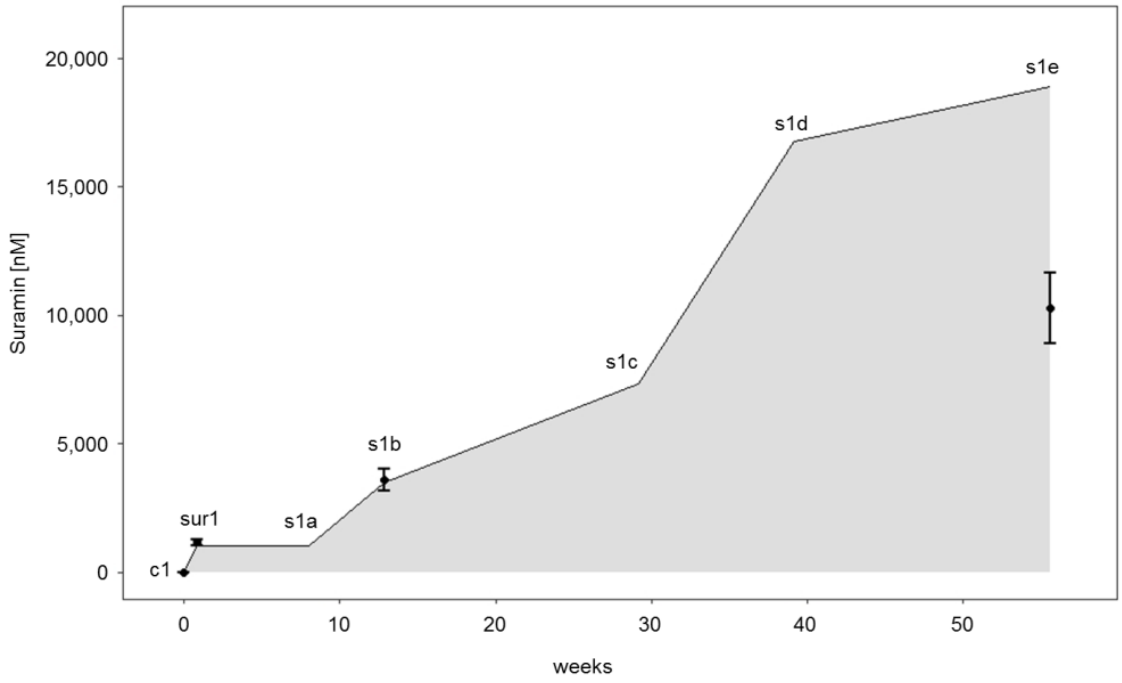

Figure 1. *In vitro* selection for suramin resistance in *T. b. rhodesiense* bloodstream form trypanosomes. Suramin concentration used for the selection is show as a line graph with gray filling. The mean 50% inhibitory concentrations of selected lines are shown as points, error bars represent standard deviations (n=4-6)

5.3.2. Phenotypic profiling of the suramin-selected lines

An increase in suramin concentration during the selection process typically abrogated, or strongly delayed, the growth of the trypanosomes. However, once the cultures had recovered in the absence of suramin, there was no apparent effect on the population doubling time in the selected lines (Figure 2A), indicating that there was no fitness cost associated with high-level suramin resistance (at least not *in vitro*; *in vivo*, trypanosomes depending on a particular VSG would be doomed). This is in agreement with the finding

that the suramin resistance phenotypes were stable in the absence of drug pressure (Figure 2B). The suramin-selected lines were moderately cross-resistant to trypan blue, but not to melarsoprol or pentamidine (Table 1).

A

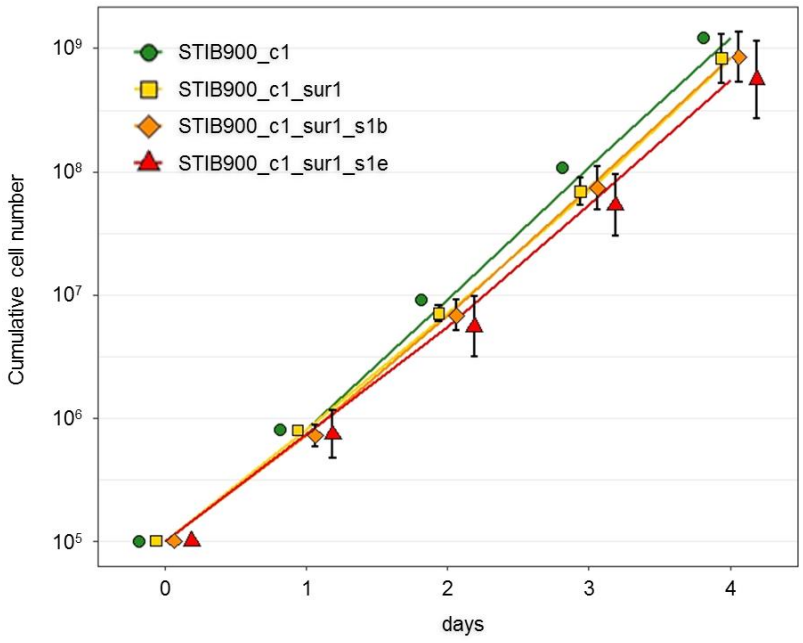

B

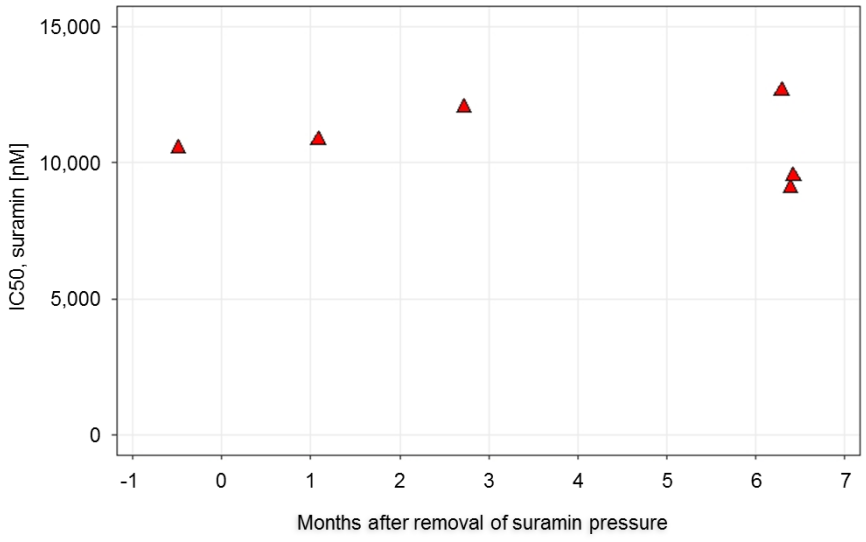

Figure 2. Phenotype of the suramin-resistant *T. b. rhodesiense* lines. (A) Growth curves of the sensitive and the resistant lines in the absence of drug pressure. Error bars represent standard deviations (n=1 for c1; n=2 for sur1; n=3 for s1b and s1e). (B) Stability of the suramin resistance in the s1e line after cultivation in absence of drug pressure, triangles represent individual drug assays.

Table 1. Drug sensitivities (IC50 in nM) of the suramin-selected *T. b. rhodesiense* lines ± standard deviations (n = 4-5)

Line	Suramin	Trypan Blue	Melarsoprol	Pentamidine
STIB900-c1	10 ± 4.4	3,300 ± 360	15 ± 3.2	4.4 ± 3.7
STIB900-c1-sur1	1,100 ± 130	13,000 ± 4,400	15 ± 4.2	2.4 ± 2.5
STIB900-c1-sur1-s1b	3,500 ± 580	19,000 ± 3,400	20 ± 5.9	2.9 ± 2.4
STIB900-c1-sur1-s1e	11,000 ± 1,2	23,000 ± 5,200	19 ± 5.5	3.6 ± 3.4

5.3.3. Further selection with suramin affected *VSG^{Sur}*

Aiming to test whether the highly suramin-resistant *T. b. rhodesiense* lines still expressed *VSG^{Sur}*, we performed quantitative PCR to measure the expression of *VSG^{Sur}*and *VSG^{900}*. The s1b and s1e lines showed a very high expression of *VSG^{Sur}*, which was in the same range as for strain sur1 and >1000-fold higher than the expression of the housekeeping gene *TERT*. To investigate whether the *VSG^{Sur}* sequence remained identical in the higher resistant strains, we amplified the expressed *VSG* gene from cDNA by PCR with primers binding to the 5' spliced leader sequence and a conserved sequence (gatatattttaaca) in the 3' untranslated region of all *VSG* genes [272,274]. Sequencing of the PCR product revealed that *VSG^{Sur}* had acquired several point mutations in the strain s1e, which showed the highest resistance. The mutant gene was named *VSG^{Supersur}*. It had acquired mutations both at the N- and C-terminus of the protein (Figure 3) and showed 98% amino acid sequence identity as compared to VSG^{Sur}. This surprising finding suggested that the mutations may have been selected for by the increasing suramin pressure.

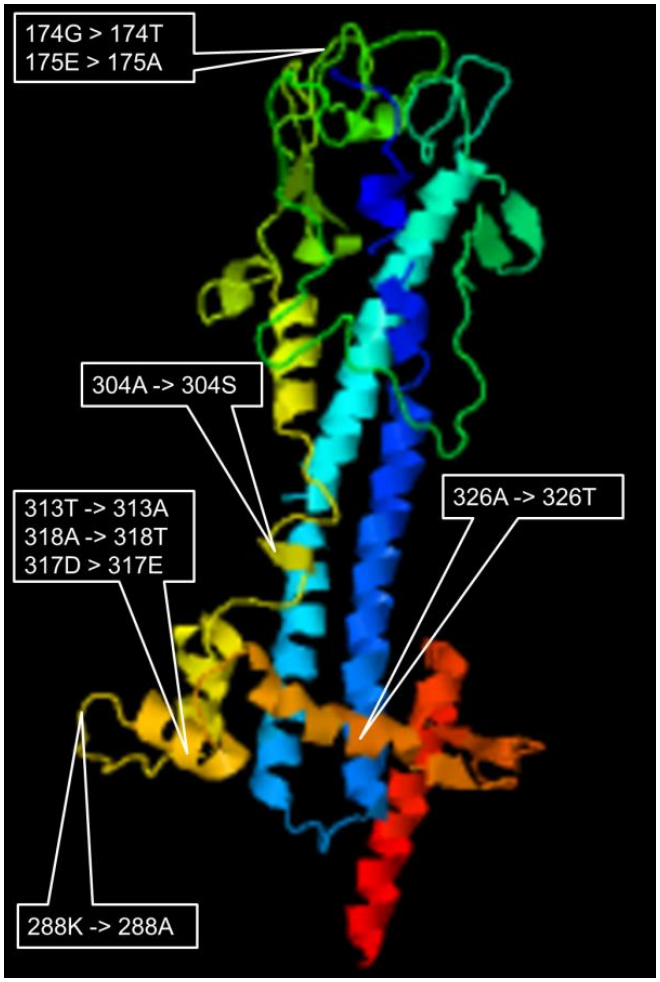

Figure 3. Variant surface glycoprotein expressed in higher suramin-resistant strains.

Amino acid substitutions in $VSG^{Supersur}$ as compared to VSG^{Sur} modeled on the known structure of Mitat 1.1 (modeled with Phyre2[297]).

5.3.4. Expression of *VSG*^{Supersur} enhances suramin resistance

To test the above hypothesis, we targeted the active *VSG* expression site of *T. b. rhodesiense* STIB900_sur1 with a *VSG*^{Supersur} construct (Figure 4A). Successful replacement of *VSG*^{Sur} in line sur1 and expression of *VSG*^{Supersur} was verified by amplification of the expressed *VSG* gene from cDNA by PCR and sequencing of the PCR product. Out of the four transfected clones two (sur1_tr1 and sur1_tr2) retained expression of *VSG*^{Sur} and two (sur1_tr3 and sur1_tr4) expressed *VSG*^{Supersur}. The clones that expressed *VSG*^{Supersur} exhibited an increased IC_{50} to suramin (Figure 4B), which was significant for clone sur1_tr4. This finding re-emphasizes the importance of VSG^{Sur} in suramin resistance, and it may provide useful information for identifying potential interaction partners. However, we still have not learned anything about the target(s) of suramin.

A

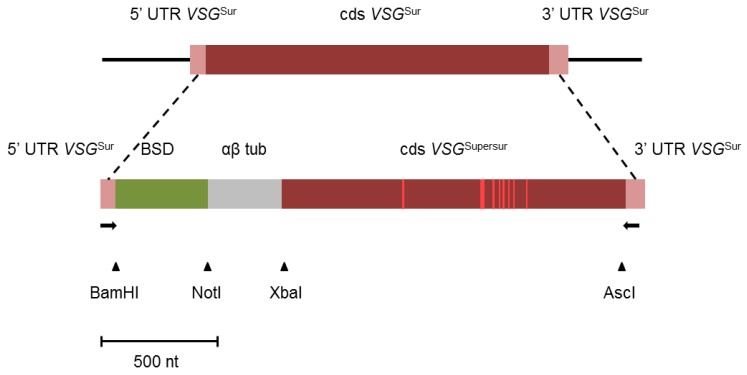

B

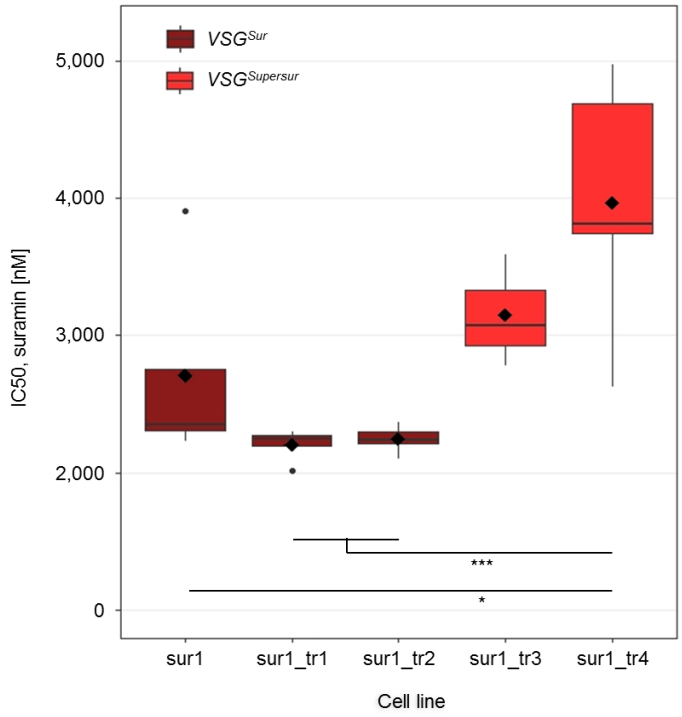

Figure 4. Genetic exchange of *VSG*^{Sur} with *VSG*^{Supersur} at the active expression site of *T. b. rhodesiense* STIB900_c1_sur1. (A) Construct used for the *VSG*^{Sur} replacement, deviations between *VSG*^{Supersur} and *VSG*^{Sur} are shown in light red within the *VSG*^{Supersur} sequence. Arrows represent primer binding sites for the amplification of the construct. The construct was framed with the 5' and 3' UTR of *VSG*^{Sur} used for the homologous recombination, it contains a blasticidine resistance gene (BSD), an αβ tubulin splice site (αβ tub) and the coding sequence of *VSG*^{Supersur}. (B) 50% inhibitory concentrations of the transfected clones and the parent strain sur1. The pseudoclones sur1_tr1 and sur1_tr2 do still express *VSG*^{Sur} and the pseudoclones sur1_tr3 and sur1_tr4 express *VSG*^{Supersur}. The boxplots represent median +/- quartiles, the mean is plotted as a black rectangle. Significant differences between the cell lines are indicated (* = p >0.05; ** = p>0.01; *** = p>0.001, Tukey multiple comparisons test).

5.3.5. Transcriptomics identifies overexpressed genes in suramin-resistant lines

The transfection experiments demonstrated that VSG^{Supersur}, while contributing to enhanced suramin resistance, could not account for the resistance factor of 1000 observed in the most resistant *T. b. rhodesiense* line as compared to the sensitive c1 line (Table 1). Indeed replacement of VSG^{Sur} with VSG^{Supersur} elevated the IC50 ~2.5-fold whereas the IC50 increased ~9-fold from the sur1 to the s1e line. Furthermore the line s1b showed already an increase in IC50 as compared to the sur1 line, whereas the expressed VSG remained the same. Therefore there must be additional modifications of gene expression or mutations that alter suramin sensitivity. To obtain a global picture on differentially expressed genes between the *T. b. rhodesiense* lines, we performed RNA-Seq on mRNA from cultures in the absence of suramin. As control strains we included the c1 and sur1 lines. The experiment was performed in triplicates from independent cultures to increase sensitivity (as compared to the first study [277]; Chapter 3).

A first comparison of the sensitive c1 line with the sur1 line confirmed the expression switch from *VSG^{900}* to *VSG^{Sur}* (Figure 5A). Four additional genes showed up as significant hits, all of them were *VSG*s with low expression levels. Inspection of the mapped data in the integrative genomics viewer revealed that only fragments of the genes were covered with mapped reads with a large number of mismatches. Both indicate that the reads derived from one or more *VSG*, not present in the database, and that they were expressed by a very small proportion of the trypanosomes. Three of the hits were expressed in the sensitive c1 strain with low expression levels. One hit was expressed by the resistant sur1 line, but the expression level was negligibly low with 6-20 mapped reads. The genes that were not significantly differentially expressed despite a large fold-change, showed a high degree of variance in the sensitive c1 line.

A comparison of the s1b with the sur1 line resulted in a larger number of significantly differentially expressed genes, most of them unregulated in the higher resistant s1b line (Figure 5B). Again all of them were *VSGs*, notably one putative *VSG* pseudogene, Tb927.9.1070, showed a high expression in the resistant s1b line. This indicates that further alterations of the VSG expression had taken place during the course of selection towards the higher resistant strains. But compared to the expression level of *VSG^{Sur}* the transcript abundance of all the differentially expressed VSGs was still much smaller.

The largest number of differentially expressed genes was detected between line s1e and s1b (Figure 5C), which was to be exptected given the long selection period (Figure 1).

The genes with a high expression and a large fold-change were all *VSG* genes or expression-site associated genes (*ESAG*). Additionally, a total of 85 genes not related to *VSGs* were significantly differentially expressed, out of which 45 were upregulated and 40 were downregulated in the highly resistant s1e line as compared to the s1b line (Supplementary Tables S1A and S1B).

A

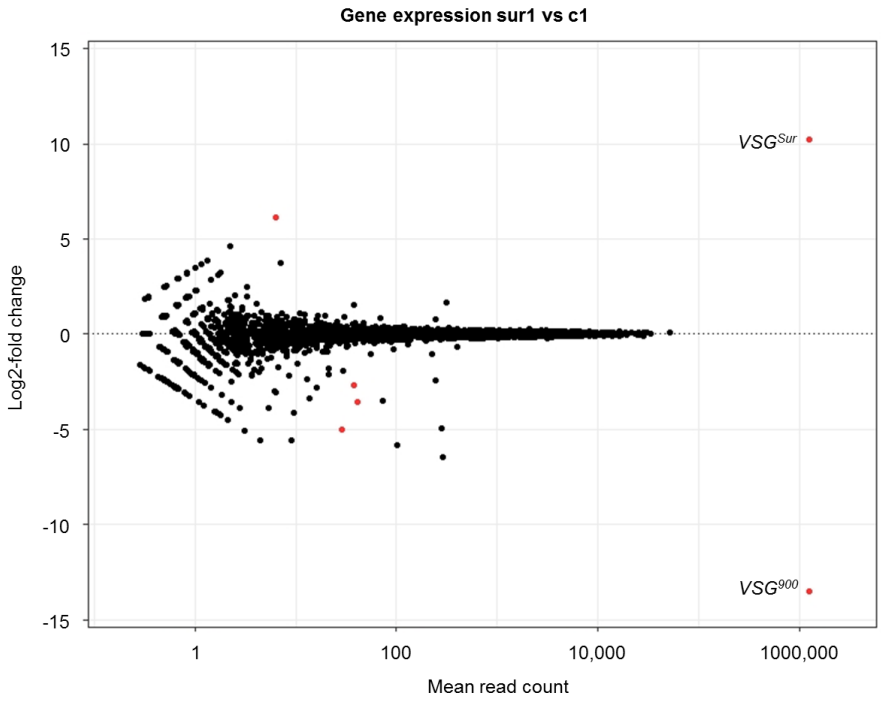

B

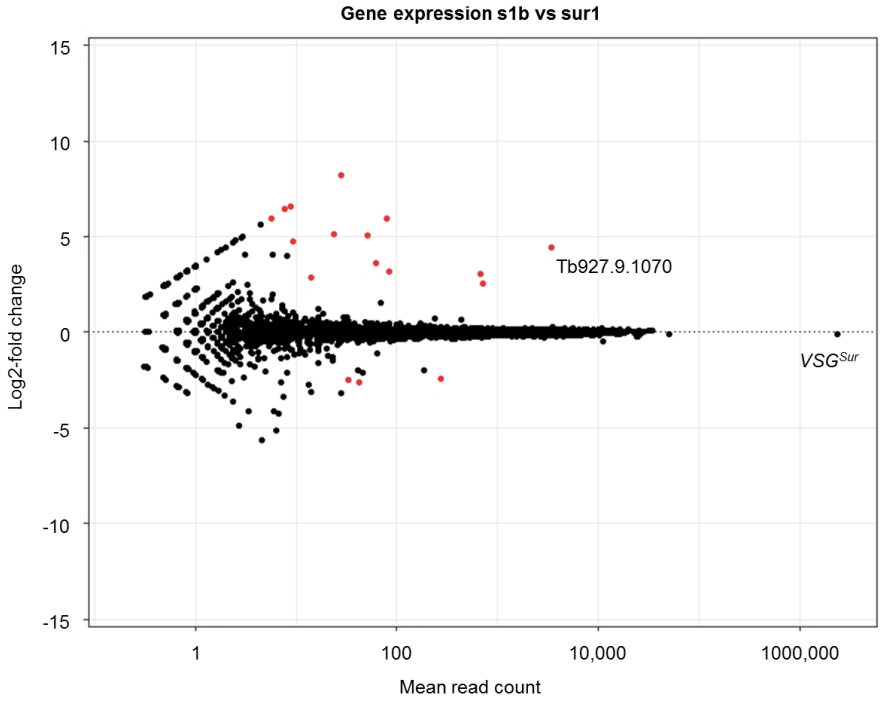

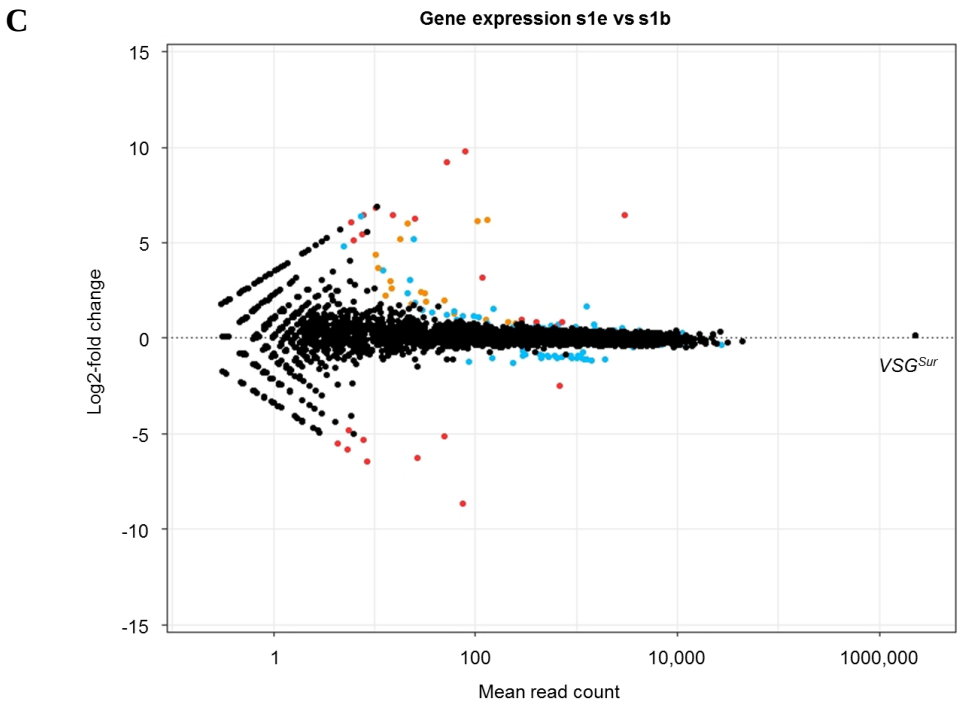

Figure 5. Alterations in gene expression associated with increased suramin resistance

Pair-wise comparison of the gene expression between the four *T. b. rhodesiense* lines as analyzed with DESeq2[270]. The x-axis represents the number of reads mapped per transcript; the y-axis the log2-fold change in transcript abundance between the compared lines. Transcripts with an adjusted p-value<0.05 are plotted in colour: *VSG* genes and pseudogenes in red; expression-site associated genes in orange and other differentially expressed genes in blue. (A) comparison of the suramin sensitive c1 line with the resistant sur1 line; (B) comparison of the sur1 with the s1b line; (C) comparison of the s1b with the s1e line.

Table S1A: Genes overexpressed in the highly suramin resistant s1e line as compared to the s1b line (*VSG*s not shown).

Transcript	Base Mean	log2Fold Change	padj	description
FM162580_gene5	130	6.18	2.74E-36	ESAG2
FM162580_gene7	105	6.16	1.46E-29	ESAG1
Tb927.2.1380	1278	1.68	2.30E-13	leucine-rich repeat protein (LRRP), putative
Tb927.9.11580	1511	0.75	8.18E-09	glycosomal membrane protein
FM162567_gene11	49	1.97	6.55E-08	ESAG11
Tb10.v4.0058	24	5.19	2.53E-07	Noncoding RNA, putative
FM162576_gene1	31	2.38	3.48E-07	ESAG7
FM162581_gene9	29	2.45	9.50E-07	ESAG2

Tb927.11.16180	23	3.05	1.16E-06	hypothetical protein
Tb927.9.3260	663	0.73	2.43E-06	hypothetical protein
FM162577_gene3	18	5.17	6.10E-06	ESAG3
FM162578_gene7	21	6.01	7.96E-06	ESAG1
FM162567_gene6	61	1.30	7.05E-05	ESAG4
Tb927.9.7770	1543	0.46	8.25E-05	spermidine synthase
Tb11.v5.0495	149	1.54	0.0001	retrotransposon hot spot (RHS), putative
Tb927.4.220	21	2.37	0.0002	retrotransposon hot spot protein 2 (RHS2), interrupted, degenerate
Tb927.2.960	61	1.41	0.0002	hypothetical protein
Tb11.v5.0712	108	1.09	0.0003	calcium-transporting ATPase, putative
Tb927.6.2200	1644	0.38	0.0007	DJ-1 family protein, putative
FM162581_gene11	127	0.99	0.0007	ESAG1
Tb927.6.210	95	1.14	0.0008	leucine-rich repeat protein (LRRP, pseudogene), putative
Tb927.1.3760	74	1.17	0.0010	hypothetical protein, conserved
Tb927.2.5710	12	3.55	0.0011	hypothetical protein
FM162577_gene4	10	4.36	0.0016	ESAG4
Tb10.v4.0059	7	6.36	0.0017	chrX additional, unordered contig
Tb927.2.4930	1096	0.36	0.0026	esterase, putative
Tb927.7.2640	1382	0.35	0.0029	cytoskeleton associated protein, putative
Tb927.11.12100	1154	0.41	0.0037	protein tyrosine phosphatase, putative
FM162577_gene1	15	2.60	0.0041	ESAG6
Tb927.2.1344	25	1.83	0.0043	retrotransposon hot spot protein 1 (RHS1), interrupted
FM162578_gene5	11	3.66	0.0045	ESAG2
FM162576_gene2	14	2.98	0.0057	ESAG6
Tb927.8.1990	4663	0.28	0.0066	peroxidoxin
Tb927.8.5470	4175	0.42	0.0081	flagellar calcium-binding 24 kDa protein
Tb927.2.1120	420	0.60	0.0085	retrotransposon hot spot protein 4 (RHS4), point mutation
Tb927.8.3530	11052	0.27	0.0087	glycerol-3-phosphate dehydrogenase [NAD+], glycosomal
Tb927.11.6210	1905	0.32	0.0132	Lanosterol 14-alpha demethylase
Tb927.8.6110	2879	0.32	0.0132	3-hydroxy-3-methylglutaryl-CoA synthase, putative
FM162578_gene1	23	1.78	0.0143	ESAG6
Tb927.8.2850	389	0.57	0.0146	Poly(A)-specific ribonuclease PARN-1
Tb927.10.10220	65	0.95	0.0169	procyclin-associated gene 2 (PAG2) protein
Tb927.8.5460	991	0.50	0.0169	Flagellar calcium-binding 44 kDa protein
Tb927.3.4020	560	0.66	0.0184	phosphatidylinositol 4-kinase alpha, putative

Tb927.4.5100	1173	0.36	0.0187	Endoplasmic Reticulum-Golgi Intermediate Compartment (ERGIC)/Endoplasmic reticulum vesicle transporter, putative
Tb927.7.1930	131	0.80	0.0188	nucleoside diphosphatase, putative
Tb927.2.5040	668	0.39	0.0189	MORN repeat, putative
Tb927.9.8450	1249	0.36	0.0250	UMP/CMP kinase
Tb927.10.10610	2078	0.31	0.0284	protein tyrosine phosphatase, putative
FM162577_gene0	32	1.91	0.0286	ESAG7
Tb927.10.9550	37	1.32	0.0286	hypothetical protein
Tb927.9.10650	688	0.42	0.0290	hypothetical protein
Tb09.v4.0042	52	1.20	0.0309	leucine-rich repeat protein (LRRP, pseudogene), putative
Tb927.8.6390	2400	0.41	0.0309	lysophospholipase, putative
Tb927.9.11230	1565	0.40	0.0309	calmodulin-like protein, putative
FM162579_gene1	13	2.24	0.0325	ESAG6
Tb927.4.230	236	0.57	0.0326	DNA-directed RNA polymerase III subunit, pseudogene, putative
Tb927.11.11410	983	0.57	0.0349	trans-sialidase, putative
Tb927.3.2520	209	0.85	0.0349	ESAG1 protein, putative
Tb927.4.1210	30	1.47	0.0392	hypothetical protein
Tb927.7.7040	2802	0.51	0.0405	methylthioadenosine phosphorylase, putative
Tb927.3.2530	248	0.76	0.0411	ESAG11, degenerate
Tb927.8.5380	476	0.54	0.0426	ubiquitin fold modifier protein, putative
Tb927.9.800	5	4.78	0.0438	UDP-Gal or UDP-GlcNAc-dependent glycosyltransferase, putative

Tabe S1B: Genes downregulated in the highly suramin resistant s1e line as compared to the s1b line (*VSG*s not shown).

Transcript	**Base Mean**	**log2Fold Change**	**padj**	**description**
Tb927.10.12360	1008	-1.03	1.18E-28	hypothetical protein, conserved
Tb927.10.12520	1401	-1.16	2.05E-27	hypothetical protein, conserved
Tb927.10.12470	1184	-1.08	9.16E-25	hypothetical protein, conserved
Tb927.10.12380	1036	-0.91	3.63E-20	chaperone protein DnaJ, putative
Tb927.10.12290	874	-0.91	1.01E-17	UDP-Gal or UDP-GlcNAc-dependent glycosyltransferase, putative
Tb927.10.12350	443	-1.06	2.66E-17	hypothetical protein, conserved
Tb927.10.12310	1259	-1.08	1.18E-15	helicase-like protein
Tb927.10.12490	1941	-1.09	1.26E-14	kinesin, putative
Tb927.10.12440	718	-1.01	2.12E-13	kinesin, putative
Tb927.10.12430	909	-1.03	4.19E-13	Noc2p family, putative

Tb927.10.12370	1119	-1.07	9.27E-13	gamma-glutamylcysteine synthetase
Tb927.10.12500	650	-1.02	4.08E-11	P-type H+-ATPase, putativ
Tb927.10.12550	293	-0.94	2.45E-10	hypothetical protein, conserved
Tb927.10.12320	522	-0.93	2.50E-10	hypothetical protein
Tb927.10.12390	866	-0.97	1.35E-09	hypothetical protein, conserved
Tb927.10.12530	234	-1.28	1.18E-08	chaperone protein DnaJ, putative
Tb927.10.12300	462	-0.91	1.45E-08	hypothetical protein, conserved
Tb927.10.12480	465	-0.92	1.58E-08	UAA transporter family, putative
Tb927.10.12420	307	-0.88	8.80E-08	predicted S. cerevisiae Got1 homologue
Tb927.10.12400	609	-0.95	1.17E-06	membrane transporter protein, putative
Tb927.10.12540	535	-0.95	2.64E-06	NADH-ubiquinone oxidoreductase complex I subunit, putative
Tb927.10.12460	440	-0.84	3.12E-06	Zinc finger, C3HC4 type (RING finger), putative
Tb927.10.12450	148	-1.03	3.74E-06	SNARE domain-containing protein, putative
Tb927.10.12410	1162	-0.73	3.05E-05	hypothetical protein, conserved
Tb927.10.12340	86	-1.22	4.15E-05	hypothetical protein
Tb927.10.12330	294	-0.65	0.0008	zinc finger protein family member, putative
Tb927.8.1870	13936	-0.33	0.0011	Golgi/lysosome glycoprotein 1
Tb927.8.8290	3688	-0.46	0.0017	amino acid transporter AATP5
Tb927.5.1950	2838	-0.36	0.0047	hypothetical protein, conserved
Tb927.5.3240	2475	-0.32	0.0068	hypothetical protein, conserved
Tb927.7.2660	11468	-0.38	0.0087	zinc finger protein family member, putative
Tb927.9.13380	6871	-0.34	0.0127	Autophagy-related protein 24
Tb927.4.4570	2772	-0.34	0.0160	hypothetical protein, conserved
Tb927.9.10770	27571	-0.36	0.0203	polyadenylate-binding protein 2
Tb927.6.1020	4171	-0.38	0.0217	cysteine peptidase, Clan CA, family C1, Cathepsin L-like
Tb927.10.8940	25000	-0.28	0.0232	flagellum targeting protein kharon1, putative
Tb927.8.7780	5667	-0.28	0.0240	hypothetical protein, conserved
Tb927.10.13720	2584	-0.29	0.0367	RNA-binding protein 29, putative
Tb927.10.5810	12756	-0.34	0.0399	The ARF-like 2 binding protein BART, putative
Tb927.5.2600	1453	-0.31	0.0474	methyltransferase domain containing protein, putative

5.3.6. Genomics identifies mutated genes in suramin-resistant lines

To identify mutations such as nucleotide polymorphisms or short indels that had occurred during the selection for high-level suramin resistance, the mapped illumina RNA-Seq reads were screened for deviation from the *T. b. brucei* TREU927 reference genome. The dataset was filtered for mutations only present in the highly suramin-resistant s1b and/or s1e lines but not in the 100-fold resistant *T. b. rhodesiense* STIB900_sur1 and the sensitive parent clone STIB900_c1. Stringent filtering for the presence of the mutation in the three replicates per line and the absence thereof in the three replicates of STIB900_sur1 and STIB900_c1 returned 30 candidate variants. These were scrutinized by inspection of the aligned sequencing reads in a genome browser. Stringent criteria were used to exclude false positives: We excluded (1) variants which laid within highly diverse regions with a low quality of the alignment, (2) variants within *VSG* genes and pseudogenes and (3) variants that were wrongly called due to small differences in allele frequencies. This left five candidate variants for suramin resistance, summarized in Table 2.

Table 2. Mutations identified. Variants that were present in the highly suramin-resistant s1b and/or s1e lines and absent in the c1 and sur1 lines. The variants in Tb927.11.760 and Tb427.BES129.12 were only present in <30% of the sequencing reads (*).

Gene ID	Gene Name	Mutation	Effect	s1b	s1e
Tb927.4.1270	putative ruvB-like DNA helicase	c.934A>G	missense I312V	0/1	1/1
Tb927.11.760	putative protein phosphatase 2C	c.798_799insCC	frameshift N267fs	0/1*	0/1*
Tb427.BES129.12	expression site-associated gene 11	Haplotype of 7 SNPs upstr. of ESAG11	Possible modifier	0/0	0/1*
Tb927.1.3050	putative tRNA (Uracil-5-)-methyltransferase	c.141T>C	synonymous S47S	0/0	0/1
Tb927.11.3700	Uncharacterised ACR, YagE family COG1723, putative, unspecified prod.	c.1064T>C	missense L355P	0/0	0/1

5.3.7. RuvB-like helicase is a candidate intracellular target of suramin

Of the five identified mutations (Table 2), the A to G transition in ruvB-like helicase (Tb927.4.1270) was the most interesting for different reasons: (1) it was non-synonymous; (2) it was heterozygous in *T. b. rhodesiense* line s1b and homozygous in s1e, the line with the highest degree of suramin resistance; and (3) it is an essential gene in *T. brucei* bloodstream form parasites. The mutation is non-synonymous, changing isoleucine^{312} to valine (Figure 6). Position 312 lies within the AAA+ ATPase domain, four residues after the ATP-binding Walker-B motif of the helicase [298–300]. Homology-based modeling [301] resulted in the best Global Model Quality Estimation score for a model based on the RuvB-like helicase derived from cryo-electron microscopy structure of the evolutionarily conserved core of the INO80 complex from the fungus *Chaetomium thermophilum* [302] with a coverage of 98% and a sequence identity of 69% (Fig. 6A). The second best hit was a model based on the homo-hexamer crystal structure of human RuvBL1 [300] with a coverage of 96% and a sequence identity of 63% (Fig. 6B). The change from isoleucine to valine may seem inconspicuous. However, we have performed whole genome sequencing of a suramin-resistant *T. evansi* field isolates and in one of them (Westry 2, [60]) and found isoleucine^{312} of the *T. evansi* ruvB-like helicase (TevSTIB805.4.1310) to be heterozygously mutated as well, in this case to leucine (Figure 6C). The helicase sequences of the reference genomes, *T. evansi* STIB805 and *T. b. brucei* TREU927, are identical. The isoleucine at position 312 is conserved across kinetoplastidae as seen in a comparative blast search using 10 adjacent amino acids. Thus the RuvB -like helicase is a promising candidate for an intracellular target that is relevant for the susceptibility of African trypanosomes to suramin.

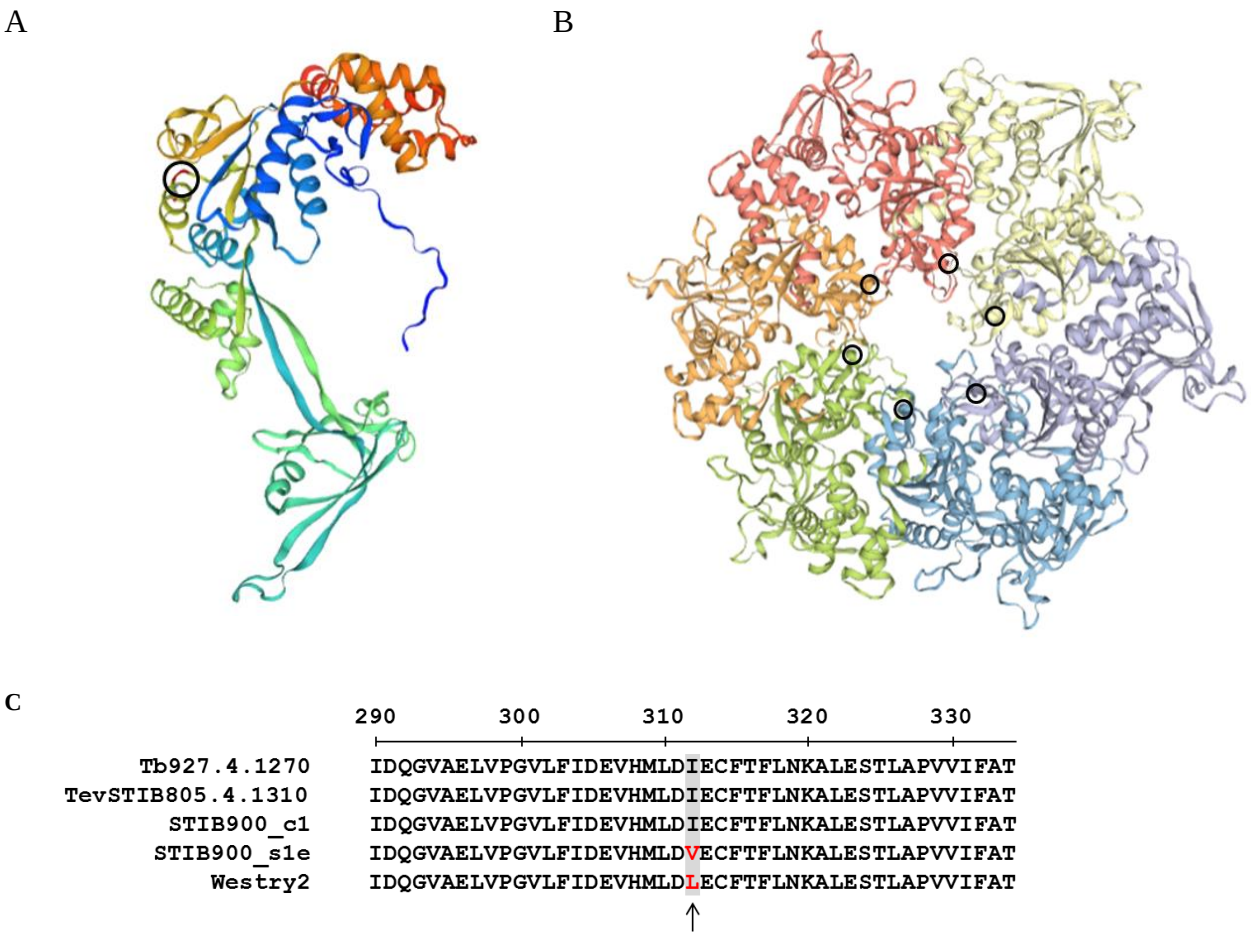

Figure 6. Amino acid substitution at position 312 of the RuvB -like helicase Tb927.4.1270

(A) Monomeric and (B) hexameric structures based on homology modeling. The mutated residue at position 312 is marked with black circles. (C) Amino acid alignment of RuvB –like helicases. The reference sequences of *T. brucei* (TREU 927) and *T. evansi* (STIB 805) are identical. However, the suramin-resistant *T. b. rhodesiense* STIB900 derivative s1e and the suramin-resistant *T. evansi* field isolate Westry2 both have acquired a point mutation at position 312. The mutation is absent in *T. b. rhodesiense* STIB900_c1 parent.

5.4. Discussion

We have previously shown that expression of *VSG*^{Sur} in *T. brucei* bloodstream forms causes 100-fold resistance to suramin [277]; (Chapter 3 & 4). The finding that *VSG*^{Sur}, after selection for high-level resistance, expressed a mutated version of *VSG*^{Sur} that further seem to enhance suramin resistance, substantiates the role of VSG^{Sur} in suramin susceptibility. However, the link between *VSG*^{Sur} expression and suramin resistance is unlikely to be relevant for the treatment of human African trypanosomiasis. In fact, it might be the explanation why there are no problems with suramin resistance in the treatment of HAT, since trypanosomes locked to *VSG*^{Sur} expression would be eliminated by the adaptive immune system. Nevertheless, the established link between VSG^{Sur} and suramin resistance is of fundamental interest to the biology of *T. brucei*, since this is the first link between two main research areas in African trypanosomes: antigenic variation and drug resistance. Our discovery of *VSG*^{Supersur} affirms this link. While the predominantly expressed *VSG* remained *VSG*^{Sur} respectively *VSG*^{Supersur} mRNA sequencing revealed ongoing dynamics of the *VSG* expression during the selection process. The expression level of these *VSG*s was negligibly low compared to the expression levels of *VSG*^{Sur} and *VSG*^{Supersur}, but the fact that some of them remained expressed after several months of selection indicates that their expression at least does not bare any fitness costs under suramin pressure as compared to cells expressing *VSG*^{Sur}. The nature of these VSGs and their effect on suramin sensitivity still remains to be investigated.

The highest resistant line, *T. b. rhodesiense* STIB900 s1e, was the only line that showed significant changes in expression of genes other than *VSG*s. A total of 18 ESAGs were differentially expressed, all of them upregulated. This could be explained by the ongoing dynamics of *VSG* expression or an expression-site switch to *VSG*^{Supersur}. Even though we do not know whether *VSG*^{Supersur} evolved through mutations of *VSG*^{Sur} or whether *VSG*^{Supersur} was already present in the genomic archive and subsequently activated through a VSG switch.

Of the differentially expressed genes other than ESAGs, five had been previously identified in a RIT-Seq screen for suramin resistance [42]: a Golgi/lysosome glycoprotein (Tb927.8.1870), an amino acid transporter (Tb927.8.8290), an autophagy-related protein (Tb927.9.13380), a cysteine peptidase (Tb927.6.1020) and the ARF-like 2 binding protein

BART (Tb927.10.5810). In agreement with the RIT-Seq data, these genes were slightly downregulated in the line s1e.

Analysis of nucleotide sequence variations in the mRNA sequencing data yielded a manageable number of variants that presumabely arose during the selection process. The most promising candidate was the non-synonymous point mutation in the ruvB-like DNA helicase. It was absent in the original *T. b. rhodesiense* line of resistance factor 100, heterozygous when the line had reached a resistance factor of 350, and homozygous at a resistance factor of 1,100. In contrast to the situation with human African trypanosomiasis, there are substantial problems with suramin resistance in animal trypanosomiases, in particular in *T. evansi*-infected camels and water buffalos [60,61]. We performed whole genome sequencing of suramin-resistant *T. evansi* field isolates and in one of them found the same residue in the ruvB-like DNA helicase to be mutated as well. The amino acid substitution from isoleucine to valine, respectively leucine, is not a dramatic change. But isoleucine^{312} is highly conserved, therefore more dramatic changes might interfere with the functionality of the protein. Since Tb927.4.1270 is essential in *T. brucei* bloodstream form [303] an impaired functionality would most probably reduce viability of the parasites. This was not the case in our highly suramin-resistant *T. b. rhodesiense* lines as indicated by the absence of a growth phenotype. Interestingly, DNA helicase is a known antiviral target of suramin: DNA helicases of Dengue virus, Chikungunya virus and Zika virus have been validated as suramin targets [100,168,207]. Thus, we are confident that the forward genetic approach finally provided a promising intracellular candidate target for suramin action in *T. brucei* bloodstream form parasites.

5.5. Material and Methods

Trypanosoma spp. strains

The *T. b. rhodesiense* STIB900 strain originates from a patient isolate collected from a male patient at St. Francis Hospital in Ifakara, Tanzania in 1982.

The *T. evansi* Westry2 strain was isolated in 1995 from a camel in Sudan [60].

Cultivation, selection and determination of the growth rate

The *T. b. rhodesiense* parasites were cultivated in Iscove's Modified Dulbecco's Medium (Sigma) supplemented according to Hirumi [262] with 15% of heat-inactivated horse-serum, at 37°C, 5% CO_2. Initial selection was carried out for six days at 1050 nM suramin (Sigma). Further selection was carried out as shown in Fig 1 by step-wise elevation of the suramin concentration. Cells were kept at the respective suramin concentrations until they showed a close-to-normal growth phenotype, subsequently the suramin concentration was increased.

For the determination of the growth rate, cells were incubated in standard growth medium at a concentration of 10^5 cells/ml, after 24 hours the cell density was quantified and the cells diluted back to 10^5 cells/ml. This procedure was repeated during four consecutive days.

Drug sensitivity testing

Drug sensitivities for suramin sodium salt (S2671, Sigma, now Merck), pentamidine isethionate (P0547, Sigma, now Merck), trypan blue (93590, Fluka, now Merck) and melarsoprol (Sanofi-Aventis/WHO) were evaluated with Alamar blue assays [15]. Serial drug dilutions were prepared with standard growth medium in a 96-well plate. The parasites were added to a final concentration of 2×10^4 cells/ml and incubated for 68 hours. Subsequently, resazurin was added to a concentration of 11.4 µg/ml and the plates incubated for 3-4 more hours. The fluorescence of viable cells was measured with a SpectraMax reader (Molecular Devices) and SoftMax Pro 5.4.5 Software. Fitting of the dose-response curves (non-linear regression model, variable slope; four parameters, lowest value set to zero) and calculation of the IC50 values were carried out with GraphPad Prism 6.00.

RNA isolation

The four parasite strains (STIB900_c1, STIB900_sur1, s1b and s1e) were grown in parallel in the absence of suramin and RNA was isolated from ~10^7 cells during the exponential growth phase using the RNAeasy Mini Kit (Qiagen). DNA was removed either with an on-column DNase treatment during RNA isolation or after isolation using a DNA-freeTM kit (Ambion). RNA was isolated three times, resulting in three technical replicates per strain, and kept at -80°C.

RT-PCR and sequencing of VSG

Complementary DNA (cDNA) was synthetized from 1-2.5 µg RNA using oligo(dT) primer and the SuperScript III Reverse Transcriptase (Invitrogen via Thermo Fisher Scientific). To amplify the predominantly expressed *VSG*, PCR was carried out with a forward primer binding to the spliced leader sequence (cgctattattagaacagtttctgtac) and a reverse primer binding to the conserved 15 nucleotides in the 3'UTR of *VSG* (gtgttaaaatatatc). After purification, the PCR product was directly sequenced with VSG^{Sur}-specific primer (agcaaaagaggggccttttaataa, tcattcgtttggccatacgc, tctgggttcatatgcgctgc and ttactgacagacgaaccggc).

Plasmid and transfection of trypanosomes

The coding sequence of $VSG^{Supersur}$ was PCR amplified from cDNA of strain s1e using primers that contained XbaI respectively AscI restriction site overhangs (taatctagaatgcaagccgtaacacgc and aatggcgcgccttaaaaaagcaaaaatgcaagc). The VSG sequence within the pUC57 plasmid described before [277]; (Chapter 3 & 4) was cut out with XbaI and AscI. And the $VSG^{Supersur}$ coding sequence was cloned into the plamid backbone using the LigaFast™ Rapid DNA Ligation System (Promega) according to the manufacturers' protocol. The resulting plasmid contained a construct that was framed with the 3' and 5'UTR of VSG^{Sur} and that contained a blasticidine resistance marker, an αβ tubulin splice site and the coding sequence of $VSG^{Supersur}$. The construct was amplified by PCR and after clean-up (Macherey-Nagel), the PCR product was directly used for the transfection of the trypanosomes. A total of 4×10^7 cells were transfected with 5µg PCR product in bloodstream form transfection buffer [50] using program Z-001 of an Amaxa Nucleofector (Lonza). The transfectants were cloned by limiting dilution and after 24 hours, blasticidine was added to a

concentration of 5µg/ml. After one week, four blasticidine resistant clones were recovered, their expressed VSG was analyzed by PCR and Sanger sequencing as described above.

RNA-Sequencing and mapping of reads

Sequencing libraries were prepared individually for the three technical replicates per line, using the TruSeq Stranded mRNA Library preparation kit (illumina). 126 nucleotide single-end sequencing was carried out on an illumina HiSeq 2500. A combination of the TREU927 reference sequence (TryTrypDB-38) with the Lister427 bloodstream expression sites and the sequences of VSG^{900} (GenBank accession MF093646) and VSG^{Sur} (GenBank accession MF093647) was used as a reference sequence. The quality of the sequencing reads was determined with fastqc [304] and untrimmed reads were mapped to the reference sequence with the Burrows-Wheeler Aligner [267] using the default settings. The sam-files were converted to bam-files using samtools [268] and sorted and indexed with picard [305]. Reads mapped per transcript were quantified with HTSeq [269] based on a gff-file that consisted of a combination of the TREU927 reference annotation (TryTrypDB-38), the annotation of the Lister427 bloodstream expression sites and the sequences of VSG^{900} and VSG^{Sur}. Differential gene expression analysis was carried out with the DESeq2 [270] package in R (cooks-cutoff and independent filtering disabled).

Detection of variants

The sorted bam-files of the aligned mRNA-Seq (STIB900) reads were further processed for the analysis of genomic variants. Read duplicates were marked and read group identifiers were added using picard. Variants were called with the gatk (version 4.0.7.0) haplotypecaller in gvcf-mode [306]. The individual g.vcf-files were combined using gatk combinegvcfs and genotyped using gatk genotypegvcfs. Variant annotation was calculated using snpEff (version 4.3T) based on a gff file consisting of the TREU927 reference annotation (TryTrypDB-38), the annotation of the Lister427 bloodstream expression sites and the sequences of VSG^{900} and VSG^{Sur} [307].

DNA isolation, sequencing and mapping

The *T. evansi* strains were propagated in a mouse and after heart puncture at high parasitemia, the trypanosomes were separated from the blood with a diethylaminoethyl cellulose column. The genomic DNA was isolated by chloroform/phenol extraction. Sequencing libraries were prepared using illumina's KAPA Hyper Prep Kit and paired-end

126 nt sequencing was carried out on an illumina HiSeq 2500. Raw sequencing reads were trimmed with trimmomatic [266] (removal of low quality bases and illumina adaptors) and mapped to the *T. evansi* reference genome TevansiSTIB805 (TriTrypDB-9.0) using bwa [267]. The sam-file was converted to a bam-file using samtools [268] and sorted and indexed using picard [305]. The aligned genome was visualized with the integrative genomics viewer [308,309].

6. General discussion

6.1. VSGs – more than immune evasion

VSGs are the most abundant proteins of bloodstream-form trypanosomes; densely packed on the cell membrane, they cover the whole surface of the cell [310]. Up to more than 2000 *VSG* genes and pseudogenes can be found in the genomic archive of trypanosomes [274] but due to allelic exclusion only one specific *VSG* is expressed at a certain time [311]. Transcription of *VSG* genes is driven by RNA polymerase I and takes place at the active bloodstream expression site [312]. Sporadic switching of the expressed *VSG* leads to antigenic variation and confers protection against the hosts' immune response by escaping the adaptive immune system [311]. Have VSGs ever been attributed any functions other than immune escape? Even though it is thought that a *VSG* gene gave rise to the serum resistance associated gene, which confers protection of *T. b. rhodesiense* from the human trypanolytic factor, the resulting protein is a truncated version of a VSG and has lost the typical characteristics of VSGs [313,314]. At some point a VSG was identified to be associated with *in vitro* generated TLF1 resistance in *T. b. brucei* [315] but follow-up studies excluded its direct involvement in TLF1 resistance [316]. Thus, with VSG^{Sur} we describe for the first time a gene, which based on its sequence and high expression levels clearly encodes a VSG, that has an impact on the cell that goes beyond immune escape. The link between expression of VSG^{Sur} and the phenotype of suramin resistance and reduced substrate uptake is surprising and opens up a number of questions: How does VSG^{Sur} confer resistance? Is the uptake machinery affected and if yes, which part? Does VSG^{Sur} interact with other surface proteins? And finally, what are the features that make VSG^{Sur} so special?

In the following I will discuss different possible hypotheses on how VSG^{Sur} could act on the cell and mediate the observed phenotype.

(1) Reduced binding of suramin to its receptor

One possibility how VSG^{Sur} could confer suramin resistance is through inhibition of suramin binding to its receptor. An unusual structure or multimeric state of VSG^{Sur} could sterically occlude the suramin receptor; even electrostatic forces could be involved since suramin is highly negatively charged. Do our data support such a hypothesis?

(i) Trypan blue: binding of trypan blue to the cell surface was similar in *VSG*^{Sur} and *VSG*^{900} expressing cells for concentrations below 400 µg/ml, and elevated at a concentration of 400 µg/ml (Chapter 3). We speculated about the presence of a high-affinity and a low-affinity receptor with impact of VSG^{Sur} only on the low-affinity receptor. But we have to bear in mind, that the uptake of trypan blue was reduced already at the lower concentrations in *VSG*^{Sur} expressors, thus the uptake data cannot be fully explained by a reduced binding to a potential low-affinity transporter. Furthermore, the concentration at which *VSG*^{900} expressing cells showed an increase of trypan blue binding was very high and led to toxicity, which could have biased the results and led to a higher fluorescence (since trypan blue permeates dead cells). A similar experiment in 2T1 with shorter incubation times did not show any difference in trypan blue binding between *VSG*^{Sur} and *VSG*^{221} expressing cells even at the highest concentration (Wiedemar, data not shown). Thus, I conclude that the reduced trypan blue uptake is not mediated by a reduced binding. Of course, experiments with trypan blue only give us a proxy for the situation with suramin; trypan blue is smaller than suramin and it bears four negative charges, in contrast to suramin with six negative charges. But the fact that *VSG*^{Sur} expressing cells showed cross-resistance to trypan blue and a reduced uptake makes it likely, that the effect of VSG^{Sur} on trypan blue binding and uptake is comparable with the effects on binding and uptake of suramin.

(ii) Transferrin and LDL: VSG^{Sur} did not only have an effect on the uptake of suramin but also on the uptake of LDL and transferrin. Is it possible that the changes of the VSG^{Sur} structure are that massive, that the VSG not only occludes the suramin receptor but also the transferrin and the elusive LDL receptor?

The transferrin receptor is an ESAG6/7 heterodimer [317], and structural analysis showed that it does not extend above the densely packed VSG-layer [318]. If the VSG surmounts and mantels the transferrin receptor, it is conceivable that structural and/or electrostatic changes of the VSG could indeed have an effect on the binding of transferrin to its receptor. I did perform binding assays, which showed a certain decrease of cell associated LDL and transferrin in *VSG*^{Sur} expressing cells. But the decrease was not big enough to explain the reduced uptake of both substrates. Furthermore, the difference might as well

have been a technical bias: Endocytosis happens very fast [319], and thus the very high concentrations of substrates used in the binding assay would quickly lead to an increase of intracellular fluoresce of *VSG*^{221} expressing cells if just very little endocytosis had taken place.

(iii) TLF1: There was no difference in TLF1 uptake between *VSG*^{Sur} and *VSG*^{221} expressing cells. Under the above hypothesis this would mean, that VSG^{Sur} does not prevent binding of TLF1 to the HpHb receptor. Indeed structural analysis of the HpHb receptor showed, that the receptor surmounts the VSGs [320]; this makes it plausible, that a potential abnormal VSG has less of an effect on such a long protein.

All in all, the hypothesis of a VSG^{Sur} mediated reduced receptor binding alone seems to be rather unlikely but it cannot be completely excluded based on our data. The one key experiment that once and for all clarifies this question would be a binding experiment with radiolabeled suramin, preferentially carried out in a cold-room to guarantee absence of any endocytosis.

(2) Altered movement and localization of surface proteins

VSGs circulate very quickly; they move over the trypanosome surface to the flagellar pocket where they are endocytosed, sorted, and subsequently recycled to the cell surface via the flagellar pocket. This whole process happens within only 12 minutes [261]. The speed at which VSGs are able to diffuse over the cell surface depends on the size of the VSG [321] and its glycosylation [322]. Recently, it was shown that a flexible part between the C- and N-terminal domain of the 3D structure allows VSGs to adopt two different conformations that influence the speed of VSG movement [323]. It was even proposed that this flexibility allowed VSGs to slide over trans-membrane proteins [323]. Currently it is not known how the movement and localization of other surface proteins are regulated [324]. But one could speculate that their localization and transport to the flagellar pocket is driven or influenced by the fast movement of the dense VSG coat. Under such a scenario, it would be plausible that an atypical 3D structure, multimeric state, glycosylation or flexibility of VSG^{Sur} could influence the diffusion rate of the VSG itself. The movement and localization of other surface proteins could be influenced either indirectly through modified VSG kinetics or directly by changing VSG-protein interactions.

How is such a hypothesis to be assessed in view of our data?

(i) ISG75: We did not observe any alterations in ISG75 turnover (half-life). But it is likely that ISG75 is recycled back to the cell surface after endocytosis [325], therefore we do not know whether the endocytosis rate correlates with the turnover rate. We cannot exclude that the movement of ISG75 from the cell surface [326] to the flagellar pocket is somehow hampered by VSG^{Sur}.

(ii) Transferrin: The transferrin receptor is already located in the flagellar pocket [327] and does not have to be trafficked over the cell surface to the site of endocytosis. The VSG is not only endocytosed but also exocytosed at the flagellar pocket, and subsequently moves back to the external cell surface. With all this bidirectional movements of VSGs within the flagellar pocket, it is possible that a VSG^{Sur} with an unusual structure or kinetics has a secondary effect on location and micro-movement of the transferrin receptor as well.

(iii) Concanavaline A: Measurement of the ConA uptake showed that VSG^{Sur} is endocytosed at a level not much lower than VSG^{221}. Still there seems to be a small difference, especially if the increased ConA binding to VSG^{Sur} is taken into account. This could be derived from alterations of VSG kinetics.

(iv) TLF1: The sensitivity to TLF1 was unchanged upon expression of $\textit{VSG}^{\textit{Sur}}$. This could be explained by a lack of interaction of the HpHb receptor with the VSGs due to the long and slender conformation of the HpHb receptor [320].

All in all, the suggested hypothesis is rather speculative, but based on our data it is a plausible scenario. Testing this hypothesis would be experimentally challenging. To have a first idea one could look at the surface localization of the transferrin receptor by fluorescence microscopy: Mislocalized ESAG6/7 outside of the flagellar pocket would indicate an influence of VSG^{Sur} on the movement and localization of surface proteins. But such conclusions have to be drawn with caution, as mislocalization of ESAG6/7 can also be a secondary effect of iron starvation (even though that was shown to be associated with ESAG6/7 overexpression, which was not the case in our RNA-Seq data) [328]. To comprehensively investigate the hypothesis one would have to monitor surface movements of the proteins in real time. This is highly challenging, but it is possible and has been done with VSGs [261]. Further, crystallography of the VSG^{Sur} structure could reveal potential alterations of the flexible part, which would suggest an effect on surface movement (or

possibly also endocytosis). A third way to find evidence for the suggested hypothesis would be to seek for binding partners of VSG^{Sur} and VSG^{221}; if surface proteins indeed bind to one but not the other, this would be a strong indication for interactions on the cell surface.

(3) Alteration of the endocytic system

A third hypothesis is a specific defect of the endocytosis apparatus that only affects certain surface proteins. In bloodstream-form trypanosomes, surface proteins, notably VSG and the transferrin receptor, are endocytosed at a very high rate [261,319]. This not only allows the parasite to efficiently take up the required nutrients, but it supports evasion of the immune system, since antibodies bound to VSGs are intracellularly cleaved off and the VSG recycled to the cell membrane [261,329]. Endocytosis and exocytosis exclusively take place at the flagellar pocket, which is located at the posterior end of the trypanosomes. After endocytosis, the different surface proteins localize to different endosomal compartements: VSG and the transferrin receptor (both GPI-anchored proteins) are located in early Rab5A endosomes, while the transmembrane protein ISG100 localizes to Rab5B endosomes [330]. This led to the hypothesis that Rab5A confers endosomal traffic of GPI-anchored proteins. In the endosomal compartement, the proteins are sorted and either directed to the lysosome or recycled back to the flagellar pocket via Rab11 endosomes [329]. A VSG with an unusual structure could interfere with this system; if, for example, intracellular traffic and sorting were somehow hampered or modified by VSG^{Sur}, this could have an effect on the whole endocytosis apparatus and lead to miss-trafficking or mislocalization in the endosomal compartment.

Do our results support this hypothesis?

(i) General endocytosis: The *VSG^{Sur}* expressing cells did not show a big-eye phenotype (enlargement of flagellar pocket that is usually seen in trypanosomes with a general endocytosis-defect). Further, their viability and growth rate was comparable to *VSG^{221}* and *VSG^{900}* expressing parasites (even though, in certain media their growth was reduced to some extent; Wiedemar and Zwyer, unpublished). Based on these data we can exclude a general endocytosis defect, but not a defect that only affects certain parts of the endocytosis apparatus.

(ii) The uptake of transferrin was highly reduced while the uptake of ConA was not strongly altered. Both, the transferrin receptor and the VSG (that mediates ConA

uptake) localize to Rab5A endosomes. Furthermore, the uptake of TLF1, and thus the endocytosis of the HpHb receptor, was not reduced. If the assumption were true that Rab5A endosomes confer trafficking of all GPI-anchored proteins, the HpHb receptor would also be localized to the Rab5A compartment. In this case, there would be at least three surface proteins located to the Rab5A, out of which some are affected by expression of VSG^{Sur} and others are not. Thus, we cannot narrow down the phenotype on a general defect of Rab5A-mediated transport.

Even though our data does not prove a specific endocytosis defect, it is a plausible scenario that an altered endocytosis apparatus, leading to mislocalization of proteins within the endosomal compartement, would cause such an endocytosis defect. To experimentally address this hypothesis, immune fluorescence microscopy could be useful: co-staining of different parts of the endosomal compartment (Rab5A, Rab5B, Rab11) with different substrates (transferrin, ConA, LDL) and receptors (ISG75) could identify alterations and mislocalizations in the endocytic system.

Conclusion

In summary, I propose three main hypotheses on how VSG^{Sur} could lead to suramin resistance and the uptake defect. VSG^{Sur} could act on the level of binding, on surface transport, or on the endocytic system. It might also be a combination of the hypothesized mechanisms that leads to the observed phenotype. Based on our data we can conclude that VSGs can indeed influence processes beyond the well-studied topic of immune evasion, and that they might interact with other surface proteins and/or influence the endocytic system. This brings us to the next question: What are the special features of VSG^{Sur} allowing such an impact on the cells?

Structural peculiarities of VSG^{Sur}

Even if we presently cannot name them, there must be some unusual structural features in VSG^{Sur}. VSGs, which usually form homodimers [331], have their N-terminal domain exposed to the surface and their C-terminal domain attached to the cell membrane through a GPI-anchor [332,333]. They can bear different numbers of C- and N-glycosylation sites [334]. Based on the cysteine residues in the N- and C-termini, VSGs can be classified in different groups [335]. The number and positions of cysteines implies that VSG^{Sur} is a

typical A2 type VSG, and preliminary computational models have not shown any abnormalities of the 3D structure compared to other VSGs (Wiedemar & Zoltner, unpublished). But even if they are subtle, there must be some peculiar structural features within the 3D structure, glycosylation and/or multimeric state of VSG^{Sur}. A recently discovered additional O-glycosylation site on top of certain VSGs was associated with alterations of the 3D structure and the multimeric state [336]. Similar changes of VSG^{Sur} could possibly carry out the observed phenotype. Indeed, VSG^{Sur} contains a cysteine-flanked loop with a threonine at position 164 similar to what was described by Pinger et al [336]. Interestingly, preliminary investigations of the multimeric state using blue-native gels indicate that VSG^{Sur} indeed forms a higher multimeric state than the classical dimer (Wiedemar & Zoltner, unpublished). Thus, hopefully, we will be able to identify the structure of VSG^{Sur} by further experiments like crystallography and size-exclusion chromatography. Another way to narrow down the parts of the VSG^{Sur} that are causal for the phenotype would be to investigate mutant and chimeric VSGs. The $VSG^{Supersur}$ mutant is a first step in that direction; if the enhancement of resistance in $VSG^{Supersur}$ expressing cells can be confirmed, this could depict structural key positions mediating the alterations. Additionally, one could systematically produce chimeras of VSG^{Sur} and VSG^{221}, starting with a pair of chimeras that bear the VSG^{Sur} N-terminal domain and the VSG^{221} C-terminal domain and vice versa.

6.2. What do we learn about suramin uptake?

Based on the observation that *ISG75* knock-down led to suramin resistance and reduced binding of suramin to the cell surface [42], it was proposed that ISG75 acts as the suramin receptor in *T. brucei*. But failure to show direct binding of suramin to ISG75 *in vitro* (unpublished data Martin Zoltner [337]) indicates the presence of additional factors involved in suramin binding. Our data are in agreement with a suramin uptake model that involves ISG75: The ISG75 knock-down experiments with VSG^{221} expressing cells showed a similar decrease in suramin susceptibility as observed by Alsford et al [42] and an even larger effect in VSG^{Sur} expressors. Even though the ISG75 turnover (half-live) was unchanged, a VSG^{Sur}-mediated defect of suramin binding, trafficking and/or endocytosis via ISG75 is basically possible. Concurrently we have made the following observations that indicate the presence of additional factors:

a) ISG75 knock-down had as stronger effect on *VSG*^{Sur} expressing cells than on the *VSG*^{221} expressing parent. Thus, ISG75 is even more important for suramin uptake in *VSG*^{Sur} expressing cells while for *VSG*^{221} expressing cells there might be an additional receptor or pathway involved.

b) Suramin sensitivity (and thus suramin uptake) was enhanced in the presence of LDL in *VSG*^{221} but not in *VSG*^{Sur} expressing cells (similar results in *VSG*^{Sur} and *VSG*^{900} expressing *T. b. rhodesiense* STIB900 cells confirmed this finding; Wiedemar & Cal, data not shown).

c) Suramin reduced LDL uptake in *VSG*^{221} but not in *VSG*^{Sur} expressing cells. This observation at first glance seems to contradict b), but it is in agreement with the literature [59] and points out the presence of an interdependence of suramin and LDL uptake.

Together, these three observations indicate the presence of two suramin receptors. One receptor (R^{Sur}) binds free suramin; it is or it involves ISG75. The other receptor binds suramin in complex with LDL (R^{LDL_Sur}). LDL was proposed to bind to two receptors; a high affinity and a low-affinity receptor [296]. I suggest that R^{LDL_Sur} is one of these LDL receptors. If the uptake of suramin-LDL by R^{LDL_Sur} is less efficient than the uptake of LDL alone, this would explain the inhibitory effect of suramin on LDL uptake. If we assume that VSG^{Sur} completely abrogates the function of R^{LDL_Sur}, while having only a minor effect on R^{Sur} (through the above suggested reduced binding, traffic or uptake), we could also explain observations a) and b). Based on this model, suramin uptake in *VSG*^{Sur} expressing cells would then only take place through the ISG75 involving R^{Sur} and be independent of LDL. Of course there are critical points challenging this model: upon addition of LDL to serum-free medium we did not see any shift in IC50 of the *VSG*^{Sur} expressors. But should they not take up less suramin if part of the suramin is bound to LDL? Possibly, but not necessarily: the LDL levels used in the assay were rather low and might just confer a small decrease of the unbound suramin pool.

What about other models; could VSG itself act as a suramin receptor? In the course of my studies this was actually the first hypothesis we had. It could go in both directions: (i) All VSG confer suramin binding except for VSG^{Sur}; or (ii) VSG^{Sur} is the only VSG that confers suramin binding. In scenario (ii) one could further speculate that due to a binding of suramin to VSG^{Sur}, it does not bind to its usual receptor and is, after endocytosis,

exocytosed together with VSG^{Sur}. In my opinion, such models seem rather unlikely in the meantime because they do not provide any explanation of the highly reduced uptake of transferrin and LDL.

Taken together, the effects of VSG^{Sur} are not simple and cannot easily be explained. VSG^{Sur} has a direct or indirect influence on different surface proteins. For suramin uptake itself, I propose a new model that includes two receptors: R^{Sur} involves ISG75 and confers uptake of unbound suramin; R^{LDL_Sur} is one of the LDL receptors and confers uptake of suramin in complex with LDL.

6.3. Helicase – a potential target of suramin in *T. brucei*

In light of the many enzymes that can be inhibited by suramin (Chapter 2), it is likely that the cytotoxic action in *T. brucei* cannot be narrowed down to one single target but is carried out through a combination of different inhibitory effects. Nevertheless, we can assume that these various targets are not equally suramin sensitive, and that their inhibition is not equally harmful to the trypanosome. Thus, it is likely that there is a major target, mutation or upregulation of which can confer a certain degree of suramin resistance. With the RuvB-like helicase (Tb927.4.1270) we might have identified this target. The fact that the isoleucin^{312} to valine (I312V) mutation in the RuvB-like helicase was absent in the *T. b. rhodesiense* line STIB900 before suramin selection, then at first appeared heterozygously, and later-on turned homozygous while the parasites were selected for higher and higher suramin resistance, is a strong indication that the mutation confers resistance. Theoretically, such a shift from wildtype to heterozygous to homozygous could as well be a hitchhiking effect and the real cause of resistance genetically linked to the mutated RuvB-like helicase. But, for the following reasons, we have strong indications that the mutation itself causes suramin resistance:

a) There were no other mutations on that chromosome or elsewhere in the transcriptome that showed such a shift from wildtype to heterozygous to homozygous.
b) The very same residue of RuvB-like helicase was found to be mutated in a completely independent parasite, which even belongs to another subspecies: a suramin-resistant field isolate of *T. evansi*.
c) The mutated residue is highly conserved among kinetoplastids and beyond.

d) Suramin inhibits viral helicases already at nanomolar to low micromolar concentrations [100,168,207].

RuvB-like helicases are involved in transcription activation via chromatin remodeling and removal of histone modifications, in DNA damage repair, oncogenesis and production of small nuclear ribonucleoproteins [299]. They also affect mitosis as they act on the replication fork and the spindle apparatus through interactions with microtubules [299] with an impact on chromosomal alignment and segregation [338]. They were further shown to bind to Holliday junctions [339] and might thus catalyze branch migration at the sites of homologous recombination, as do their bacterial orthologues [340]. RuvB-like helicases are also involved in telomere maintenance through interactions with telomere reverse transcriptase [341]. The activity of RuvB-like helicase is dose-sensitive, and heterozygous gene loss leads to haploinsufficiency in yeast [339]. Could an inhibition of the RuvB-like helicase confer the cytotoxic activity of suramin in *T. brucei*?

In sight of the above described functions of RuvB-like helicases, an inhibition of the enzyme might lead to problems in transcription, replication and mitosis, with an onset of drug action within the first cell cycle, thus within a couple of hours in the quickly dividing *T. brucei*. Indeed, if *T. brucei* is exposed to suramin, onset of action can be seen after five hours [249]. Recent studies showed an elevated proportion of *T. brucei* cells with more than two nuclei after suramin exposure for 24 hours, which indicates a cytokinesis defect with maintained mitosis [34]. One could speculate that such a phenotype is mediated through an inhibitory effect of suramin on the interaction of RuvB-like helicase with microtubules, which play a role in cytokinesis [342].

If the RuvB-like helicase is indeed a target, how could the identified mutations I312V in the lab-selected *T. b. rhodesiense* and I312L in the resistant *T. evansi* field isolate confer protection from suramin?

The *T. brucei* RuvB-like helicase is an essential enzyme in bloodstream-form *T. brucei* [303], thus any nonsynonymous SNP must preserve helicase function. RuvB-like helicases can be present as monomers or as hexameric rings [299]. They contain three different domains: Domain I confers ATP binding, domain III, which is in close proximity to domain I, caps the ATP binding site, and domain II mediates binding to nucleic acids [300]. The mutated isoleucine is located within the second subunit of domain I, four residues after the

Walker B motif, which is thought to be responsible for ATP hydrolysis [300]. For the Zika virus helicase, 3D modeling indicated binding of suramin either to the ATP binding site or the RNA binding site [100]. If suramin binds to the ATP binding site in the *T. brucei* RuvB-like helicase, the I312V substitution could protect from suramin action by an impairment of suramin binding. If suramin binds to and inhibits the nucleic acid binding site, the I312V amino acid exchange might not interfere with suramin binding directly as it is located elsewhere, in domain I close to the ATP binding site. But it might increase the activity of RuvB-like helicase and even out the inhibitory suramin action to some extent. This would not completely antagonize the action of suramin, but might lead to some degree of resistance as observed in the *T. b. rhodesiense* cells with the mutated RuvB-like helicase.

To sum up, we have strong indications that the identified RuvB-like helicase is an intracellular target for suramin in *T. brucei*. To challenge this hypothesis I am currently performing reverse genetic experiments and introducing the mutated allele in wildtype and heterozygously mutated *T. brucei* cells. The outcome of these experiments will hopefully provide a clear answer and show whether I312V in *T. brucei* RuvB-like helicase indeed confers suramin resistance.

6.4. Final conclusion

Through analysis of the transcriptome of suramin-resistant *T. b. rhodesiense* cells, I have discovered a new variant surface glycoprotein, VSG^{Sur}, expression of which causes suramin resistance and a reduced uptake of different substrates. Even though the exact impact of VSG^{Sur} on suramin uptake is not yet fully understood, these results revealed a new mechanism, which is the first link between antigenic variation and drug resistance. The discovery of VSG^{Sur} even raises questions that go beyond the research area of drug resistance and affect fundamental biology of trypanosomes and the function of VSGs in general.

With the RuvB-like helicase, I further identified a previously unknown candidate target for suramin action in *T. brucei*. If the described mutation in the RuvB-like helicase indeed leads to resistance, this will be the first observation of drug resistance mediated by an altered drug target in *T. brucei*.

All in all, the results of this PhD thesis increase our knowledge on drug resistance in *T. brucei* by adding two new potential resistance mechanisms (Fig 1). I hope that this new

knowledge will provide a better understanding of drug uptake and drug action, which will hopefully be useful for future basic biological research as well as drug development.

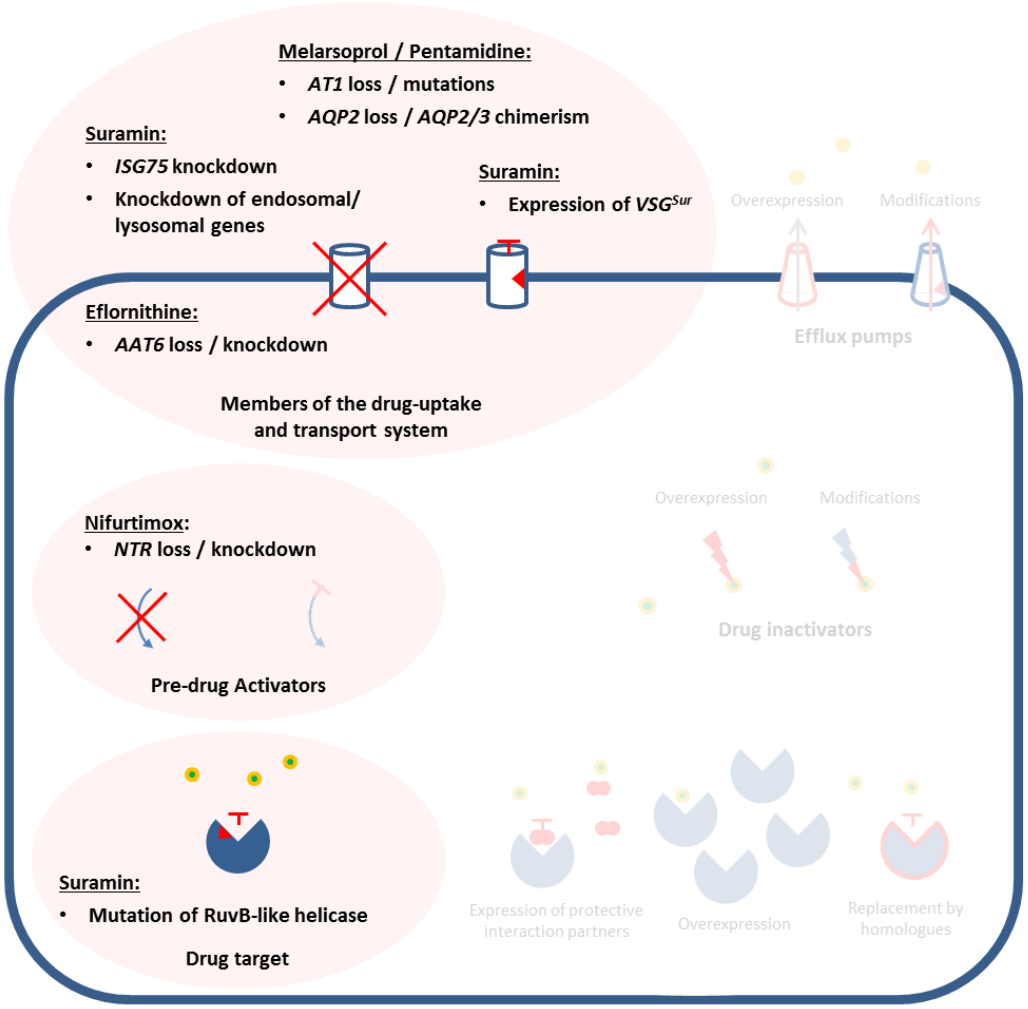

Figure 1: Mechanisms of drug resistance in *T. brucei*. Two new resistance mechanisms against suramin are added compared to Figure 3 of Chapter 1: The VSG^{Sur}-mediated resistance, which is an alteration of the uptake system; and the mutation in RuvB-like helicase, which could potentially be a modification of the drug target.

References

1. Iyidogan P, Anderson KS. Current perspectives on HIV-1 antiretroviral drug resistance. Viruses. 2014;6: 4095–4139. doi:10.3390/v6104095
2. Gross M. Antibiotics in crisis. Curr Biol CB. 2013;23: R1063-1065.
3. Perlin DS, Rautemaa-Richardson R, Alastruey-Izquierdo A. The global problem of antifungal resistance: prevalence, mechanisms, and management. Lancet Infect Dis. 2017;17: e383–e392. doi:10.1016/S1473-3099(17)30316-X
4. Vanaerschot M, Huijben S, Van den Broeck F, Dujardin J-C. Drug resistance in vectorborne parasites: multiple actors and scenarios for an evolutionary arms race. FEMS Microbiol Rev. 2014;38: 41–55. doi:10.1111/1574-6976.12032
5. Barok M, Joensuu H, Isola J. Trastuzumab emtansine: mechanisms of action and drug resistance. Breast Cancer Res BCR. 2014;16: 209. doi:10.1186/bcr3621
6. Morrone LA, Scuteri D, Rombolà L, Mizoguchi H, Bagetta G. Opioids Resistance in Chronic Pain Management. Curr Neuropharmacol. 2017;15: 444–456. doi:10.2174/1570159X14666161101092822
7. Allouche S, Noble F, Marie N. Opioid receptor desensitization: mechanisms and its link to tolerance. Front Pharmacol. 2014;5: 280. doi:10.3389/fphar.2014.00280
8. Wozniak A, Villagra NA, Undabarrena A, Gallardo N, Keller N, Moraga M, et al. Porin alterations present in non-carbapenemase-producing Enterobacteriaceae with high and intermediate levels of carbapenem resistance in Chile. J Med Microbiol. 2012;61: 1270–1279. doi:10.1099/jmm.0.045799-0
9. Blair JMA, Webber MA, Baylay AJ, Ogbolu DO, Piddock LJV. Molecular mechanisms of antibiotic resistance. Nat Rev Microbiol. 2015;13: 42–51. doi:10.1038/nrmicro3380
10. Alibert S, N'gompaza Diarra J, Hernandez J, Stutzmann A, Fouad M, Boyer G, et al. Multidrug efflux pumps and their role in antibiotic and antiseptic resistance: a pharmacodynamic perspective. Expert Opin Drug Metab Toxicol. 2017;13: 301–309. doi:10.1080/17425255.2017.1251581
11. Jacoby GA. AmpC beta-lactamases. Clin Microbiol Rev. 2009;22: 161–182, Table of Contents. doi:10.1128/CMR.00036-08
12. Gniadkowski M. Evolution of extended-spectrum beta-lactamases by mutation. Clin Microbiol Infect Off Publ Eur Soc Clin Microbiol Infect Dis. 2008;14 Suppl 1: 11–32. doi:10.1111/j.1469-0691.2007.01854.x
13. Unissa AN, Subbian S, Hanna LE, Selvakumar N. Overview on mechanisms of isoniazid action and resistance in Mycobacterium tuberculosis. Infect Genet Evol J Mol Epidemiol Evol Genet Infect Dis. 2016;45: 474–492. doi:10.1016/j.meegid.2016.09.004
14. Ando H, Kitao T, Miyoshi-Akiyama T, Kato S, Mori T, Kirikae T. Downregulation of katG expression is associated with isoniazid resistance in Mycobacterium

tuberculosis. Mol Microbiol. 2011;79: 1615–1628. doi:10.1111/j.1365-2958.2011.07547.x

15. Jacoby GA, Walsh KE, Mills DM, Walker VJ, Oh H, Robicsek A, et al. qnrB, another plasmid-mediated gene for quinolone resistance. Antimicrob Agents Chemother. 2006;50: 1178–1182. doi:10.1128/AAC.50.4.1178-1182.2006

16. Palmer AC, Kishony R. Opposing effects of target overexpression reveal drug mechanisms. Nat Commun. 2014;5: 4296. doi:10.1038/ncomms5296

17. Ehrlich P. Chemotherapeutische Trypanosomen-Studien. Berliner klinische Wochenschrift. 1907;44: 310–314.

18. Ehrlich P. Address in Pathology, ON CHEMIOTHERAPY: Delivered before the Seventeenth International Congress of Medicine. Br Med J. 1913;2: 353–359.

19. Voegtlin C, Dyer HA, Miller DW. On Drug-Resistance of Trypanosomes with Particular Reference to Arsenic. J Pharmacol Exp Ther. 1924;23: 55–36.

20. Yorke W. DRUG-RESISTANCE. Br J Vener Dis. 1933;9: 83–97.

21. Wainwright M. Dyes, trypanosomiasis and DNA: a historical and critical review. Biotech Histochem Off Publ Biol Stain Comm. 2010;85: 341–354. doi:10.3109/10520290903297528

22. Lawson TL. Trypanosomiasis treated with “Pentamidine.” The Lancet. 1942;240: 480–483. doi:https://doi.org/10.1016/S0140-6736(00)58164-1

23. Friedheim E a. H. Mel B in the treatment of human trypanosomiasis. Am J Trop Med Hyg. 1949;29: 173–180.

24. Steverding D. The development of drugs for treatment of sleeping sickness: a historical review. Parasit Vectors. 2010;3: 15. doi:10.1186/1756-3305-3-15

25. Burri C, Stich A, Brun R. Current Chemotherapy of Human African Trypanosomiasis. In: Maudlin I, Holmes PH, Miles MA, editors. The Trypanosomiases. CABI Publishing; 2004. p. 403.

26. Taelman H, Schechter PJ, Marcelis L, Sonnet J, Kazyumba G, Dasnoy J, et al. Difluoromethylornithine, an effective new treatment of Gambian trypanosomiasis. Results in five patients. Am J Med. 1987;82: 607–614.

27. Iten M, Matovu E, Brun R, Kaminsky R. Innate lack of susceptibility of Ugandan Trypanosoma brucei rhodesiense to DL-alpha-difluoromethylornithine (DFMO). Trop Med Parasitol Off Organ Dtsch Tropenmedizinische Ges Dtsch Ges Tech Zusammenarbeit GTZ. 1995;46: 190–194.

28. Checchi F, Piola P, Ayikoru H, Thomas F, Legros D, Priotto G. Nifurtimox plus Eflornithine for late-stage sleeping sickness in Uganda: a case series. PLoS Negl Trop Dis. 2007;1: e64. doi:10.1371/journal.pntd.0000064

29. Torreele E, Bourdin Trunz B, Tweats D, Kaiser M, Brun R, Mazué G, et al. Fexinidazole--a new oral nitroimidazole drug candidate entering clinical development for the treatment of sleeping sickness. PLoS Negl Trop Dis. 2010;4: e923. doi:10.1371/journal.pntd.0000923

30. Kaiser M, Bray MA, Cal M, Bourdin Trunz B, Torreele E, Brun R. Antitrypanosomal activity of fexinidazole, a new oral nitroimidazole drug candidate for treatment of

sleeping sickness. Antimicrob Agents Chemother. 2011;55: 5602–5608. doi:10.1128/AAC.00246-11

31. Deeks ED. Fexinidazole: First Global Approval. Drugs. 2019. doi:10.1007/s40265-019-1051-6

32. Fairlamb AH, Henderson GB, Cerami A. Trypanothione is the primary target for arsenical drugs against African trypanosomes. Proc Natl Acad Sci U S A. 1989;86: 2607–2611.

33. Worthen C, Jensen BC, Parsons M. Diverse effects on mitochondrial and nuclear functions elicited by drugs and genetic knockdowns in bloodstream stage Trypanosoma brucei. PLoS Negl Trop Dis. 2010;4: e678. doi:10.1371/journal.pntd.0000678

34. Thomas JA, Baker N, Hutchinson S, Dominicus C, Trenaman A, Glover L, et al. Insights into antitrypanosomal drug mode-of-action from cytology-based profiling. PLoS Negl Trop Dis. 2018;12: e0006980. doi:10.1371/journal.pntd.0006980

35. Rollo IM, Williamson J. Acquired resistance to "Melarsen", tryparsamide and amidines in pathogenic trypanosomes after treatment with "Melarsen" alone. Nature. 1951;167: 147–148.

36. Frommel TO, Balber AE. Flow cytofluorimetric analysis of drug accumulation by multidrug-resistant Trypanosoma brucei brucei and T. b. rhodesiense. Mol Biochem Parasitol. 1987;26: 183–191.

37. Carter NS, Fairlamb AH. Arsenical-resistant trypanosomes lack an unusual adenosine transporter. Nature. 1993;361: 173–176. doi:10.1038/361173a0

38. Carter NS, Berger BJ, Fairlamb AH. Uptake of diamidine drugs by the P2 nucleoside transporter in melarsen-sensitive and -resistant Trypanosoma brucei brucei. J Biol Chem. 1995;270: 28153–28157.

39. Mäser P, Sütterlin C, Kralli A, Kaminsky R. A nucleoside transporter from Trypanosoma brucei involved in drug resistance. Science. 1999;285: 242–244.

40. Matovu E, Geiser F, Schneider V, Mäser P, Enyaru JC, Kaminsky R, et al. Genetic variants of the TbAT1 adenosine transporter from African trypanosomes in relapse infections following melarsoprol therapy. Mol Biochem Parasitol. 2001;117: 73–81.

41. Matovu E, Stewart ML, Geiser F, Brun R, Mäser P, Wallace LJM, et al. Mechanisms of arsenical and diamidine uptake and resistance in Trypanosoma brucei. Eukaryot Cell. 2003;2: 1003–1008.

42. Alsford S, Eckert S, Baker N, Glover L, Sanchez-Flores A, Leung KF, et al. High-throughput decoding of antitrypanosomal drug efficacy and resistance. Nature. 2012;482: 232–236. doi:10.1038/nature10771

43. Graf FE, Ludin P, Arquint C, Schmidt RS, Schaub N, Kunz Renggli C, et al. Comparative genomics of drug resistance in Trypanosoma brucei rhodesiense. Cell Mol Life Sci CMLS. 2016;73: 3387–3400. doi:10.1007/s00018-016-2173-6

44. Graf FE, Ludin P, Wenzler T, Kaiser M, Brun R, Pyana PP, et al. Aquaporin 2 mutations in Trypanosoma brucei gambiense field isolates correlate with decreased susceptibility to pentamidine and melarsoprol. PLoS Negl Trop Dis. 2013;7: e2475. doi:10.1371/journal.pntd.0002475

45. Munday JC, Eze AA, Baker N, Glover L, Clucas C, Aguinaga Andrés D, et al. Trypanosoma brucei aquaglyceroporin 2 is a high-affinity transporter for pentamidine and melaminophenyl arsenic drugs and the main genetic determinant of resistance to these drugs. J Antimicrob Chemother. 2014;69: 651–663. doi:10.1093/jac/dkt442

46. Song J, Baker N, Rothert M, Henke B, Jeacock L, Horn D, et al. Pentamidine Is Not a Permeant but a Nanomolar Inhibitor of the Trypanosoma brucei Aquaglyceroporin-2. PLoS Pathog. 2016;12: e1005436. doi:10.1371/journal.ppat.1005436

47. Bacchi CJ, Nathan HC, Hutner SH, McCann PP, Sjoerdsma A. Polyamine metabolism: a potential therapeutic target in trypanosomes. Science. 1980;210: 332–334.

48. Vincent IM, Creek D, Watson DG, Kamleh MA, Woods DJ, Wong PE, et al. A molecular mechanism for eflornithine resistance in African trypanosomes. PLoS Pathog. 2010;6: e1001204. doi:10.1371/journal.ppat.1001204

49. Baker N, Alsford S, Horn D. Genome-wide RNAi screens in African trypanosomes identify the nifurtimox activator NTR and the eflornithine transporter AAT6. Mol Biochem Parasitol. 2011;176: 55–57. doi:10.1016/j.molbiopara.2010.11.010

50. Schumann Burkard G, Jutzi P, Roditi I. Genome-wide RNAi screens in bloodstream form trypanosomes identify drug transporters. Mol Biochem Parasitol. 2011;175: 91–94. doi:10.1016/j.molbiopara.2010.09.002

51. Pépin J, Khonde N, Maiso F, Doua F, Jaffar S, Ngampo S, et al. Short-course eflornithine in Gambian trypanosomiasis: a multicentre randomized controlled trial. Bull World Health Organ. 2000;78: 1284–1295.

52. Iten M, Mett H, Evans A, Enyaru JC, Brun R, Kaminsky R. Alterations in ornithine decarboxylase characteristics account for tolerance of Trypanosoma brucei rhodesiense to D,L-alpha-difluoromethylornithine. Antimicrob Agents Chemother. 1997;41: 1922–1925.

53. Tsuhako MH, Alves MJ, Colli W, Filardi LS, Brener Z, Augusto O. Comparative studies of nifurtimox uptake and metabolism by drug-resistant and susceptible strains of Trypanosoma cruzi. Comp Biochem Physiol C. 1991;99: 317–321.

54. Docampo R. Sensitivity of parasites to free radical damage by antiparasitic drugs. Chem Biol Interact. 1990;73: 1–27.

55. Boiani M, Piacenza L, Hernández P, Boiani L, Cerecetto H, González M, et al. Mode of action of nifurtimox and N-oxide-containing heterocycles against Trypanosoma cruzi: is oxidative stress involved? Biochem Pharmacol. 2010;79: 1736–1745. doi:10.1016/j.bcp.2010.02.009

56. Wilkinson SR, Taylor MC, Horn D, Kelly JM, Cheeseman I. A mechanism for cross-resistance to nifurtimox and benznidazole in trypanosomes. Proc Natl Acad Sci U S A. 2008;105: 5022–5027. doi:10.1073/pnas.0711014105

57. Wang CC. Molecular mechanisms and therapeutic approaches to the treatment of African trypanosomiasis. Annu Rev Pharmacol Toxicol. 1995;35: 93–127. doi:10.1146/annurev.pa.35.040195.000521

58. Fairlamb AH, Bowman IB. Uptake of the trypanocidal drug suramin by bloodstream forms of Trypanosoma brucei and its effect on respiration and growth rate in vivo. Mol Biochem Parasitol. 1980;1: 315–333.

59. Vansterkenburg EL, Coppens I, Wilting J, Bos OJ, Fischer MJ, Janssen LH, et al. The uptake of the trypanocidal drug suramin in combination with low-density lipoproteins by Trypanosoma brucei and its possible mode of action. Acta Trop. 1993;54: 237–250.

60. El Rayah IE, Kaminsky R, Schmid C, El Malik KH. Drug resistance in Sudanese Trypanosoma evansi. Vet Parasitol. 1999;80: 281–287.

61. Zhou J, Shen J, Liao D, Zhou Y, Lin J. Resistance to drug by different isolates Trypanosoma evansi in China. Acta Trop. 2004;90: 271–275. doi:10.1016/j.actatropica.2004.02.002

62. Zoltner M, Leung KF, Alsford S, Horn D, Field MC. Modulation of the Surface Proteome through Multiple Ubiquitylation Pathways in African Trypanosomes. PLoS Pathog. 2015;11: e1005236. doi:10.1371/journal.ppat.1005236

63. Brun R, Blum J, Chappuis F, Burri C. Human African trypanosomiasis. Lancet Lond Engl. 2010;375: 148–159. doi:10.1016/S0140-6736(09)60829-1

64. Burri C, Chappuis F, Brun R. Human African Trypanosomiasis. 23rd ed. Manson's Tropical Diseases. 23rd ed. Saunders Ltd.; 2014. pp. 606–691.

65. Giordani F, Morrison LJ, Rowan TG, DE Koning HP, Barrett MP. The animal trypanosomiases and their chemotherapy: a review. Parasitology. 2016;143: 1862–1889. doi:10.1017/S0031182016001268

66. Bisaggio DFR, Adade CM, Souto-Padrón T. In vitro effects of suramin on Trypanosoma cruzi. Int J Antimicrob Agents. 2008;31: 282–286. doi:10.1016/j.ijantimicag.2007.11.001

67. Santos EC, Novaes RD, Cupertino MC, Bastos DSS, Klein RC, Silva EAM, et al. Concomitant Benznidazole and Suramin Chemotherapy in Mice Infected with a Virulent Strain of Trypanosoma cruzi. Antimicrob Agents Chemother. 2015;59: 5999–6006. doi:10.1128/AAC.00779-15

68. Khanra S, Kumar YP, Dash J, Banerjee R. In vitro screening of known drugs identified by scaffold hopping techniques shows promising leishmanicidal activity for suramin and netilmicin. BMC Res Notes. 2018;11: 319. doi:10.1186/s13104-018-3446-y

69. Fleck SL, Birdsall B, Babon J, Dluzewski AR, Martin SR, Morgan WD, et al. Suramin and suramin analogues inhibit merozoite surface protein-1 secondary processing and erythrocyte invasion by the malaria parasite Plasmodium falciparum. J Biol Chem. 2003;278: 47670–47677. doi:10.1074/jbc.M306603200

70. Müller HM, Reckmann I, Hollingdale MR, Bujard H, Robson KJ, Crisanti A. Thrombospondin related anonymous protein (TRAP) of Plasmodium falciparum binds specifically to sulfated glycoconjugates and to HepG2 hepatoma cells suggesting a role for this molecule in sporozoite invasion of hepatocytes. EMBO J. 1993;12: 2881–2889.

71. Hawking F. Chemotherapy of onchocerciasis. Trans R Soc Trop Med Hyg. 1958;52: 109–111.

72. Ashburn LL, Burch TA, Brady FJ. Pathologic effects of suramin, hetrazan and arsenamide on adult Onchocerca volvulus. Boletin Oficina Sanit Panam Pan Am Sanit Bur. 1949;28: 1107–1117.

73. Burch TA, Ashburn LL. Experimental therapy of onchocerciasis with suramin and hetrazan; results of a three-year study. Am J Trop Med Hyg. 1951;31: 617–623.

74. Babalola OE. Ocular onchocerciasis: current management and future prospects. Clin Ophthalmol Auckl NZ. 2011;5: 1479–1491. doi:10.2147/OPTH.S8372

75. Coyne PE, Maxwell C. Suramin and therapy of onchocerciasis. Arch Dermatol. 1992;128: 698.

76. Voogd TE, Vansterkenburg EL, Wilting J, Janssen LH. Recent research on the biological activity of suramin. Pharmacol Rev. 1993;45: 177–203.

77. Reiter B, Oram JD. Inhibition of streptococcal bacteriophage by suramin. Nature. 1962;193: 651–652.

78. Herrmann-Erlee MP, Wolff L. Inhibition of mumps virus reproduction by congored and suramine. Arch Int Pharmacodyn Ther. 1957;110: 340–341.

79. De Clercq E. Suramin: a potent inhibitor of the reverse transcriptase of RNA tumor viruses. Cancer Lett. 1979;8: 9–22.

80. Mitsuya H, Popovic M, Yarchoan R, Matsushita S, Gallo RC, Broder S. Suramin protection of T cells in vitro against infectivity and cytopathic effect of HTLV-III. Science. 1984;226: 172–174.

81. Broder S, Yarchoan R, Collins JM, Lane HC, Markham PD, Klecker RW, et al. Effects of suramin on HTLV-III/LAV infection presenting as Kaposi's sarcoma or AIDS-related complex: clinical pharmacology and suppression of virus replication in vivo. Lancet Lond Engl. 1985;2: 627–630.

82. Kaplan LD, Wolfe PR, Volberding PA, Feorino P, Levy JA, Abrams DI, et al. Lack of response to suramin in patients with AIDS and AIDS-related complex. Am J Med. 1987;82: 615–620.

83. Cheson BD, Levine AM, Mildvan D, Kaplan LD, Wolfe P, Rios A, et al. Suramin therapy in AIDS and related disorders. Report of the US Suramin Working Group. JAMA. 1987;258: 1347–1351.

84. Yahi N, Sabatier JM, Nickel P, Mabrouk K, Gonzalez-Scarano F, Fantini J. Suramin inhibits binding of the V3 region of HIV-1 envelope glycoprotein gp120 to galactosylceramide, the receptor for HIV-1 gp120 on human colon epithelial cells. J Biol Chem. 1994;269: 24349–24353.

85. Chen Y, Maguire T, Hileman RE, Fromm JR, Esko JD, Linhardt RJ, et al. Dengue virus infectivity depends on envelope protein binding to target cell heparan sulfate. Nat Med. 1997;3: 866–871.

86. Aguilar JS, Rice M, Wagner EK. The polysulfonated compound suramin blocks adsorption and lateral difusion of herpes simplex virus type-1 in vero cells. Virology. 1999;258: 141–151. doi:10.1006/viro.1999.9723

87. Garson JA, Lubach D, Passas J, Whitby K, Grant PR. Suramin blocks hepatitis C binding to human hepatoma cells in vitro. J Med Virol. 1999;57: 238–242.

88. Alarcón B, Lacal JC, Fernández-Sousa JM, Carrasco L. Screening for new compounds with antiherpes activity. Antiviral Res. 1984;4: 231–244.

89. Offensperger WB, Offensperger S, Walter E, Blum HE, Gerok W. Suramin prevents duck hepatitis B virus infection in vivo. Antimicrob Agents Chemother. 1993;37: 1539–1542.

90. Tsiquaye K, Zuckerman A. Suramin inhibits duck hepatitis B virus DNA polymerase activity. J Hepatol. 1985;1: 663–669.

91. Tsiquaye KN, Collins P, Zuckerman AJ. Antiviral activity of the polybasic anion, suramin and acyclovir in Hepadna virus infection. J Antimicrob Chemother. 1986;18 Suppl B: 223–228.

92. Loke RH, Anderson MG, Coleman JC, Tsiquaye KN, Zuckerman AJ, Murray-Lyon IM. Suramin treatment for chronic active hepatitis B--toxic and ineffective. J Med Virol. 1987;21: 97–99.

93. Wang Y, Qing J, Sun Y, Rao Z. Suramin inhibits EV71 infection. Antiviral Res. 2014;103: 1–6. doi:10.1016/j.antiviral.2013.12.008

94. Ren P, Zou G, Bailly B, Xu S, Zeng M, Chen X, et al. The approved pediatric drug suramin identified as a clinical candidate for the treatment of EV71 infection-suramin inhibits EV71 infection in vitro and in vivo. Emerg Microbes Infect. 2014;3: e62. doi:10.1038/emi.2014.60

95. Ren P, Zheng Y, Wang W, Hong L, Delpeyroux F, Arenzana-Seisdedos F, et al. Suramin interacts with the positively charged region surrounding the 5-fold axis of the EV-A71 capsid and inhibits multiple enterovirus A. Sci Rep. 2017;7: 42902. doi:10.1038/srep42902

96. Albulescu IC, van Hoolwerff M, Wolters LA, Bottaro E, Nastruzzi C, Yang SC, et al. Suramin inhibits chikungunya virus replication through multiple mechanisms. Antiviral Res. 2015;121: 39–46. doi:10.1016/j.antiviral.2015.06.013

97. Ho Y-J, Wang Y-M, Lu J, Wu T-Y, Lin L-I, Kuo S-C, et al. Suramin Inhibits Chikungunya Virus Entry and Transmission. PloS One. 2015;10: e0133511. doi:10.1371/journal.pone.0133511

98. Kuo S-C, Wang Y-M, Ho Y-J, Chang T-Y, Lai Z-Z, Tsui P-Y, et al. Suramin treatment reduces chikungunya pathogenesis in mice. Antiviral Res. 2016;134: 89–96. doi:10.1016/j.antiviral.2016.07.025

99. Henß L, Beck S, Weidner T, Biedenkopf N, Sliva K, Weber C, et al. Suramin is a potent inhibitor of Chikungunya and Ebola virus cell entry. Virol J. 2016;13: 149. doi:10.1186/s12985-016-0607-2

100. Tan CW, Sam I-C, Chong WL, Lee VS, Chan YF. Polysulfonate suramin inhibits Zika virus infection. Antiviral Res. 2017;143: 186–194. doi:10.1016/j.antiviral.2017.04.017

101. Williams WL. The Effects of Suramin (Germanin), Azo Dyes, and Vasodilators on Mice with Transplanted Lymphosarcomas. AACR. 1946;6: 344–353.

102. Osswald H, Youssef M. Suramin enhancement of the chemotherapeutic actions of cyclophosphamide or adriamycin of intramuscularly-implanted Ehrlich carcinoma. Cancer Lett. 1979;6: 337–343.

103. Stein CA, LaRocca RV, Thomas R, McAtee N, Myers CE. Suramin: an anticancer drug with a unique mechanism of action. J Clin Oncol Off J Am Soc Clin Oncol. 1989;7: 499–508. doi:10.1200/JCO.1989.7.4.499

104. Bowden CJ, Figg WD, Dawson NA, Sartor O, Bitton RJ, Weinberger MS, et al. A phase I/II study of continuous infusion suramin in patients with hormone-refractory prostate cancer: toxicity and response. Cancer Chemother Pharmacol. 1996;39: 1–8.

105. Rosen PJ, Mendoza EF, Landaw EM, Mondino B, Graves MC, McBride JH, et al. Suramin in hormone-refractory metastatic prostate cancer: a drug with limited efficacy. J Clin Oncol Off J Am Soc Clin Oncol. 1996;14: 1626–1636. doi:10.1200/JCO.1996.14.5.1626

106. Dawson NA, Figg WD, Cooper MR, Sartor O, Bergan RC, Senderowicz AM, et al. Phase II trial of suramin, leuprolide, and flutamide in previously untreated metastatic prostate cancer. J Clin Oncol Off J Am Soc Clin Oncol. 1997;15: 1470–1477. doi:10.1200/JCO.1997.15.4.1470

107. Hussain M, Fisher EI, Petrylak DP, O'Connor J, Wood DP, Small EJ, et al. Androgen deprivation and four courses of fixed-schedule suramin treatment in patients with newly diagnosed metastatic prostate cancer: A Southwest Oncology Group Study. J Clin Oncol Off J Am Soc Clin Oncol. 2000;18: 1043–1049. doi:10.1200/JCO.2000.18.5.1043

108. Small EJ, Meyer M, Marshall ME, Reyno LM, Meyers FJ, Natale RB, et al. Suramin therapy for patients with symptomatic hormone-refractory prostate cancer: results of a randomized phase III trial comparing suramin plus hydrocortisone to placebo plus hydrocortisone. J Clin Oncol Off J Am Soc Clin Oncol. 2000;18: 1440–1450. doi:10.1200/JCO.2000.18.7.1440

109. Calvo E, Cortés J, Rodríguez J, Sureda M, Beltrán C, Rebollo J, et al. Fixed higher dose schedule of suramin plus hydrocortisone in patients with hormone refractory prostate carcinoma a multicenter Phase II study. Cancer. 2001;92: 2435–2443.

110. Small EJ, Halabi S, Ratain MJ, Rosner G, Stadler W, Palchak D, et al. Randomized study of three different doses of suramin administered with a fixed dosing schedule in patients with advanced prostate cancer: results of intergroup 0159, cancer and leukemia group B 9480. J Clin Oncol Off J Am Soc Clin Oncol. 2002;20: 3369–3375. doi:10.1200/JCO.2002.10.022

111. Vogelzang NJ, Karrison T, Stadler WM, Garcia J, Cohn H, Kugler J, et al. A Phase II trial of suramin monthly x 3 for hormone-refractory prostate carcinoma. Cancer. 2004;100: 65–71. doi:10.1002/cncr.11867

112. Safarinejad MR. Combination chemotherapy with docetaxel, estramustine and suramin for hormone refractory prostate cancer. Urol Oncol. 2005;23: 93–101. doi:10.1016/j.urolonc.2004.10.003

113. Mirza MR, Jakobsen E, Pfeiffer P, Lindebjerg-Clasen B, Bergh J, Rose C. Suramin in non-small cell lung cancer and advanced breast cancer. Two parallel phase II studies. Acta Oncol Stockh Swed. 1997;36: 171–174.

114. Ord JJ, Streeter E, Jones A, Le Monnier K, Cranston D, Crew J, et al. Phase I trial of intravesical Suramin in recurrent superficial transitional cell bladder carcinoma. Br J Cancer. 2005;92: 2140–2147. doi:10.1038/sj.bjc.6602650

115. Uchio EM, Linehan WM, Figg WD, Walther MM. A phase I study of intravesical suramin for the treatment of superficial transitional cell carcinoma of the bladder. J Urol. 2003;169: 357–360. doi:10.1097/01.ju.0000032745.90528.dc

116. Grossman SA, Phuphanich S, Lesser G, Rozental J, Grochow LB, Fisher J, et al. Toxicity, efficacy, and pharmacology of suramin in adults with recurrent high-grade gliomas. J Clin Oncol Off J Am Soc Clin Oncol. 2001;19: 3260–3266. doi:10.1200/JCO.2001.19.13.3260

117. Laterra JJ, Grossman SA, Carson KA, Lesser GJ, Hochberg FH, Gilbert MR, et al. Suramin and radiotherapy in newly diagnosed glioblastoma: phase 2 NABTT CNS Consortium study. Neuro-Oncol. 2004;6: 15–20. doi:10.1215/S1152851703000127

118. Hosang M. Suramin binds to platelet-derived growth factor and inhibits its biological activity. J Cell Biochem. 1985;29: 265–273. doi:10.1002/jcb.240290310

119. Coffey RJ, Leof EB, Shipley GD, Moses HL. Suramin inhibition of growth factor receptor binding and mitogenicity in AKR-2B cells. J Cell Physiol. 1987;132: 143–148. doi:10.1002/jcp.1041320120

120. Pollak M, Richard M. Suramin blockade of insulinlike growth factor I-stimulated proliferation of human osteosarcoma cells. J Natl Cancer Inst. 1990;82: 1349–1352.

121. Spigelman Z, Dowers A, Kennedy S, DiSorbo D, O'Brien M, Barr R, et al. Antiproliferative effects of suramin on lymphoid cells. Cancer Res. 1987;47: 4694–4698.

122. Takano S, Gately S, Engelhard H, Tsanaclis AM, Brem S. Suramin inhibits glioma cell proliferation in vitro and in the brain. J Neurooncol. 1994;21: 189–201.

123. Guo XJ, Fantini J, Roubin R, Marvaldi J, Rougon G. Evaluation of the effect of suramin on neural cell growth and N-CAM expression. Cancer Res. 1990;50: 5164–5170.

124. Song S, Yu B, Wei Y, Wientjes MG, Au JL-S. Low-dose suramin enhanced paclitaxel activity in chemotherapy-naive and paclitaxel-pretreated human breast xenograft tumors. Clin Cancer Res Off J Am Assoc Cancer Res. 2004;10: 6058–6065. doi:10.1158/1078-0432.CCR-04-0595

125. Xin Y, Lyness G, Chen D, Song S, Wientjes MG, Au JL-S. Low dose suramin as a chemosensitizer of bladder cancer to mitomycin C. J Urol. 2005;174: 322–327. doi:10.1097/01.ju.0000161594.86931.ea

126. Kosarek CE, Hu X, Couto CG, Kisseberth WC, Green EM, Au JLS, et al. Phase I evaluation of low-dose suramin as chemosensitizer of doxorubicin in dogs with naturally occurring cancers. J Vet Intern Med. 2006;20: 1172–1177.

127. Singla AK, Bondareva A, Jirik FR. Combined treatment with paclitaxel and suramin prevents the development of metastasis by inhibiting metastatic colonization of circulating tumor cells. Clin Exp Metastasis. 2014;31: 705–714. doi:10.1007/s10585-014-9661-6

128. Gan Y, Lu J, Yeung BZ, Cottage CT, Wientjes MG, Au JL-S. Pharmacodynamics of telomerase inhibition and telomere shortening by noncytotoxic suramin. AAPS J. 2015;17: 268–276. doi:10.1208/s12248-014-9703-7

129. Villalona-Calero MA, Wientjes MG, Otterson GA, Kanter S, Young D, Murgo AJ, et al. Phase I study of low-dose suramin as a chemosensitizer in patients with advanced non-small cell lung cancer. Clin Cancer Res Off J Am Assoc Cancer Res. 2003;9: 3303–3311.

130. Villalona-Calero MA, Otterson GA, Wientjes MG, Weber F, Bekaii-Saab T, Young D, et al. Noncytotoxic suramin as a chemosensitizer in patients with advanced non-small-cell lung cancer: a phase II study. Ann Oncol Off J Eur Soc Med Oncol. 2008;19: 1903–1909. doi:10.1093/annonc/mdn412

131. Stocker K, Fischer H, Meier J. Thrombin-like snake venom proteinases. Toxicon Off J Int Soc Toxinology. 1982;20: 265–273.

132. Monteiro RQ, Campana PT, Melo PA, Bianconi ML. Suramin interaction with human alpha-thrombin: inhibitory effects and binding studies. Int J Biochem Cell Biol. 2004;36: 2077–2085. doi:10.1016/j.biocel.2004.03.007

133. Murakami MT, Arruda EZ, Melo PA, Martinez AB, Calil-Eliás S, Tomaz MA, et al. Inhibition of myotoxic activity of Bothrops asper myotoxin II by the anti-trypanosomal drug suramin. J Mol Biol. 2005;350: 416–426. doi:10.1016/j.jmb.2005.04.072

134. Aragão EA, Vieira DS, Chioato L, Ferreira TL, Lourenzoni MR, Silva SR, et al. Characterization of suramin binding sites on the human group IIA secreted phospholipase A2 by site-directed mutagenesis and molecular dynamics simulation. Arch Biochem Biophys. 2012;519: 17–22. doi:10.1016/j.abb.2012.01.002

135. Salvador GHM, Dreyer TR, Cavalcante WLG, Matioli FF, Dos Santos JI, Velazquez-Campoy A, et al. Structural and functional evidence for membrane docking and disruption sites on phospholipase A2-like proteins revealed by complexation with the inhibitor suramin. Acta Crystallogr D Biol Crystallogr. 2015;71: 2066–2078. doi:10.1107/S1399004715014443

136. Salvador GHM, Dreyer TR, Gomes AAS, Cavalcante WLG, Dos Santos JI, Gandin CA, et al. Structural and functional characterization of suramin-bound MjTX-I from Bothrops moojeni suggests a particular myotoxic mechanism. Sci Rep. 2018;8: 10317. doi:10.1038/s41598-018-28584-7

137. Zhou X, Tan T-C, Valiyaveettil S, Go ML, Kini RM, Velazquez-Campoy A, et al. Structural characterization of myotoxic ecarpholin S from Echis carinatus venom. Biophys J. 2008;95: 3366–3380. doi:10.1529/biophysj.107.117747

138. El-Kik CZ, Fernandes FFA, Tomaz MA, Gaban GA, Fonseca TF, Calil-Elias S, et al. Neutralization of Apis mellifera bee venom activities by suramin. Toxicon Off J Int Soc Toxinology. 2013;67: 55–62. doi:10.1016/j.toxicon.2013.02.007

139. Arruda EZ, Silva NMV, Moraes R a. M, Melo PA. Effect of suramin on myotoxicity of some crotalid snake venoms. Braz J Med Biol Res Rev Bras Pesqui Medicas E Biol. 2002;35: 723–726.

140. Fathi B, Amani F, Jami-al-ahmadi A, Zare A. Antagonistc effect of suramin against the venom of the Iranian snake Echis carinatus in mice. Iranian J Vet Sci Technol. 2010;2: 19–15.

141. The Lancet, Editorial. Snake-bite envenoming: a priority neglected tropical disease. Lancet Lond Engl. 2017;390: 2. doi:10.1016/S0140-6736(17)31751-8

142. Arnold C. Vipers, mambas and taipans: the escalating health crisis over snakebites. Nature. 2016;537: 26–28. doi:10.1038/537026a

143. den Hertog A, Nelemans A, Van den Akker J. The inhibitory action of suramin on the P2-purinoceptor response in smooth muscle cells of guinea-pig taenia caeci. Eur J Pharmacol. 1989;166: 531–534.

144. Kuruppu S, Chaisakul J, Smith AI, Hodgson WC. Inhibition of presynaptic neurotoxins in taipan venom by suramin. Neurotox Res. 2014;25: 305–310. doi:10.1007/s12640-013-9426-z

145. Grishin S, Shakirzyanova A, Giniatullin A, Afzalov R, Giniatullin R. Mechanisms of ATP action on motor nerve terminals at the frog neuromuscular junction. Eur J Neurosci. 2005;21: 1271–1279. doi:10.1111/j.1460-9568.2005.03976.x

146. Ong WY, Motin LG, Hansen MA, Dias LS, Ayrout C, Bennett MR, et al. P2 purinoceptor blocker suramin antagonises NMDA receptors and protects against excitatory behaviour caused by NMDA receptor agonist (RS)-(tetrazol-5-yl)-glycine in rats. J Neurosci Res. 1997;49: 627–638. doi:10.1002/(SICI)1097-4547(19970901)49:5<627::AID-JNR13>3.0.CO;2-S

147. Kharlamov A, Jones SC, Kim DK. Suramin reduces infarct volume in a model of focal brain ischemia in rats. Exp Brain Res. 2002;147: 353–359. doi:10.1007/s00221-002-1251-1

148. Dupre TV, Doll MA, Shah PP, Sharp CN, Kiefer A, Scherzer MT, et al. Suramin protects from cisplatin-induced acute kidney injury. Am J Physiol Renal Physiol. 2016;310: F248-258. doi:10.1152/ajprenal.00433.2015

149. Doggrell SA. Suramin: potential in acute liver failure. Expert Opin Investig Drugs. 2004;13: 1361–1363. doi:10.1517/13543784.13.10.1361

150. Chi Y, Gao K, Zhang H, Takeda M, Yao J. Suppression of cell membrane permeability by suramin: involvement of its inhibitory actions on connexin 43 hemichannels. Br J Pharmacol. 2014;171: 3448–3462. doi:10.1111/bph.12693

151. Bourguignon T, Benoist L, Chadet S, Miquelestorena-Standley E, Fromont G, Ivanes F, et al. Stimulation of murine P2Y11-like purinoreceptor protects against hypoxia/reoxygenation injury and decreases heart graft rejection lesions. J Thorac Cardiovasc Surg. 2019;158: 780–790.e1. doi:10.1016/j.jtcvs.2018.12.014

152. Sahu D, Saroha A, Roy S, Das S, Srivastava PS, Das HR. Suramin ameliorates collagen induced arthritis. Int Immunopharmacol. 2012;12: 288–293. doi:10.1016/j.intimp.2011.12.003

153. Zou CJ, Onaka TO, Yagi K. Effects of suramin on neuroendocrine and behavioural responses to conditioned fear stimuli. Neuroreport. 1998;9: 997–999.

154. Denkinger M, Shive CL, Pantenburg B, Forsthuber TG. Suramin has adjuvant properties and promotes expansion of antigen-specific Th1 and Th2 cells in vivo. Int Immunopharmacol. 2004;4: 15–24. doi:10.1016/j.intimp.2003.09.004

155. Dunn PM, Blakeley AG. Suramin: a reversible P2-purinoceptor antagonist in the mouse vas deferens. Br J Pharmacol. 1988;93: 243–245.

156. Bernardes CF, Fagian MM, Meyer-Fernandes JR, Castilho RF, Vercesi AE. Suramin inhibits respiration and induces membrane permeability transition in isolated rat liver mitochondria. Toxicology. 2001;169: 17–23.

157. Naviaux RK, Zolkipli Z, Wang L, Nakayama T, Naviaux JC, Le TP, et al. Antipurinergic therapy corrects the autism-like features in the poly(IC) mouse model. PloS One. 2013;8: e57380. doi:10.1371/journal.pone.0057380

158. Naviaux JC, Schuchbauer MA, Li K, Wang L, Risbrough VB, Powell SB, et al. Reversal of autism-like behaviors and metabolism in adult mice with single-dose antipurinergic therapy. Transl Psychiatry. 2014;4: e400. doi:10.1038/tp.2014.33

159. Naviaux RK, Curtis B, Li K, Naviaux JC, Bright AT, Reiner GE, et al. Low-dose suramin in autism spectrum disorder: a small, phase I/II, randomized clinical trial. Ann Clin Transl Neurol. 2017;4: 491–505. doi:10.1002/acn3.424

160. Town BW, Wills ED, Wilson EJ, Wormall A. Studies on suramin; the action of the drug on enzymes and some other proteins. General considerations. Biochem J. 1950;47: 149–158. doi:10.1042/bj0470149

161. Willson M, Callens M, Kuntz DA, Perié J, Opperdoes FR. Synthesis and activity of inhibitors highly specific for the glycolytic enzymes from Trypanosoma brucei. Mol Biochem Parasitol. 1993;59: 201–210.

162. Morgan HP, McNae IW, Nowicki MW, Zhong W, Michels PAM, Auld DS, et al. The trypanocidal drug suramin and other trypan blue mimetics are inhibitors of pyruvate kinases and bind to the adenosine site. J Biol Chem. 2011;286: 31232–31240. doi:10.1074/jbc.M110.212613

163. Stoppani AO, Brignone JA. Inhibition of succinic dehydrogenase by polysulfonated compounds. Arch Biochem Biophys. 1957;68: 432–451.

164. Ono K, Nakane H, Fukushima M. Differential inhibition of various deoxyribonucleic and ribonucleic acid polymerases by suramin. Eur J Biochem. 1988;172: 349–353.

165. Jindal HK, Anderson CW, Davis RG, Vishwanatha JK. Suramin affects DNA synthesis in HeLa cells by inhibition of DNA polymerases. Cancer Res. 1990;50: 7754–7757.

166. Mastrangelo E, Pezzullo M, Tarantino D, Petazzi R, Germani F, Kramer D, et al. Structure-based inhibition of Norovirus RNA-dependent RNA polymerases. J Mol Biol. 2012;419: 198–210. doi:10.1016/j.jmb.2012.03.008

167. Waring MJ. The effects of antimicrobial agents on ribonucleic acid polymerase. Mol Pharmacol. 1965;1: 1–13.

168. Basavannacharya C, Vasudevan SG. Suramin inhibits helicase activity of NS3 protein of dengue virus in a fluorescence-based high throughput assay format. Biochem Biophys Res Commun. 2014;453: 539–544. doi:10.1016/j.bbrc.2014.09.113

169. Bojanowski K, Lelievre S, Markovits J, Couprie J, Jacquemin-Sablon A, Larsen AK. Suramin is an inhibitor of DNA topoisomerase II in vitro and in Chinese hamster fibrosarcoma cells. Proc Natl Acad Sci U S A. 1992;89: 3025–3029.

170. Ren C, Morohashi K, Plotnikov AN, Jakoncic J, Smith SG, Li J, et al. Small-molecule modulators of methyl-lysine binding for the CBX7 chromodomain. Chem Biol. 2015;22: 161–168. doi:10.1016/j.chembiol.2014.11.021

171. Feng Y, Li M, Wang B, Zheng YG. Discovery and mechanistic study of a class of protein arginine methylation inhibitors. J Med Chem. 2010;53: 6028–6039. doi:10.1021/jm100416n

172. Trapp J, Meier R, Hongwiset D, Kassack MU, Sippl W, Jung M. Structure-activity studies on suramin analogues as inhibitors of NAD+-dependent histone deacetylases (sirtuins). ChemMedChem. 2007;2: 1419–1431. doi:10.1002/cmdc.200700003

173. Schuetz A, Min J, Antoshenko T, Wang C-L, Allali-Hassani A, Dong A, et al. Structural basis of inhibition of the human NAD+-dependent deacetylase SIRT5 by suramin. Struct Lond Engl 1993. 2007;15: 377–389. doi:10.1016/j.str.2007.02.002

174. Hosoi Y, Matsumoto Y, Tomita M, Enomoto A, Morita A, Sakai K, et al. Phosphorothioate oligonucleotides, suramin and heparin inhibit DNA-dependent protein kinase activity. Br J Cancer. 2002;86: 1143–1149. doi:10.1038/sj.bjc.6600191

175. Hensey CE, Boscoboinik D, Azzi A. Suramin, an anti-cancer drug, inhibits protein kinase C and induces differentiation in neuroblastoma cell clone NB2A. FEBS Lett. 1989;258: 156–158.

176. El-Kik CZ, Fernandes FFA, Tomaz MA, Gaban GA, Fonseca TF, Calil-Elias S, et al. Neutralization of Apis mellifera bee venom activities by suramin. Toxicon Off J Int Soc Toxinology. 2013;67: 55–62. doi:10.1016/j.toxicon.2013.02.007

177. Murakami MT, Arruda EZ, Melo PA, Martinez AB, Calil-Eliás S, Tomaz MA, et al. Inhibition of myotoxic activity of Bothrops asper myotoxin II by the anti-trypanosomal drug suramin. J Mol Biol. 2005;350: 416–426. doi:10.1016/j.jmb.2005.04.072

178. Zhang YL, Keng YF, Zhao Y, Wu L, Zhang ZY. Suramin is an active site-directed, reversible, and tight-binding inhibitor of protein-tyrosine phosphatases. J Biol Chem. 1998;273: 12281–12287.

179. Lominski I, Gray S. Inhibition of lysozyme by "Suramin." Nature. 1961;192: 683.

180. Vicik R, Hoerr V, Glaser M, Schultheis M, Hansell E, McKerrow JH, et al. Aziridine-2,3-dicarboxylate inhibitors targeting the major cysteine protease of Trypanosoma brucei as lead trypanocidal agents. Bioorg Med Chem Lett. 2006;16: 2753–2757. doi:10.1016/j.bmcl.2006.02.026

181. Cadène M, Duranton J, North A, Si-Tahar M, Chignard M, Bieth JG. Inhibition of neutrophil serine proteinases by suramin. J Biol Chem. 1997;272: 9950–9955.

182. Eisen V, Loveday C. Effects of suramin on complement, blood clotting, fibrinolysis and kinin formation. Br J Pharmacol. 1973;49: 678–687.

183. Eichhorst ST, Krueger A, Müerköster S, Fas SC, Golks A, Gruetzner U, et al. Suramin inhibits death receptor-induced apoptosis in vitro and fulminant apoptotic liver damage in mice. Nat Med. 2004;10: 602–609. doi:10.1038/nm1049

184. Tayel A, Ebrahim MA, Ibrahim AS, El-Gayar AM, Al-Gayyar MM. Cytotoxic effects of suramin against HepG2 cells through activation of intrinsic apoptotic pathway. J BUON Off J Balk Union Oncol. 2014;19: 1048–1054.

185. Fortes PA, Ellory JC, Lew VL. Suramin: a potent ATPase inhibitor which acts on the inside surface of the sodium pump. Biochim Biophys Acta. 1973;318: 262–272.

186. Demenis MA, Furriel RPM, Leone FA. Characterization of an ectonucleoside triphosphate diphosphohydrolase 1 activity in alkaline phosphatase-depleted rat osseous plate membranes: possible functional involvement in the calcification process. Biochim Biophys Acta. 2003;1646: 216–225.

187. Magalhães L, de Oliveira AHC, de Souza Vasconcellos R, Mariotini-Moura C, de Cássia Firmino R, Fietto JLR, et al. Label-free assay based on immobilized capillary enzyme reactor of Leishmania infantum nucleoside triphosphate diphosphohydrolase (LicNTPDase-2-ICER-LC/UV). J Chromatogr B Analyt Technol Biomed Life Sci. 2016;1008: 98–107. doi:10.1016/j.jchromb.2015.11.028

188. Luo H, Wood K, Shi F-D, Gao F, Chang Y. Suramin is a novel competitive antagonist selective to α1β2γ2 GABAA over ρ1 GABAC receptors. Neuropharmacology. 2018;141: 148–157. doi:10.1016/j.neuropharm.2018.08.036

189. Nakazawa K, Inoue K, Ito K, Koizumi S, Inoue K. Inhibition by suramin and reactive blue 2 of GABA and glutamate receptor channels in rat hippocampal neurons. Naunyn Schmiedebergs Arch Pharmacol. 1995;351: 202–208.

190. Chung W-C, Kermode JC. Suramin disrupts receptor-G protein coupling by blocking association of G protein alpha and betagamma subunits. J Pharmacol Exp Ther. 2005;313: 191–198. doi:10.1124/jpet.104.078311

191. El-Ajouz S, Ray D, Allsopp RC, Evans RJ. Molecular basis of selective antagonism of the P2X1 receptor for ATP by NF449 and suramin: contribution of basic amino acids in the cysteine-rich loop. Br J Pharmacol. 2012;165: 390–400. doi:10.1111/j.1476-5381.2011.01534.x

192. Stevis PE, Deecher DC, Lopez FJ, Frail DE. Pharmacological characterization of soluble human FSH receptor extracellular domain: facilitated secretion by coexpression with FSH. Endocrine. 1999;10: 153–160. doi:10.1385/ENDO:10:2:153

193. La Rocca RV, Stein CA, Danesi R, Cooper MR, Uhrich M, Myers CE. A pilot study of suramin in the treatment of metastatic renal cell carcinoma. Cancer. 1991;67: 1509–1513.

194. Fong JS, Good RA. Suramin--a potent reversible and competitive inhibitor of complement systems. Clin Exp Immunol. 1972;10: 127–138.

195. Tsiftsoglou SA, Sim RB. Human complement factor I does not require cofactors for cleavage of synthetic substrates. J Immunol Baltim Md 1950. 2004;173: 367–375. doi:10.4049/jimmunol.173.1.367

196. Tsiftsoglou SA, Willis AC, Li P, Chen X, Mitchell DA, Rao Z, et al. The catalytically active serine protease domain of human complement factor I. Biochemistry (Mosc). 2005;44: 6239–6249. doi:10.1021/bi047680t

197. Nunziante M, Kehler C, Maas E, Kassack MU, Groschup M, Schätzl HM. Charged bipolar suramin derivatives induce aggregation of the prion protein at the cell surface

and inhibit PrPSc replication. J Cell Sci. 2005;118: 4959–4973. doi:10.1242/jcs.02609

198. Shukla SJ, Sakamuru S, Huang R, Moeller TA, Shinn P, Vanleer D, et al. Identification of clinically used drugs that activate pregnane X receptors. Drug Metab Dispos Biol Fate Chem. 2011;39: 151–159. doi:10.1124/dmd.110.035105

199. Klinger M, Freissmuth M, Nickel P, Stäbler-Schwarzbart M, Kassack M, Suko J, et al. Suramin and suramin analogs activate skeletal muscle ryanodine receptor via a calmodulin binding site. Mol Pharmacol. 1999;55: 462–472.

200. Fairlamb AH, Bowman IB. Trypanosoma brucei: suramin and other trypanocidal compounds' effects on sn-glycerol-3-phosphate oxidase. Exp Parasitol. 1977;43: 353–361.

201. Dias DA, de Barros Penteado B, Dos Santos LD, Dos Santos PM, Arruda CCP, Schetinger MRC, et al. Characterization of ectonucleoside triphosphate diphosphohydrolase (E-NTPDase; EC 3.6.1.5) activity in mouse peritoneal cavity cells. Cell Biochem Funct. 2017;35: 358–363. doi:10.1002/cbf.3281

202. Oses JP, Cardoso CM, Germano RA, Kirst IB, Rücker B, Fürstenau CR, et al. Soluble NTPDase: An additional system of nucleotide hydrolysis in rat blood serum. Life Sci. 2004;74: 3275–3284. doi:10.1016/j.lfs.2003.11.020

203. Vasconcellos RDS, Mariotini-Moura C, Gomes RS, Serafim TD, Firmino R de C, Silva E Bastos M, et al. Leishmania infantum ecto-nucleoside triphosphate diphosphohydrolase-2 is an apyrase involved in macrophage infection and expressed in infected dogs. PLoS Negl Trop Dis. 2014;8: e3309. doi:10.1371/journal.pntd.0003309

204. Santos RF, Pôssa MAS, Bastos MS, Guedes PMM, Almeida MR, Demarco R, et al. Influence of Ecto-nucleoside triphosphate diphosphohydrolase activity on Trypanosoma cruzi infectivity and virulence. PLoS Negl Trop Dis. 2009;3: e387. doi:10.1371/journal.pntd.0000387

205. Iqbal J, Lévesque SA, Sévigny J, Müller CE. A highly sensitive CE-UV method with dynamic coating of silica-fused capillaries for monitoring of nucleotide pyrophosphatase/phosphodiesterase reactions. Electrophoresis. 2008;29: 3685–3693. doi:10.1002/elps.200800013

206. Andréola ML, Tharaud D, Litvak S, Tarrago-Litvak L. The ribonuclease H activity of HIV-1 reverse transcriptase: further biochemical characterization and search of inhibitors. Biochimie. 1993;75: 127–134.

207. Mukherjee S, Hanson AM, Shadrick WR, Ndjomou J, Sweeney NL, Hernandez JJ, et al. Identification and analysis of hepatitis C virus NS3 helicase inhibitors using nucleic acid binding assays. Nucleic Acids Res. 2012;40: 8607–8621. doi:10.1093/nar/gks623

208. Marchand C, Lea WA, Jadhav A, Dexheimer TS, Austin CP, Inglese J, et al. Identification of phosphotyrosine mimetic inhibitors of human tyrosyl-DNA phosphodiesterase I by a novel AlphaScreen high-throughput assay. Mol Cancer Ther. 2009;8: 240–248. doi:10.1158/1535-7163.MCT-08-0878

209. Kakuguchi W, Nomura T, Kitamura T, Otsuguro S, Matsushita K, Sakaitani M, et al. Suramin, screened from an approved drug library, inhibits HuR functions and attenuates malignant phenotype of oral cancer cells. Cancer Med. 2018;7: 6269–6280. doi:10.1002/cam4.1877

210. Paulson CN, John K, Baxley RM, Kurniawan F, Orellana K, Francis R, et al. The anti-parasitic agent suramin and several of its analogues are inhibitors of the DNA binding protein Mcm10. Open Biol. 2019;9: 190117. doi:10.1098/rsob.190117

211. Horiuchi KY, Eason MM, Ferry JJ, Planck JL, Walsh CP, Smith RF, et al. Assay development for histone methyltransferases. Assay Drug Dev Technol. 2013;11: 227–236. doi:10.1089/adt.2012.480

212. Peinado RDS, Olivier DS, Eberle RJ, de Moraes FR, Amaral MS, Arni RK, et al. Binding studies of a putative C. pseudotuberculosis target protein from Vitamin B12 Metabolism. Sci Rep. 2019;9: 6350. doi:10.1038/s41598-019-42935-y

213. Howitz KT, Bitterman KJ, Cohen HY, Lamming DW, Lavu S, Wood JG, et al. Small molecule activators of sirtuins extend Saccharomyces cerevisiae lifespan. Nature. 2003;425: 191–196. doi:10.1038/nature01960

214. Trueblood KE, Mohr S, Dubyak GR. Purinergic regulation of high-glucose-induced caspase-1 activation in the rat retinal Müller cell line rMC-1. Am J Physiol Cell Physiol. 2011;301: C1213-1223. doi:10.1152/ajpcell.00265.2011

215. Stark S, Schuller A, Sifringer M, Gerstner B, Brehmer F, Weber S, et al. Suramin induces and enhances apoptosis in a model of hyperoxia-induced oligodendrocyte injury. Neurotox Res. 2008;13: 197–207.

216. Marques AF, Esser D, Rosenthal PJ, Kassack MU, Lima LMTR. Falcipain-2 inhibition by suramin and suramin analogues. Bioorg Med Chem. 2013;21: 3667–3673. doi:10.1016/j.bmc.2013.04.047

217. Beiler JM, Martin GJ. Inhibition of hyaluronidase action by derivatives of hesperidin. J Biol Chem. 1948;174: 31–35.

218. Constantopoulos G, Rees S, Cragg BG, Barranger JA, Brady RO. Experimental animal model for mucopolysaccharidosis: suramin-induced glycosaminoglycan and sphingolipid accumulation in the rat. Proc Natl Acad Sci U S A. 1980;77: 3700–3704. doi:10.1073/pnas.77.6.3700

219. Bachmann A, Russ U, Quast U. Potent inhibition of the CFTR chloride channel by suramin. Naunyn Schmiedebergs Arch Pharmacol. 1999;360: 473–476.

220. Peoples RW, Li C. Inhibition of NMDA-gated ion channels by the P2 purinoceptor antagonists suramin and reactive blue 2 in mouse hippocampal neurones. Br J Pharmacol. 1998;124: 400–408. doi:10.1038/sj.bjp.0701842

221. Sharma A, Yogavel M, Sharma A. Structural and functional attributes of malaria parasite diadenosine tetraphosphate hydrolase. Sci Rep. 2016;6: 19981. doi:10.1038/srep19981

222. Vieira DS, Aragão EA, Lourenzoni MR, Ward RJ. Mapping of suramin binding sites on the group IIA human secreted phospholipase A2. Bioorganic Chem. 2009;37: 41–45. doi:10.1016/j.bioorg.2009.01.002

223. Quemé-Peña M, Juhász T, Mihály J, Cs Szigyártó I, Horváti K, Bősze S, et al. Manipulating Active Structure and Function of Cationic Antimicrobial Peptide CM15 with the Polysulfonated Drug Suramin: A Step Closer to in Vivo Complexity. Chembiochem Eur J Chem Biol. 2019. doi:10.1002/cbic.201800801

224. Abdeen S, Salim N, Mammadova N, Summers CM, Goldsmith-Pestana K, McMahon-Pratt D, et al. Targeting the HSP60/10 chaperonin systems of Trypanosoma brucei as a strategy for treating African sleeping sickness. Bioorg Med Chem Lett. 2016;26: 5247–5253. doi:10.1016/j.bmcl.2016.09.051

225. Stevens M, Abdeen S, Salim N, Ray A-M, Washburn A, Chitre S, et al. HSP60/10 chaperonin systems are inhibited by a variety of approved drugs, natural products, and known bioactive molecules. Bioorg Med Chem Lett. 2019;29: 1106–1112. doi:10.1016/j.bmcl.2019.02.028

226. Wierenga RK, Swinkels B, Michels PA, Osinga K, Misset O, Van Beeumen J, et al. Common elements on the surface of glycolytic enzymes from Trypanosoma brucei may serve as topogenic signals for import into glycosomes. EMBO J. 1987;6: 215–221.

227. Opperdoes FR, Borst P. Localization of nine glycolytic enzymes in a microbody-like organelle in Trypanosoma brucei: the glycosome. FEBS Lett. 1977;80: 360–364.

228. Fairlamb A. A study of glycerophosphate oxidase in Trypanosoma brucei. Ph.D. Thesis, University of Edinburgh. 1975.

229. Morty RE, Troeberg L, Pike RN, Jones R, Nickel P, Lonsdale-Eccles JD, et al. A trypanosome oligopeptidase as a target for the trypanocidal agents pentamidine, diminazene and suramin. FEBS Lett. 1998;433: 251–256.

230. Zimmermann S, Hall L, Riley S, Sørensen J, Amaro RE, Schnaufer A. A novel high-throughput activity assay for the Trypanosoma brucei editosome enzyme REL1 and other RNA ligases. Nucleic Acids Res. 2016;44: e24. doi:10.1093/nar/gkv938

231. Roveri OA, Franke de Cazzulo BM, Cazzulo JJ. Inhibition by suramin of oxidative phosphorylation in Crithidia fasciculata. Comp Biochem Physiol B. 1982;71: 611–616.

232. Thomas JA, Baker N, Hutchinson S, Dominicus C, Trenaman A, Glover L, et al. Insights into antitrypanosomal drug mode-of-action from cytology-based profiling. PLoS Negl Trop Dis. 2018;12: e0006980. doi:10.1371/journal.pntd.0006980

233. Gagliardi AR, Taylor MF, Collins DC. Uptake of suramin by human microvascular endothelial cells. Cancer Lett. 1998;125: 97–102.

234. Baghdiguian S, Boudier JL, Boudier JA, Fantini J. Intracellular localisation of suramin, an anticancer drug, in human colon adenocarcinoma cells: a study by quantitative autoradiography. Eur J Cancer Oxf Engl 1990. 1996;32A: 525–532.

235. Sanderson L, Khan A, Thomas S. Distribution of suramin, an antitrypanosomal drug, across the blood-brain and blood-cerebrospinal fluid interfaces in wild-type and P-glycoprotein transporter-deficient mice. Antimicrob Agents Chemother. 2007;51: 3136–3146. doi:10.1128/AAC.00372-07

236. Baghdiguian S, Boudier JL, Boudier JA, Fantini J. Intracellular localisation of suramin, an anticancer drug, in human colon adenocarcinoma cells: a study by quantitative autoradiography. Eur J Cancer Oxf Engl 1990. 1996;32A: 525–532.

237. Coppens I, Opperdoes FR, Courtoy PJ, Baudhuin P. Receptor-mediated endocytosis in the bloodstream form of Trypanosoma brucei. J Protozool. 1987;34: 465–473.

238. Pal A, Hall BS, Field MC. Evidence for a non-LDL-mediated entry route for the trypanocidal drug suramin in Trypanosoma brucei. Mol Biochem Parasitol. 2002;122: 217–221.

239. Lozano RM, Jiménez M, Santoro J, Rico M, Giménez-Gallego G. Solution structure of acidic fibroblast growth factor bound to 1,3, 6-naphthalenetrisulfonate: a minimal model for the anti-tumoral action of suramins and suradistas. J Mol Biol. 1998;281: 899–915.

240. Huang H-W, Mohan SK, Yu C. The NMR solution structure of human epidermal growth factor (hEGF) at physiological pH and its interactions with suramin. Biochem Biophys Res Commun. 2010;402: 705–710. doi:10.1016/j.bbrc.2010.10.089

241. Lima LMTR, Becker CF, Giesel GM, Marques AF, Cargnelutti MT, de Oliveira Neto M, et al. Structural and thermodynamic analysis of thrombin:suramin interaction in solution and crystal phases. Biochim Biophys Acta. 2009;1794: 873–881. doi:10.1016/j.bbapap.2009.03.011

242. Jiao L, Ouyang S, Liang M, Niu F, Shaw N, Wu W, et al. Structure of severe fever with thrombocytopenia syndrome virus nucleocapsid protein in complex with suramin reveals therapeutic potential. J Virol. 2013;87: 6829–6839. doi:10.1128/JVI.00672-13

243. Prigozhina NL, Heisel AJ, Seldeen JR, Cosford NDP, Price JH. Amphiphilic suramin dissolves Matrigel, causing an "inhibition" artefact within in vitro angiogenesis assays. Int J Exp Pathol. 2013;94: 412–417. doi:10.1111/iep.12043

244. Vansterkenburg EL, Wilting J, Janssen LH. Influence of pH on the binding of suramin to human serum albumin. Biochem Pharmacol. 1989;38: 3029–3035.

245. Alsford S, Field MC, Horn D. Receptor-mediated endocytosis for drug delivery in African trypanosomes: fulfilling Paul Ehrlich's vision of chemotherapy. Trends Parasitol. 2013;29: 207–212. doi:10.1016/j.pt.2013.03.004

246. Pépin J, Milord F. The treatment of human African trypanosomiasis. Adv Parasitol. 1994;33: 1–47.

247. Fang Y, Ye WX, Nei HY, Wang YL. In vitro development of suramin-resistant clones of Trypanosoma evansi. Acta Trop. 1994;58: 79–83.

248. Scott AG, Tait A, Turner CM. Characterisation of cloned lines of Trypanosoma brucei expressing stable resistance to MelCy and suramin. Acta Trop. 1996;60: 251–262.

249. Wenzler T, Steinhuber A, Wittlin S, Scheurer C, Brun R, Trampuz A. Isothermal microcalorimetry, a new tool to monitor drug action against Trypanosoma brucei and Plasmodium falciparum. PLoS Negl Trop Dis. 2012;6: e1668. doi:10.1371/journal.pntd.0001668

250. Parsons M, Nelson RG, Watkins KP, Agabian N. Trypanosome mRNAs share a common 5’ spliced leader sequence. Cell. 1984;38: 309–316.

251. Nielsen H, Engelbrecht J, Brunak S, von Heijne G. A neural network method for identification of prokaryotic and eukaryotic signal peptides and prediction of their cleavage sites. Int J Neural Syst. 1997;8: 581–599.

252. Fankhauser N, Mäser P. Identification of GPI anchor attachment signals by a Kohonen self-organizing map. Bioinforma Oxf Engl. 2005;21: 1846–1852. doi:10.1093/bioinformatics/bti299

253. van Luenen HGAM, Kieft R, Mussmann R, Engstler M, ter Riet B, Borst P. Trypanosomes change their transferrin receptor expression to allow effective uptake of host transferrin. Mol Microbiol. 2005;58: 151–165. doi:10.1111/j.1365-2958.2005.04831.x

254. Hertz-Fowler C, Figueiredo LM, Quail MA, Becker M, Jackson A, Bason N, et al. Telomeric expression sites are highly conserved in Trypanosoma brucei. PloS One. 2008;3: e3527. doi:10.1371/journal.pone.0003527

255. Avelar-Freitas BA, Almeida VG, Pinto MCX, Mourão F a. G, Massensini AR, Martins-Filho OA, et al. Trypan blue exclusion assay by flow cytometry. Braz J Med Biol Res Rev Bras Pesqui Medicas E Biol. 2014;47: 307–315. doi:10.1590/1414-431X20143437

256. Brickman MJ, Cook JM, Balber AE. Low temperature reversibly inhibits transport from tubular endosomes to a perinuclear, acidic compartment in African trypanosomes. J Cell Sci. 1995;108 (Pt 11): 3611–3621.

257. Hawking F. Chemotherapy of Trypanosomiasis. In: Schnitzer RJ, Hawking F, editors. Experimental Chemotherapy. Academic Press; 1963.

258. Bernhard SC, Nerima B, Mäser P, Brun R. Melarsoprol- and pentamidine-resistant Trypanosoma brucei rhodesiense populations and their cross-resistance. Int J Parasitol. 2007;37: 1443–1448. doi:10.1016/j.ijpara.2007.05.007

259. El-Sayed NM, Hegde P, Quackenbush J, Melville SE, Donelson JE. The African trypanosome genome. Int J Parasitol. 2000;30: 329–345.

260. Leach TM, Roberts CJ. Present status of chemotherapy and chemoprophylaxis of animal trypanosomiasis in the Eastern hemisphere. Pharmacol Ther. 1981;13: 91–147.

261. Engstler M, Thilo L, Weise F, Grünfelder CG, Schwarz H, Boshart M, et al. Kinetics of endocytosis and recycling of the GPI-anchored variant surface glycoprotein in Trypanosoma brucei. J Cell Sci. 2004;117: 1105–1115. doi:10.1242/jcs.00938

262. Hirumi H, Hirumi K. Continuous cultivation of Trypanosoma brucei blood stream forms in a medium containing a low concentration of serum protein without feeder cell layers. J Parasitol. 1989;75: 985–989.

263. Baltz T, Baltz D, Giroud C, Crockett J. Cultivation in a semi-defined medium of animal infective forms of Trypanosoma brucei, T. equiperdum, T. evansi, T. rhodesiense and T. gambiense. EMBO J. 1985;4: 1273–1277.

264. Mäser P, Grether-Bühler Y, Kaminsky R, Brun R. An anti-contamination cocktail for the in vitro isolation and cultivation of parasitic protozoa. Parasitol Res. 2002;88: 172–174.

265. Räz B, Iten M, Grether-Bühler Y, Kaminsky R, Brun R. The Alamar Blue assay to determine drug sensitivity of African trypanosomes (T.b. rhodesiense and T.b. gambiense) in vitro. Acta Trop. 1997;68: 139–147.

266. Bolger AM, Lohse M, Usadel B. Trimmomatic: a flexible trimmer for Illumina sequence data. Bioinforma Oxf Engl. 2014;30: 2114–2120. doi:10.1093/bioinformatics/btu170

267. Li H, Durbin R. Fast and accurate short read alignment with Burrows-Wheeler transform. Bioinforma Oxf Engl. 2009;25: 1754–1760. doi:10.1093/bioinformatics/btp324

268. Li H, Handsaker B, Wysoker A, Fennell T, Ruan J, Homer N, et al. The Sequence Alignment/Map format and SAMtools. Bioinforma Oxf Engl. 2009;25: 2078–2079. doi:10.1093/bioinformatics/btp352

269. Anders S, Pyl PT, Huber W. HTSeq--a Python framework to work with high-throughput sequencing data. Bioinforma Oxf Engl. 2015;31: 166–169. doi:10.1093/bioinformatics/btu638

270. Love MI, Huber W, Anders S. Moderated estimation of fold change and dispersion for RNA-seq data with DESeq2. Genome Biol. 2014;15: 550. doi:10.1186/s13059-014-0550-8

271. Grabherr MG, Haas BJ, Yassour M, Levin JZ, Thompson DA, Amit I, et al. Full-length transcriptome assembly from RNA-Seq data without a reference genome. Nat Biotechnol. 2011;29: 644–652. doi:10.1038/nbt.1883

272. Aline R, MacDonald G, Brown E, Allison J, Myler P, Rothwell V, et al. (TAA)n within sequences flanking several intrachromosomal variant surface glycoprotein genes in Trypanosoma brucei. Nucleic Acids Res. 1985;13: 3161–3177.

273. Brenndörfer M, Boshart M. Selection of reference genes for mRNA quantification in Trypanosoma brucei. Mol Biochem Parasitol. 2010;172: 52–55. doi:10.1016/j.molbiopara.2010.03.007

274. Cross GAM, Kim H-S, Wickstead B. Capturing the variant surface glycoprotein repertoire (the VSGnome) of Trypanosoma brucei Lister 427. Mol Biochem Parasitol. 2014;195: 59–73. doi:10.1016/j.molbiopara.2014.06.004

275. Field MC, Horn D, Fairlamb AH, Ferguson MAJ, Gray DW, Read KD, et al. Anti-trypanosomatid drug discovery: an ongoing challenge and a continuing need. Nat Rev Microbiol. 2017;15: 217–231. doi:10.1038/nrmicro.2016.193

276. Pal A, Hall BS, Field MC. Evidence for a non-LDL-mediated entry route for the trypanocidal drug suramin in Trypanosoma brucei. Mol Biochem Parasitol. 2002;122: 217–221.

277. Wiedemar N, Graf FE, Zwyer M, Ndomba E, Kunz Renggli C, Cal M, et al. Beyond immune escape: a variant surface glycoprotein causes suramin resistance in Trypanosoma brucei. Mol Microbiol. 2018;107: 57–67. doi:10.1111/mmi.13854

278. Alsford S, Kawahara T, Glover L, Horn D. Tagging a T. brucei RRNA locus improves stable transfection efficiency and circumvents inducible expression position effects. Mol Biochem Parasitol. 2005;144: 142–148. doi:10.1016/j.molbiopara.2005.08.009

279. Schindelin J, Arganda-Carreras I, Frise E, Kaynig V, Longair M, Pietzsch T, et al. Fiji: an open-source platform for biological-image analysis. Nat Methods. 2012;9: 676–682. doi:10.1038/nmeth.2019

280. Van der Ploeg LH, Schwartz DC, Cantor CR, Borst P. Antigenic variation in Trypanosoma brucei analyzed by electrophoretic separation of chromosome-sized DNA molecules. Cell. 1984;37: 77–84.

281. Harrisson F, Callebaut M, Vakaet L. Microspectrographic analysis of trypan blue-induced fluorescence in oocytes of the Japanese quail. Histochemistry. 1981;72: 563–578.

282. Steverding D. The transferrin receptor of Trypanosoma brucei. Parasitol Int. 2000;48: 191–198.

283. Coppens I, Opperdoes FR, Courtoy PJ, Baudhuin P. Receptor-mediated endocytosis in the bloodstream form of Trypanosoma brucei. J Protozool. 1987;34: 465–473.

284. Koval A, Ahmed K, Katanaev VL. Inhibition of Wnt signalling and breast tumour growth by the multi-purpose drug suramin through suppression of heterotrimeric G proteins and Wnt endocytosis. Biochem J. 2016;473: 371–381. doi:10.1042/BJ20150913

285. Schwede A, Macleod OJS, MacGregor P, Carrington M. How Does the VSG Coat of Bloodstream Form African Trypanosomes Interact with External Proteins? PLoS Pathog. 2015;11: e1005259. doi:10.1371/journal.ppat.1005259

286. Raper J, Fung R, Ghiso J, Nussenzweig V, Tomlinson S. Characterization of a novel trypanosome lytic factor from human serum. Infect Immun. 1999;67: 1910–1916.

287. Vanhamme L, Paturiaux-Hanocq F, Poelvoorde P, Nolan DP, Lins L, Van Den Abbeele J, et al. Apolipoprotein L-I is the trypanosome lytic factor of human serum. Nature. 2003;422: 83–87. doi:10.1038/nature01461

288. Lecordier L, Uzureau P, Tebabi P, Pérez-Morga D, Nolan D, Schumann Burkard G, et al. Identification of Trypanosoma brucei components involved in trypanolysis by normal human serum. Mol Microbiol. 2014;94: 625–636. doi:10.1111/mmi.12783

289. Vanhollebeke B, De Muylder G, Nielsen MJ, Pays A, Tebabi P, Dieu M, et al. A haptoglobin-hemoglobin receptor conveys innate immunity to Trypanosoma brucei in humans. Science. 2008;320: 677–681. doi:10.1126/science.1156296

290. Pal A, Hall BS, Nesbeth DN, Field HI, Field MC. Differential endocytic functions of Trypanosoma brucei Rab5 isoforms reveal a glycosylphosphatidylinositol-specific endosomal pathway. J Biol Chem. 2002;277: 9529–9539. doi:10.1074/jbc.M110055200

291. Pal A, Hall BS, Jeffries TR, Field MC. Rab5 and Rab11 mediate transferrin and anti-variant surface glycoprotein antibody recycling in Trypanosoma brucei. Biochem J. 2003;374: 443–451. doi:10.1042/BJ20030469

292. Field MC, Allen CL, Dhir V, Goulding D, Hall BS, Morgan GW, et al. New approaches to the microscopic imaging of Trypanosoma brucei. Microsc Microanal Off J Microsc Soc Am Microbeam Anal Soc Microsc Soc Can. 2004;10: 621–636. doi:10.1017/S1431927604040942

293. Coppens I, Levade T, Courtoy PJ. Host plasma low density lipoprotein particles as an essential source of lipids for the bloodstream forms of Trypanosoma brucei. J Biol Chem. 1995;270: 5736–5741.

294. Schell D, Borowy NK, Overath P. Transferrin is a growth factor for the bloodstream form of Trypanosoma brucei. Parasitol Res. 1991;77: 558–560.

295. Kabiri M, Steverding D. Studies on the recycling of the transferrin receptor in Trypanosoma brucei using an inducible gene expression system. Eur J Biochem. 2000;267: 3309–3314.

296. Coppens I, Baudhuin P, Opperdoes FR, Courtoy PJ. Receptors for the host low density lipoproteins on the hemoflagellate Trypanosoma brucei: purification and involvement in the growth of the parasite. Proc Natl Acad Sci U S A. 1988;85: 6753–6757.

297. Kelley LA, Mezulis S, Yates CM, Wass MN, Sternberg MJE. The Phyre2 web portal for protein modeling, prediction and analysis. Nat Protoc. 2015;10: 845–858. doi:10.1038/nprot.2015.053

298. Torreira E, Jha S, López-Blanco JR, Arias-Palomo E, Chacón P, Cañas C, et al. Architecture of the pontin/reptin complex, essential in the assembly of several macromolecular complexes. Struct Lond Engl 1993. 2008;16: 1511–1520. doi:10.1016/j.str.2008.08.009

299. Jha S, Dutta A. RVB1/RVB2: running rings around molecular biology. Mol Cell. 2009;34: 521–533. doi:10.1016/j.molcel.2009.05.016

300. Matias PM, Gorynia S, Donner P, Carrondo MA. Crystal structure of the human AAA+ protein RuvBL1. J Biol Chem. 2006;281: 38918–38929. doi:10.1074/jbc.M605625200

301. Waterhouse A, Bertoni M, Bienert S, Studer G, Tauriello G, Gumienny R, et al. SWISS-MODEL: homology modelling of protein structures and complexes. Nucleic Acids Res. 2018;46: W296–W303. doi:10.1093/nar/gky427

302. Eustermann S, Schall K, Kostrewa D, Lakomek K, Strauss M, Moldt M, et al. Structural basis for ATP-dependent chromatin remodelling by the INO80 complex. Nature. 2018;556: 386–390. doi:10.1038/s41586-018-0029-y

303. Alsford S, Turner DJ, Obado SO, Sanchez-Flores A, Glover L, Berriman M, et al. High-throughput phenotyping using parallel sequencing of RNA interference targets in the African trypanosome. Genome Res. 2011;21: 915–924. doi:10.1101/gr.115089.110

304. Babraham Bioinformatics - FastQC A Quality Control tool for High Throughput Sequence Data. 6 Apr 2017 [cited 6 Apr 2017]. Available: http://www.bioinformatics.babraham.ac.uk/projects/fastqc/

305. Picard Tools - By Broad Institute. 6 Apr 2017 [cited 6 Apr 2017]. Available: http://broadinstitute.github.io/picard/

306. McKenna A, Hanna M, Banks E, Sivachenko A, Cibulskis K, Kernytsky A, et al. The Genome Analysis Toolkit: a MapReduce framework for analyzing next-generation DNA sequencing data. Genome Res. 2010;20: 1297–1303. doi:10.1101/gr.107524.110

307. Cingolani P, Platts A, Wang LL, Coon M, Nguyen T, Wang L, et al. A program for annotating and predicting the effects of single nucleotide polymorphisms, SnpEff: SNPs in the genome of Drosophila melanogaster strain w1118; iso-2; iso-3. Fly (Austin). 2012;6: 80–92. doi:10.4161/fly.19695

308. Robinson JT, Thorvaldsdóttir H, Winckler W, Guttman M, Lander ES, Getz G, et al. Integrative genomics viewer. Nat Biotechnol. 2011;29: 24–26. doi:10.1038/nbt.1754

309. Thorvaldsdóttir H, Robinson JT, Mesirov JP. Integrative Genomics Viewer (IGV): high-performance genomics data visualization and exploration. Brief Bioinform. 2013;14: 178–192. doi:10.1093/bib/bbs017

310. Cross GA. Identification, purification and properties of clone-specific glycoprotein antigens constituting the surface coat of Trypanosoma brucei. Parasitology. 1975;71: 393–417.

311. Horn D. Antigenic variation in African trypanosomes. Mol Biochem Parasitol. 2014;195: 123–129. doi:10.1016/j.molbiopara.2014.05.001

312. Günzl A, Bruderer T, Laufer G, Schimanski B, Tu L-C, Chung H-M, et al. RNA polymerase I transcribes procyclin genes and variant surface glycoprotein gene expression sites in Trypanosoma brucei. Eukaryot Cell. 2003;2: 542–551.

313. De Greef C, Hamers R. The serum resistance-associated (SRA) gene of Trypanosoma brucei rhodesiense encodes a variant surface glycoprotein-like protein. Mol Biochem Parasitol. 1994;68: 277–284.

314. Campillo N, Carrington M. The origin of the serum resistance associated (SRA) gene and a model of the structure of the SRA polypeptide from Trypanosoma brucei rhodesiense. Mol Biochem Parasitol. 2003;127: 79–84.

315. Faulkner SD, Oli MW, Kieft R, Cotlin L, Widener J, Shiflett A, et al. In vitro generation of human high-density-lipoprotein-resistant Trypanosoma brucei brucei. Eukaryot Cell. 2006;5: 1276–1286. doi:10.1128/EC.00116-06

316. Kieft R, Stephens NA, Capewell P, MacLeod A, Hajduk SL. Role of expression site switching in the development of resistance to human Trypanosome Lytic Factor-1 in Trypanosoma brucei brucei. Mol Biochem Parasitol. 2012;183: 8–14. doi:10.1016/j.molbiopara.2011.12.004

317. Salmon D, Geuskens M, Hanocq F, Hanocq-Quertier J, Nolan D, Ruben L, et al. A novel heterodimeric transferrin receptor encoded by a pair of VSG expression site-associated genes in T. brucei. Cell. 1994;78: 75–86.

318. Mehlert A, Wormald MR, Ferguson MAJ. Modeling of the N-glycosylated transferrin receptor suggests how transferrin binding can occur within the surface coat of Trypanosoma brucei. PLoS Pathog. 2012;8: e1002618. doi:10.1371/journal.ppat.1002618

319. Kabiri M, Steverding D. Studies on the recycling of the transferrin receptor in Trypanosoma brucei using an inducible gene expression system. Eur J Biochem. 2000;267: 3309–3314.

320. Lane-Serff H, MacGregor P, Lowe ED, Carrington M, Higgins MK. Structural basis for ligand and innate immunity factor uptake by the trypanosome haptoglobin-haemoglobin receptor. eLife. 2014;3: e05553. doi:10.7554/eLife.05553

321. Hartel AJW, Glogger M, Guigas G, Jones NG, Fenz SF, Weiss M, et al. The molecular size of the extra-membrane domain influences the diffusion of the GPI-anchored VSG on the trypanosome plasma membrane. Sci Rep. 2015;5: 10394. doi:10.1038/srep10394

322. Hartel AJW, Glogger M, Jones NG, Abuillan W, Batram C, Hermann A, et al. N-glycosylation enables high lateral mobility of GPI-anchored proteins at a molecular crowding threshold. Nat Commun. 2016;7: 12870. doi:10.1038/ncomms12870

323. Bartossek T, Jones NG, Schäfer C, Cvitković M, Glogger M, Mott HR, et al. Structural basis for the shielding function of the dynamic trypanosome variant surface glycoprotein coat. Nat Microbiol. 2017;2: 1523–1532. doi:10.1038/s41564-017-0013-6

324. Schwede A, Macleod OJS, MacGregor P, Carrington M. How Does the VSG Coat of Bloodstream Form African Trypanosomes Interact with External Proteins? PLoS Pathog. 2015;11: e1005259. doi:10.1371/journal.ppat.1005259

325. Koumandou VL, Boehm C, Horder KA, Field MC. Evidence for recycling of invariant surface transmembrane domain proteins in African trypanosomes. Eukaryot Cell. 2013;12: 330–342. doi:10.1128/EC.00273-12

326. Ziegelbauer K, Multhaup G, Overath P. Molecular characterization of two invariant surface glycoproteins specific for the bloodstream stage of Trypanosoma brucei. J Biol Chem. 1992;267: 10797–10803.

327. Grab DJ, Shaw MK, Wells CW, Verjee Y, Russo DC, Webster P, et al. The transferrin receptor in African trypanosomes: identification, partial characterization and subcellular localization. Eur J Cell Biol. 1993;62: 114–126.

328. Mussmann R, Engstler M, Gerrits H, Kieft R, Toaldo CB, Onderwater J, et al. Factors affecting the level and localization of the transferrin receptor in Trypanosoma brucei. J Biol Chem. 2004;279: 40690–40698. doi:10.1074/jbc.M404697200

329. Morgan GW, Hall BS, Denny PW, Carrington M, Field MC. The kinetoplastida endocytic apparatus. Part I: a dynamic system for nutrition and evasion of host defences. Trends Parasitol. 2002;18: 491–496.

330. Pal A, Hall BS, Nesbeth DN, Field HI, Field MC. Differential endocytic functions of Trypanosoma brucei Rab5 isoforms reveal a glycosylphosphatidylinositol-specific endosomal pathway. J Biol Chem. 2002;277: 9529–9539. doi:10.1074/jbc.M110055200

331. Auffret CA, Turner MJ. Variant specific antigens of Trypanosoma brucei exist in solution as glycoprotein dimers. Biochem J. 1981;193: 647–650.

332. Ferguson MA, Homans SW, Dwek RA, Rademacher TW. Glycosyl-phosphatidylinositol moiety that anchors Trypanosoma brucei variant surface glycoprotein to the membrane. Science. 1988;239: 753–759.

333. Freymann DM, Metcalf P, Turner M, Wiley DC. 6 A-resolution X-ray structure of a variable surface glycoprotein from Trypanosoma brucei. Nature. 1984;311: 167–169.

334. Mehlert A, Zitzmann N, Richardson JM, Treumann A, Ferguson MA. The glycosylation of the variant surface glycoproteins and procyclic acidic repetitive proteins of Trypanosoma brucei. Mol Biochem Parasitol. 1998;91: 145–152.

335. Carrington M, Miller N, Blum M, Roditi I, Wiley D, Turner M. Variant specific glycoprotein of Trypanosoma brucei consists of two domains each having an independently conserved pattern of cysteine residues. J Mol Biol. 1991;221: 823–835.

336. Pinger J, Nešić D, Ali L, Aresta-Branco F, Lilic M, Chowdhury S, et al. African trypanosomes evade immune clearance by O-glycosylation of the VSG surface coat. Nat Microbiol. 2018;3: 932–938. doi:10.1038/s41564-018-0187-6

337. Zoltner M, Horn D, de Koning HP, Field MC. Exploiting the Achilles' heel of membrane trafficking in trypanosomes. Curr Opin Microbiol. 2016;34: 97–103. doi:10.1016/j.mib.2016.08.005

338. Gentili C, Castor D, Kaden S, Lauterbach D, Gysi M, Steigemann P, et al. Chromosome Missegregation Associated with RUVBL1 Deficiency. PloS One. 2015;10: e0133576. doi:10.1371/journal.pone.0133576

339. Radovic S, Rapisarda VA, Tosato V, Bruschi CV. Functional and comparative characterization of Saccharomyces cerevisiae RVB1 and RVB2 genes with bacterial Ruv homologues. FEMS Yeast Res. 2007;7: 527–539. doi:10.1111/j.1567-1364.2006.00205.x

340. Lilley DM. Homologous recombination. A ring for a warhead. Curr Biol CB. 1994;4: 1152–1154.

341. Venteicher AS, Meng Z, Mason PJ, Veenstra TD, Artandi SE. Identification of ATPases pontin and reptin as telomerase components essential for holoenzyme assembly. Cell. 2008;132: 945–957. doi:10.1016/j.cell.2008.01.019

342. Vaughan S, Gull K. The structural mechanics of cell division in Trypanosoma brucei. Biochem Soc Trans. 2008;36: 421–424. doi:10.1042/BST0360421

343. Büscher P, Cecchi G, Jamonneau V, Priotto G. Human African trypanosomiasis. Lancet Lond Engl. 2017;390: 2397–2409. doi:10.1016/S0140-6736(17)31510-6

344. Matovu E, Enyaru JC, Legros D, Schmid C, Seebeck T, Kaminsky R. Melarsoprol refractory T. b. gambiense from Omugo, north-western Uganda. Trop Med Int Health TM IH. 2001;6: 407–411.

345. Robays J, Nyamowala G, Sese C, Betu Ku Mesu Kande V, Lutumba P, Van der Veken W, et al. High failure rates of melarsoprol for sleeping sickness, Democratic Republic of Congo. Emerg Infect Dis. 2008;14: 966–967. doi:10.3201/eid1406.071266

346. Berger BJ, Carter NS, Fairlamb AH. Characterisation of pentamidine-resistant Trypanosoma brucei brucei. Mol Biochem Parasitol. 1995;69: 289–298.

347. Baker N, Glover L, Munday JC, Aguinaga Andrés D, Barrett MP, de Koning HP, et al. Aquaglyceroporin 2 controls susceptibility to melarsoprol and pentamidine in African trypanosomes. Proc Natl Acad Sci U S A. 2012;109: 10996–11001. doi:10.1073/pnas.1202885109

348. Bernhard SC, Nerima B, Mäser P, Brun R. Melarsoprol- and pentamidine-resistant Trypanosoma brucei rhodesiense populations and their cross-resistance. Int J Parasitol. 2007;37: 1443–1448. doi:10.1016/j.ijpara.2007.05.007

349. Volpon L, D'Orso I, Young CR, Frasch AC, Gehring K. NMR structural study of TcUBP1, a single RRM domain protein from Trypanosoma cruzi: contribution of a beta hairpin to RNA binding. Biochemistry (Mosc). 2005;44: 3708–3717. doi:10.1021/bi047450e

350. D'Orso I, Frasch AC. TcUBP-1, a developmentally regulated U-rich RNA-binding protein involved in selective mRNA destabilization in trypanosomes. J Biol Chem. 2001;276: 34801–34809. doi:10.1074/jbc.M102120200

351. Cassola A, Frasch AC. An RNA recognition motif mediates the nucleocytoplasmic transport of a trypanosome RNA-binding protein. J Biol Chem. 2009;284: 35015–35028. doi:10.1074/jbc.M109.031633

352. Richardson JB, Evans B, Pyana PP, Van Reet N, Sistrom M, Büscher P, et al. Whole genome sequencing shows sleeping sickness relapse is due to parasite regrowth and not reinfection. Evol Appl. 2016;9: 381–393. doi:10.1111/eva.12338

Appendix 1.

PLOS | PATHOGENS

RESEARCH ARTICLE

Aquaglyceroporin-null trypanosomes display glycerol transport defects and respiratory-inhibitor sensitivity

Laura Jeacock[1‡], Nicola Baker[1¤‡], Natalie Wiedemar[2,3], Pascal Mäser[2,3], David Horn[1*]

1 The Wellcome Trust Centre for Anti-Infectives Research, School of Life Sciences, University of Dundee, Dow Street, Dundee, United Kingdom, **2** Parasite Chemotherapy Unit, Swiss Tropical and Public Health Institute, Basel, Switzerland, **3** University of Basel, Basel, Switzerland

¤ Current address: Centre for Immunology & Infection, University of York, Heslington, York, United Kingdom
‡ These authors are co-first authors.
* d.horn@dundee.ac.uk

OPEN ACCESS

Citation: Jeacock L, Baker N, Wiedemar N, Mäser P, Horn D (2017) Aquaglyceroporin-null trypanosomes display glycerol transport defects and respiratory-inhibitor sensitivity. PLoS Pathog 13(3): e1006307. https://doi.org/10.1371/journal.ppat.1006307

Editor: Scott M Landfear, Oregon Health & Science University, UNITED STATES

Received: December 4, 2016

Accepted: March 22, 2017

Published: March 30, 2017

Data Availability Statement: All relevant data are within the paper and its Supporting Information files.

Funding: This research was jointly funded by the UK Medical Research Council (MRC) and the UK Department for International Development (DFID) under the MRC/DFID Concordat agreement, and is also part of the EDCTP2 programme supported by the European Union (MR/K000500/1 to DH), by the Wellcome Trust (100320/Z/12/Z; Investigator Award to DH), and by the Swiss National Science

Abstract

Aquaglyceroporins (AQPs) transport water and glycerol and play important roles in drug-uptake in pathogenic trypanosomatids. For example, AQP2 in the human-infectious African trypanosome, *Trypanosoma brucei gambiense*, is responsible for melarsoprol and pentamidine-uptake, and melarsoprol treatment-failure has been found to be due to AQP2-defects in these parasites. To further probe the roles of these transporters, we assembled a *T. b. brucei* strain lacking all three *AQP*-genes. Triple-null *aqp1-2-3 T. b. brucei* displayed only a very moderate growth defect *in vitro*, established infections in mice and recovered effectively from hypotonic-shock. The *aqp1-2-3* trypanosomes did, however, display glycerol uptake and efflux defects. They failed to accumulate glycerol or to utilise glycerol as a carbon-source and displayed increased sensitivity to salicylhydroxamic acid (SHAM), octyl gallate or propyl gallate; these inhibitors of trypanosome alternative oxidase (TAO) can increase intracellular glycerol to toxic levels. Notably, disruption of *AQP2* alone generated cells with glycerol transport defects. Consistent with these findings, *AQP2*-defective, melarsoprol-resistant clinical isolates were sensitive to the TAO inhibitors, SHAM, propyl gallate and ascofuranone, relative to melarsoprol-sensitive reference strains. We conclude that African trypanosome AQPs are dispensable for viability and osmoregulation but they make important contributions to drug-uptake, glycerol-transport and respiratory-inhibitor sensitivity. We also discuss how the AQP-dependent inverse sensitivity to melarsoprol and respiratory inhibitors described here might be exploited.

Author summary

Protein channels in cell membranes transport specific molecules in and out of cells, and can also facilitate drug-uptake. One such protein, known as an aquaglyceroporin (AQP), allows parasitic African trypanosomes, the cause of lethal diseases in humans and livestock, to accumulate an arsenic-based drug known as melarsoprol. Unfortunately,

Foundation (310030_156264). The funders had no role in study design, data collection and analysis, decision to publish, or preparation of the manuscript.

Competing interests: The authors have declared that no competing interests exist.

parasites with a mutated AQP have resisted this drug and have spread, leading to treatment-failure in >50% of patients in some areas. The functions of this particular AQP, and two other similar AQPs normally expressed by these parasites, remain to be fully characterised in trypanosomes. We therefore generated and characterised parasites lacking all three AQPs. The cells grow well and, to our surprise, continue to effectively allow water to flow in and out of the cell. Glycerol uptake and efflux are both perturbed, however. As a consequence, drugs that cause these parasites to produce toxic quantities of glycerol are more effective against parasites lacking the AQPs. Indeed, even the melarsoprol-resistant, patient-derived parasites described above are more sensitive to these drugs. Our findings not only reveal the relative contributions of the AQPs to glycerol transport, they also point to therapies that could be more effective in the many patients infected by melarsoprol-resistant parasites.

Introduction

African trypanosomes are parasitic protozoa and the causative agents of human and animal African trypanosomiasis (HAT and AAT, respectively). These parasites are typically transmitted by tsetse-flies, which are restricted to sub-Saharan Africa. HAT is typically fatal without treatment, classified as a 'neglected tropical disease', and caused primarily by *T. brucei gambiense* (Western-Africa) but also by *T. brucei rhodesiense* (Eastern Africa). AAT is typically caused by *T. vivax*, *T. congolense* or *T. b. brucei*, important veterinary and livestock pathogens; *T. b. brucei* is a less-prevalent veterinary parasite and the favoured experimental sub-species. Vaccine development is challenging and therapies suffer problems with toxicity, resistance, cost, limited efficacy and difficulties with administration [1]. In addition, in the case of HAT, diagnostic tools must define the stage of the disease if the appropriate therapy is to be selected [1]. For treatment of the second stage for example, when parasites have entered the central nervous system, the nifurtimox-eflornithine combination therapy is favoured [2]. The other option is melarsoprol, but this is toxic [1]. Unfortunately, eflornithine is ineffective against *T. b. rhodesiense* [3] so melarsoprol is currently the only option, despite its toxicity, against advanced disease caused by this parasite.

Melarsoprol treatment-failure, in >50% of patients in some areas, has been reported for both *T. b. rhodesiense* [4] and *T. b. gambiense* infections [5]. Melarsoprol-resistance can arise due to reduced accumulation of drug, following aquaglyceroporin 2 (AQP2) mutation [6]. Both a trypanosome P2 adenosine transporter [7,8] and AQP2, an aquaglyceroporin with an unusual arrangement of pore-lining residues comprising the 'selectivity filter' [9,10], contribute to melarsoprol-uptake; laboratory-engineered defects in these transporters render cells melarsoprol-resistant. These cells also display cross-resistance to pentamidine [6], a drug used to treat trypanosomiasis prior to central nervous system involvement. This may have little impact in the clinic, however, because pentamidine remains effective at the high doses administered [11]. In terms of melarsoprol-resistance and treatment-failure, clinical isolates from both the Democratic Republic of the Congo and South Sudan, dating back to the 1970s, display *AQP2*-defects [12,13], and a clinical isolate was re-sensitised to both melarsoprol and pentamidine by the addition of an intact *AQP2* gene [14]. A defect in a related *Leishmania* AQP has been linked to widespread antimonial-resistant *Leishmania* infections in India [15].

There are three AQPs encoded in the *T. b. brucei* genome. AQP1 has been reported to localise to the flagellar membrane in bloodstream-form cells [16], while plasma membrane localisation is indicated in insect-stage cells [17]. AQP3 displays a plasma membrane localisation in

both bloodstream-form cells [9,16] and insect-stage cells [9]. AQP2, on the other hand, is largely restricted to the flagellar pocket membrane in bloodstream-form cells, and then becomes distributed more widely in the plasma membrane in insect-stage cells [9]. Heterologous expression of the *T. b. brucei* AQPs reveals their ability to transport water, mass: 18 Da; ammonia, mass: 17 Da [18]; boric acid, mass: 62 Da [19]; glycerol, mass: 92 Da [20] and some forms of trivalent arsenic, mass: 83–198 Da; and trivalent antimony, mass: 122–292 Da [21]. *AQP2* gene-knockout in *T. b. brucei* reveals that this AQP can also specifically mediate uptake of melarsoprol; mass: 398 Da, and pentamidine; mass: 340 Da [9,10]. These drugs have a substantially greater mass than other known AQP-substrates and recent evidence indicates that pentamidine, rather than being a permeant, binds to and inhibits AQP2, suggesting that uptake of this drug might require endocytosis [22].

To further probe AQP-function, we deleted all three *T. b. brucei AQP* genes from the *T. b. brucei* genome. We found that trypanosomes tolerate the loss of all three *AQPs*. The triple *aqp1-2-3* null-strains, surprisingly, tolerated hypotonic shock, but were defective in glycerol uptake, utilisation and efflux and, consequently, were sensitised to trypanosome alternative oxidase (TAO) inhibitors that increase the intracellular glycerol concentration to toxic levels. Notably, trypanosomes lacking only *AQP2* were also defective in glycerol utilisation and efflux and, as predicted by our *T. b. brucei* studies, clinical melarsoprol-resistant *T. b. gambiense* isolates were also more sensitive to respiratory inhibitors relative to melarsoprol sensitive reference strains.

Results

T. b. brucei tolerates the loss of all three *AQPs*

T. b. brucei AQP1 (Tb927.6.1520) is on chromosome 6 and *AQP2* (Tb927.10.14170) and *AQP3* (Tb927.10.14160) are adjacent to each other on chromosome 10 (see Fig 1A). The *AQP2-AQP3* locus is dispensable for growth [23]. *AQP1* knockdown, using RNA interference was not associated with any substantial growth-defect [16], but knockout of *AQP1* has not, to our knowledge, been attempted. *T. b. brucei* is diploid so we sequentially replaced the *AQP1* alleles with selectable markers (*NPT* and *PAC*) to determine whether *AQP1* was dispensable (see Fig 1A). We readily obtained *aqp1*-null strains, as confirmed by Southern blotting (Fig 1B).

We next devised a strategy to assemble triple *aqp*-null strains in a background that would facilitate conditional expression of wild-type or mutant *AQPs* for complementation studies. In order to recycle the limited number of selectable-markers available, we used a multi-step strategy employing the meganuclease, I-*Sce*I (see Materials and methods). Briefly, we set up strains in the 2T1-background [24] in which meganuclease induction triggered the replacement of a chromosomal knockout-cassette, bearing an I-*Sce*I cleavage-site, with an allelic knockout-cassette lacking an I-*Sce*I cleavage-site. The cassette-integration and chromosomal allele-replacement process was carried out for the *AQP2-AQP3* locus and then repeated for the *AQP1* locus, such that the resulting strains bore a *BLA*-marker at both *aqp2-aqp3* null alleles and an *NPT*-marker at both *aqp1* null alleles (Fig 1A). Southern blotting confirmed the absence of *AQP1* (Fig 1B), *AQP2* and *AQP3* (Fig 1C) in the resulting *aqp1-2-3* null strains. Thus, *T. b. brucei* tolerates the loss of all three *AQPs*.

The *T. b. brucei* AQPs have minimal impact on fitness or osmoregulation

We assessed fitness in cell-culture for the new *aqp1* and *aqp1-2-3* strains and compared these to the wild-type and the previously described *aqp2-3* strains [9]. The growth-curves indicated a modest defect in the *aqp1-2-3* strains and no apparent defect in the *aqp1* or in the *aqp2-3* strains (Fig 2A). The *aqp1-2-3* strains were also able to establish infections *in vivo* in a mouse

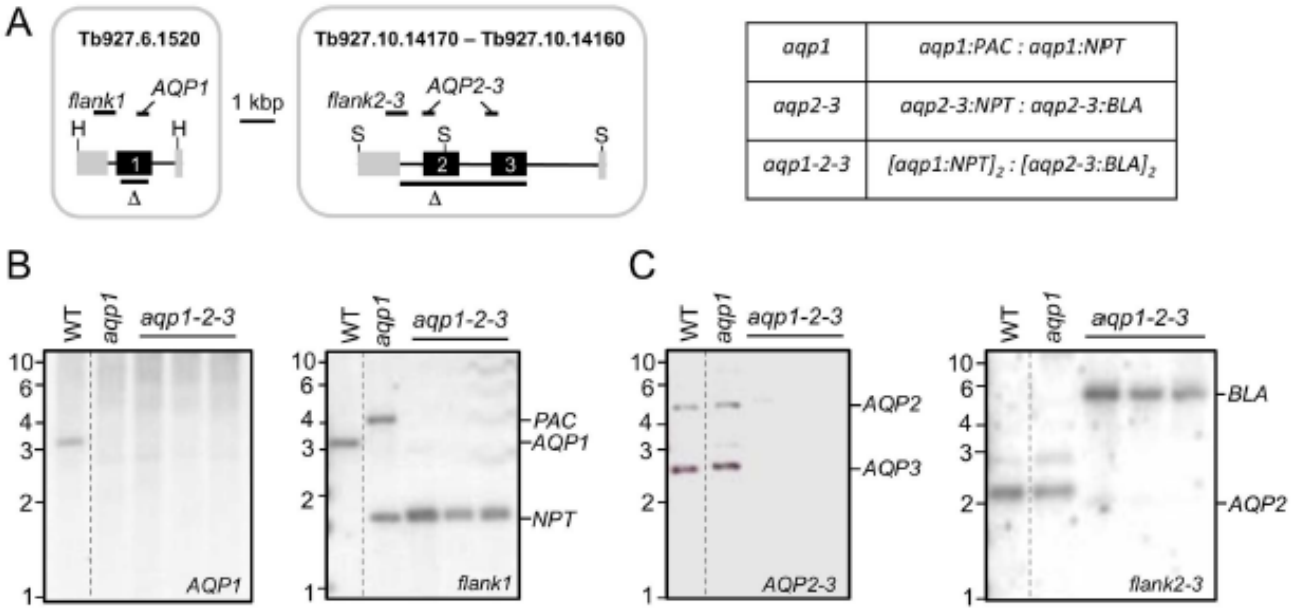

Fig 1. *T. b. brucei* tolerates the loss of all three *AQPs*. (A) The schematic maps indicate the *AQP1* and *AQP2-3* regions replaced by selectable markers as also indicated on the right. Δ indicates the regions deleted while the probes used for Southern blotting are shown above the maps. H, *Hpa*I; S, *Sad*I. (B) The Southern blots indicate deletion of the *AQP1* alleles in *aqp1* and three independent *aqp1-2-3* strains. Wild-type (WT) is shown for comparison. Genomic DNA was digested with *Hpa*I. (C) The Southern blots indicate deletion of the *AQP2-3* alleles in *aqp1-2-3* strains. WT is shown for comparison. Genomic DNA was digested with *Sad*I.

https://doi.org/10.1371/journal.ppat.1006307.g001

model; parasitaemia in all three mice was between 4 x 10^6 and 4 x 10^7 per ml of blood four days after inoculation. These *aqp1-2-3* strains also differentiated to the insect mid-gut stage *in vitro*; equivalent to wild-type after one week in insect-stage growth-medium. Thus, we observed only a modest fitness-defect in bloodstream-form cells in the absence of all three *AQPs* but not in the absence of either *AQP1* or *AQP2-AQP3*.

AQP2 specifically controls melarsoprol and pentamidine-uptake and has a particularly pronounced impact on pentamidine-sensitivity *in vitro* [9]. Dose-response assays confirmed the expected pentamidine-resistance in the *aqp2-3* strains and indicated no additional resistance in the *aqp1-2-3* strains (Fig 2B); EC_{50}-values were increased by approximately 30-fold relative to wild-type in both cases. These results are consistent with the established specific role for AQP2 in pentamidine (and melarsoprol) uptake and cross-resistance [9,12,23].

AQPs can transport water or small solutes. To explore the contribution of the *T. b. brucei* AQPs to osmoregulation, we exposed cells to hypo-osmotic shock and monitored the response. Under these conditions, cells swell rapidly and then, more slowly (10–20 min), return to their original volume. We saw no, or only moderate, differences in the time taken to recover for *aqp1*, *aqp2-3* or *aqp1-2-3* null-cells relative to wild-type trypanosomes (Fig 2C). We conclude that the *T. b. brucei* AQPs have minimal impact on fitness or regulatory volume-decrease after osmotic shock.

Glycerol uptake and utilisation are perturbed in *aqp* null *T. b. brucei*

We next assessed the ability of the *aqp1-2-3* null *T. b. brucei* strains to use glycerol as a carbon-source, which is possible in bloodstream form trypanosomes under aerobic conditions [25]. In preliminary experiments, *aqp1-2-3* cells displayed sustained motility in 5 mM glucose and

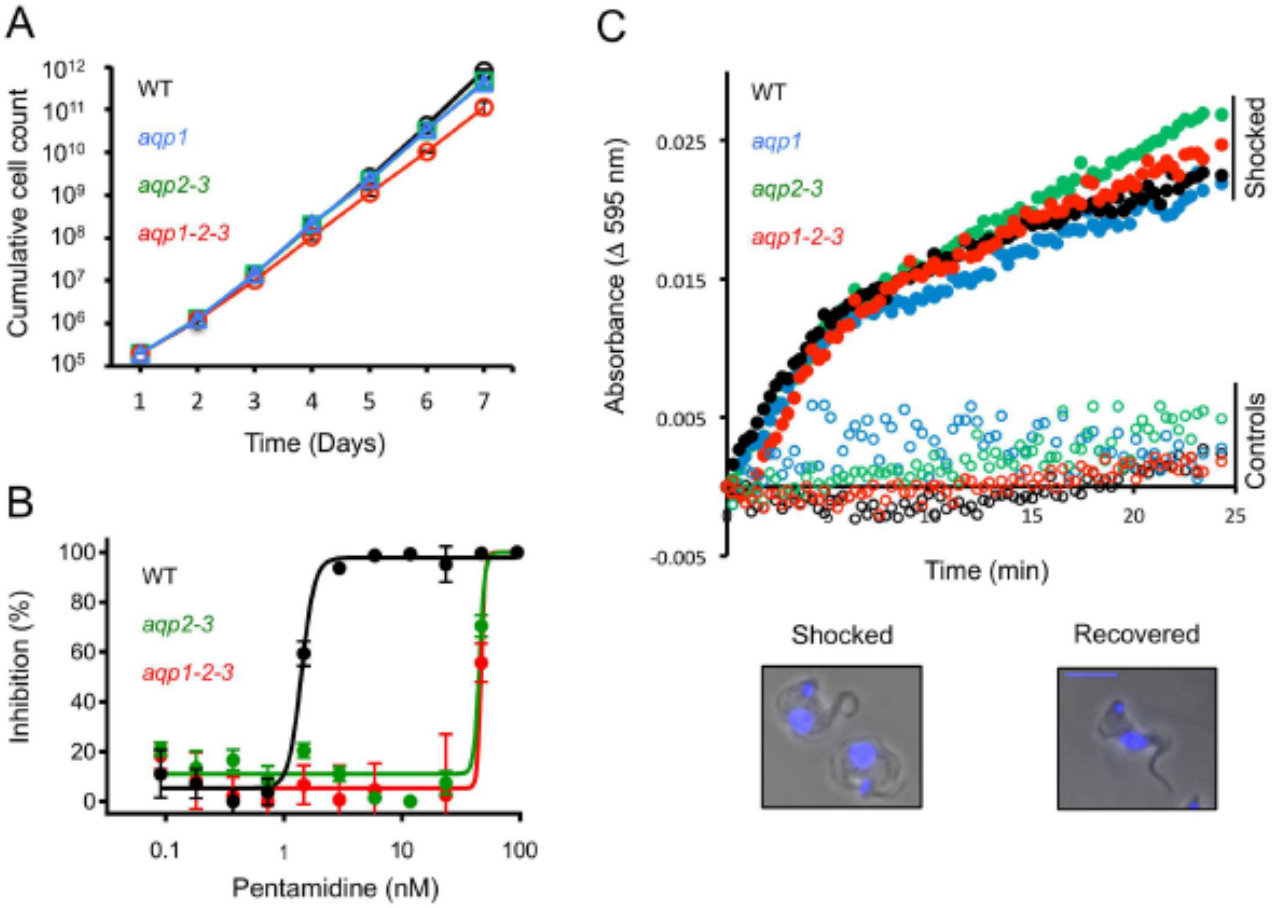

Fig 2. The *T. b. brucei* AQPs have minimal impact on fitness or osmoregulation. (A) Cumulative growth-curves for wild-type (WT), *aqp1*, *aqp2-3* and *aqp1-2-3* null-strains. (B) Dose-response curves for pentamidine. (C) Hypo-osmotic shock assay. Open symbols, Earle's salt buffer; filled symbols, buffer diluted 50:50 with H_2O. The recovery phase is shown. The phase-contrast images show two shocked and swollen cells (at left) and a recovered cell (at right). Scale-bar, 5 μm. DNA was counter-stained with DAPI (blue).

https://doi.org/10.1371/journal.ppat.1006307.g002

fructose but these cells were immotile within 15-minutes in 5 mM glycerol. To quantify the ATP-levels in cells incubated in 5 mM glucose or glycerol, we used a luminescence assay and this confirmed that *aqp1-2-3* cells were able to use glucose as a carbon-source but were unable to utilise glycerol (Fig 3A). Since ATP-levels were significantly depleted ($P<0.001$) relative to wild-type in *aqp1-2-3* cells incubated in glycerol, we exploited this assay to assess the impact of the various AQPs on glycerol utilisation; cells were harvested before they became immotile in this assay so as to record quantitative differences among strains. As expected, ATP-levels were not significantly diminished in any of the *aqp*-defective strains tested in glucose (Fig 3A). In glycerol though, ATP-levels were significantly depleted ($P<0.001$) in *aqp2*, *aqp2-3* and *aqp1-2-3* cells but not in *aqp1* cells (Fig 3A). These results suggest that, among the AQPs, AQP2 makes the greatest contribution to glycerol utilisation; this interpretation is supported by both effective utilisation of glycerol by *aqp1* null cells and no increase in the glycerol-utilisation defect in *aqp2-3* cells relative to *aqp2* cells.

Since glycerol utilisation does not directly reflect glycerol uptake, we next measured glycerol uptake; in wild-type, triple-null and *AQP2*-complemented cells. The *aqp1-2-3* cells

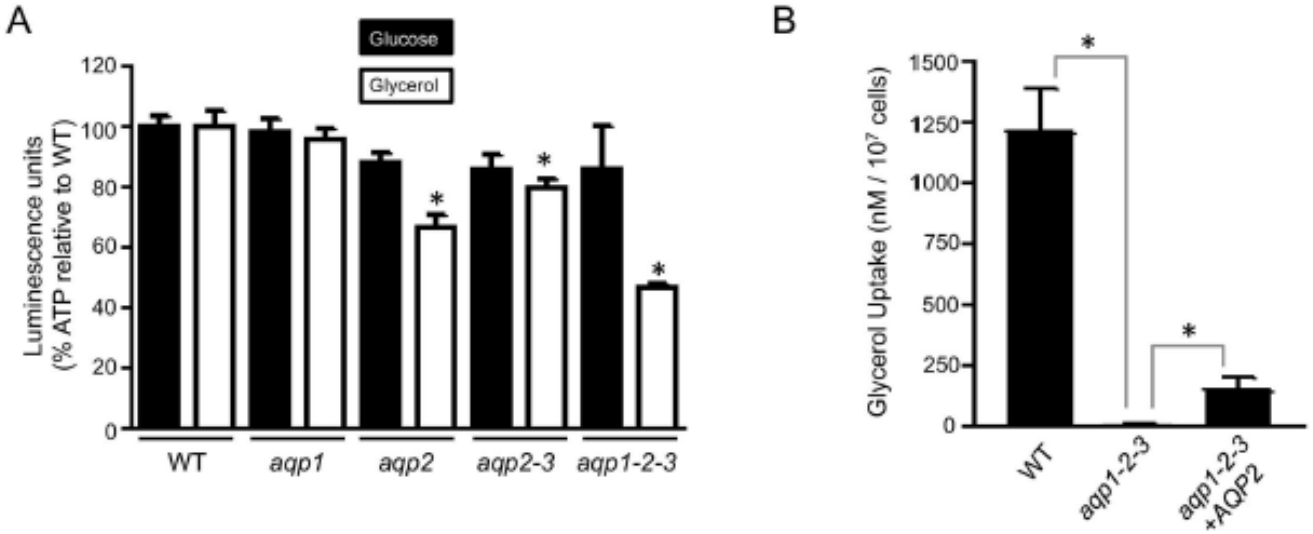

Fig 3. Glycerol uptake and utilisation is perturbed in *aqp*-null *T. b. brucei*. (A) ATP levels were assessed in the strains indicated after incubation in 5 mM glucose or glycerol. Readings were taken in triplicate and normalised to substrate only. * indicates significantly different ($P<0.001$) to wild-type (WT) using an ANOVA test in GraphPad Prism. Error bars, SD. (B) Radiolabelled glycerol uptake was assessed in the strains indicated. Readings were taken in quadruplicate. * indicates significant difference ($P<0.05$) using a Student's *t*-test. Error bars, SD.

https://doi.org/10.1371/journal.ppat.1006307.g003

revealed almost complete ablation of glycerol-uptake (Fig 3B), consistent with minimal diffusion of glycerol across the plasma membrane. *AQP2* provided complementation of this defect, albeit only partial (Fig 3B). Thus, AQP2 appears to make the greatest contribution to glycerol utilisation but not the major contribution to glycerol uptake into the cell, possibly reflecting an impact on transport into glycosomes, where glycerol is utilised [25].

T. b. brucei aqp-null cells display a glycerol efflux defect and respiratory inhibitor-sensitivity

We next asked whether *aqp*-defective trypanosomes displayed glycerol-efflux defects as well as the glycerol-uptake defects described above. Salicylhydroxamic acid (SHAM) increases intracellular glycerol levels by inhibiting the trypanosome alternative oxidase (TAO) [26], a ubiquinol oxygen oxidoreductase that is cyanide-insensitive and maintains redox balance as part of the glycerol-3-phosphate oxidase system (see Fig 4A, left-hand panels). Consistent with a glycerol-efflux defect, dose-response curves revealed that *aqp1-2-3* null-cells were SHAM-sensitive (EC_{50} decreased >7-fold) relative to wild-type cells (Fig 4A, right-hand panel: EC_{50} 1.6 and 12 μM, respectively). SHAM plus glycerol rapidly kills bloodstream-form African trypanosomes [27] (see Fig 4B, left-hand panel), but we predicted that the impact of added glycerol would not be pronounced in glycerol-uptake defective *aqp1-2-3* null-cells. Indeed, SHAM dose-response curves generated in the presence of 10 mM glycerol (Fig 4B, right-hand panel) revealed a substantial impact of glycerol against wild-type cells but only a very weak impact against *aqp1-2-3* null-cells; glycerol reduced SHAM EC_{50} values by 13 and 1.8-fold, respectively; to 0.9 μM in both cases (compare Fig 4A and 4B). We also tested the additional TAO inhibitors, propyl gallate and octyl gallate [28], against wild-type and *aqp1-2-3* null-cells. Once again, and consistent with a glycerol-efflux defect, dose-response curves revealed that *aqp1-2-3* null-cells were TAO inhibitor sensitive relative to wild-type cells (Fig 4C); EC_{50} was reduced by 4-fold and 5-fold, respectively.

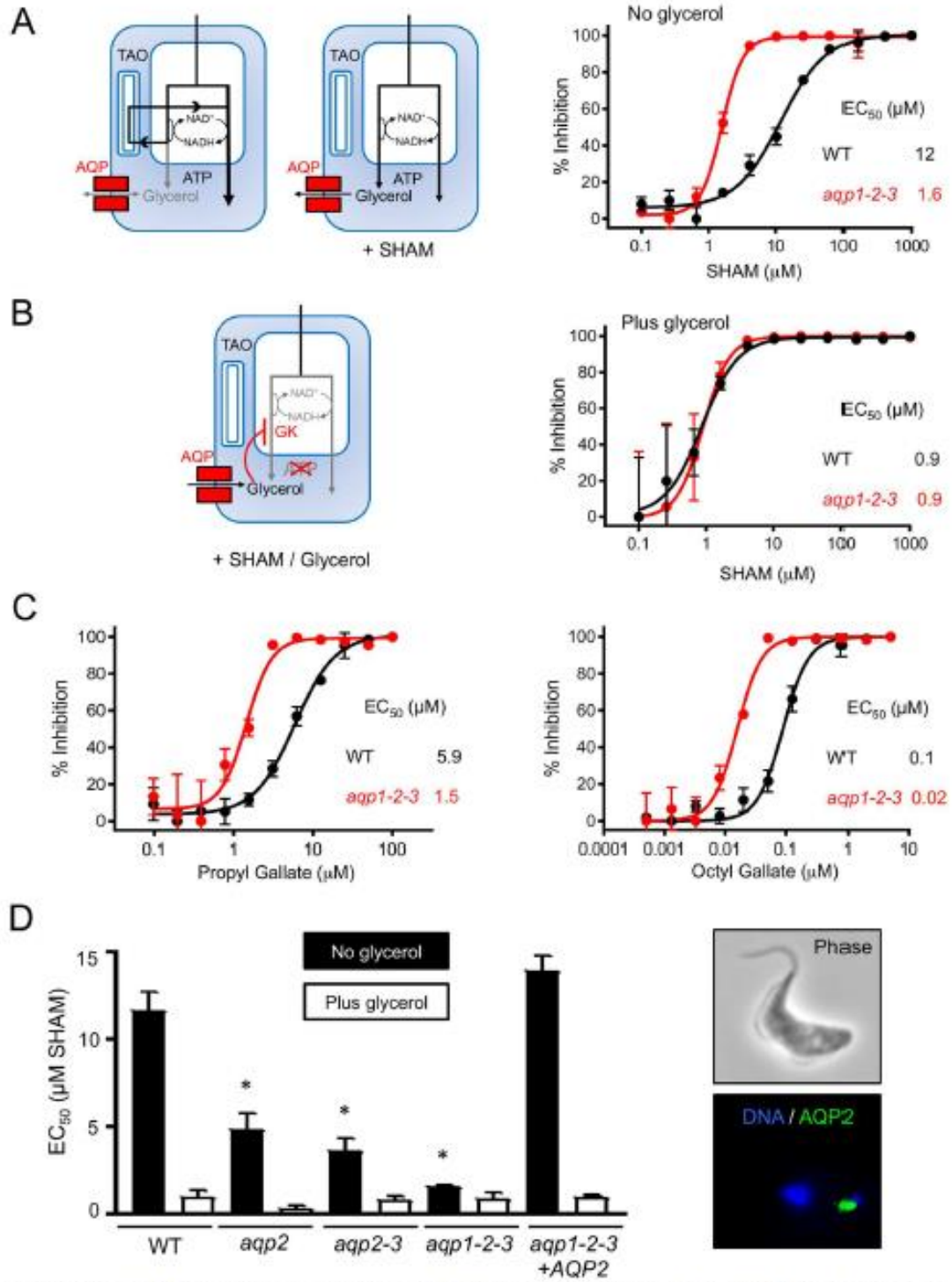

Fig 4. *aqp*-null *T. b. brucei* display defective glycerol-efflux and respiratory inhibitor-sensitivity. (A) Bloodstream *T. brucei* express a SHAM-sensitive mitochondrial trypanosome alternative oxidase (TAO). Under aerobic conditions, TAO activity allows ATP production without glycerol production as indicated by the black lines (left-hand blue 'cell'). SHAM blocks TAO-activity, leading to the anaerobic production of glycerol, which is toxic if not removed, as indicated by the black lines (right-hand blue 'cell'). SHAM dose-response curves for wild-type (WT) and *aqp1-2-3* null-cells. EC_{50} values are indicated.

(B) In the presence of SHAM and glycerol, the glycerol inhibits glycerol kinase (GK), also preventing ATP-production by the anaerobic route (blue 'cell'). SHAM dose-response curves as in A but in the presence of 10 mM glycerol. (C) Propyl gallate and octyl gallate dose-response curves for wild-type (WT) and *aqp1-2-3* null-cells. EC_{50} values are indicated. (D) SHAM EC_{50} values +/- 10 mM glycerol from A-B and also from *aqp2*, *aqp2-3* and *aqp1-2-3* cells re-expressing ^{GFP}AQP2. * indicates significantly different ($P<0.01$) to WT using an ANOVA test in GraphPad Prism. Pairwise comparisons +/- glycerol, except in the case of the *aqp1-2-3* null, indicated significant ($P<0.001$) differences using a Student's *t*-test. Error bars, SD. The images to the right show re-expression of ^{GFP}AQP2 in *aqp1-2-3* null-cells.

https://doi.org/10.1371/journal.ppat.1006307.g004

Since our glycerol-utilisation assays indicated a defect in *aqp2* null *T. b. brucei*, we next asked whether these cells also displayed increased sensitivity to SHAM, consistent with a glycerol-efflux defect. We also tested SHAM-sensitivity in *aqp2-3* null cells and in *aqp1-2-3* null cells re-expressing *AQP2*; re-expressed AQP2 was localised to the flagellar pocket (Fig 4D, right-hand side), as expected [9]. The full set of SHAM (plus glycerol) EC_{50} values are shown in Fig 4D. SHAM-sensitivity was indeed observed in *aqp2* null (2.4-fold) *aqp2-3* null (3.2-fold) and *aqp1-2-3* null cells (see above); these cells were all significantly more sensitive to SHAM than wild type (Fig 4D), and AQP2 re-expression effectively reversed SHAM-sensitivity in the *aqp1-2-3* null background (Fig 4D). Also, 10 mM glycerol reduced SHAM EC_{50} values to <1 μM in all cell types and this reduction was significant in all but the *aqp1-2-3* null cells (Fig 4D), again consistent with almost complete ablation of glycerol transport in the latter case only.

Melarsoprol-resistant clinical isolates display respiratory inhibitor-sensitivity

TAO inhibitor-sensitivity in *aqp*-null *T. b. brucei* may help to predict how trypanosomes in patients will respond to respiratory inhibitors. In particular, naturally occurring melarsoprol-resistant clinical *T. b. gambiense* isolates display chimerisation of the *AQP2/3* genes [14]. Indeed, a substantial proportion, >50% in some areas, of circulating *T. b. gambiense* may be *AQP2*-defective [12,13]; probably due to selection with melarsoprol since the 1940s. To analyse whether this *AQP2* defect might have an impact on respiratory inhibitor-sensitivity in clinical isolates, we generated SHAM dose-response curves. The isolates selected were the melarsoprol/pentamidine sensitive STIB930 and STIB891 strains (EC_{50} <10 and <2 nM, respectively, according to [12]), the melarsoprol/pentamidine resistant K03048 and 40 AT isolates from melarsoprol-relapsed patients (EC_{50} >20 and >50 nM, respectively, according to [12]) and a 40 AT-derivative that re-expresses *AQP2* and is consequently restored to melarsoprol/pentamidine sensitivity [14]. The STIB930 and STIB891 strains are from patients in Côte d'Ivoire in 1978 [29] and Uganda in 1995 [30] and the K03048 and 40 AT isolates are from patients in South Sudan in 2003 [31] and the Democratic Republic of the Congo in 2006 [13], respectively. The STIB930 and STIB891 strains have intact *AQP2* genes, while neither of the latter isolates has an intact *AQP2* gene [12].

As our studies on *T. b. brucei* had predicted, dose-response curves for the *T. b. gambiense* strains revealed significantly lower EC_{50} values for both *aqp2*-defective strains relative to the *AQP2* controls (Fig 5A); the strains that lacked AQP2 were also confirmed to be pentamidine-resistant (Fig 5A, inset), as previously reported [12]. These results suggest a glycerol-efflux defect in the *aqp2*-defective clinical isolates. Re-expression of *AQP2* in 40 AT cells did not significantly alter SHAM-sensitivity, however (Fig 5A). This may indicate that the AQP2/3 chimera interferes with glycerol efflux by recombinant AQP2, possibly due to the formation of AQP hetero-tetramers that, despite the glycerol efflux defect, continue to contribute to pentamidine uptake by endocytosis [22]. The addition of 10 mM glycerol significantly reduced SHAM EC_{50} values to <1 μM in all five cell-types (Fig 5A), indicating, as predicted, continued

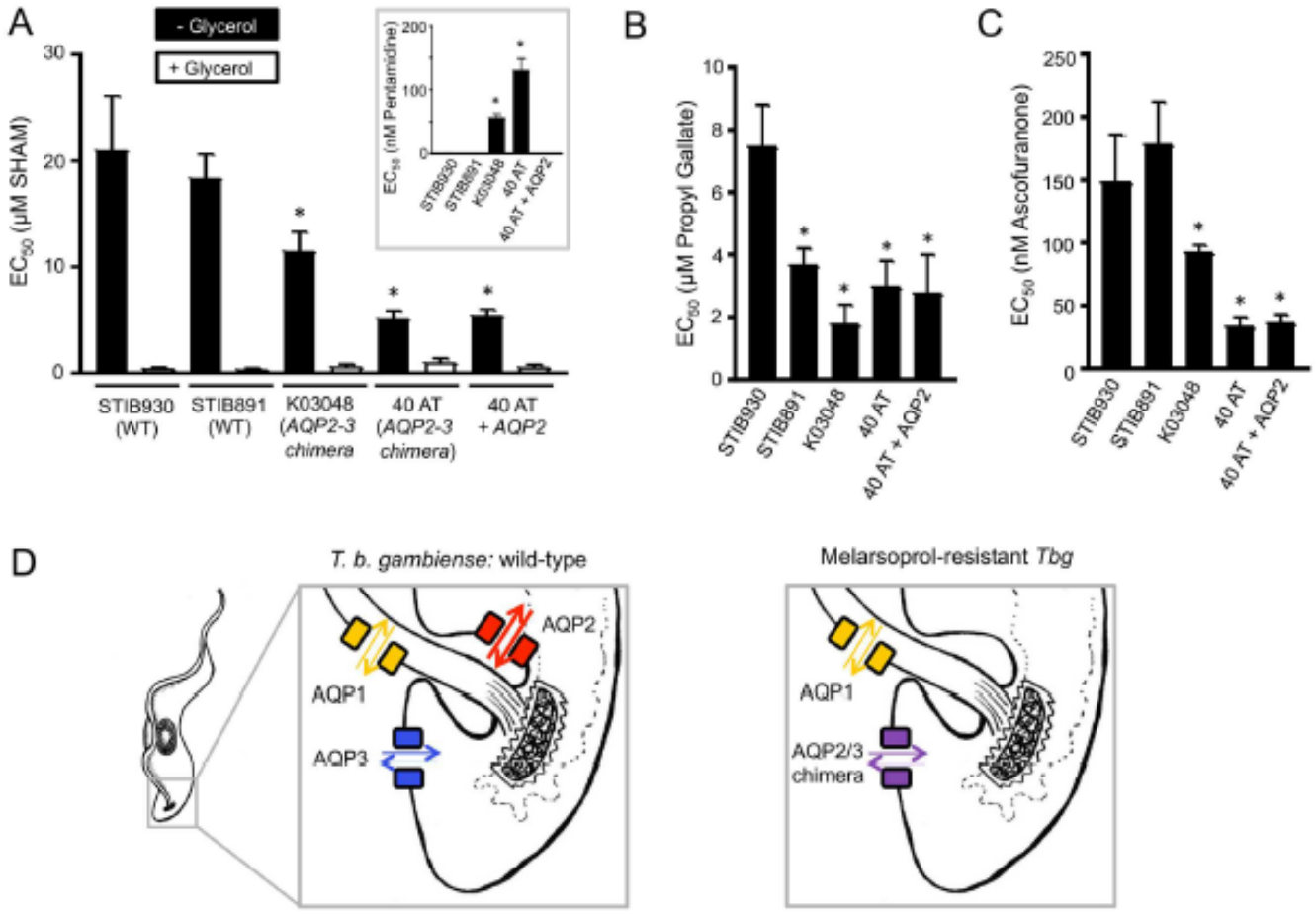

Fig 5. Respiratory inhibitor-sensitivity in *T. b. gambiense* isolates and AQP-mediated glycerol transport. (A) SHAM EC_{50} values for the *T. b gambiense* strains are indicated +/- glycerol. The inset shows pentamidine EC_{50} values. * indicates significantly different ($P<0.05$) to STIB930 using an ANOVA test in GraphPad Prism. All pairwise comparisons +/- 10 mM glycerol also indicated significant ($P<0.001$) differences using a Student's *t*-test. Error bars, SD. (B) Propyl gallate and (C) Ascofuranone EC_{50} values. Other details as in A. (D) Model for glycerol transport by AQPs in *T. b. gambiense*. The weight of the arrows indicates relative impact on glycerol utilisation and efflux, with AQP2 being the major contributor; note that transport across both the plasma and glycosomal membranes contributes to glycerol utilisation and efflux, see the text for more details. The right-hand panel indicates the situation in melarsoprol-resistant (reduced melarsoprol uptake) and SHAM-sensitive (reduced glycerol efflux) clinical isolates where a chimeric AQP2/3 replaces AQP2 and AQP3.

https://doi.org/10.1371/journal.ppat.1006307.g005

glycerol influx in each case. To extend these findings, we examined the impact of two additional TAO inhibitors, propyl gallate and ascofuranone [32], on the same set of strains described above. Dose-responses for propyl gallate (Fig 5B) and ascofuranone (Fig 5C) revealed similar EC_{50} profiles as detailed above for SHAM. Although the STIB891 EC_{50} for propyl gallate was relatively low, both *aqp2*-defective strains displayed an even lower EC_{50}, and both were significantly more sensitive to the respiratory inhibitors than the STIB930 control (Fig 5B and 5C). Once again, re-expression of *AQP2* in 40 AT cells did not significantly alter respiratory inhibitor sensitivity (Fig 5B and 5C).

Together, our results indicate that triple *aqp*-null and *aqp2* null *T. b. brucei* exhibit defects in bidirectional glycerol flux. The evidence is three-fold; first, failure to take up or effectively utilise glycerol as a carbon source; second, sensitivity to multiple respiratory inhibitors which produce toxic levels of intracellular glycerol; and third, no significant increase in SHAM-

sensitivity in excess glycerol in triple-null cells. Thus, glycerol flux appears to be almost absent in *aqp1-2-3* triple-null cells. Our results also indicate that AQP2 makes a key contribution to glycerol utilisation and efflux. This interpretation is supported by a substantial defect in glycerol utilisation and sensitivity to SHAM in *aqp2* null-cells; a phenotype that is reversed by AQP2 re-expression in *aqp1-2-3* triple-null cells. Importantly, analysis of melarsoprol/pentamidine sensitive *T. b. gambiense* reference strains and melarsoprol/pentamidine resistant clinical-isolates supports the idea that AQP2 also makes a key contribution to glycerol efflux in trypanosomes in patients (see Fig 5D). We propose that it is the replacement of *AQP2* with the *AQP2-3* chimera in clinical isolates (Fig 5D) that increases sensitivity to respiratory inhibitors. Notably, although the chimera comprises <15% of the AQP3-sequence at the *C*-terminus, like AQP3 [9], the chimera is distributed within the plasma membrane [10]; AQP2 by contrast is concentrated in the flagellar pocket in bloodstream-form cells [9].

Discussion

Here, we describe bloodstream-form *T. b. brucei* strains that lack all three AQPs. These strains exhibit only a minimal fitness-defect and no apparent osmoregulation-defect. They do, however, exhibit bidirectional defects in glycerol transport. AQP2 is an important determinant of cross-resistance to melarsoprol and pentamidine and this AQP was also found to make a key contribution to glycerol transport. Finally, following analysis of clinical isolates, we propose that the AQPs behave similarly in parasites in patients, suggesting that TAO-inhibitors may be more effective against melarsoprol-resistant African trypanosome infections.

The triple *aqp*-null strain was assembled with the primary purpose of dissecting AQP-functions. We note though that successful generation of such a strain indicates that the AQPs are unlikely to be suitable therapeutic targets for inhibition. It was also possible to generate malaria parasites that lacked the single encoded *AQP* gene; these *aqp*-null *Plasmodium* parasites displayed defective glycerol uptake and moderately reduced virulence [33]. We find that *aqp1-2-3* null *T. b. brucei* establish parasitemia in mice. Indeed, strains isolated from patients following melarsoprol treatment-failure, in an area where treatment-failure is common, display fusion of *AQP2* and *AQP3* to form an *AQP2/3* chimera [12,13]. This suggests, either that these *AQPs* are dispensable at all stages of the life-cycle, or that the chimera complements the defect(s). It remains possible that AQP1 or the AQP2/3 chimera have essential functions in other life-cycle stages, but we were able to differentiate triple-null cells to the procyclic stage *in vitro* and also note that *T. vivax* and *T. congolense* appear to lack both the *AQP1* and *AQP2* genes [34].

The three *T. b. brucei* AQPs were previously reported to play a role in osmoregulation [16]. The same study indicated an additional glycerol transport activity in *T. b. brucei* [16]. In contrast, we observe minimal or no defect in osmoregulation and detected minimal residual glycerol flux in triple *aqp*-null cells. The former difference could potentially reflect adaptation in null cells but the latter difference is likely explained by only 36% AQP2 knockdown or 73% triple AQP knockdown in the former study [16]. Notably, adaptation, if it operates, would also be expected in clinical and veterinary isolates that lack *AQP* genes. How is osmoregulation achieved in other parasitic trypanosomatids? A contractile vacuole/spongiome complex is present in *Trypanosoma cruzi* and *Leishmania major*, and aqua(glycero)porins have been localised to these organelles [35,36]; the *T. cruzi* aquaporin is not closely related to the *T. brucei* AQPs but *Leishmania* AQP1 is closely related [6] and does play a role is osmoregulation [37]. However, water can diffuse across membranes and alternative mechanisms of osmoregulation do operate. In both *L. major* [38] and *Crithidia luciliae* [39], cells tolerate hypotonic stress through the efflux of amino acids and, in *Leishmania donovani*, also through the efflux of inorganic osmolytes [40]. Thus, *T. brucei* AQPs may contribute to osmoregulation, but we suggest

that the primary roles of these AQPs in bloodstream-form cells are the transport of glycerol and other solutes.

Under aerobic conditions, *T. b. brucei* can use glycerol as a carbon source [41]. We found that triple *aqp*-null cells, and even *aqp2*-null cells, fail to effectively utilise glycerol. This indicates that AQPs contribute to glycerol-uptake and utilisation and that AQP2 makes a key contribution. Since glycerol utilisation and production under anaerobic conditions occurs inside glycosomes [25], we must consider glycosomal transport as well as transport across the plasma membrane. A *T. cruzi* aquaporin is localised to acidocalcisomes [36] but AQPs have not been reported to be associated with glycosomes. It is possible that the *T. brucei* AQPs are also present in glycosomal membranes but there may equally be alternative glycerol transporters associated with these organelles.

Carbohydrate catabolism in African trypanosomes has been considered a promising potential antitrypanosomal therapeutic target for >40 years. Indeed, a SHAM plus glycerol combination blocks aerobic and anaerobic glycolysis *in vivo* and clears parasites from the blood of experimental animals within 5 min [27]. Since this combination is so effective, glycerol-efflux has remained of particular interest [26]. SHAM inhibits TAO, which is upregulated in the bloodstream-form and not found in other trypanosomatids or in the mammalian host [26]. TAO inhibition blocks the aerobic pathway and increases the production of ATP via the reverse-action of glycerol kinase [41]. The glycerol produced by this anaerobic glycolysis will become toxic if not removed from the cell. If glycerol is not removed, it reverses the action of glycerol kinase by mass-action and also blocks the anaerobic pathway, explaining the toxic effect of SHAM plus glycerol. Our findings indicate that this SHAM-glycerol effect is dependent upon the AQPs. Indeed, our results show that *aqp2*, *aqp2-3* and *aqp1-2-3* cells, and clinical isolates lacking *AQP2* but with an *AQP2/3* chimera, display increased sensitivity to multiple respiratory inhibitors in the absence of exogenous glycerol. Thus, AQP2 plays a key role in both glycerol utilisation and efflux.

The combination of SHAM with a large dose of glycerol, required at up to 15 g per kg, remains impractical as a therapy [42]. More potent antitrypanosomal TAO inhibitors have been developed, however [42,43,44]. Our finding, therefore, that *aqp2*-deficiency is associated with TAO-inhibitor sensitivity, has implications for potential future therapeutic strategies. For example, new TAO-inhibitors may be effective as mono-therapies against melarsoprol-resistant *T. b. rhodesiense* [4], or *T. b. gambiense*, known to lack *AQP2* in the latter case [12]. This may also be the case for *T. vivax* and *T. congolense*, where the reference genomes indicate the absence of both the *AQP1* and *AQP2* genes and the presence of only an *AQP3*-like gene (Tvy486_1013610 and TcIL3000_10_12040, respectively) [34]. Indeed, although SHAM alone is ineffective against *T. vivax* [45], ascofuranone is effective against *T. vivax* infections in mice without added glycerol [32]. This and other TAO inhibitors are thought to function by mimicking ubiquinol and blocking electron transfer to the oxidase [46].

Melarsoprol has been highly effective against trypanosomiasis but clinical resistance, due to an *aqp2*-defect, has become widespread [12]. An option, therefore, could be to apply TAO-inhibitors and melarsoprol sequentially or in combination; this could establish a counter-resistance approach whereby AQP2 is required for both the uptake and efflux of toxins. Further similar options may emerge from on-going efforts to develop safer and orally available arsenical formulations [47]. Ultimately, reciprocal shifts in drug-sensitivity, such as the example we describe here, may be exploited to develop novel paradigms of targeted-therapy. Such strategies could restrict or even reverse the emergence and spread of drug resistance in human and livestock parasites, which would be of great value given the high cost of developing new therapies.

Our studies on *aqp*-null *T. b. brucei* and on clinical isolates of *T. b. gambiense* have revealed bidirectional defects in glycerol transport and the key contribution of AQP2, the AQP

specifically responsible for melarsoprol- and pentamidine-sensitivity, now also shown to impact respiratory inhibitor sensitivity. Thus, AQPs impact the efficacy of three major classes of antitrypanosomal drugs. These new mechanistic insights into differential sensitivities to antitrypanosomal drugs, in both clinical and veterinary settings, are potentially exploitable.

Materials and methods

T. b. brucei growth and manipulation

Bloodstream-form *T. brucei*, Lister 427, MiTat 1.2, clone 221a, and all derivatives were cultured in HMI-11 as previously described [48]. Bloodstream-form *T. b. gambiense* were cultured in the same media but with 15% FCS and 5% human serum. 2T1 [24], *aqp2* [9], *aqp2-3* [23], STIB930, STIB891, K03048, 40 AT [12] and 40 AT plus AQP2 [14] strains were described previously. SHAM, glycerol, octyl gallate and propyl gallate were from Sigma. SHAM was dissolved in DMSO, the gallates were dissolved in 70% ethanol or DMSO and ascofuranone was dissolved in DMSO. EC_{50} assays were performed using the AlamarBlue method as described [49] with 10 mM glycerol added as appropriate; drug exposure was for 66–67 h and AlamarBlue incubation was for 5–6 h. Plates were read on an Infinite 200 Pro plate-reader (Tecan). Growth rates in culture were monitored by splitting to 1 x 10^5 cells/ml and by counting daily. Three Balb/c mice were infected with *aqp1-2-3* triple-null trypanosomes by intraperitoneal injection of 10^4 cells in 0.2 ml of growth medium. Parasitaemia was determined daily following tail bleeds. Mice were purchased from Envigo, UK. Differentiation to insect-stage, procyclic form cells was initiated by washing 2 x 10^7 cells twice in DTM [50] and re-suspending in 5 ml DTM supplemented with citrate (3 mM) and cis-aconitate (3 mM) at 27˚C.

Plasmids and strain construction

For *AQP*-knockout plasmid constructs, AQP-flanking sequences were inserted on both sides of selectable marker cassettes. Restriction enzyme cleavage at the distal ends of the AQP targeting regions was used to linearise plasmid constructs prior to transfection. The AQP2-3 locus was disrupted by replacing a 4,772 bp fragment [9] with *BLA* and a modified *NPT* selectable marker cassette. The *AQP1* locus was disrupted by replacing a 647 bp fragment with *NPT* and (a modified) *PAC* selectable marker cassettes. The *AQP1*:*PAC* and *AQP2-3*:*NPT* cassettes were modified using annealed oligonucleotides (XSceF: CTAGTAGGGATAACAGGGTAAT, and XSceR: CTAGGATTACCCTGTTATCCCTA) to engineer an I-*Sce*I site at an *Xba*I site adjacent to each 5'-targeting region. Other oligonucleotide sequences are available upon request.

During creation of the *aqp1-2-3* triple-null strains, selectable markers were recovered using I-*Sce*I meganuclease-induction in a 2T1 (*BLE*:*PAC*) background [48]. Briefly, a $pRPa^{Sce}$ [51] construct (*HYG* recovers *PAC*) was introduced at the tagged locus on chromosome 2 and the *AQP2-3* alleles were replaced with *BLA* and *NPT*-cassettes, the latter containing the flanking I-*Sce*I cleavage site. Induction with 1 $\mu g.ml^{-1}$ tetracycline triggered I-*Sce*I cleavage and duplication of the *BLA*-cassette (*NPT* recovered). A similar process was repeated for *AQP1* alleles but this time with *NPT* and *PAC*-cassettes (*PAC* recovered). The ph3E construct [48] was then used to remove the I-*Sce*I cassette (*PAC* recovered *HYG*). A $pRPa^{AQP2}$ construct (*HYG* recovers *PAC*) was then used for expression of recombinant *AQP2* in the 2T1-*aqp1-2-3* null-background (*BLE*:*BLA*:*NEO*:*PAC*). Selectable-marker recovery was confirmed by screening individual clones in multi-well plates. Strains were transfected using a Nucleofector (Lonza) and cytomix. Transformants were selected with phleomycin (1 $\mu g.ml^{-1}$), blasticidin (10 $\mu g.ml^{-1}$), G418 (2 $\mu g.ml^{-1}$), puromycin (2 $\mu g.ml^{-1}$) and hygromycin (2.5 $\mu g.ml^{-1}$) as appropriate and *AQP* knockout was confirmed by Southern blotting, carried out according to standard protocols.

Hypo-osmotic shock assays

Cell volume during hypo-osmotic shock was assessed using a light-scattering assay. Briefly, 5 x 10^7 cells were pelleted and resuspended in ice cold Earle's salt buffer (116 mM NaCl, 1.8 mM $CaCl_2$, 5mM KCl, 0.8 mM $MgSO_4$, 1 mM NaH_2PO_4, 30 mM HEPES, 30 mM glucose, pH 7.4). 1.3 x10^4 cells in 100 µl per well were added to 96-well plates. Either 100 µl of cold deionised water (hypo-osmotic) or Earle's salt buffer (iso-osmotic) was added to each well. Results were then immediately read at 18-s intervals over a course of 25-min, using a Tecan Infinite 200 pro plate-reader at 595 nM absorbance.

Microscopy

For phase and fluorescence microscopy, cells were fixed in 1% paraformaldehyde, settled onto slides and mounted in Vectashield (Vector Laboratories) containing 4,6-diamidino-2-phenylindole (DAPI). Images were captured using an Axiovert 200 epifluorescence microscope in conjunction with an Axiocam 105 colour camera (Zeiss) and were processed using Zen digital imaging suite.

ATP quantification

We used the CellTiter-Glo luminescence assay (Promega). Briefly 5 x 10^6 cells were washed twice with cold PBS and re-suspended in 1 ml of 37˚C PBS with either 5 mM glucose or glycerol in PBS for 20-min before performing the assay as per the manufacturers' instructions. Plates were read on an Infinite 200 Pro plate-reader (Tecan). Values were compared to an ATP standard-curve.

Glycerol uptake assay

We used a [^{14}C] glycerol centrifugation method [52] with minor modifications. Briefly, cells were pelleted by centrifugation (1,000 g, 10 min), washed twice in transport buffer (33 mM HEPES, 98 mM NaCl, 4.6 mM KCl, 0.55 $CaCl_2$, 0.07 $MgSO_4$, 5.8 mM Na_2PO_4, 0.3 mM $NaHCO_3$, 14 mM glucose, pH 7.3) and diluted to 1 x 10^8/ml in transport buffer on ice. Uptake was measured (at 37˚C) by introducing 100 µl of cells to 100 µl transport buffer, containing 0.25 uCi glycerol. This reaction mixture was immediately loaded onto 100 µl of dibutyl phthalate (Sigma) in 1.5 ml Eppendorf tubes. After incubation for 5 min, cells were pelleted through the oil layer by centrifugation (16,000g, 1 min). The tubes were then frozen on liquid nitrogen and the bottoms of the tubes, containing pellets, were snipped directly into scintillation vials. Pellets were solubilised overnight in 150 µl 1 M NaOH, before mixing with 2 ml of scintillation fluid and reading on a scintillation counter (Beckman LS 6500) for 1 min.

Ethics statement

All animal experiments were approved by the Ethical Review Committee at the University of Dundee and performed under the Animals (Scientific Procedures) Act 1986 (UK Home Office Project Licence PPL 70/8274) in accordance with the European Communities Council Directive (86/609/EEC).

Acknowledgments

We thank L. Glover (Institut Pasteur) for advice on meganuclease cleavage, A. Fairlamb and N. Sienkiewicz (University of Dundee) for advice on glycerol uptake and utilisation assays, the TrypTag team (University of Oxford) for permission to cite data from their website (TrypTag.com) and B. Dujon (Institut Pasteur) for the I-*Sce*I gene.

Author Contributions

Conceptualization: LJ NB NW PM DH.

Investigation: LJ NB NW.

Supervision: PM DH.

Writing – original draft: LJ NB DH.

Writing – review & editing: LJ DH.

References

1. Brun R, Blum J, Chappuis F, Burri C (2010) Human African trypanosomiasis. Lancet 375: 148–159. https://doi.org/10.1016/S0140-6736(09)60829-1 PMID: 19833383
2. Priotto G, Kasparian S, Mutombo W, Ngouama D, Ghorashian S, et al. (2009) Nifurtimox-eflornithine combination therapy for second-stage African *Trypanosoma brucei gambiense* trypanosomiasis: a multicentre, randomised, phase III, non-inferiority trial. Lancet 374: 56–64. https://doi.org/10.1016/S0140-6736(09)61117-X PMID: 19559476
3. Iten M, Mett H, Evans A, Enyaru JC, Brun R, et al. (1997) Alterations in ornithine decarboxylase characteristics account for tolerance of *Trypanosoma brucei rhodesiense* to D,L-α-difluoromethylornithine. Antimicrob Agents Chemother 41: 1922–1925. PMID: 9303385
4. Kibona SN, Matemba L, Kaboya JS, Lubega GW (2006) Drug-resistance of *Trypanosoma b. rhodesiense* isolates from Tanzania. Trop Med Int Health 11: 144–155. https://doi.org/10.1111/j.1365-3156.2005.01545.x PMID: 16451338
5. Robays J, Nyamowala G, Sese C, Betu Ku Mesu Kande V, Lutumba P, et al. (2008) High failure rates of melarsoprol for sleeping sickness, Democratic Republic of Congo. Emerg Infect Dis 14: 966–967. https://doi.org/10.3201/eid1406.071266 PMID: 18507916
6. Baker N, de Koning HP, Maser P, Horn D (2013) Drug resistance in African trypanosomiasis: the melarsoprol and pentamidine story. Trends Parasitol 29: 110–118. https://doi.org/10.1016/j.pt.2012.12.005 PMID: 23375541
7. Carter NS, Fairlamb AH (1993) Arsenical-resistant trypanosomes lack an unusual adenosine transporter. Nature 361: 173–176. https://doi.org/10.1038/361173a0 PMID: 8421523
8. Maser P, Sutterlin C, Kralli A, Kaminsky R (1999) A nucleoside transporter from *Trypanosoma brucei* involved in drug resistance. Science 285: 242–244. PMID: 10398598
9. Baker N, Glover L, Munday JC, Aguinaga Andres D, Barrett MP, et al. (2012) Aquaglyceroporin 2 controls susceptibility to melarsoprol and pentamidine in African trypanosomes. Proc Natl Acad Sci U S A 109: 10996–11001. https://doi.org/10.1073/pnas.1202885109 PMID: 22711816
10. Munday JC, Eze AA, Baker N, Glover L, Clucas C, et al. (2014) *Trypanosoma brucei* aquaglyceroporin 2 is a high-affinity transporter for pentamidine and melaminophenyl arsenic drugs and the main genetic determinant of resistance to these drugs. J Antimicrob Chemother 69: 651–663. https://doi.org/10.1093/jac/dkt442 PMID: 24235095
11. Bronner U, Gustafsson LL, Doua F, Ericsson O, Miezan T, et al. (1995) Pharmacokinetics and adverse reactions after a single dose of pentamidine in patients with *Trypanosoma gambiense* sleeping sickness. British Journal of Clinical Pharmacology 39: 289–295. PMID: 7619671
12. Graf FE, Ludin P, Wenzler T, Kaiser M, Brun R, et al. (2013) Aquaporin 2 mutations in *Trypanosoma brucei gambiense* field isolates correlate with decreased susceptibility to pentamidine and melarsoprol. PLoS Negl Trop Dis 7: e2475. https://doi.org/10.1371/journal.pntd.0002475 PMID: 24130910
13. Pyana Pati P, Van Reet N, Mumba Ngoyi D, Ngay Lukusa I, Karhemere Bin Shamamba S, et al. (2014) Melarsoprol sensitivity profile of *Trypanosoma brucei gambiense* isolates from cured and relapsed sleeping sickness patients from the Democratic Republic of the Congo. PLoS Negl Trop Dis 8: e3212. https://doi.org/10.1371/journal.pntd.0003212 PMID: 25275572
14. Graf FE, Baker N, Munday JC, de Koning HP, Horn D, et al. (2015) Chimerization at the *AQP2-AQP3* locus is the genetic basis of melarsoprol-pentamidine cross-resistance in clinical *Trypanosoma brucei gambiense* isolates. Int J Parasitol Drugs Drug Resist 5: 65–68. https://doi.org/10.1016/j.ijpddr.2015.04.002 PMID: 26042196
15. Gourbal B, Sonuc N, Bhattacharjee H, Legare D, Sundar S, et al. (2004) Drug uptake and modulation of drug resistance in *Leishmania* by an aquaglyceroporin. J Biol Chem 279: 31010–31017. https://doi.org/10.1074/jbc.M403959200 PMID: 15138256

16. Bassarak B, Uzcategui NL, Schonfeld C, Duszenko M (2011) Functional characterization of three aquaglyceroporins from *Trypanosoma brucei* in osmoregulation and glycerol transport. Cell Physiol Biochem 27: 411–420. https://doi.org/10.1159/000327968 PMID: 21471730

17. Dean S, Sunter JD, Wheeler RJ (2017) TrypTag.org: A Trypanosome Genome-wide Protein Localisation Resource. Trends Parasitol 33: 80–82. https://doi.org/10.1016/j.pt.2016.10.009 PMID: 27863903

18. Zeuthen T, Wu B, Pavlovic-Djuranovic S, Holm LM, Uzcategui NL, et al. (2006) Ammonia permeability of the aquaglyceroporins from *Plasmodium falciparum*, *Toxoplasma gondii* and *Trypansoma brucei*. Mol Microbiol 61: 1598–1608. https://doi.org/10.1111/j.1365-2958.2006.05325.x PMID: 16889642

19. Marsiccobetre S, Rodriguez-Acosta A, Lang F, Figarella K, Uzcategui NL (2017) Aquaglyceroporins Are the Entry Pathway of Boric Acid in *Trypanosoma brucei*. Biochim Biophys Acta 1859: 679–685. https://doi.org/10.1016/j.bbamem.2017.01.011 PMID: 28087364

20. Uzcategui NL, Szallies A, Pavlovic-Djuranovic S, Palmada M, Figarella K, et al. (2004) Cloning, heterologous expression, and characterization of three aquaglyceroporins from *Trypanosoma brucei*. J Biol Chem 279: 42669–42676. https://doi.org/10.1074/jbc.M404518200 PMID: 15294911

21. Uzcategui NL, Figarella K, Bassarak B, Meza NW, Mukhopadhyay R, et al. (2013) *Trypanosoma brucei* aquaglyceroporins facilitate the uptake of arsenite and antimonite in a pH dependent way. Cell Physiol Biochem 32: 880–888. https://doi.org/10.1159/000354490 PMID: 24217645

22. Song J, Baker N, Rothert M, Henke B, Jeacock L, et al. (2016) Pentamidine Is not a permeant but a nanomolar inhibitor of the *Trypanosoma brucei* aquaglyceroporin-2. PLoS Pathog 12: e1005436. https://doi.org/10.1371/journal.ppat.1005436 PMID: 26828608

23. Alsford S, Eckert S, Baker N, Glover L, Sanchez-Flores A, et al. (2012) High-throughput decoding of antitrypanosomal drug efficacy and resistance. Nature 482: 232–236. https://doi.org/10.1038/nature10771 PMID: 22278056

24. Alsford S, Horn D (2008) Single-locus targeting constructs for reliable regulated RNAi and transgene expression in *Trypanosoma brucei*. Mol Biochem Parasitol 161: 76–79. https://doi.org/10.1016/j.molbiopara.2008.05.006 PMID: 18588918

25. Haanstra JR, van Tuijl A, Kessler P, Reijnders W, Michels PA, et al. (2008) Compartmentation prevents a lethal turbo-explosion of glycolysis in trypanosomes. Proc Natl Acad Sci U S A 105: 17718–17723. https://doi.org/10.1073/pnas.0806664105 PMID: 19008351

26. Chaudhuri M, Ott RD, Hill GC (2006) Trypanosome alternative oxidase: from molecule to function. Trends Parasitol 22: 484–491. https://doi.org/10.1016/j.pt.2006.08.007 PMID: 16920028

27. Clarkson AB Jr., Brohn FH (1976) Trypanosomiasis: an approach to chemotherapy by the inhibition of carbohydrate catabolism. Science 194: 204–206. PMID: 986688

28. Grady RW, Bienen EJ, Clarkson AB Jr., (1986) Esters of 3,4-dihydroxybenzoic acid, highly effective inhibitors of the sn-glycerol-3-phosphate oxidase of *Trypanosoma brucei* brucei. Mol Biochem Parasitol 21: 55–63. PMID: 3773935

29. Felgner P, Brinkmann U, Zillmann U, Mehlitz D, Abu-Ishira S (1981) Epidemiological studies on the animal reservoir of gambiense sleeping sickness. Part II. Parasitological and immunodiagnostic examination of the human population. Tropenmedizin und Parasitologie 32: 134–140. PMID: 6285560

30. Matovu E, Geiser F, Schneider V, Maser P, Enyaru JC, et al. (2001) Genetic variants of the *TbAT1* adenosine transporter from African trypanosomes in relapse infections following melarsoprol therapy. Mol Biochem Parasitol 117: 73–81. PMID: 11551633

31. Maina NW, Oberle M, Otieno C, Kunz C, Maeser P, et al. (2007) Isolation and propagation of *Trypanosoma brucei gambiense* from sleeping sickness patients in south Sudan. Trans R Soc Trop Med Hyg 101: 540–546. https://doi.org/10.1016/j.trstmh.2006.11.008 PMID: 17275053

32. Yabu Y, Suzuki T, Nihei C, Minagawa N, Hosokawa T, et al. (2006) Chemotherapeutic efficacy of ascofuranone in *Trypanosoma vivax*-infected mice without glycerol. Parasitol Int 55: 39–43. https://doi.org/10.1016/j.parint.2005.09.003 PMID: 16288933

33. Promeneur D, Liu Y, Maciel J, Agre P, King LS, et al. (2007) Aquaglyceroporin PbAQP during intraerythrocytic development of the malaria parasite *Plasmodium berghei*. Proc Natl Acad Sci U S A 104: 2211–2216. https://doi.org/10.1073/pnas.0610843104 PMID: 17284593

34. Jackson AP, Berry A, Aslett M, Allison HC, Burton P, et al. (2012) Antigenic diversity is generated by distinct evolutionary mechanisms in African trypanosome species. Proc Natl Acad Sci U S A 109: 3416–3421. https://doi.org/10.1073/pnas.1117313109 PMID: 22331916

35. Figarella K, Uzcategui NL, Zhou Y, LeFurgey A, Ouellette M, et al. (2007) Biochemical characterization of *Leishmania major* aquaglyceroporin LmAQP1: possible role in volume regulation and osmotaxis. Mol Microbiol 65: 1006–1017. https://doi.org/10.1111/j.1365-2958.2007.05845.x PMID: 17640270

36. Montalvetti A, Rohloff P, Docampo R (2004) A functional aquaporin co-localizes with the vacuolar proton pyrophosphatase to acidocalcisomes and the contractile vacuole complex of *Trypanosoma cruzi*. J Biol Chem 279: 38673–38682. https://doi.org/10.1074/jbc.M406304200 PMID: 15252016

37. Plourde M, Ubeda JM, Mandal G, Monte-Neto RL, Mukhopadhyay R, et al. (2015) Generation of an aquaglyceroporin AQP1 null mutant in *Leishmania major*. Mol Biochem Parasitol 201: 108–111. https://doi.org/10.1016/j.molbiopara.2015.07.003 PMID: 26222914

38. Vieira LL, Lafuente E, Gamarro F, Cabantchik Z (1996) An amino acid channel activated by hypotonically induced swelling of *Leishmania major* promastigotes. Biochem J 319 (Pt 3): 691–697. PMID: 8920968

39. Bursell JD, Kirk J, Hall ST, Gero AM, Kirk K (1996) Volume-regulatory amino acid release from the protozoan parasite *Crithidia luciliae*. J Membrane Biol 154: 131–141.

40. Lefurgey A, Gannon M, Blum J, Ingram P (2005) *Leishmania donovani* amastigotes mobilize organic and inorganic osmolytes during regulatory volume decrease. The J Euk Microbiol 52: 277–289. https://doi.org/10.1111/j.1550-7408.2005.00030.x PMID: 15927005

41. Bakker BM, Michels PA, Opperdoes FR, Westerhoff HV (1997) Glycolysis in bloodstream form *Trypanosoma brucei* can be understood in terms of the kinetics of the glycolytic enzymes. J Biol Chem 272: 3207–3215. PMID: 9013556

42. Nihei C, Fukai Y, Kita K (2002) Trypanosome alternative oxidase as a target of chemotherapy. Biochim Biophys Acta 1587: 234–239. PMID: 12084465

43. Grady RW, Bienen EJ, Dieck HA, Saric M, Clarkson AB Jr. (1993) *N*-n-alkyl-3,4-dihydroxybenzamides as inhibitors of the trypanosome alternative oxidase: activity *in vitro* and *in vivo*. Antimicrob Agents Chemother 37: 1082–1085. PMID: 8517695

44. Menzies SK, Tulloch LB, Florence GJ, Smith TK (2016) The trypanosome alternative oxidase: a potential drug target? Parasitology: 1–9.

45. Evans DA, Holland MF (1978) Effective treatment of *Trypanosoma vivax* infections with salicylhydroxamic acid (SHAM). Trans R Soc Trop Med Hyg 72: 203–204. PMID: 653794

46. Shiba T, Kido Y, Sakamoto K, Inaoka DK, Tsuge C, et al. (2013) Structure of the trypanosome cyanide-insensitive alternative oxidase. Proc Natl Acad Sci U S A 110: 4580–4585. https://doi.org/10.1073/pnas.1218386110 PMID: 23487766

47. Kennedy PG (2012) An alternative form of melarsoprol in sleeping sickness. Trends Parasitol 28: 307–310. https://doi.org/10.1016/j.pt.2012.05.003 PMID: 22704910

48. Alsford S, Kawahara T, Glover L, Horn D (2005) Tagging a *T. brucei RRNA* locus improves stable transfection efficiency and circumvents inducible expression position effects. Mol Biochem Parasitol 144: 142–148. https://doi.org/10.1016/j.molbiopara.2005.08.009 PMID: 16182389

49. Raz B, Iten M, Grether-Buhler Y, Kaminsky R, Brun R (1997) The Alamar Blue assay to determine drug sensitivity of African trypanosomes (*T. b. rhodesiense* and *T. b. gambiense*) *in vitro*. Acta Trop 68: 139–147. PMID: 9386789

50. Czichos J, Nonnengaesser C, Overath P (1986) *Trypanosoma brucei*: *cis*-aconitate and temperature reduction as triggers of synchronous transformation of bloodstream to procyclic trypomastigotes *in vitro*. Exp Parasitol 62: 283–291. PMID: 3743718

51. Alsford S, Turner DJ, Obado SO, Sanchez-Flores A, Glover L, et al. (2011) High-throughput phenotyping using parallel sequencing of RNA interference targets in the African trypanosome. Genome Res 21: 915–924. https://doi.org/10.1101/gr.115089.110 PMID: 21363968

52. Wille U, Schade B, Duszenko M (1998) Characterization of glycerol uptake in bloodstream and procyclic forms of *Trypanosoma brucei*. Eur J Biochem 256: 245–250. PMID: 9746370

I have performed the drug sensitivity assays of the melarsoprol-pentamidine resistant *T. b. gambiense* field isolates (Figure 5A-C).

Appendix 2. The enigmatic role of uridine-rich-binding protein 1 in melarsoprol/ pentamidine cross-resistance of *Trypanosoma brucei*

Natalie Wiedemar[1,2], Fabrice E. Graf[1,2], Remo S. Schmidt[1,2], Pascal Mäser[1,2]

[1] Swiss Tropical and Public Health Institute, CH-4002 Basel, Switzerland

[2] University of Basel, CH-4001 Basel, Switzerland

Working manuscript, January 2019

I have performed all the experiments.

Abstract

Melarsoprol and pentamidine are drugs that have been used to treat human African trypanosomiasis (HAT) for decades. It has been known for a long time that resistance against one of the drugs confers cross-resistance to the other. This has been attributed to shared transporters: AT1 and AQP2, which both mediate cellular uptake of melarsoprol and pentamidine. In a previous study we have identified mutations in both genes in two *in vitro* selected melarsoprol and pentamidine resistant *Trypanosoma brucei rhodesiense* lines. Additionally, both lines carried a homozygous mutation in uridine-rich-binding protein 1 (*UBP1*), follow-up on which was inconclusive. In the present study, we re-introduce the wildtype *UBP1* sequence into one of the selected lines and investigate the effects on drug sensitivity. The transfected clones do not show a clear loss of resistance in presence of the wildtype allele, thus the *UBP1* mutation could not be confirmed as cause for the melarsoprol-pentamidine cross-resistance.

UBP1 and MPXR

Cure for human African trypanosomiasis (HAT) exclusively relies on successful drug treatment. HAT is caused by two subspecies of the protozoan parasite *Trypanosoma brucei*: *T. b. gambiense* and *T. b. rhodesiense.* During the first stage, when the trypanosomes have not yet invaded the central nervous system, the disease is treated with pentamidine for *T. b. gambiense* HAT or suramin for *T. b. rhodesiense* HAT [1]. The treatment of the second stage with involvement of the central nervous system relies on drugs that are able to cross the blood-brain barrier, for a long time melarsoprol was the only option. In the last decade a combination of eflornithine and nifurtimox have been used to treat *T. b. gambiense* HAT [1], and most recently fexinidazole [2] has been approved for treatment of all stages. Besides complicated administration and unacceptable side effects, especially in case of melarsoprol, increasing reports of treatment failures, possibly due to drug resistance, hamper treatment with the current drugs [3,4]. Shortly after the introduction of melarsoprol [5], laboratory induced melarsoprol resistance with cross-resistance to pentamidine was reported [6]. This melarsoprol-pentamidine cross-resistance (MPXR) was attributed to a defective drug transporter and consequently a reduced drug uptake [7,8]. The transporter itself was later on identified as an adenosine transporter [7,9] encoded by the gene *TbAT1* [10]. Mutations in *TbAT1* were also identified in MPXR patient isolates [11]. A second transporter was identified in a genome-wide RNAi library screen: aquaglyceroporin 2, encoded by the gene *TbAQP2*, which also leads to MPXR under knockdown [12,13]. Aquaporin 2 mutations were also shown to be present in the field, as deletions and chimerism of *TbAQP2*/*TbAQP3* were identified in drug-resistant field isolates [14].

In a past study we selected the *T. b. rhodesiense* STIB900 line independently with melarsoprol (STIB900-M) and pentamidine (STIB900-P) over the course of two years [15]. Both lines showed MPXR and were subjected to mRNA and whole genome sequencing. STIB900-M carried a 25 kb deletion encompassing *TbAT1* while STIB900-P had acquired a point mutation in *TbAT1* that rendered the protein non-functional regarding drug transport [16]. Additionally, both lines contained a 1.8 kb deletion leading to a loss of *AQP2*. These findings were in agreement with the model of loss of drug import as the cause of MPXR. However, simultaneous knock-out of *TbAQP2* and *TbAT1* in *T. b. brucei* cells did not lead to such a strong MPXR phenotype as observed in the selected lines, which indicates that additional mutations must be involved in drug resistance [16]. Only few non-synonymous

mutations were identified in STIB900-M and STIB900-P. Most noticeable, both lines had acquired the same point mutation, a G to T transversion at position 392 of the coding sequence in Tb927.11.500, the gene encoding the RNA-binding protein UBP1 (uridine-rich-binding protein 1). UBP1 contains a well-conserved RNA-recognition motive (RRM) that binds to AU-rich instability elements in the 3' UTR of certain mRNAs and decreases their half-life as shown in *T. cruzi* [17,18]. The identified mutation is located within the RRM and leads to the amino acid substitution arginine^{131} to leucine (R131L) [16]. UBP1 is an essential gene in *T. brucei* bloodstream forms [19].

Additional lines of evidence point towards a potential role for UBP1 in drug resistance: (i) the orthologue in *T. cruzi*, TcUBP1, relocalized from the cytoplasm to the nucleus during arsenite stress, and this process was inhibited by mutations that affected RNA-binding [20]. (ii) a paralogue in *T. brucei*, UBP2, was identified as a secondary hit for pentamidine resistance by genome-wide RNAi, and UBP1 showed a pentamidine signature as well [12]. (iii) Whole-genome sequencing of clinical isolates derived from *T. b. gambiense* relapse patients after melarsoprol treatment identified heterozygous single-nucleotide polymorphism in *UBP1* [21].

Experimental investigation on the mutation R131L in *T. b. brucei* 2T1 was inconclusive: parasites overexpressing GFP-UBP1-R131L became slightly hypersensitive to pentamidine, while *in situ* introduction of the mutated allele did not alter melarsoprol and pentamidine sensitivity [16]. However, it was still possible that the UBP1 mutation would mediate drug resistance only in the STIB900-M and STIB900-P background, i.e. loss of function for TbAT1 and TbAQP2.

To investigate this hypothesis we introduced the *UBP1* wildtype allele *in situ* into the resistant STIB900-P and STIB900-M lines. Therefore parasites were transfected with a construct consisting of the intergenic region upstream of *UBP1*, a βα tubulin splice site, the blasticidine resistance gene, an αβ tubulin splice site, the 5' untranslated region of *UBP1* and the first part of the *UBP1* coding sequence (cds) including the site of the mutation (Fig. 1A). As the original construct [16] contained the mutant T allele at position 392, we used a primer that spanned the mutation but contained a G at the respective position to insert the wildtype allele into the amplified product. Transfection of trypanosomes was carried out [16] and pseudoclones were picked after one week. Subsequently DNA was isolated and the first part of the *UBP1* cds was PCR amplified and sequenced to check for

the presence of the wildtype allele. In an initial round of transfection, only one out of six recovered clones was homozygous GG, the remaining clones had integrated parts of the construct including the blasticidine resistance gene but without the last part of the *UBP1* cds. Thus, the homologous recombination event in those clones must have happened further upstream of the mutated position, which is located at the very end of the construct in the last nine nucleotides. To increase chances of a correct replacement of the mutated with the wildtype allele in a second round of transfection we extended the construct by using a primer with a 49 nucleotide overhang. Of the 13 recovered clones, four were homozygous GG and nine remained homozygous TT. Clones that showed any additional mutations in the coding sequence were excluded from further experiments. Sequencing revealed that STIB900 as well as STIB900-M and STIB900-P had an additional AAC deletion when compared to the Tb927.11.500 reference sequence, leading to a loss of a glutamine at position 29. At the given position the transfectants were identical to the Tb927.11.500 reference sequence on which the construct was based on.

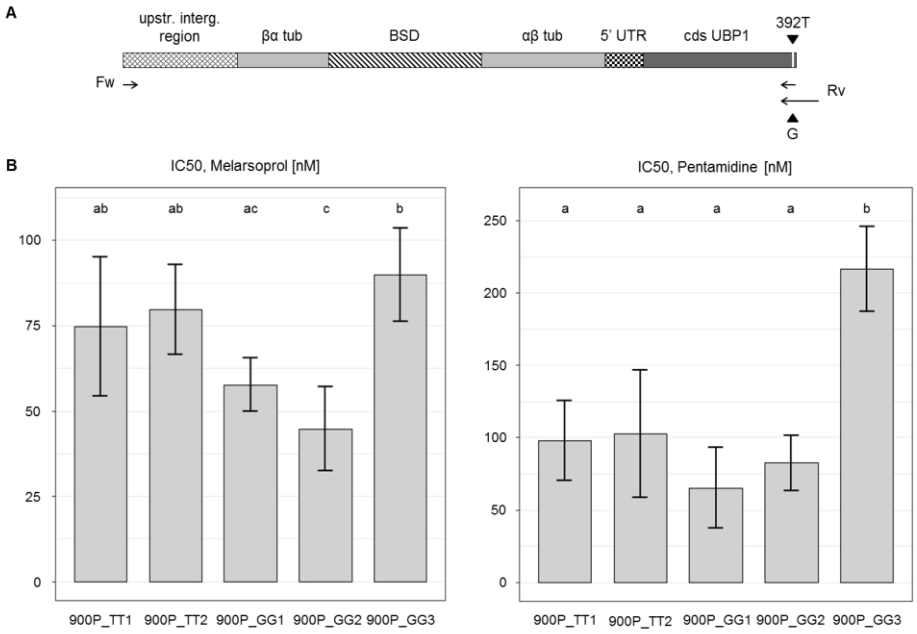

Figure 1: Reverse genetics of *UBP1* and the effect on drug sensitivity (A) Construct used to replace the mutated *UBP1* by the wildtype allele with the upstream intergenic region of *UBP1* (upstr. inerg. region) as homologous region on the 5' end of the construct, a βα tubulin splice site (βα tub), blasticidine resistance gene (BSD), αβ tubulin splice site (αβ tub), 5'UTR of *UBP1* and the first 400 nucleotides of the *UBP1* coding sequence including the 392G>T mutation (black triangle). Primers used for amplification of the construct prior

to transfection are shown as black arrows; the reverse primers (Rv) contained the wildtype G allele at position 392 of the *UBP1* coding sequence. (B) Drug sensitivities for melarsoprol and pentamidine are shown for the transfected STIB900-P clones. Two transfectants (TT) had retained the mutated T allele and three transfectants (GG) carried the wildtype G allele. Error bars represent standard deviations of five replicates, different letters indicate significant differences between the clones (Tukey multiple comparison test).

Drug sensitivities of the parental STIB900-P, three homozygous GG, and two homozygous TT transfectants (as additional controls) were determined using Alamar Blue assays [22]. For melarsoprol, STIB900-P showed an IC50 of 95 nM, the transfectants with the retained TT mutation had an IC_{50} of 75 and 80 nM, and the transfectants reverted back to the wildtype allele GG had an IC50 of 58, 45 and 90 nM (Fig 1B). For pentamidine the IC_{50} was at 183 nM in STIB900-P, 98 and 103 nM for the TT transfectants and 65, 82 and 216 nM for the GG transfectants (Fig 1B). Comparison of the three GG clones with the lines carrying the TT genotype yielded an overall p-value of 0.91 for pentamidine and 0.29 for melarsoprol (Welch Two Sample t-test).

In summary, neither did the introduction of the R131L mutation cause MPXR in sensitive *T. b. brucei* cells [16], nor did its reversion in abrogate resistance in MPXR *T. b. rhodesiense* cells (Tab 1). Interestingly, four out of five transfectants showed trend of decreased IC50 for melarsoprol and pentamidine irrespective of their genotype. In light of the faint observed signatures in the RNAi library screen [12], one could speculate that the resistance phenotype is rather influenced by gene dosage and that the introduction of the construct leads to alterations of mRNA abundance and thus generally decreases the melarsoprol and pentamidine sensitivity. Taken together these results do not support the hypothesis that UBP1 is involved in drug sensitivity and that the mutation R131L causes melarsoprol/pentamidine cross-resistance in *T. brucei*. Nevertheless, the role of UBP1 remains somehow puzzling and an involvement in drug sensitivity cannot definitely be ruled out.

Table 1: Melarsoprol and Pentamidine sensitivities of different cell lines carrying either wildtype arginine or the mutated leucine at position 131 of UBP1

Line	UBP1	IC50 ± standard deviation [nM]	
		Melarsoprol	Pentamidine
STIB900	Arg^{131}	6.0 ± 3.4	2.8 ± 0.8
STIB900_P	Leu^{131}	84 ± 52	130 ± 69
STIB900_M	Leu^{131}	170 ± 63	210 ± 93
2T1	Arg^{131}	16 ± 3.3	2.1 ± 0.9
2T1 _H	Leu^{131}	15 ± 4.0	2.6 ± 1.2
2T1 _L	Leu^{131}	17 ± 4.2	2.5 ± 0.9
STIB900_P	Leu^{131}	95 ± 18	183 ± 55
900P_TT1	Leu^{131}	75 ± 20	98 ± 28
900P_TT2	Leu^{131}	80 ± 13	103 ± 44
900P_GG1	Arg^{131}	58 ± 7.9	65 ± 28
900P_GG2	Arg^{131}	45 ± 12	82 ± 19
900P_GG3	Arg^{131}	90 ± 14	216 ± 29

References

1. Büscher P, Cecchi G, Jamonneau V, Priotto G. Human African trypanosomiasis. Lancet Lond Engl. 2017;390: 2397–2409. doi:10.1016/S0140-6736(17)31510-6

2. Deeks ED. Fexinidazole: First Global Approval. Drugs. 2019. doi:10.1007/s40265-019-1051-6

3. Matovu E, Enyaru JC, Legros D, Schmid C, Seebeck T, Kaminsky R. Melarsoprol refractory T. b. gambiense from Omugo, north-western Uganda. Trop Med Int Health TM IH. 2001;6: 407–411.

4. Robays J, Nyamowala G, Sese C, Betu Ku Mesu Kande V, Lutumba P, Van der Veken W, et al. High failure rates of melarsoprol for sleeping sickness, Democratic Republic of Congo. Emerg Infect Dis. 2008;14: 966–967. doi:10.3201/eid1406.071266

5. Friedheim E a. H. Mel B in the treatment of human trypanosomiasis. Am J Trop Med Hyg. 1949;29: 173–180.

6. Rollo IM, Williamson J. Acquired resistance to "Melarsen", tryparsamide and amidines in pathogenic trypanosomes after treatment with "Melarsen" alone. Nature. 1951;167: 147–148.

7. Carter NS, Fairlamb AH. Arsenical-resistant trypanosomes lack an unusual adenosine transporter. Nature. 1993;361: 173–176. doi:10.1038/361173a0

8. Berger BJ, Carter NS, Fairlamb AH. Characterisation of pentamidine-resistant Trypanosoma brucei brucei. Mol Biochem Parasitol. 1995;69: 289–298.

9. Carter NS, Berger BJ, Fairlamb AH. Uptake of diamidine drugs by the P2 nucleoside transporter in melarsen-sensitive and -resistant Trypanosoma brucei brucei. J Biol Chem. 1995;270: 28153–28157.

10. Mäser P, Sütterlin C, Kralli A, Kaminsky R. A nucleoside transporter from Trypanosoma brucei involved in drug resistance. Science. 1999;285: 242–244.

11. Matovu E, Geiser F, Schneider V, Mäser P, Enyaru JC, Kaminsky R, et al. Genetic variants of the TbAT1 adenosine transporter from African trypanosomes in relapse infections following melarsoprol therapy. Mol Biochem Parasitol. 2001;117: 73–81.

12. Alsford S, Eckert S, Baker N, Glover L, Sanchez-Flores A, Leung KF, et al. High-throughput decoding of antitrypanosomal drug efficacy and resistance. Nature. 2012;482: 232–236. doi:10.1038/nature10771

13. Baker N, Glover L, Munday JC, Aguinaga Andrés D, Barrett MP, de Koning HP, et al. Aquaglyceroporin 2 controls susceptibility to melarsoprol and pentamidine in African trypanosomes. Proc Natl Acad Sci U S A. 2012;109: 10996–11001. doi:10.1073/pnas.1202885109

14. Graf FE, Ludin P, Wenzler T, Kaiser M, Brun R, Pyana PP, et al. Aquaporin 2 mutations in Trypanosoma brucei gambiense field isolates correlate with decreased susceptibility to pentamidine and melarsoprol. PLoS Negl Trop Dis. 2013;7: e2475. doi:10.1371/journal.pntd.0002475

15. Bernhard SC, Nerima B, Mäser P, Brun R. Melarsoprol- and pentamidine-resistant Trypanosoma brucei rhodesiense populations and their cross-resistance. Int J Parasitol. 2007;37: 1443–1448. doi:10.1016/j.ijpara.2007.05.007

16. Graf FE, Ludin P, Arquint C, Schmidt RS, Schaub N, Kunz Renggli C, et al. Comparative genomics of drug resistance in Trypanosoma brucei rhodesiense. Cell Mol Life Sci CMLS. 2016;73: 3387–3400. doi:10.1007/s00018-016-2173-6

17. Volpon L, D'Orso I, Young CR, Frasch AC, Gehring K. NMR structural study of TcUBP1, a single RRM domain protein from Trypanosoma cruzi: contribution of a beta hairpin to RNA binding. Biochemistry (Mosc). 2005;44: 3708–3717. doi:10.1021/bi047450e

18. D'Orso I, Frasch AC. TcUBP-1, a developmentally regulated U-rich RNA-binding protein involved in selective mRNA destabilization in trypanosomes. J Biol Chem. 2001;276: 34801–34809. doi:10.1074/jbc.M102120200

19. Alsford S, Turner DJ, Obado SO, Sanchez-Flores A, Glover L, Berriman M, et al. High-throughput phenotyping using parallel sequencing of RNA interference targets in the African trypanosome. Genome Res. 2011;21: 915–924. doi:10.1101/gr.115089.110

20. Cassola A, Frasch AC. An RNA recognition motif mediates the nucleocytoplasmic transport of a trypanosome RNA-binding protein. J Biol Chem. 2009;284: 35015–35028. doi:10.1074/jbc.M109.031633

21. Richardson JB, Evans B, Pyana PP, Van Reet N, Sistrom M, Büscher P, et al. Whole genome sequencing shows sleeping sickness relapse is due to parasite regrowth and not reinfection. Evol Appl. 2016;9: 381–393. doi:10.1111/eva.12338

22. Räz B, Iten M, Grether-Bühler Y, Kaminsky R, Brun R. The Alamar Blue assay to determine drug sensitivity of African trypanosomes (T.b. rhodesiense and T.b. gambiense) in vitro. Acta Trop. 1997;68: 139–147.

Acknowledgements

First of all I deeply thank Pascal Mäser, my supervisor, for his support and for giving me the opportunity to carry out the presented work. His encouraging, open-minded leadership style gave me the freedom to dive into the subject and project, and his unprejudiced and creative way to address research questions was a constant inspiration for me.

I further thank all the current and past members of the Parasite Chemotherapy Unit of the Swiss TPH. You made me feel at home at work. The positive and familiar atmosphere in our group, the funny, deep and interesting discussions and the many times we literally laughed tears, made me enjoy my working hours. Special thanks go to Remo Schmidt, for not only showing me many molecular biological techniques, but also for thorough and fruitful discussions, and for his patience and open ear to the small and big sorrows of us PhD students. I warmly thank Monica Cal for introducing me in the cell culture lab and providing me with enough knowledge to make my trypanosomes feel happy; and for her friendship. Special thanks also to Christina Kunz for showing me how to clone trypanosomes and for many helpful advices. I am further very grateful to our two MSc students Michaela Zwyer and Silvan Hälg, they did not only let me gain first experience as a supervisor, but their motivation and very good work advanced the progress and the success of our project significantly. I also warmly thank Anna Fesser for her friendship, for many coffee hours and for all the inspiring work-related and non-work-related conversations. I am further very thankful to Tanja Wenzler, Emiliana Ndomba and Fabrice Graf for the pilot work they had performed on the project before the start of my PhD, without their discoveries and their results my project would not have come into existence.

I am very grateful also to Mark Field, Martin Zoltner and the whole Field-lab at the School of Life Sciences in Dundee for hosting me for two months and for many fruitful discussions. Special thanks go to Martin Zoltner, who spent a lot of time introducing me to new techniques and for his help with the ISG75 turnover and the endocytosis assays.

There is large number of people who have inspired and helped me during my PhD and it is impossible to name all of them. I am grateful to Mike Ferguson and Mark Carrington for their input on the structure of VSG^{Sur}. I further thank Sam Alsford for discussions and input on the human serum resistance assays.

I am also very thankful to André Schneider and Tosso Leeb for joining the PhD committee and for their time and inputs.

I further warmly thank all my past and present colleagues and friends at the Swiss TPH who made me adopt Basel as a second home very quickly. I thank my former office mates for all the fun we had and the biostats group members for lunch company and many coffees, walks, rhine swims and parties. I further thank the Thirsty Thursday crew for many hang-outs and barbeques at the rhine. And many thanks to my salsa-buddies for their company, friendship and for joining me when I needed to dance off the stress!

I further thank my flat-mates for providing me with a family in Basel and for feeding me through once in a while. And I am grateful to my friends from church for their support, and prayers.

I am very grateful also to my friends in Bern who know me inside out, for allowing me to move to far away Basel, for their constant support, encouragement and friendship.

Finally, I am deeply thankful to my parents and my whole family, who equipped me with the needed self-confidence, who have supported and encouraged me in every situation and with everything I did, and who are always there for me.